A NOVEL FRAMEWORK FOR CONSTRUCTING FLEXIBLE LIFETIME DISTRIBUTIONS WITH APPLICATIONS IN RELIABILITY

Thesis submitted to the University of Calicut

for the award of the degree of

DOCTOR OF PHILOSOPHY

IN

STATISTICS

under the Faculty of Science

by

GREESHMA CHANDRAN

under the guidance of

Prof. (Dr.) M. MANOHARAN

DEPARTMENT OF STATISTICS

UNIVERSITY OF CALICUT

KERALA - 673 635

INDIA

May - 2025

DEPARTMENT OF STATISTICS
UNIVERSITY OF CALICUT

Prof. (Dr.) M. Manoharan
M.Sc., Ph.D.

Calicut University P.O.
Kerala, India 673 635.
Mob : 91-9447424043
Email : manumavila@gmail.com

CERTIFICATE

I hereby certify that, this thesis entitled **"A novel framework for constructing flexible lifetime distributions with applications in reliability"** is a bonafide record of research work carried out by **Mrs. Greeshma Chandran.**, Research Scholar, Department of Statistics, University of Calicut, under my supervision and guidance for the award of the Degree of Doctor of Philosophy in Statistics, of the University of Calicut. The work reported herein does not form part of any other thesis or dissertation submitted previously for the award of any degree or diploma of any other university or institution. Also certified that the contents of the thesis have been checked using anti-plagiarism data base and no unacceptable similarity was found through the software check.

University of Calicut

Date: 26/05/2025

Dr. M. Manoharan

Research Supervisor

Dr. M. MANOHARAN
Senior Professor, Dept. of Statistics
University of Calicut
Calicut University P.O., Malappuram (Dt.)
Kerala. PIN-673635

DEPARTMENT OF STATISTICS
UNIVERSITY OF CALICUT

Prof. (Dr.) M. Manoharan
M.Sc., Ph.D.

Calicut University P.O.
Kerala, India 673 635.
Mob : 91-9447424043
Email : manumavila@gmail.com

CERTIFICATE

Certified that the corrections/suggestions recommended by the adjudicators of the Ph.D thesis entitled **"A novel framework for constructing flexible lifetime distributions with applications in reliability"** submitted by **Ms. Greeshma Chandran**, Research Scholar, Department of Statistics, University of Calicut, under my supervision and guidance have been incorporated in the thesis and that the contents in the thesis and the soft copy are one and the same.

University of Calicut
Date: 12/10/2025

Dr. M. Manoharan
Research Supervisor

Dr. M. MANOHARAN
Senior Professor, Dept. of Statistics
University of Calicut
Calicut University P.O., Malappuram (Dt.)
Kerala. PIN-673635

DECLARATION

I, Greeshma Chandran., hereby declare that this thesis entitled **"A novel framework for constructing flexible lifetime distributions with applications in reliability"** is based on the original work done by me under the guidance of Dr. M. Manoharan, Senior Professor (Retd.), Department of Statistics, University of Calicut and has not been included in any other thesis submitted previously for the award of any degree. The contents of the thesis have undergone plagiarism check using the *iThenticate* software at C.H.M.K Library, University of Calicut, and the similarity index found within permissible limit. I also declare that the thesis is free from AI-generated content.

26/05/2025 **Greeshma Chandran**

Dr. M. MANOHARAN
Senior Professor, Dept. of Statistics
University of Calicut
Calicut University P.O., Malappuram (Dt.)
Kerala. PIN-673635

Acknowledgments

I take this opportunity with immense pleasure and gratitude to thank all those who have supported and guided me throughout the course of my journey toward completing this thesis.

First and foremost, I would like to express my heartfelt gratitude to my guide and mentor, Dr. Manoharan M, Senior Professor (Retd.), Department of Statistics, University of Calicut, for his invaluable guidance, constant encouragement, and insightful suggestions throughout this research.

I extend my sincere thanks to Dr. Krishnarani S. D, Head of the Department; Dr. Dileepkumar M, Assistant Professor; Dr. Jayakumar K, Senior Professor; and Dr. Chandran C, Senior Professor (Retd.), Department of Statistics, University of Calicut, for their valuable suggestions, academic encouragement, and approachable nature that helped shape my ideas with greater clarity.

I am deeply grateful to the librarian and non-teaching staff of the department, whose timely assistance greatly contributed to the smooth progress of my academic work. I also extend special thanks to my fellow research scholars, whose constant support and encouragement have made this journey memorable.

I wish to express my deep respect and gratitude to my former teachers, especially Mr. Shajeeb and Mr. Sasi Kumar, whose early guidance and encouragement laid the foundation for my passion for learning and research.

I gratefully acknowledge the Kerala State Council for Science, Technology and Environment (KSCSTE) for their financial support, which greatly facilitated my research work.

I am forever grateful to my parents and sibling for their unwavering love, constant encouragement, and invaluable support, which have been the foundation of my strength and perseverance. I also express my sincere gratitude to my in-laws, whose kindness, blessings, and encouragement have been a continuous source of strength and motivation throughout this journey. A special mention goes to my adorable stress busters, Hyzu, Milu, Tyzu, and Toby, who filled my days with joy, comfort, and calm during the most challenging phases.

I also wish to remember with love and gratitude my grandparents, whose blessings have always guided me, and in particular my beloved grandmother, Thathi, whose memory continues to be a source of strength and inspiration.

A heartfelt thanks to my life partner, Anand, my special companion, for his unwavering love, support, and encouragement, which have been my greatest source of strength throughout this journey. Above all, I owe a special debt of gratitude to my father, whose sacrifices, guidance, and silent strength have laid the foundation for all my achievements. This work is a reflection of both his values and dreams. Finally, my sincere thanks to science for inspiring curiosity, discovery, and the pursuit of knowledge.

Abstract

The growing complexity of real-world data demands highly adaptable probability models capable of capturing diverse distributional behaviors. This thesis proposes a novel approach for constructing flexible families of probability distributions, termed the QT-transformation and its dual concept, QT_d-transformation. By combining the quantile function $Q(\cdot)$ with a continuous function $T(\cdot)$ (or T_d), the approach accommodates a variety of mathematical forms, enabling the generation of diverse distributions with different shapes and tail behaviors. Several functional forms of $T(\cdot)$, including widely used sigmoid functions (logistic, arctangent, and error sigmoid), as well as known transformations (Yun and sigmoidal), are employed. Besides these established functions, a simple arbitrary function satisfying the necessary conditions of $T(\cdot)$ is used to develop a new family of distributions. The study mainly focuses on modifications of the exponential distribution; the structural and reliability properties, as well as parameter estimation of all the submodels using the exponential as the baseline, are examined. The thesis further explores the utility of the proposed model in reliability through stress-strength reliability analysis. For single-component systems, estimation is carried out using both maximum likelihood estimation (MLE) and Bayesian estimation, accompanied by the construction of asymptotic confidence intervals, Bayesian credible intervals, and highest posterior density intervals. This analysis is then extended to s-out-of-k systems under progressive type II censoring, employing MLE, Bayesian, and uniformly minimum variance unbiased estimation techniques. In all cases, the efficacy and applicability of the proposed methods are validated through comprehensive simulation studies and real data applications. The thesis concludes by highlighting the capability of the proposed methods to generate flexible distributional forms, thereby paving the way for future research opportunities and practical implementations.

Keywords: Lifetime distributions, QT-transformation, Classical estimation, Bayesian estimation, Stress-strength reliability

പഠനസംഗ്രഹം

നിലവിലെ ലോക-ഡാറ്റയുടെ സങ്കീർണ്ണത വർദ്ധിച്ചുകൊണ്ടിരിക്കുന്ന സാഹചര്യത്തിൽ, വിവിധ വിതരണ സ്വഭാവങ്ങൾ പിടികൂടാൻ കഴിയുന്ന, അത്യന്തം അനുയോജ്യമായ പ്രൊബബിലിറ്റി മോഡലുകൾ ആവശ്യമാണ്. ഈ ആവശ്യം പരിഹരിക്കാൻ, ഈ പ്രബന്ധം പുതിയൊരു സമീപനം നിർദ്ദേശിക്കുന്നു: QT-പരിവർത്തനം എന്നതും അതിന്റെ ഡ്യുവൽ ആശയം QT_d-പരിവർത്തനം എന്നതുമാണ്. ക്വാണ്ടൈൽ ഫംഗ്ഷൻ $Q(\cdot)$ നെ ഒരു തുടർച്ചയായ ഫംഗ്ഷൻ $T(\cdot)$ (അഥവാ T_d) യുമായി സംയോജിപ്പിച്ച്, ഈ സമീപനം വിവിധ ഗണിത രൂപങ്ങൾ ഉൾക്കൊള്ളാൻ കഴിയുന്ന രീതിയിൽ രൂപകൽപ്പന ചെയ്യപ്പെട്ടിരിക്കുന്നു, ഇതിലൂടെ വ്യത്യസ്ത ആകൃതികളും ടെയിൽ ബിഹേവിയറുകളുമുള്ള വൈവിധ്യമാർന്ന വിതരണങ്ങളുടെ ഉത്പാദനത്തെ പ്രാപ്തമാക്കുന്നു. $T(\cdot)$ എന്ന ഫംഗ്ഷന്റെ നിരവധി രൂപങ്ങൾ, ഉദാഹരണത്തിന്, വ്യാപകമായി ഉപയോഗിക്കുന്ന സിഗ്മോയ്ഡ് ഫംഗ്ഷനുകൾ (ലൊജിസ്റ്റിക്, ആർക്ടാൻജന്റ്, എറർ സിഗ്മോയ്ഡ്) കൂടാതെ അറിയപ്പെടുന്ന പരിവർത്തനങ്ങൾ (യുൻ, സിഗ്മോയ്ഡൽ) എന്നിവ ഉപയോഗിച്ചിരിക്കുന്നു. ഈ സ്ഥാപിത ഫംഗ്ഷനുകൾക്ക് പുറമേ, $T(\cdot)$ ന്റെ ആവശ്യമായ നിബന്ധനകൾ പാലിക്കുന്ന ഒരു ലളിതമായ ആർബിറ്ററി ഫംഗ്ഷൻ ഉപയോഗിച്ച് പുതിയൊരു വിതരണ കുടുംബം വികസിപ്പിച്ചിരിക്കുന്നു. ഈ പഠനം പ്രധാനമായും എക്സ്പൊണൻഷ്യൽ വിതരണത്തിന്റെ ഭേദഗതികളിൽ കേന്ദ്രീകരിച്ചിരിക്കുന്നു; ഘടനാപരവും വിശ്വാസ്യതാപരവുമായ ഗുണങ്ങളും, എക്സ്പോണൻഷ്യൽ അടിസ്ഥാനമായി ഉപയോഗിക്കുന്ന എല്ലാ ഉപമോഡലുകളുടെയും പാരാമീറ്റർ എസ്റ്റിമേഷനും പരിശോധിക്കുന്നു. പ്രസ്താവിച്ച മോഡലിന്റെ റിലയബിലിറ്റി അനാലിസിസ് ലെ പ്രയോജനം, സ്ട്രെസ്-സ്ട്രെങ്ത് റിലയബിലിറ്റി വിശകലനം വഴി കൂടുതൽ ആഴത്തിൽ പരിശോധിച്ചിരിക്കുന്നു. ഒറ്റ ഘടകമുള്ള സിസ്റ്റങ്ങൾക്കായി, മാക്സിമം ലൈക്ലിഹുഡ് എസ്റ്റിമേഷൻ (MLE) ബേസിയൻ എസ്റ്റിമേഷൻ ഉപയോഗിച്ച് റിലയബിലിറ്റി എസ്റ്റിമേഷൻ നടത്തുകയും, അതോടൊപ്പം അസിംപ്റ്റോട്ടിക് കോൺഫിഡൻസ് ഇന്റർവലുകൾ, ബേസിയൻ ക്രെഡിബിൾ ഇന്റർവലുകൾ, ഹൈയസ്റ്റ് പോസ്റ്റീരിയർ ഡെൻസിറ്റി (HPD) ഇന്റർവലുകൾ എന്നിവ നിർമ്മിക്കുകയും ചെയ്തിരിക്കുന്നു. ഈ വിശകലനം, പ്രോഗ്രസീവ് ടൈപ്പ് II സെൻസറിംഗ് ഉള്ള s-ഓട്ട്-ഓഫ്-k സിസ്റ്റങ്ങളിലേക്ക് വിപുലീകരിച്ചിരിക്കുന്നു, ഇവിടെ MLE, ബേസിയൻ, യൂണിഫോം മിനിമം വേരിയൻസ് അൺബയാസ്ഡ് എസ്റ്റിമേഷൻ (UMVUE) സാങ്കേതിക വിദ്യകൾ ഉപയോഗിച്ചിരിക്കുന്നു. എല്ലാ സാഹചര്യങ്ങളിലും, സമഗ്രമായ സിമുലേഷൻ പഠനങ്ങളിലൂടെയും യഥാർത്ഥ ഡാറ്റ ആപ്ലിക്കേഷനുകളിലൂടെയും നിർദ്ദിഷ്ട രീതികളുടെ ഫലപ്രാപ്തിയും പ്രയോഗക്ഷമതയും സാധൂകരിക്കപ്പെടുന്നു. ഈ പ്രബന്ധം, നിർദ്ദേശിച്ച രീതികൾക്ക് അനുയോജ്യമായ വിതരണ രൂപങ്ങൾ സൃഷ്ടിക്കാൻ ശേഷിയുള്ളതിനെ ഉദാഹരിച്ച്, ഭാവിയിലെ ഗവേഷണ സാധ്യതകൾക്കും പ്രായോഗിക പ്രയോഗങ്ങൾക്കും വഴി തുറക്കുന്നു.

സൂചകപദങ്ങൾ: ആജീവനാന്ത വിതരണങ്ങൾ, QT-പരിവർത്തനം, പരമ്പരാഗത മൂല്യനിർണ്ണയം, ബേയ്സിയൻ മൂല്യനിർണ്ണയം, സ്ട്രെസ്-സ്ട്രെങ്ത് റിലയബിലിറ്റി

Contents

List of Figures

List of Tables

Acronyms

AB absolute bias

ACI asymptotic confidence interval

AGPT alpha gamma power transformation

AGPTE alpha gamma power transformed exponential

AIL average interval length

ASG arctangent sigmoid {Gumbel}

ASGE arctangent sigmoid {Gumbel}-exponential

BCI Bayesian credible intervals

BT bathtub

CDF cumulative distribution function

CRHF cumulative reverse hazard function

CS censoring schemes

CP coverage probabilities

DHR decreasing hazard rate

ECDF empirical cumulative distribution function

ESG error sigmoid {Gumbel}

ESGE error sigmoid {Gumbel}-exponential

GLD generalized lambda distribution

HPD highest posterior density

HR hazard rate

IHR increasing hazard rate

K-S Kolmogorov-Smirnov

LSG logistic sigmoid {Gumbel}

LSGE logistic sigmoid {Gumbel}-exponential

MCMC Markov chain Monte-Carlo

MH Metropolis-Hastings

ML maximum likelihood

MLE maximum likelihood estimation

MRL mean residual life

MSE mean square error

MWT mean waiting time

NFE new flexible exponential

PDF probability density function

$Q(u)$ quantile function

R stress-strength raliability

RHF reverse hazard function

SN skew-normal

SUE sigmoidal type-I {unit exponential}

SUEE sigmoidal type-I {unit exponential}-exponential

TTT total time on test

UBT upside down bathtub

UMVU uniformly minimum variance unbiased

UMVUE uniformly minimum variance unbiased estimation

YUG Yun {unit Gumbel}

YUGE Yun {unit Gumbel}-exponential

Chapter 1

Introduction

Life testing experiments are essential for evaluating the reliability and durability of systems, components, and products across various fields. In large-scale industries and manufacturing units, these experiments help to ensure product quality, optimize maintenance schedules, design safer systems, reduce costs, and enhance customer satisfaction. The purpose of life testing in the medical field is to determine the longevity and safety of medical implants and devices, to ensure the safety of patients, and to improve treatment outcomes.

Life testing experiments are typically represented by lifetime random variables that describe the probabilistic nature of failure times. These variables enable the development of statistical models that accurately capture failure patterns and estimate key reliability metrics.

Reliability theory is a branch of statistics that utilizes lifetime distributions to analyze system performance and the probability that components or systems will function under specified conditions for a given period of time. It has a wide range of applications across various fields, including engineering, manufacturing, healthcare, risk management, etc., ensuring the safety, efficiency, and longevity of systems. Let's explore some key areas of reliability modeling and their practical applications:

- **Failure time analysis**: Lifetime distributions model the time until a component or system experiences failure, enabling the manufacturers to forecast and assess failure patterns over time.

  Application: In automobile engineering, lifetime distributions are used to predict the failure time of critical components such as brake pads or engine parts. By analyzing the failure times of these components under normal operating conditions, manufacturers can determine their expected lifespan and thereby design parts that are more durable and efficient.

- **Stress-strength model:** These models determine whether a system is likely to withstand applied stresses, which is essential for ensuring reliable performance under various conditions.

  Application: In aerospace, the stress-strength reliability of key components like aircraft engines is modeled using lifetime distributions. For instance, the lifetime model helps to ensure whether the engine parts can withstand the extreme thermal and mechanical stresses encountered during flight.

- **Predictive maintenance and warranty analysis:** Lifetime distributions are used in predictive maintenance to estimate the probability of product failure over time, helping to schedule maintenance and set warranty periods, thereby reducing unexpected downtime and optimizing service costs.

  Application: In the energy sector, the failure behavior of turbine blades in wind power plants is modeled using lifetime distributions. Thus, the operator can plan predictive maintenance tasks, minimize unscheduled downtime, and maximize uptime.

- **Accelerated life testing:** In this technique, product reliability is evaluated by exposing them to extreme or accelerated conditions like high temperature, high voltage, etc., to induce failures faster, allowing researchers to predict lifespan under normal conditions.

  Application: In electronic manufacturing units, components like microprocessors or batteries may not fail within a short testing period under normal conditions. Accelerated testing, combined with appropriate lifetime distributions, enables manufacturers to predict long-term performance and reliability.

- **Degradation model:** These models describe how a system's performance gradually deteriorates over time due to various factors like wear and tear, exposure to environmental conditions, or internal chemical reactions. Based on the observed degradation trends, the remaining useful life can be predicted.

  Application: The capacity of a battery might be tracked over time using a degradation model, which considers factors such as charging cycles and temperature in order to predict the point at which the battery will no longer be able to hold a charge.

- **Shock and damage model:** These models analyze the failure mechanism of a system subjected to the cumulative damage from sudden disruptive events called shocks that occur over time. Each shock contributes a certain amount of damage, and eventually the system fails when the cumulative damage exceeds the critical threshold.

  Application: Continuous use of biomedical devices, like pacemakers, combined with occasional extreme physiological events, leads to gradual wear and tear. The shock-damage model can be used to predict the failure and guide replacement schedules.

Thus, the lifetime distributions serve as a foundation for many reliability models, allowing researchers and engineers to make precise decisions about system design, optimize maintenance strategies, and effectively manage risk. As technology develops, the systems are becoming more complex and operating under diverse and dynamic conditions, making it challenging to capture intricate failure mechanisms using traditional lifetime models. This growing complexity necessitates the development of more flexible and adaptive lifetime models to ensure the reliability of modern systems across various fields.

This study contributes to developing flexible lifetime models by introducing a method to generate families of distributions. The proposed models are then applied to a critical aspect of reliability analysis, the stress-strength reliability. The analysis covers both single component systems and the more complex s-out-of-k systems, with extensions to practical scenarios involving complete and censored samples. This comprehensive approach highlights the practical relevance and adaptability of the proposed models in capturing real-world reliability behaviors.

1.1 Lifetime random variable

In life testing experiments, it is known that the exact failure times are typically unknown and impossible to predict with certainty. This uncertainty in failure times arises because they follow specific probability distributions, which describe the likelihood of failure occurring at any given time. These distributions model the random nature of failure times, considering factors such as environmental conditions, material properties, and external stresses that impact the failure process. Given this uncertainty, the concept of a lifetime random variable becomes fundamental in reliability analysis and survival studies. The lifetime random variable X is defined as a non-negative random variable that measures the time until a specific event occurs. The value of X depends on the nature of the events and can be continuous or discrete, depending on how the failure time is measured in the context.

- **Continuous lifetime variables:** In systems where time can be measured in infinitely small units, for example, hours, minutes, seconds, etc.
- **Discrete lifetime variables:** For systems where time is measured in discrete intervals, for example, days, months, etc.

In this study, we focus on the continuous lifetime random variables. One of the classic lifetime models is the exponential distribution. Let's discuss it in the next section.

1.1.1 Exponential distribution

The exponential distribution is a widely used continuous lifetime distribution, valued for its simplicity, versatility, and unique properties. The cumulative distribution function (CDF) and probability density function (PDF) of exponential distribution is given as

$$\begin{aligned} F(x,\lambda) &= 1-e^{-\lambda x}, \quad x>0,\ \lambda>0, \\ f(x,\lambda) &= \lambda e^{-\lambda x}, \quad x>0,\ \lambda>0, \end{aligned}$$

where λ is the scale parameter. The corresponding mean and variance are $1/\lambda$ and $1/\lambda^2$, respectively. A key characteristic of this distribution is the memoryless property, which implies the failure time is independent of the elapsed time. Mathematically, we can express it as $P(X > t+s|X > t) = P(X > s)$, $t, s > 0$. This property makes the exponential distribution suitable for modeling systems with a constant failure rate. Also note that this is the only continuous distribution having a constant hazard rate.

The exponential distribution has a wide range of applications, not only in reliability analysis but also in queuing theory and survival analysis. In queuing theory, it is commonly used to model inter-arrival times between events, whereas in survival analysis, it is used to analyze time-to-event data, such as patient survival data in the medical field. Despite its broad applicability, it has certain limitations. Modeling with a constant failure rate may not always be realistic in many practical situations, highlighting the need to develop more flexible models.

1.2 Background and motivation of the study

As we have seen the significance of the exponential distribution in modeling lifetime data, it also has certain limitations, particularly when dealing with data that exhibit non-constant failure rates, which are commonly observed in real-world applications. For example, mechanical components may undergo wear-out failures with increasing failure rates, while electronic systems might exhibit early-life failures with decreasing failure rates. These limitations led to the development of more flexible distributions, such as the Weibull distribution proposed by Weibull (1951). The Weibull distribution is a simple extension of the exponential distribution, constructed by incorporating a shape parameter, which enables it to exhibit increasing, decreasing, and constant failure rates.

But many real-world applications exhibit more complex failure patterns, such as bathtub-shaped (characterized by an initial decreasing failure rate, followed by a constant failure rate, and then an increasing failure rate) or upside-down bathtub-shaped (characterized by an initial increasing failure rate, followed by a constant failure rate, and then a decreasing failure rate) hazard functions. Moreover, the real-world data often exhibits heavy tails, skewness, and other intricate behaviors that the traditional distributions struggle to model. These scenarios necessitate more advanced models, which led to the development of distributions such as the log-normal, gamma, generalized exponential distributions, etc. Each of these distributions has distinct features designed to meet specific modeling requirements.

Considerable efforts have been made by researchers to introduce new flexible distributions with desirable properties. Over time, the focus shifted towards enhancing the techniques used to construct these adaptable distributions. This progression led to the creation of families of distributions, allowing for more general models that extend and improve the features of the baseline models.

Vicari and Kotz (2005) gave a detailed survey of the key milestones in the early development of statistical distributions. Further, Lee et al. (2013) classified the primary techniques developed before and after 1980, offering a comprehensive overview. The approaches proposed prior to 1980 can be broadly classified into three categories: methods based on differential equations, transformation techniques, and quantile functions. Since 1980, the focus on generating new distributions has shifted towards adding parameters to existing distributions or combining multiple distributions. These methods are often referred to as methods of combinations. Even though the method offers great flexibility, the complexity of the model leads to challenges in parameter estimation, computational efficiency, and model interpretability. Thus, the balance between flexibility and tractability is a key consideration in the development of new distributions.

Most methodologies for generating new distributions are based on extending or combining existing distributions rather than incorporating other useful mathematical functions that could enhance their flexibility and applicability. This limitation motivated us to introduce a non-traditional method that facilitates the construction of new classes of distributions with specific characteristics derived from well-known mathematical functions. This study aims to develop a novel approach that incorporates useful mathematical functions for generating families of distributions. Numerous mathematical functions, each with unique properties, are well documented in the literature. The primary objective is to extract these properties to create classes of distributions that exhibit the desired characteristics. In particular, we focus on developing lifetime models using the exponential distribution as the baseline. Furthermore, we apply these models to stress-strength reliability analysis, a critical aspect of system performance evaluation.

1.3 Objectives of the study

The main objectives of the study are as follows:

1. To review existing methodologies for constructing families of distributions.
2. To propose a method for generating families of distributions.
3. To develop new lifetime models using the exponential distribution as a baseline within the proposed framework.
4. To study the statistical and reliability properties of the newly constructed

models.

5. To estimate the parameters of the proposed models.

6. To validate the applicability of the proposed models using real-world data.

7. To evaluate stress-strength reliability using the proposed model under both complete and censored samples.

8. To perform inference on stress-strength reliability using both classical and Bayesian approaches.

9. To evaluate the real-world applicability of stress-strength reliability estimation.

A detailed literature survey on advancements in probability distributions will be discussed in the next section.

1.4 Literature review on statistical distributions

As discussed in the introduction, the approaches for generating statistical distributions developed before 1980 can be broadly categorized into three methods: methods based on differential equations, methods based on transformations, and methods based on quantile functions. A significant contribution using the differential equation approach was presented by Pearson (1895). In this work, Pearson (1895) developed a system of continuous distributions where each probability density function (PDF) satisfies the following differential equation:

$$\frac{1}{f(x)}\frac{df(x)}{dx} = \frac{a+x}{b_0 + b_1 x + b_2 x^2},$$

where a, b_0, b_1 and b_2 are the parameters. Burr (1942) introduced a system of continuous distribution which satisfies the following differential equation:

$$\frac{dF(x)}{dx} = F(x)(1-F(x))g(x),$$

where $0 \leq F(x) \leq 1$ and $g(x)$ is a non-negative function of x. A system of discrete distributions is developed by Ord (1967) using a difference equation analogous to Pearson's differential equation. Dunning and Hanson (1977) proposed a generalized form of Pearson differential equation given as

$$\frac{df(x)}{dx} = \frac{(a_0 + a_1 x + a_2 x^2 + \cdots + a_m x^m) f(x)}{b_0 + b_1 x + b_2 x^2 + \cdots + b_n x^n},$$

where $m,\ n > 0$.

The foundational work on transformation also known as translation was introduced by Johnson (1949), who developed a system for generating distributions using normalization transformations having the general form

$$Z = \gamma + \delta f\left(\frac{X - \xi}{\lambda}\right),$$

where $f(\cdot)$ represents the transformation function, Z is a standardized normal random variable, γ and δ are the shape parameters, λ is the scale parameter and ξ is the location parameter. The Johnson system includes three types:

- The log-normal system (S_L):

$$Z = \gamma + \delta \log(X - \xi), \quad X \geq \xi.$$

- The system of bounded distributions (S_B):

$$Z = \gamma + \delta \log\left(\frac{X - \xi}{\xi + \lambda - X}\right), \quad \xi \leq X \leq \xi + \lambda.$$

- The system of unbounded distributions (S_U):

$$Z = \gamma + \delta \log\left\{\left(\frac{X - \xi}{\lambda}\right) + \left(\left(\frac{X - \xi}{\lambda}\right)^2 + 1\right)^{1/2}\right\}, \quad -\infty < X < \infty.$$

These system of distributions has the ability to include commonly used models like normal, log-normal, beta, gamma, exponential, and other distributions, along with its flexible parameters, making it a useful and versatile tool for statistical modeling and data analysis. Another study based on transformation is Tukey (1977), which introduced the $g-h$ family of distributions by transforming the standard normal variable Z using the following transformation:

$$T_{g,h}(Z) = \frac{(\exp(gZ) - 1)\exp(hZ^2/2)}{g}, \quad g \in \mathbb{R},\ h > 0.$$

Later, a generalization of $g-h$ family of distributions was provided by Jiménez et al. (2015) by considering a continuous normalized (*i.e.*, with mean 0 and variance 1) random variable instead of the standard normal variable.

Hastings Jr et al. (1947) introduced a class of distributions based on the quantile function, which does not have a closed form expression for its distribution function. This marked a significant advancement in the use of quantile functions for representing probability distributions. Later, the class of distributions proposed by Hastings Jr et al. (1947) was refined by Tukey (1960), leading to the development of the Tukey's lambda distribution, with the percentile function given by

$$Q(p) = \frac{p^{\lambda} - (1-p)^{\lambda}}{\lambda}, \quad \lambda \neq 0.$$

Tukey's lambda distribution was later generalized by Ramberg and Schmeiser (1972, 1974) and Ramberg et al. (1979) resulting in the generalized lambda distribution (GLD). This family of distributions is defined in terms of its percentile function, given by

$$Q(p) = \lambda_1 + \frac{p^{\lambda_3} - (1-p)^{\lambda_4}}{\lambda_2}, \quad 0 \leq p \leq 1,$$

where λ_1 and λ_2 are the location and scale parameters and λ_3 and λ_4 determine the skewness and kurtosis of the distribution, respectively. Later, a more general form of the GLD, known as the extended generalized lambda distribution, was introduced by Karian et al. (1996).

The methodologies for generating new distributions after 1980 have shifted towards adding parameters to existing distributions or combining multiple distributions. Therefore, we categorize the methods developed after 1980 as "methods of combination." Notable developments using these methods of combination are summarized below:

Azzalini (1985) proposed the class of skew-normal (SN) distribution by combining two symmetric distribution, defined as follows: Let X and Y are two independent random variable which are symmetric about 0. Then for any $\lambda \in \mathbb{R}$

$$P(X - \lambda Y < 0) = \int_{-\infty}^{\infty} f_Y(y) F_X(\lambda y) dy = \frac{1}{2},$$

where $f_Y(\cdot)$ is the PDF of Y and $F_X(\cdot)$ is the CDF of X. Thus

$$f(x; \lambda) = 2 f_Y(x) F_X(x), \tag{1.1}$$

is a valid CDF. If X and Y follows standard normal distribution, then

$$f(x; \lambda) = 2\phi(x)\Phi(x),$$

where $\phi(x)$ and $\Phi(x)$ are PDF and CDF of standard normal variable respectively. This represents the PDF of the skew-normal family of distributions. Many specific skewed distribution have been derived from the general framework of (1.1) by using different choices of $f_Y(\cdot)$ and $F_X(\cdot)$. For example, Nadarajah and Kotz (2006c) derived the skew-uniform, skew-t, skew-Cauchy, skew-Laplace, and skew-logistic distributions and studied their properties. Moreover Additionally, various extensions of the SN distribution have been developed, with some extensions based on the normal distribution and others based on different symmetric distributions. Pewsey (2000) proposed the wrapped SN distribution for modeling circular data. Arellano-Valle et al. (2004) introduced an extension of the skew-normal distribution, referred to as the skew-generalized normal distribution. Azzalini and Valle (1996) presented a multivariate parametric family where the marginal densities are scalar skew-normal and studied its properties, with special emphasis on the bivariate case. Another generalization of Azzalini (1985) framework is the approach based on a weighted function proposed by Chang and Genton (2007), which includes Azzalini (1985) model as a special case. This approach is defined as follows: Let X be a symmetric random variable with PDF $f(x;\Theta)$, where Θ represents a vector of unknown parameters. In practical scenarios, there are instance where obtaining a random sample directly from $f(\cdot)$ may be challenging or expensive. If the PDF $f(x,\Theta)$ is modified by some multiplicative non negative weighting function $w(x,\eta)$, where η denotes an additional vector of unknown parameters, then the observed data will follow a distribution with the modified PDF,

$$g(x,\Theta,\eta) = f(x,\Theta)\frac{w(x,\Theta,\eta)}{E(w(x,\Theta,\eta))}, \tag{1.2}$$

where $g(\cdot)$ is said to be the PDF of a weighted distribution.

Another prominent approach for generating new families of distribution is the method of adding parameters. Early developments in this method include the exponentiated approach, which is described generally as follows: if X is a random variable with CDF $F(x)$, then the exponentiated version of X has a CDF of the form

$$F_E(x) = (F(x))^a, \tag{1.3}$$

where $a > 0$ is an additional parameter. Such a family of distributions generated from a baseline distributions by raising to a positive power is also known as Lehman family of distributions. The pioneering work on this method was presented by Mudholkar et al. (1995), who introduced the exponentiated Weibull distribution. Gupta et al. (1998) gave a systematic treatment of (1.3). Gupta and Kundu (1999) and Gupta and Kundu (2001) introduced the exponentiated exponential distribution as a generalization of the standard exponential distribution. Nadarajah and Kotz (2006b) conducted an extensive study of various exponentiated X distributions including the exponentiated exponential, gamma, Weibull, Gumbel, and Fréchet distributions. Gupta and Kundu (2007) provided a comprehensive review of the developments related to generalized exponential distributions. Additionally, Nadarajah et al. (2013) presented a detailed survey on the properties and applications of exponentiated Weibull distributions. In addition to the exponentiated approach, several alternative methods have been proposed to generate flexible families of distributions by utilizing various functions of $F(x)$. For instance, Gera (1997) defined a family of distributions with the following CDF

$$F_E(x) = e^{-\lambda x^{\gamma}} F(x), \quad \lambda,\ \gamma > 0.$$

Also, Gera (1997) introduced the modified exponentiated Weibull distribution by using the exponentiated Weibull distribution as the baseline. Marshall and Olkin (1997) proposed a novel approach for introducing an additional parameter to any existing distribution. The survival function of the Marshall-Olkin family of distributions, based on a baseline $F(x)$, is defined as:

$$\bar{G}(x) = \frac{\alpha \bar{F}(x)}{1 - (1-\alpha)\bar{F}(x)}, \quad \alpha > 0.$$

Additionally, Marshall and Olkin (1997) provided a detailed examination of cases when $F(x)$ is exponential and Weibull.

Eugene et al. (2002) introduced a new family of distributions using the beta distribution as a generator, known as the beta-generated family of distributions. The CDF of the beta-generated family is defined as

$$G(x) = \int_0^{F(x)} b(t)\, dt, \tag{1.4}$$

where $b(t)$ is the PDF of beta random variable and $F(x)$ is the CDF of any random variable. This family of distribution can also be viewed as a generalization of the distributions of order statistics for the random variable X with CDF $F(x)$. In the literature, several beta-generated distributions have been developed by applying different baseline distributions in (1.4). For instance, Nadarajah and Gupta (2004) generated a Beta-Fréchet, Nadarajah and Kotz (2004) generated a

Beta-Gumbel, Nadarajah and Kotz (2006a) generated a Beta-Exponential distributions, Akinsete et al. (2008)generated a Beta-Pareto distribution, Silva et al. (2010) generated a Beta-Modified Weibull distribution and Alshawarbeh et al. (2012) generated a Beta-Cauchy distribution.

Cordeiro and De Castro (2011) introduced a family of distributions called the Kumaraswamy-generalized distribution (Kw-G), which extends the beta-generated family by replacing the beta distribution with the Kumaraswamy distribution in (1.4). For an arbitrary parent distribution $F(x)$, the CDF of kw-G is defined as

$$G(x) = 1 - (1 - F(x)^a)^b, a > 0,\ b > 0,$$

where a and b are two additional parameter introduced to control skewness and tail behavior. Later, Cordeiro et al. (2013) propose a new class of distributions that extend the exponentiated type distributions known as exponentiated generalized class of distributions, whose CDF is defined as

$$G(x) = \left(1 - (1 - F(x))^a\right)^b, a > 0\ b > 0,$$

where a and b are two additional shape parameters. Alzaatreh et al. (2013) proposed a more general version of the beta-generated family, referred to as the $T - X$ family of distributions, which allows any continuous PDF to be used as the generator and is defined as: Suppose T is a continuous random variable with PDF, $r(t)$ defined on $[a, b]$ and X be a random variable with CDF $F(x)$. Then the CDF of $T - X$ family is defined as

$$G(x) = \int_a^{W(F(x))} r(t)\ dt,$$

where $W(F(x))$ satisfies the following conditions:

- $W(F(x)) \in [a, b]$.
- $W(F(x))$ is differentiable and monotonically no,n-decreasing.
- $W(F(x)) \to a$ as $x \to -\infty$ and $W(F(x)) \to b$ as $x \to \infty$.

For different choices of $W(\cdot)$, and various combinations of distribution functions for T and X, researchers have developed different families of $T-X$ distributions. Additionally, Alzaatreh et al. (2012) generated a discrete $T-X$ family of distributions by considering the distribution of X as a geometric distribution.

Since these approaches introduce additional parameters, they can sometimes make the model more complex. To address this issue, Kumar et al. (2015a) proposed a new transformation known as the DUS transformation. For the baseline distribution $F(x)$, the CDF of DUS transformation is defined as

$$G(x) = \frac{e^{F(x)} - 1}{e - 1}.$$

DUS transformations are widely used to create more flexible statistical models based on different baseline distributions. For instance, Maurya et al. (2017b) proposed a distribution called exponential transformed Lindley by using the Lindley distribution as the baseline in the DUS transformation. Similarly, Karakaya et al. (2021) introduced the DUS-Kumaraswamy distribution by applying the Kumaraswamy distribution as the baseline. Later, Maurya et al. (2017a) applied the DUS transformation to the exponentiated CDF to propose the generalized DUS transformation. Additionally, Kumar et al. (2015b) introduced another parsimonious model using the sine function, referred to as the SS transformation. A similar parsimonious transformation is the Kavya-Manoharan (KM) transformation, proposed by Kavya and Manoharan (2021), and its CDF is defined as

$$G(x) = \frac{e}{e-1}\left(1 - e^{-F(x)}\right),$$

where $F(x)$ is the baseline distribution.

Mahdavi and Kundu (2017a) introduced a new method for generating lifetime distributions, known as the alpha power transformation (APT) method. For any continuous baseline distribution $F(x)$, the CDF of APT is defined as

$$G(x) = \begin{cases} \frac{\alpha^{F(x)}-1}{\alpha-1}, & \text{if } \alpha > 0,\ \alpha \neq 0, \\ F(x), & \text{if } \alpha = 1. \end{cases}$$

Further, Mahdavi and Kundu (2017a) introduced the alpha-power exponential distribution by using the exponential distribution as the baseline. Following this, numerous lifetime models have been developed by various authors using the APT method. For instance, Nassar et al. (2017), Ramadan and Magdy (2018), Dey et al. (2019), Malik and Ahmad (2019), Ahmed (2020), and Eghwerido et al. (2021) introduced the AP-Weibull, AP-Inverse Weibull, AP-Lindley, AP-Inverse Rayleigh, AP-Kumaraswamy, and AP-Gompertz distributions, respectively.

In the past few years, further modifications have been made to the APT method to generate more flexible lifetime models. By inverting the CDF of APT, Nassar et al. (2018) proposed a new class of distributions whose CDF is defined as

$$G(x) = \frac{\log(1+(\alpha-1)F(x))}{\log \alpha}, \quad \alpha > 0.$$

Elbatal et al. (2018) introduced the new alpha power transformation (NAPT) and its CDF is given by

$$G(x) = \frac{F(x)\ \alpha^{F(x)}}{F(x)}, \quad \alpha > 0.$$

Ahmad et al. (2019) proposed a new family of lifetime distribution namely, extended alpha power transformation (Ex-APT) and it's CDF is defined as

$$G(x) = \frac{\alpha^{F(x)} - e^{F(x)}}{\alpha - e}, \quad \alpha > 0.$$

Hussein et al. (2022) introduced the modified alpha power class of distribution by adding two parameter to the baseline distribution and it's CDF is given as

$$G(x) = \frac{\beta^{F^2(x)}\alpha^{F(x)} - 1}{\alpha\beta - 1}, \quad \alpha, \beta \geq 1,\ \alpha\beta \neq 1.$$

In spite of these advances, further refinements and novel methodologies re-main necessary to address emerging challenges in the field of statistical modeling. This study presents a novel approach to constructing families of distributions by incorporating well-established mathematical functions, thereby improving their flexibility and relevance in reliability analysis. In the following chapters, we will explore these developments in detail, highlighting their statistical significance, reliability properties and applications to stress-strength reliability along with their practical implications in real world scenarios.

1.5 Significance of the study

The study introduces a comprehensive framework for constructing families of distributions that enables the development of models with desired characteristics derived from widely used mathematical functions. A key significance of the proposed approach is its ability to extend classical distributions to accommodate more complex real-world phenomena by incorporating diverse tail behaviors and structural properties. In particular, the study presents various generalized versions of the exponential distribution, which belong to several important classes of distributions, including class $\mathcal{L}$, class $\mathcal{L}(\gamma)$, class $\mathcal{D}$ of dominated-variation, and sub-exponential classes. In addition, these models exhibit tail properties such as regularly varying, heavy-tailed, and long-tailed behavior, making them useful for modeling extreme events and rare occurrences.

Thus, the constructed models serve as effective statistical tools for researchers and practitioners to analyze complex structures, allowing for more accurate modeling in prediction, risk assessment, and decision making across fields such as finance, insurance, and stock market analysis. Additionally, the models have significant applications in reliability analysis, including stress-strength reliability estimation, accelerated life testing models, degradation models, and survival analysis.

Overall, this research contributes significantly to statistical distribution theory by connecting theoretical innovations with real-world applications. In particular, it paves the way for future research on the further investigation of transformation-based families of distributions and their practical significance.

1.6 Overview of the thesis

The thesis mainly focuses on developing a new approach for generating families of distributions. The proposed method, termed the QT-transformation and QT_d-transformation, is based on the combination of a quantile function $Q(\cdot)$ and a continuous function $T(\cdot)$. By selecting an appropriate function for $T(\cdot)$, a new class of distributions can be developed with enhanced flexibility and applicability. In this study, we explore three distinct choices for $T(\cdot)$: a well-known mathematical function, a widely used transformation, and an arbitrarily chosen function. Based on these choices, we construct distinct families of distribution. In this study, we focused on constructing new flexible models by choosing the exponential distribution as the baseline. We systematically analyze their statistical properties and explore their applications in reliability theory.

The thesis is organized into nine chapters, each addressing different aspects of the study, from theoretical foundations to practical applications. The introductory chapter provides the background, motivation, and objectives of the research. It also presents a comprehensive review of existing methodologies for constructing statistical models, emphasizing their strengths, limitations, and the need for the proposed approach.

In Chapter 2, we present the fundamental terminology and key concepts relevant to this study. It includes key properties of distribution functions, important estimation techniques, and model selection criteria.

Chapter 3 deals with the construction and theoretical foundation of the proposed methods, QT-transformation and its dual concept QT_d-transformation. It explores the underlying theoretical concepts, including fundamental rules of the quantile function, which are essential for the development of the proposed methodology.

As mentioned earlier, we consider the function $T(\cdot)$ as the widely used mathematical function, the sigmoid function, and present its applications in Chapter 4. Furthermore, we examine the statistical properties of the resulting models, discuss parameter estimation methods, and validate them through simulation study and real data analysis.

In Chapter 5, two types of well-known transformations are considered as the function $T(\cdot)$. Similar to the previous chapter, we explore their statistical properties and parameter estimation methods and assess the applicability of the models through simulation study and real data analysis.

In addition to the well-known functions, we consider an arbitrary function for $T(\cdot)$ that satisfies all the necessary conditions and study the statistical properties of the resulting models and evaluate their applicability through simulation study and real data analysis. These are discussed in Chapter 6.

Chapter 7 focuses on the inference of stress-strength reliability based on the models proposed in the previous chapters. A simulation study is conducted using the exponential distribution as the baseline, and the models are validated through real data analysis.

Chapter 8 presents the estimation of stress-strength reliability, where the stress and strength variables follow a special submodel of the proposed model under a progressively censored sample. This chapter also includes a comprehensive simulation study, followed by real data analysis, to evaluate the effectiveness and practical applicability of the model.

Finally, we incorporate the conclusion of the study along with recommendations for future research in Chapter 9.

Chapter 2

Some Basic Preliminaries

2.1 Introduction

In the field of statistics, a deeper understanding of probability distribution is essential for accurately interpreting data, modeling uncertain processes, and making informed predictions. The characteristics of these distributions, such as their central tendency, variability, and tail behavior, along with other statistical properties, offer valuable insights into the underlying processes that drive the data.

The purpose of this chapter is to lay a solid foundation for understanding distribution functions by covering fundamental preliminaries. We begin with an overview of the key characteristics and properties of distributions, followed by a discussion of the estimation techniques employed in this study to determine distribution parameters. Additionally, the chapter examines the model selection criteria used to identify the most suitable statistical model and support the decision-making process.

This chapter is organized as follows: Section 2.2 introduces some key properties of distribution functions that are fundamental to understanding model behavior. It covers concepts such as the quantile function, moments, order statistics, entropy, stochastic ordering, and tail behavior, including an overview of several significant classes of distributions. An overview of important estimation techniques essential for parameter inference is given in Section 2.3. Section 2.4 outlines widely used model selection criteria for evaluating model adequacy. Finally, Section 2.6 concludes the chapter with a brief summary of the concepts discussed.

2.2 Properties of distribution function

This section explores fundamental properties that describe the shape, dispersion, ordering, reliability, and tail characteristics of distributions.

2.2.1 Quantile function

The p^{th} quantile function of a random variable X with CDF is defined as

$$Q(p) = F^{-1}(p) = inf\{x \in \mathcal{R} : F(x) \geq p\}, \quad 0 < p < 1.$$

Using the quantile function, we can define the three quartiles, which divide the data into four equal parts:

- **First quartile (Q_1)**: It is also known as the lower quartile, given as $Q_1 = Q(0.25)$. This represents the value below which 25% of the data falls.
- **Second quartile (Q_2)**: It is also called the median, given as $Q_2 = Q(0.5)$. This divides the dataset into two equal halves.
- **Third quartile (Q_3)**: It is also referred to as the upper quartile, given as $Q_3 = Q(0.75)$. This represents the value below which 75% of the data falls.

To characterize the shape of a distribution, we use two key measures, skewness and kurtosis, where skewness measures the symmetry of the distribution, and kurtosis assesses the heaviness of its tails. Various methods exist in the literature for evaluating skewness and kurtosis. One such approach, based on the quantile function, includes Galton's skewness (S), introduced by Galton (1883) and Moor's kurtosis (K), proposed by Moors (1988). These measures are defined as follows:

$$\begin{aligned} S &= \frac{Q(6/8) - 2Q(4/8) + Q(2/8)}{Q(6/8) - Q(2/8)}, \\ K &= \frac{Q(7/8) - Q(5/8) + Q(3/8) - Q(1/8)}{Q(6/8) - Q(2/8)}. \end{aligned}$$

2.2.2 Moments

Moments provides valuable insight about the shape, central tendency, variability, skewness, and kurtosis of a distribution. The n^{th} moment about the origin (raw moments) of a random variable X with PDF, $f(x)$, is defined as

$$\mu_n = E(X^n) = \int_{-\infty}^{\infty} x^n f(x)\, dx.$$

Similarly, moments about mean (central moments) are defined as

$$\mu_n^{'} = E\left[(X - E(X))^n\right] = \int_{-\infty}^{\infty} (x-\mu)^n f(x)\, dx,$$

where $\mu = E(X)$ is the expected value of X. Additionally, the incomplete moments, which capture partial contributions up to a point x, are defined as

$$\mu_n(x) = \int_{-\infty}^{x} x^n f(x)\, dx.$$

The moment generating function (MGF) is a powerful tool for generating moments, and it uniquely characterizes probability distribution. It is defined as

$$M_X(t) = E(e^{tX}) = \int_{-\infty}^{\infty} e^{tX} f(x)\, dx.$$

The n^{th} moments of X can also be obtained by differentiating the MGF n times and evaluating it at $t = 0$, *i.e.*,

$$\mu_n = \left.\frac{d^n M_X(t)}{dt^n}\right|_{t=0}.$$

2.2.3 Reliability Measures

Reliability measures are important in survival analysis and reliability engineering for assessing the performance, longevity, and failure patterns of systems, components, or individuals over time. Below are some key reliability measures:

2.2.3.1 Survival function:

Let T be a non-negative random variable with CDF, $F(\cdot)$. Then the survival function is defined as

$$S(t) = P(T > t) = 1 - F(t); \quad t > 0.$$

It represents the probability that a system, component, or individual survives beyond a given time t, without failure.

2.2.3.2 Hazard rate:

The hazard rate (HR), also known as the failure rate function, is the instantaneous rate at which failures occur at time t, given that the system has survived up to that point. *i.e.*,

$$h(t) = \lim_{\Delta t \to 0} \frac{P(t < T \leq t + \Delta t | T > t)}{\Delta t}.$$

Using the PDF and the survival function, the HR can also be written as

$$h(t) = \frac{f(t)}{S(t)} = \frac{f(t)}{1 - F(t)}.$$

Based on its behavior over time $h(t)$, the hazard rate can be classified into increasing hazard rate (IHR), decreasing hazard rate (DHR), bathtub (BT), upside down bathtub (UBT), and constant hazard rate. A distribution is said to be IHR if $h(t)$ is non-decreasing and DHR pattern when $h(t)$ is non-increasing. A BT shaped hazard rate initially exhibits a decreasing pattern, followed by a constant phase, and then an increasing curve. In contrast, an UBT hazard rate starts with an increasing curve, transitions to a constant phase, and then decreases over time. Finally, a constant hazard rate remains unchanged over time, which is a key characteristic of the exponential distribution.

2.2.3.3 Mean residual life:

The mean residual life (MRL), $\mu(\cdot)$, represents the expected remaining lifetime of a system or component, given that it has already survived up to a certain time t. It is defined as

$$\mu(t) = E(T - t | T > t) = \frac{1}{S(t)} \int_t^\infty S(x)\, dx.$$

For more details one may refer to Hollander and Proschan (1975), Bryson and Siddiqui (1969), Muth (1977).

2.2.3.4 Mean waiting time:

The mean waiting time (MWT), $\bar{\mu}(\cdot)$, is the dual concept of MRL and represents the expected past lifetime of a system or component, given that it fails before a stipulated time t. It is defined as

$$\bar{\mu}(t) = E(t - T | T \leq t) = \frac{1}{F(t)} \int_0^t F(x)\, dx = t - \frac{1}{F(t)} \int_0^t x f(x)\, dx.$$

For more details one may refer to Ruiz and Navarro (1996), Chandra and Roy (2001).

2.2.3.5 Aging intensity function:

Another measure of aging is the aging intensity (AI) function, $L(t)$, proposed by Jiang et al. (2003), defined by

$$L(t) = \frac{-tf(xt)}{\bar{F}(t)\log\bar{F}(t)}. \tag{2.1}$$

It quantifies the rate at which a system deteriorates over time. Specifically, if the hazard rate remains constant, then $L(t) = 1$; if the hazard rate is increasing, $L(t) > 1$, indicating an aging system; and if the hazard rate is decreasing, $L(t) < 1$, suggesting an improving system. Moreover, the magnitude of $L(t)$ reflects the strength of the aging or anti-aging tendency.

2.2.4 Order statistics

Let $X_1, X_2, \ldots, X_n$ be a random sample of size n from any continuous distribution with CDF, $F(x)$ and PDF, $f(x)$. By sorting the sample in increasing order, the ordered statistics are obtained as

$$X_{(1)} \leq X_{(2)} \leq \cdots \leq X_{(n)}.$$

Then the CDF of the k^{th} order statistics is defined as

$$F_{X_{(k)}}(x) = \sum_{i=k}^{n} \binom{n}{k} F^i(x)\left(1 - F(x)\right)^{n-i},$$

and the corresponding PDF is given as

$$f_{X_{(k)}}(x) = \frac{1}{B(k, n-k-1)} F^{k-1}(x)\left(1 - F(x)\right)^{n-i}.$$

2.2.5 Entropy

Entropy, also known as the"measure of uncertainty" is a fundamental concept in probability theory and information science that quantifies the uncertainty or randomness in a probability distribution. One of the most widely used measures of entropy is Shannon entropy, introduced by Shannon (1948) and defined as

$$H = -\int_0^\infty f(x) \log f(x)\ dx.$$

Another significant entropy measure is the Rényi entropy, which is a generalization of Shannon entropy defined as

$$H_\delta = \frac{1}{1-\delta} \log \int_{-\infty}^{\infty} (f(x))^\delta\ dx, \quad \delta > 0.$$

Rényi entropy has numerous applications across various fields. Liu et al. (2011) utilized it for density estimation, while applied it to estimate the number of components in a multi-component non-stationary signal. Another widely used entropy measure is the q-entropy, defined as

$$H_q = \frac{1}{1-q} \left(1 - \int_{-\infty}^{\infty} (f(x))^q\ dx \right), \quad q \in \mathbb{R}.$$

2.2.6 Stochastic ordering

Stochastic ordering is a fundamental concept in probability theory used to compare random variables or probability distributions. It is especially useful in reliability theory, risk analysis, and decision theory for comparing lifetimes, risks, and system performance. Let X and Y be two continuous random variables, with CDF, $F_X(x)$ and $F_Y(x)$, and survival functions $S_X(x)$ and $S_Y(x)$, respectively. Let $f_X(x)$ and $f_Y(x)$ be the corresponding density functions. Then, the following types of stochastic orderings can be defined:

(i) X is smaller than Y in stochastic order, denoted as $X \leq_{st} Y$ if and only if $S_X(x) \leq S_Y(x)$ for all x.

(iii) X is smaller than Y in likelihood ratio order, denoted as $X \leq_{lr} Y$ if and only if $\frac{f_Y(x)}{f_X(x)}$ is increasing in x.

(ii) X is smaller than Y in hazard rate order, denoted as $X \leq_{hr} Y$ if and only if $\frac{\bar{F}_Y(x)}{\bar{F}_X(x)}$ is increasing in x.

(iv) X is smaller than Y in reversed hazard rate order, denoted as $X \leq_{rhr} Y$ if and only if $\frac{F_Y(x)}{F_X(x)}$ is increasing in x.

For more details one may refer to Shaked and Shanthikumar (2007).

2.2.7 Tail behavior and important distribution classes

The tail behavior of a distribution refers to how its probability density function behaves as the random variable assumes extreme values. This section discusses key tail properties of a distribution.

➢ **Heavy tailed distribution:** A heavy-tailed distribution is a distribution whose tail decays slower than that of an exponential distribution. Mathematically, a distribution function with survival function $S(x)$ is said to be heavy-tailed if and only if

$$\lim_{x\to\infty} e^{\lambda x} S(x) = \infty, \quad \text{for all } \lambda > 0. \tag{2.2}$$

➢ **Long tailed distribution:** Another important subclass of heavy-tailed distribution is the long-tailed distribution, whose tails are asymptotically self-similar under shifting by a constant. Formally, a distribution with survival function $S(x)$ is said to be long-tailed if

$$\lim_{x\to\infty} \frac{S(x+y)}{S(x)} = 1, \quad \text{for all } y > 0. \tag{2.3}$$

➢ **Regularly varying tails:** A regularly varying tail describes a probability distribution whose tail behavior follows a power-law decay. A distribution with survival function $S(x)$ is said to have a regularly varying tail with tail index $\alpha > 0$, if

$$\lim_{x\to\infty} \frac{S(tx)}{S(x)} = t^{-\alpha}, \quad \text{for all } t > 0. \tag{2.4}$$

There are several significant classes of distribution that characterize the tail behavior. Here we discuss some of them.

Definition 2.2.1. *(**Class** $\mathcal{L}$, Klüppelberg (1988)) A distribution function, F belongs to class $\mathcal{L}$ if*

$$\lim_{x\to\infty} \frac{S(x-y)}{S(x)} = 1, \quad \textit{for all}\, y \in \mathbb{R}.$$

Definition 2.2.2. *(**Class** $\mathcal{L}(\gamma)$, Su et al. (2004)) A distribution, F belongs to class $\mathcal{L}(\gamma)$ with $\gamma \geq 0$ if*

$$\lim_{x\to\infty} \frac{S(x+y)}{S(x)} = e^{-\gamma y}, \quad \forall\, y \in \mathbb{R}.$$

Definition 2.2.3. *(**Class** $\mathcal{D}$, Klüppelberg (1988)) A distribution F belongs to the class $\mathcal{D}$ of dominated-variation distributions if*

$$\lim_{x\to\infty} sup \frac{S(x)}{S(2x)} < \infty.$$

Definition 2.2.4. *(**Class** $\mathcal{S}$ **of subexponential**, Klüppelberg (1988)) A distribution F is belongs to class $\mathcal{S}$ of subexponential distribution if*

$$\lim_{x\to\infty} \frac{1 - F * F(x)}{1 - F(x)} = 2,$$

where '$*$' denotes the convolution operator.

For more details one may refer to Klüppelberg (1988), Foss et al. (2011), Leipus et al. (2023) and the references therein.

2.3 Statistical inference

Statistical inference is the process of making conclusions about a population based on data collected from a sample. It provides a framework for estimating population parameters, testing hypotheses, and making predictions from observed data. The two primary approaches to inference are the frequentist and Bayesian paradigms. In the frequentist approach, parameters are considered fixed and unknown quantities, and conclusions are based on the long-run frequency properties of estimators. In contrast, Bayesian inference treats parameters as random variables and incorporates prior information about these parameters through a prior distribution. Both paradigms offer various types of inference procedures: point estimation, which provides a single value that best estimates the unknown parameters; interval estimation, which gives a range of possible values within which the parameter is likely to lie, such as confidence intervals in the frequentist approach and credible intervals in the Bayesian framework; and hypothesis testing, which is used to evaluate the validity of specific assumptions or claims about the parameters. Statistical inference is a cornerstone of data-driven scientific inquiry because, by applying appropriate inferential techniques, it is possible to draw valid and reliable conclusions even when the data is incomplete or noisy. In the next subsection, we discuss more on frequentist and Bayesian paradigms of inference.

2.3.1 Method of maximum likelihood estimation

One of the most widely used frequentist approaches for estimating parameters is the maximum likelihood estimation (MLE). The methodology of MLE was first introduced by Fisher (1912), which laid the groundwork for modern statistical estimation and is defined as follows: Let $\underline{X} = (x_1, x_2, \ldots, x_n)$ be a random sample of size n from a population with PDF and CDF as $f(x|\theta)$ and $F(x|\theta)$, where

$\theta = (\theta_1, \theta_2 \ldots \theta_k)$ is a vector of k unknown parameters such that $\theta \in \Theta \subseteq \mathbb{R}$. Then the joint PDF of observed sample $\underline{X}$, known as the likelihood function $L(\theta)$, is defined as follows:

$$L(\theta) = L(\theta|\underline{x}) = f(\underline{X}|\theta) = \prod_{i=1}^{n} f(x_i|\theta).$$

Thus, we can observe that the likelihood function is a function of parameter θ. Then the MLE of θ, say $\hat{\theta}$, is the value of the parameter for which the likelihood function attains its maximum value, *i.e.*,

$$L(\hat{\theta}|\underline{X}) \geq L(\theta|\underline{X}) \implies L(\hat{\theta}|\underline{X}) = \sup_{\theta \in \Theta} L(\theta|\underline{X}).$$

For mathematical convenience, we often work with the log-likelihood function, $l(\theta) = \log L(\theta)$. To obtain the MLE, one typically follows these steps:

- Define the $l(\theta)$ based on the assumed model and observed sample.
- Take the derivative of $l(\theta)$ with respect to the parameter θ.
- Set the derivatives equal to 0 to obtain the likelihood equations.
- Solve the equations to find the value of θ.
- Verify that the obtained value corresponds to maxima by using the second derivative test.

The asymptotic properties of MLE make it suitable for constructing interval estimates for unknown parameters. Under regularity conditions, the distribution of the ML estimate is asymptotically normal with the true parameter value as mean and the variance given by the inverse Fisher information matrix. *i.e.*, for large n

$$\hat{\theta} \sim N\left(\theta, \frac{1}{nI(\theta)}\right).$$

where $I(\theta)$ is the Fisher information matrix defined as $I(\theta) = E\left(\frac{\partial^2 l}{\partial\theta_i \partial\theta_j}\right)$, $i, j = 1, 2, \ldots, k$. Using this, the $100(1-\alpha)\%$ confidence interval for θ is defined as

$$\hat{\theta} \pm z_{\alpha/2}\sqrt{Var(\hat{\theta})},$$

where, $z_{\alpha/2}$ is the upper percentile of standard normal distribution and $Var(\hat{\theta} = (nI(\theta)))^{-1}$ evaluate under $\theta = \hat{\theta}$. It should be noted that the estimators may not always be obtained analytically from the likelihood equations. In such situations, numerical iterative methods are employed to obtain the corresponding estimators. One such widely used iterative method is the Newton-Raphson method.

2.3.2 Bayesian estimation

As mentioned earlier, the Bayesian estimation combines the prior knowledge about the parameter with information from observed data to generate posterior distribution. Unlike the frequentist approach, Bayesian estimation treats parameters as random variables. This technique is fundamentally based on Bayes theorem, which offers a powerful framework for updating the probability of a hypothesis based on new evidence and is defined as follows: Suppose $\underline{X} = (x_1, x_2, \ldots, x_n)$ is a random sample of size n drawn from a population having PDF $f(x|\theta)$. The corresponding likelihood function is $L(\theta|\underline{X})$, and let $\pi(\theta)$ denote the prior distribution of the parameter θ. Then the posterior distribution of θ given data is defined as

$$\pi(\theta|\underline{X}) = \frac{L(\theta|\underline{X}).\pi(\theta)}{\int_{\Theta} L(\theta|\underline{X}).\pi(\theta)\ d\theta}.$$

This expression shows how the prior distribution $\pi(\theta)$ is updated using the likelihood function $L(\theta|\underline{X})$ to produce the updated knowledge about the parameters, called the posterior distribution.

Now, we move on to the key component of Bayesian estimation that guides the selection of an appropriate estimator from the posterior distribution known as the loss function. A loss function, denoted as $L(\hat{\theta}, \theta)$, is the cost or penalty or error associated with estimating the parameter θ by $\hat{\theta}$, when the true value is θ.

Now we evaluate the expected loss function, also known as Bayes risk, given as

$$r(\hat{\theta}) = \int L(\hat{\theta}, \theta)\pi(\theta|\underline{X})\ d\theta.$$

Our aim is to minimize the Bayes risk. The Bayes estimate of θ, say $\hat{\theta}_{Bayes}$, is the value of θ that minimizes $r(\hat{\theta})$. The resulting estimate depends on the choice of the loss function. Below, we list some of the most widely used loss functions along with their corresponding Bayes estimates:

- **Squared error loss function:** $L(\hat{\theta}, \theta) = (\hat{\theta} - \theta)^2$. The Bayes estimates is posterior mean *i.e.*, $\hat{\theta}_{Bayes} = E(\theta|\underline{X})$.
- **Absolute error loss function:** $L(\hat{\theta}, \theta) = |\hat{\theta} - \theta|$. The Bayesian estimate is the posterior median.
- **Zero-one loss function:** $L(\hat{\theta}, \theta) = \begin{cases} 0, & \hat{\theta} = \theta \\ 1, & \hat{\theta} \neq \theta \end{cases}$. The Bayesian estimate is the posterior mode.

In some cases, the Bayesian estimate cannot be obtained explicitly due to the mathematical complexity involved in analyzing the posterior distribution. To address this, various approximation techniques have been proposed by researchers. The present study also encounters a similar scenario; hence, we employ the Lindley's approximation and Markov chain Monte-Carlo (MCMC) technique to approximate the estimates. In the subsequent subsection, we will explore these methods in detail.

2.3.2.1 Lindley's approximation

In Bayesian analysis, the estimate is often seen as the ratio of two integrals, which can be challenging to evaluate analytically. To overcome this challenge, Lindley (1980) proposed an approximation method for evaluating such a ratio, and the procedure is defined as follows: Under the squared error loss function, the Bayes estimate is the posterior mean, and it takes the form

$$E(\phi(\theta)|data) = \frac{\int \phi(\theta)e^{l(\theta)+\rho(\theta)}d\theta}{\int e^{l(\theta)+\rho(\theta)}d\theta},$$

where $l(\theta)$ and $\rho(\theta)$ represent the log-likelihood function and logarithm of prior density of θ respectively. By using Lindley's approximation we have

$$E(\phi(\theta)|data) = \phi + \frac{1}{2}\sum_i\sum_j(\phi_{ij} + 2\phi_i\rho_j)\sigma_{ij} + \frac{1}{2}\sum_i\sum_j\sum_k\sum_p l_{ijk}\sigma_{ij}\sigma_{kp}\phi_p\bigg|_{\theta=\hat{\theta}},$$

where $\theta = (\theta_1, \ldots, \theta_m)$, $i, j, k, p = 1, 2, \ldots, m$, $\phi = \phi(\theta)$, $\phi_i = \partial\phi/\partial\theta_i$, $\phi_{ij} = \partial^2\phi/\partial\theta_i\partial\theta_j$, $l_{ijk} = \partial^3 l/\partial\theta_i\partial\theta_j\partial\theta_k$, $\rho_j = \partial\rho/\partial\theta_j$ and $\sigma_{ij} = (i, j)$ th element of $[I_{ij}]^{-1}|_{\theta=\hat{\theta}}$, where $[I_{ij}] = [-\partial^2 l/\partial\theta_i\partial\theta_j]$. Using this method, it is not possible to construct credible intervals. In such situations, we instead opt for the MCMC method.

2.3.2.2 MCMC method

In many cases, the posterior distribution may not be analytically tractable due to the mathematical complexity of integrals or when dealing with high-dimensional parameter spaces. This makes the analytical evaluation of Bayesian estimates, such as posterior mean, median, mode, or even credible intervals, a challenging task. To overcome these limitations, the Markov chain Monte-Carlo (MCMC) method provides a robust computational technique to approximate the posterior distribution through iterative random sampling. This method generates samples from posterior distribution by constructing a Markov chain whose stationary distribution is the desired posterior distribution. After an initial burn-in period, the distribution of the generated sample converges to the true posterior distribution. From these samples, one may evaluate the Bayes estimates.

Among the various MCMC techniques, the most widely used is the Metropolis-Hasting algorithm. It was initially introduced by Metropolis et al. (1953) and later generalized by Hastings (1970). Beginning with an initial value, the algorithm iteratively proposes new candidate values based on a proposal distribution and determines whether to accept or reject each proposal using an acceptance probability, thereby ensuring that the resulting Markov chain converges to the desired posterior distribution. The algorithm proceeds as follows:

1. Choose an initial value $\theta^{(0)}$ for the parameter θ.

2. Set $t = 1$.

3. Generate a proposal θ^* from the proposal distribution $q(\theta^*|\theta^{(t-1)})$.

4. Compute the acceptance probability.

$$\eta_\theta = min\left\{1, \frac{\pi(\theta^*|\underline{X})}{\pi(\theta^{(t-1)}|\underline{X})}\right\}.$$

5. Generate U from Uniform(0,1).

6. If $U < \eta_\theta$, accept the proposal and set $\theta^{(t)} = \theta^*$, else reject the proposal and set $\theta^{(t)} = \theta^{(t-1)}$.

7. Repeat steps 2-7, T times.

In addition to estimating posterior distributions, it is important to analyze the convergence and efficiency of the MCMC algorithm to ensure the accuracy of the Bayesian inference. For this purpose, several diagnostic tools and plots are employed. One of the most widely used diagnostics is the trace plot. It visualizes the sampled values of a parameter against the iteration number, thereby offering a visual assessment of the chain's mixing behavior. A well-mixed and converged chain typically has a trace plot that resembles random scatter without any noticeable trends or patterns.

Another important diagnostic is the ergodic mean plot, which displays the average of the parameter estimates up to a given iteration. This plot helps to assess the stability of the chain. If the chain has converged, the ergodic mean should stabilize around a constant value. An unstable or fluctuating ergodic mean indicates that the chain has not yet stabilized, and more iterations may be needed.

2.3.2.3 Bayesian credible interval and highest posterior density credible interval

In Bayesian analysis, uncertainty about an unknown parameter is expressed by its posterior distribution. One way to summarize this uncertainty is by constructing credible intervals, which provide a probabilistic range for the unknown parameter θ, based on its posterior distribution. According to Eberly and Casella (2003), a $100(1-\alpha)\%$ credible interval is defined as an interval $[l, u]$ such that

$$P(\theta < l) = \int_{-\infty}^{l} \pi(\theta|\underline{X})\, d\theta = \frac{\alpha}{2} \quad \text{and} \quad P(\theta > u) = \int_{u}^{\infty} \pi(\theta|\underline{X})\, d\theta = \frac{\alpha}{2},$$

where, $\pi(\theta|\underline{X})$ is the posterior density of θ, and l and u are the lower and upper limits of the credible interval corresponding to the significance level, α.

Each credible interval has an associated interval length, calculated as the difference between its upper and lower bounds. For the same level of credibility, $100(1-\alpha)\%$, multiple credible intervals may exist, particularly when the posterior distribution is skewed. This results in intervals of varying lengths. To address this, Chen and Shao (1999) introduced an algorithm for identifying the most appropriate credible interval, known as the highest posterior density (HPD) credible interval. The HPD credible interval is defined as the interval with the shortest possible width among all the credible intervals. Specifically, a $100(1-\alpha)\%$ HPD interval for θ is defined as

$$(L, U) = \{\theta : \pi(\theta|\underline{X}) > c\},$$

where, c is the largest constant such that $P(\theta \in (L, U)) \geq 1 - \alpha$.

2.4 Model selection criterion

In statistical modeling, the selection of an appropriate probability distribution is a crucial task. A well-chosen model not only accurately represents the data but also facilitates meaningful inferences and reliable predictions. Model selection criteria can be broadly classified into two categories: graphical techniques and formal statistical tests. Graphical techniques offer a visual analysis of how well the theoretical model aligns with the empirical data, while formal statistical tests provide a quantitative framework for evaluating model adequacy. These tests yield objective measures that support or reject the suitability of the proposed model based on the observed data. In the upcoming subsection, we explore some of the widely used model selection criteria.

2.4.1 Empirical CDF plot

The empirical cumulative distribution function (ECDF) plot is a non parametric graphical tool used to visualize and understand the distributional characteristics of a dataset. Given an ordered sample $X_{(1)} \leq X_{(2)} \leq \cdots \leq X_{(n)}$ of sample size n, the ECDF is defined as

$$F_n(x) = \frac{1}{n} \sum_{i=1}^{n} I(X_i < x),$$

where $I(\cdot)$ denotes the indicator function. The ECDF provides a step function that increases by a quantity $\frac{1}{n}$ at each sample point, which represents the proportion of observations less than or equal to a given sample point. To assess the goodness of fit of a chosen theoretical model, the ECDF is typically overlaid with the model's CDF. If the theoretical model fits the data well, the ECDF and the theoretical CDF will closely align throughout the entire range of the dataset.

2.4.2 Scaled total time on test (TTT) plot

The scaled total time on test (TTT) plot is a graphical technique used to assess the shape of the hazard behavior of the dataset. Epstein and Sobel (1953) introduced the concept of TTT plot. Later, Barlow and Campo (2024) developed the scaled version. To construct the scaled TTT plot, consider the order statistics $X_{(1)} \leq X_{(2)} \leq \cdots \leq X_{(n)}$ of sample size n. Based on the sample, TTT statistics is defined as

$$T_i = \begin{cases} \sum_{j=1}^{i} X_{(j)} + (n-i)X_{(i)}, & \text{for } i = 1, 2, \ldots, n \\ 0, & \text{for } i = 0. \end{cases}$$

Then the scaled TTT statistics is given by

$$\phi_i = \frac{T_i}{T_n}, \quad i = 0, 1, 2, \ldots, n,$$

where, $T_n = \sum_{j=1}^{n} X_{(j)}$. Plotting ϕ_i against the ECDF along with a reference diagonal line gives the scaled TTT plot. The hazard rate pattern of the dataset can be interpreted from the plot as follows: if the curve lies above the diagonal, it suggests a decreasing hazard rate; if below, an increasing hazard rate. A curve that lies above and then below indicates a bathtub-shaped hazard, while the reverse implies an upside-down bathtub shape.

2.4.3 Probability–Probability (P–P) plot

The probability–probability plot (P–P plot) is a graphical tool used to analyze the goodness of fit between a theoretical probability distribution and an observed dataset. It compares the ECDF of the sample data to the CDF of the proposed model. To construct the P–P plot, the empirical probabilities based on order statistics are plotted along the x-axis, and the corresponding theoretical CDF values are plotted along the y-axis. If the proposed model fits the data well, the points will lie approximately along the 45° diagonal line. Additionally, points lying above the diagonal indicate that the model underestimates the probabilities, while points below the diagonal suggest that the model overestimates the probabilities.

2.4.4 Quantile–Quantile (Q–Q) plot

The Q–Q plot is another widely used graphical tool to assess the fit of a candidate distribution to a dataset. Unlike the P-P plot, the Q-Q plot compares the quantile of the empirical distribution with the corresponding quantile of the theoretical distribution. To construct the Q-Q plot, the sample quantiles derived from ordered data are plotted on the x-axis, and the corresponding theoretical quantiles from the proposed distribution are plotted on the y-axis. If the model fits the data well, the plotted points will align closely along the 45° diagonal line.

2.4.5 Kolmogorov–Smirnov (K–S) test

The Kolmogorov-Smirnov (K-S) test is a widely used non parametric statistical test for model validation and is defined as follows: Suppose $x_1, x_2, \ldots, x_n$ is a random sample of size n drawn independently from a population with CDF $F(x)$, and let $F_n(x)$ be the ECDF. The K-S test statistic or distance (D) is defined as the maximum absolute difference between ECDF and the theoretical CDF, *i.e.*,

$$D = \underset{\theta}{sup}|F_n(x) - F(x)|$$

A smaller value of D indicates a good fit between the empirical and theoretical distribution. Furthermore, the P-value associated with the test helps determine whether the considered model provides a good fit to the dataset.

2.5 Statistical software and computational procedure

In this study, the numerical analyses were performed using R software, a widely used open-source platform for statistical computing and data analysis.

Specifically, various R packages such as fitdistrplus, MASS, stats4, pracma, bccp, logspline and ggplot2 were employed for parameter estimation, distribution fitting, graphical visualization, and simulation studies. In addition, custom R scripts are developed for implementing methods such as MCMC, UMVUE, and Lindley's approximation, as well as for efficiently executing the proposed models and transformations wherever necessary.

The MLE are obtained by maximizing the log-likelihood function using the optim() function in R, adopting either the BFGS or Nelder–Mead method depending on the smoothness of the likelihood surface. Convergence is verified by checking the optimizer's convergence code and ensuring stability in the log-likelihood values. The first-order condition is confirmed by evaluating the score vector at the estimated parameters, which is found to be close to zero, while the second-order condition is checked by computing the Hessian matrix at the MLE and verifying the negative definiteness of its eigenvalues. To ensure global optimality, optimization is repeated with multiple initial parameter values, and the solution yielding the highest log-likelihood is selected. For graphical visualization of distribution fitting, fitted histograms along with P-P plots or Q–Q plots are used to assess model adequacy, while the K-S test is employed as a formal goodness-of-fit measure. Furthermore, for analyses involving MCMC methods, convergence diagnostics are evaluated using trace plots and ergodic mean plots to confirm the stability and proper mixing of the generated chains.

2.6 Summary of the chapter

This chapter outlines the theoretical foundation essential for the methodological developments in this study. It outlines the fundamental concepts, definitions, and mathematical tools relevant to probability distributions and statistical modeling. Key properties of a distribution, including the quantile function, moments, reliability measures, order statistics, entropy, and stochastic orderings, are discussed to provide a deeper understanding of model behavior. In addition, various types of tail behavior and important distributional classes are introduced. The chapter also reviews important estimation techniques and model selection criteria. This foundational overview sets the stage for the subsequent chapters, which build upon these concepts to develop and apply new statistical methodologies.

Chapter 3

QT-transformation & QT_d-transformation

3.1 Introduction

As mentioned earlier, the transformation of existing distributions to generate more flexible families of distributions is a rapidly evolving area of research. In this chapter, we propose a new method to generate families of distributions. The proposed method incorporates additional mathematical functions to enhance flexibility. It is constructed using the Q-transformation rule combined with some key properties of the quantile function.

The quantile function, the inverse function of CDF, is an important function in distribution theory. As it provides direct access to the distribution's structure without the need for explicit knowledge of the PDF or CDF, making it an effective tool for statistical modeling, simulation, and distributional analysis. The Q-transformation rule is a fundamental principle related to quantile functions that offers a mathematical framework for systematically modifying the shape of a given distribution while preserving critical probabilistic properties.

Also, several mathematical functions with unique structural properties are extensively explored in the literature. Our objective is to extract these properties to create classes of distributions that exhibit desired characteristics. Furthermore, we investigate how different choices of quantile functions and transformation functions influence the resulting distributions, providing a comprehensive understanding of their structural properties.

The remainder of this chapter is structured as follows: First, to establish the foundation for the proposed method, we review some fundamental rules related to quantile functions in Section 3.2. Next, Section 3.3 presents the construction and formal definition of the proposed method, referred to as the QT-transformation, highlighting its key components and underlying principles. In Section 3.4, we introduce the dual concept of the QT-transformation, called QT_d-transformation, along with its theoretical formation and definition. Some insights into the proposed approach are provided in Section 3.5. Finally, the chapter concludes with a summary in Section 3.6.

3.2 Fundamental rules of the quantile function

The quantile function possesses several key rules that serve as the foundation for various transformations, including the one we are about to propose. Here, we briefly outline the important rules before focusing on the Q-transformation rule, which forms the basis of our methodology.

➢ **The reflection rule**

For a continuous distribution, the quantile function $(Q(u))$ satisfies

$$-Q(1-u) = Q(u).$$

i.e., $Q(u)$ can be reflected around $u = 0.5$.

➢ **The addition rule**

If $Q_X(u)$ and $Q_Y(u)$ are the quantile functions of random variables X and Y, respectively, then the quantile function for the sum $Z = X + Y$ is given by

$$Q_Z(u) = Q_X(u) + Q_Y(u).$$

➢ **The multiplication rule**

If $Q_X(u)$ and $Q_Y(u)$ are the quantile functions of positive random variables X and Y, respectively, then the quantile function for the product $Z = XY$ is given by

$$Q_Z(u) = Q_X(u) \times Q_Y(u).$$

➢ **The intermediate rule**

If $Q_X(u)$ and $Q_Y(u)$ are two quantile functions of random variables X and Y, respectively, then there exists a quantile function

$$Q_i(u) = p.Q_X(u) + (1-p).Q_Y(u), \quad 0 \leq p \leq 1,$$

such that, if $Q_X(u) < Q_{Y(u)}$, for a given u, then

$$Q_X(u) \leq Q_i(u) \leq Q_Y(u).$$

➢ **The standardization rule**

The quantile function of any distribution can be represented as

$$Q(u) = \lambda + \eta Q_Z(u),$$

where λ is the location parameter, η is the scale parameter, and $Q_Z(u)$ is the quantile function of standard distribution.

➢ **The reciprocal rule**

If X is a positive random variable with quantile function $Q_X(u)$, then the quantile function for the reciprocal $Y = \frac{1}{X}$ is given by

$$Q_Y(u) = \frac{1}{Q_X(1-u)}.$$

➢ **The uniform transformation rule**

If $Q_X(u)$ is the quantile function of a random variable X with CDF, $F_X(x)$, then the quantile function of the transformed random variable X, $Y = F_X(x)$, is given by

$$Q_Y(u) = F_X^{-1}(u).$$

i.e., the uniform transformation shows that any distribution can be regarded as a transformed uniform distribution.

➢ **The P-transformation rule**

If $f(u)$ is a non-decreasing function of u in the range $0 \leq u \leq 1$, with $f(0) = 0$ and $f(1) = 1$, then $Q(f(u))$ is also a quantile function, with the same distributional range as $Q(u)$.

➢ **Q-transformation rule**

If $T(x)$ is a non-decreasing function of x, then $T(Q(u))$ is a quantile function. On the other hand, if $T(x)$ is non-increasing, then $T(Q(1-u))$ is also a quantile function.

For further details and examples of these rules, one may refer to the work by Gilchrist (2000).

3.3 QT-transformation: Construction and definition

The proposed method utilizes the Q-transformation rule in combination with fundamental properties of the quantile function. Our initial goal is to construct the quantile function of a random variable defined on the interval $(0, 1)$. To achieve this, we will utilize the Q-transformation rule, in which we restrict the range of the function $T(\cdot)$ to $(0, 1)$. This can be accomplished through various methods, including scaling, shifting, function composition, truncation, etc. The following results illustrate these concepts.

Lemma 3.3.1. *Let $T(x) : (x_L, x_R) \to (0, 1)$ be a non-decreasing continuous function with $T(x_L) = 0$, $T(x_R) = 1$. Let $Q(\cdot)$ be a quantile function of any random variable with support (x_L, x_R), then $Q_T(u) = T(Q(u))$ is a quantile function of a random variable with support $(0, 1)$.*

Proof. From the Q-transformation rule, it follows that $Q_T(u)$ is a quantile function. We have, for a quantile function, $Q(0)$ and $Q(1)$ that give the left and right end points of support of the corresponding random variable. Then

$$\begin{aligned} Q_T(0) &= T(Q(0)) = T(x_L) = 0 \\ Q_T(1) &= T(Q(1)) = T(x_R) = 1, \end{aligned}$$

which completes the proof. □

Lemma 3.3.2. *If $Q_T(\cdot)$ is a quantile function of a random variable with support $(0, 1)$ and $F(x)$ is any continuous CDF, then $G(x) = Q_T(F(x))$ will be a valid CDF.*

Proof. Here, $Q_T(\cdot)$ and $F(\cdot)$ are continuous non-decreasing functions. Since $G(\cdot)$ is the composition of $Q_T(\cdot)$ and $F(\cdot)$, it is also continuous and non-decreasing. Also, we have

$$\begin{aligned} G(0) &= Q_T(F(0)) = Q_T(0) = 0 \\ G(\infty) &= Q_T(F(\infty)) = Q_T(1) = 1, \end{aligned}$$

which completes the proof. □

Theorem 3.3.1. *If $T(x) : (x_L, x_R) \to (0, 1)$ is a non-decreasing function with $T(x_L) = 0$, $T(x_R) = 1$, and Q($\cdot$) is any quantile function, then for any continuous CDF $F(x)$, the function*

$$G(x) = T\{Q[F(x)]\},$$

is a valid CDF.

Proof. From **Lemma 3.3.1** and **Lemma 3.3.2**, the theorem holds. □

Based on these results, we introduce a method for generating families of distributions referred to as QT_d-transformation.

Definition 3.3.1. *Consider a non-decreasing continuous function, $\tau(x)$, defined on (x_L, x_R) and a quantile function $Q(\cdot)$ of a random variable with the same support (x_L, x_R). Then, the CDF of the QT-transformed random variable is defined as*

$$G(x) = T\{Q[F(x)]\}, \tag{3.1}$$

where $F(x)$ is any CDF and $T(\cdot)$ is a scaled function of $\tau(x)$ so that $T(x) : (x_L, x_R) \to (0, 1)$ and $T(x_L) = 0$ and $T(x_R) = 1$.

Notes 1. *To restrict the range of the function $\tau(x)$ to $(0, 1)$ and ensure that it attains the values 0 and 1 at the endpoints x_L and x_R, respectively, we define a scaled version of $\tau(x)$ denoted as $T(x)$, as*

$$T(x) = \frac{\tau(x) - \tau(x_L)}{\tau(x_R) - \tau(x_L)}.$$

Thus the transformed function, $T(x)$ maps to the interval $(0, 1)$, satisfying $T(x_L) = 0$ and $T(x_R) = 1$. As an illustrative example, consider the function $\tau(x) = arctan(x)$, $x \in \mathbb{R}$. Since $\tau(x)$ approaches $-\frac{\pi}{2}$ as $x \to -\infty$ and $\frac{\pi}{2}$ as $x \to \infty$, and the corresponding scaled function becomes

$$T(x) = \frac{arctan(x) + \frac{\pi}{2}}{\pi}.$$

Remarks 1. *Since the above transformation involves a combination of quantile function $Q(\cdot)$ and a continuous function $T(\cdot)$, it is termed as "QT-transformation."*

The Figure 3.1 presents the illustration of QT-transformation, where (a, b) denotes the support of the considered baseline distribution. From this we observe that the domain of $T(Q(F(x)))$ is the same as the domain of the baseline CDF $F(x)$ and the range of $T(Q(F(x)))$ is the range of the function, $T(x)$.

Remarks 2. *The support of the QT-transformed random variable is the same as the support of the baseline random variable.*

Notes 2. *The QT-transformation allows us to generate a wide range of distribution families beyond lifetime models, depending on the choice of the baseline distribution and its support. However, in this study, we focus specifically on lifetime models and their applications in reliability analysis.*

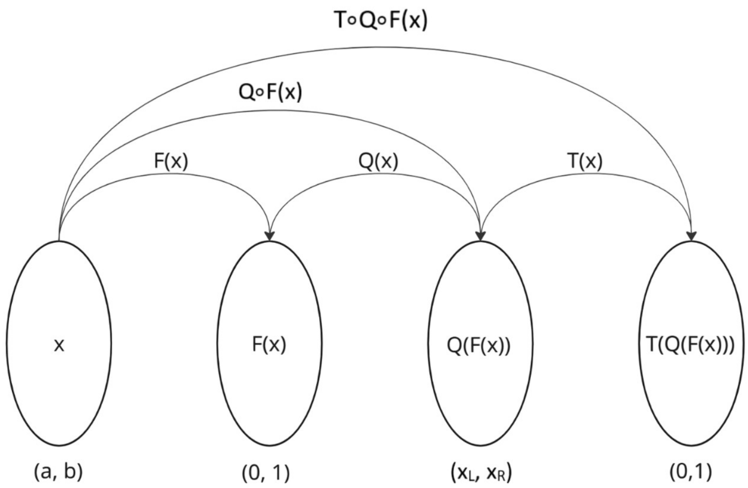

Figure 3.1: Illustration of QT-transformation

Now, we present an example to illustrate the effective application of the QT-transformation in generating the well-known Weibull-G family of distributions.

Example 3.3.1. *Consider the Weibull-G family introduced by Bourguignon et al. (2014), which is characterized by its CDF*

$$F(x;\alpha,\beta,\eta) = 1 - \exp\left\{-\alpha\left[\frac{F(x)}{1-F(x)}\right]^{\beta}\right\}, \quad \alpha,\beta > 0. \tag{3.2}$$

where $F(x)$ is the baseline distribution. Now, we will generate this family of distributions using the QT-transformation as follows:

Using **Definition 3.3.1**, consider the non-decreasing continuous function $T(x) : (x_L, x_R) \to (0,1)$ with $T(x_L) = 0$ and $T(x_R) = 1$ as

$$T(x) = 1 - e^{-x^b}, \quad b > 0,\ x > 0. \tag{3.3}$$

Since the domain of $T(x)$ is $(0, \infty)$, we have to choose a quantile function, $Q(u)$, with support on $(0, \infty)$. Here, we choose $Q(u)$ to be the quantile function of the log-logistic distribution with scale and shape parameters α and λ, respectively, given by

$$Q(u) = \alpha\left(\frac{u}{1-u}\right)^{1/\lambda}.$$

Thus

$$\begin{aligned} T(Q(u)) &= 1 - e^{-\alpha\left(\frac{u}{1-u}\right)^{b/\lambda}} \\ &= 1 - e^{-\alpha\left(\frac{u}{1-u}\right)^{\beta}}, \quad \beta = b/\lambda. \end{aligned}$$

Then by substituting u with the baseline CDF $F(x)$, we can generate the Weibull-G family.

3.4 QT_d-transformation: Construction and definition

Similarly, by considering the other side of the Q-transformation rule and applying the same underlying principles, we introduce the dual concept of the QT-transform, referred to as the QT_d-transform. Now, let us consider the following results:

Lemma 3.4.1. *Let $T(x) : (x_L, x_R) \to (0,1)$ be a non-increasing continuous function with $T(x_L) = 1$, $T(x_R) = 0$. Let $Q(\cdot)$ be a quantile function of any random variable with support (x_L, x_R), then $Q_T(u) = T(Q(1-u))$ is a quantile function of a random variable with support $(0,1)$.*

Proof. From the Q-transformation rule, it follows that $Q_T(\cdot)$ is a quantile function. We have, for a quantile function, $Q(0)$ and $Q(1)$ that give the left and right end points of support of the corresponding random variable. Then

$$\begin{aligned} Q_T(0) &= T(Q(1)) = T(x_R) = 0 \\ Q_T(1) &= T(Q(0)) = T(x_L) = 1, \end{aligned}$$

which completes the proof. □

Theorem 3.4.1. *If $T(x) : (x_L, x_R) \to (0, 1)$ is a non-decreasing function with $T(x_L) = 1$, $T(x_R) = 0$, and $Q(\cdot)$ is any quantile function, then for any continuous CDF $F(x)$, the function*

$$G(x) = T\{Q[1 - F(x)]\}, \tag{3.4}$$

is a valid CDF.

Proof. From **Lemma 3.3.1** and **Lemma 3.4.1**, the theorem holds. □

Based on these findings, we present the QT_d-Transformation.

Definition 3.4.1. *(QT_d-Transformation) Consider a non-increasing continuous function, $\tau_d(x)$, defined on (x_L, x_R) and a quantile function, $Q(\cdot)$, of a random variable with support (x_L, x_R), Then, the CDF of QT_d-transformation is defined as*

$$G(x) = T_d\{Q[1 - F(x)]\}, \tag{3.5}$$

where $F(x)$ is any CDF and $T_{d\cdot}(\cdot)$ is a scaled function of $\tau_d(x)$ so that $T_d(x) : (x_L, x_R) \to (0, 1)$ and $T_d(x_L) = 1$ and $T_d(x_R) = 0$.

Remarks 3. *As this transformation combines the quantile function with a continuous function $T_d(\cdot)$, it is referred to as the "QT_d-Transformation."*

We then provide an example to show how the QT_d-transformation can be used effectively to generate the well-known odd Fréchet-G family of distributions.

Example 3.4.1. *Consider the odd Fréchet-G family of distributions proposed by ul Haq and Elgarhy (2018) with the CDF*

$$F(x;\theta,\eta) = \exp\left\{-\left(\frac{1-G(x)}{G(x)}\right)^{\theta}\right\}, \quad \theta > 0,$$

where $F(x)$ is the baseline CDF. We now proceed to generate this family of distributions using the QT-transformation as follows:

Using **Definition 3.4.1**, consider the function

$$T_d(x) = e^{-\frac{1}{x^{\beta}}}, \quad x, \beta > 0.$$

Here also, $T_d(\cdot)$ is defined on $(0,\infty)$. So, consider $Q(u)$ as the same function given in **Example 3.3.1**. Thus

$$T_d(Q(u)) = e^{-\alpha\left(\frac{1-u}{u}\right)^{b/\lambda}}. \tag{3.6}$$

Then by substituting u with the baseline CDF $F(x)$ and assuming $\alpha = 1$ and $\theta = b/\lambda$, we get the odd Fréchet-G family.

3.5 Some insights into the proposed approach

The QT and QT_d-transformations are two related methods designed to generate new families of distributions by combining a quantile function and a continuous function. While they aim to enhance or modify distributional properties, their construction differs. The QT-transformation utilizes a continuous, non-decreasing function, while the QT_d-transformation applies a continuous, non-increasing function.

The proposed method can also be viewed as an extension of the $T-X\{Y\}$ family of distributions proposed by Aljarrah et al. (2014), but derived through an alternative approach. As discussed in Chapter 1, the $T-X\{Y\}$ family is derived based on both CDF and survival function. However, with our approach, even though the function $T(\cdot)$ satisfies the properties of CDF, it need not be a known CDF. This offers some flexibility in the choice of the function $T(\cdot)$, allowing us to incorporate some useful mathematical functions and explore their characteristics in generating new families of distributions.

From a mathematical perspective, the proposed CDF $G(x)$ given in (3.1) and (3.5) can be interpreted as the composition of three functions $T(\cdot)$, $Q(\cdot)$, and $F(\cdot)$. In this composition, $T(\cdot)$ serves as the outermost function, applying a final transformation to the results of $Q(\cdot)$ and $F(\cdot)$. Thus the behavior of $T(\cdot)$ and $T_d(\cdot)$ plays a crucial role in shaping $G(x)$, making its choice an important factor in the model construction. In the upcoming chapters, we will explore various mathematical functions that can be used within the QT-transformation framework. We will analyze how these functions influence the properties of the resulting models, examining their flexibility in adapting to different data types and their applicability across a range of statistical contexts.

3.6 Summary of the chapter

In this chapter, we proposed a new method for generating families of distributions, called QT-transformation, along with its dual concept, QT_d-transformation. The proposed method is constructed using a fundamental rule related to quantile functions, known as the Q-transformation rule. For this, we begin by reviewing fundamental definitions and key mathematical concepts related to quantile functions. Then, a detailed discussion on the construction, definition, and properties of the proposed method is presented. This chapter serves as the groundwork for the subsequent chapters, where we further explore their applications and theoretical implications by constructing new flexible families of distributions using the proposed method.

Chapter 4

Application of QT-transformation using sigmoid function

4.1 Introduction

Numerous mathematical functions, each with unique properties and applications, are extensively discussed in the literature. As mentioned in previous chapters, the selection of the function $T(\cdot)$, given in the definition of the QT-transformation, is vital. In this chapter, we explore various mathematical functions and their applications within the QT-transformation framework, focusing on properties such as kurtosis, skewness, tail behavior, and more in the resultant models.

A particularly significant function in this context is the sigmoid function, which maps any real-valued number into a range between 0 and 1, offering a smooth gradient that is crucial for optimization processes. This characteristic makes it especially suitable for various applications, including statistics, artificial intelligence, machine learning, neural networks, and biological modeling, where nonlinear relationships frequently occur. While numerous types of sigmoid functions exist, this chapter will concentrate specifically on three distinct types: logistic, arctangent, and error sigmoid functions. Using these functions, we propose three new families of distributions.

The rest of the chapter is structured as follows: In Section 4.2, we provide a brief overview of the sigmoid function, introducing the three specific types and their key properties. The subsequent Sections 4.3–4.5 explore the construction of the three families of distributions: logistic sigmoid {Gumbel} (LSG), arctangent Sigmoid Gumbel (arctangent sigmoid {Gumbel} (ASG)), and Error Sigmoid Gumbel (error sigmoid {Gumbel} (ESG)) family along with their properties. In Section 4.6, we introduce three modified exponential distributions, derived as sub-models of the proposed families. Section 4.7 presents an extensive simulation study, followed by real data analysis in Section 4.8. Finally, the chapter concludes with a summary in Section 4.9.

4.2 Overview of sigmoid function

The sigmoid function is a fundamental mathematical function known for its characteristic S-shaped curve, which provides a smooth transition between two asymptotic values, typically 0 and 1. The concept of sigmoid functions has been developed over time by various mathematicians and scientists, and it doesn't have a single founder attributed to it. However, certain researchers have contributed significantly to the development and popularization of sigmoid functions in different contexts. For example, Pierre François Verhulst, a Belgian mathematician, introduced the logistic growth model in Verhulst (1838), which gave rise to the logistic sigmoid function. Here are some of the key properties of sigmoid functions:

- **S-shaped Curve**: Sigmoid functions are characterized by their "S-shaped" curve.
- **Monotonic**: Sigmoid functions are monotonically increasing everywhere.
- **Differentiable**: Sigmoid functions are smooth and differentiable across their entire domain.

- **Continuous**: Sigmoid function is continuous every where.
- **Bounded**: Sigmoid functions are bounded.

It has been observed that the sigmoid function satisfies all the necessary properties of $\tau(x)$ as outlined in **Definition 3.3.1**. Furthermore, the sigmoid function exists in various forms, each with distinct parameters that can be adjusted to meet the desired characteristics of $T(x)$. In this study, we focus on three particular types of sigmoid functions: the logistic, arctangent, and error sigmoid functions. In the subsequent sections, we will explore the applications and properties of these sigmoid functions and demonstrate how to transform them to the range $(0, 1)$ to satisfy the desired characteristics of $T(\cdot)$ in the context of the QT-transformation.

4.2.1 Logistic sigmoid function

The Verhulst logistic sigmoid function, often simply referred to as the logistic function, was introduced in the 18$^{\text{th}}$ century to model population growth. The standard form of the logistic function is given by

$$\sigma(x) = \frac{1}{1 + \exp(-x)}, \quad x \in \mathbb{R}.$$

The plot of the standard logistic sigmoid function is provided in Figure 4.1. Some of its key properties are discussed below:

- **Asymptotic Behavior:** As $x \to -\infty$, $\sigma(x)$ approaches 0 and $x \to \infty$, $\sigma(x)$ approaches 1.
- **Derivative:** $\sigma(x)$ is infinitely differentiable. Its first derivative is given as

$$\sigma'(x) = \sigma(x)(1 - \sigma(x)).$$

- **Inverse:** Inverse of $\sigma(x)$ is known as logit function given by

$$\sigma^{-1}(x) = \log\left(\frac{y}{1-y}\right).$$

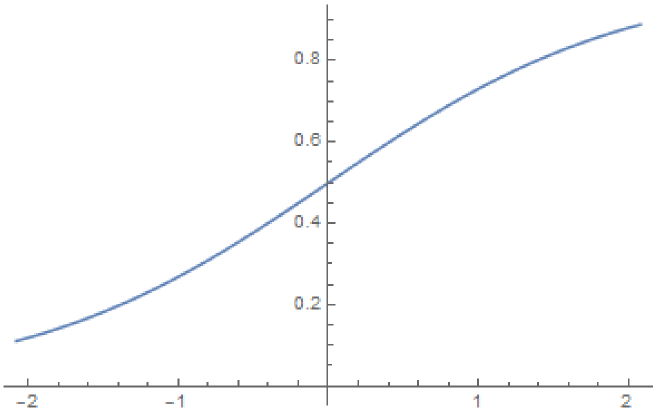

Figure 4.1: Plot of Logistic sigmoid function

This function maps any real-valued number into the range $(0, 1)$, making it highly useful across various fields. For example, it serves as a non-linear activation function in neural networking, where its smoothness, differentiability, and bounded output make it suitable for gradient-based optimization techniques in machine learning. Also, it is useful in statistical modeling, especially in logistic regression. Further, it is widely used as a population growth model in many disciplines, such as biology, ecology, and demography. For further applications of the logistic sigmoid function, one may refer to Raeside (1988), Rezaeian Zadeh et al. (2010), Matis and Al-Muhammed (2010), Menon et al. (1996), ZAIDI (2022), and Jónás (2007).

4.2.2 Arctangent sigmoid function

The arctangent sigmoid function is a mathematical function derived from the inverse tangent function given as

$$f(x) = \arctan(x) = \tan^{-1}(x), \quad x \in \mathbb{R}.$$

This function smoothly maps the entire real line to the interval $\left(-\frac{\pi}{2}, \frac{\pi}{2}\right)$. The plot of the arctangent sigmoid function is shown in Figure 4.2. Some of its key properties are outlined below:

- **Asymptotic Behavior:** As $x \to -\infty$, $f(x)$ approaches $-\frac{\pi}{2}$ and $x \to \infty$, $f(x)$ approaches $\frac{\pi}{2}$.
- **Derivative:** The derivative of $f(x)$ is given by

$$f'(x) = \frac{1}{1+x^2}.$$

- **Inverse:** The inverse of f(x) is the tangent function.
- **Tail behavior:** This function approaches its its asymptotic values more slowly than the logistic sigmoid function, resulting in a less steep at the extremes.

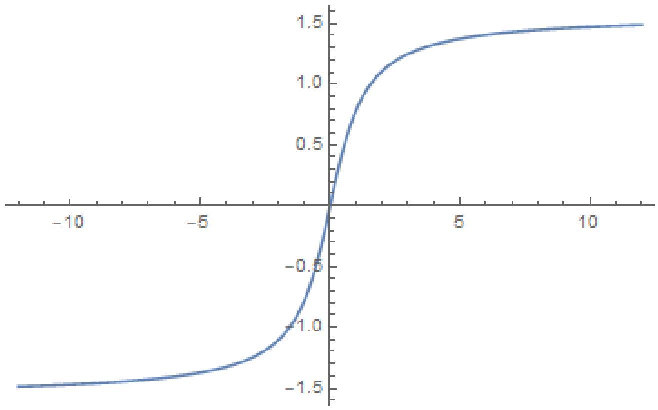

Figure 4.2: Plot of arctangent sigmoid function

Similar to the logistic sigmoid function, the arctangent sigmoid function can serve as a non-linear activation function in neural networks and machine learning. Also, its slower growth toward the extremes and smoother gradients help to reduce the risk of issues like vanishing gradients during training. It also finds applicability in signal processing, control systems, and fuzzy logic, where a gradual and bounded response is essential. In statistics, it is used as a link function in certain regression models. Also, in disciplines like psychology and biology, the arctangent sigmoid function is also used to model phenomena that exhibit saturation effects, like dose-response relationships in pharmacology and stimulus-response curves in psychometrics. More applications of the arctangent sigmoid function can be found in Kamruzzaman (2002), Anastassiou (2025), Yang et al.

(2021), Anastassiou (2022), and Sivri et al. (2022). Since our study requires the range of the function to be $(0, 1)$, the transformed function can be written as

$$f(x) = \frac{\arctan(x) + (\pi/2)}{\pi}, \quad x \in \mathbb{R}.$$

4.2.3 Error sigmoid function

The error function is a non-elementary integral denoted by $erf(x)$ and is another type of sigmoid function, defined as

$$f(x) = erf(x) = \frac{2}{\sqrt{\pi}} \int_0^x e^{-t^2} dt, \quad x \in \mathbb{R}.$$

The plot of the error sigmoid function is presented in Figure 4.3. Some of its key properties are as follows:

- **Asymptotic Behavior:** As $x \to -\infty$, $f(x)$ approaches -1 and $x \to \infty$, $f(x)$ approaches 1.
- **Derivative:** The derivative of $f(x)$ is given by

$$f'(x) = \frac{2}{\sqrt{\pi}} e^{-x^2}.$$

- **Inverse:** The error function does not have a closed-form expression for its inverse; however, many researchers have developed various approximations for both the inverse function and the error function itself.

This function maps the entire real line into the interval $(-1, 1)$. It is also closely related to the CDF of the normal distribution. Furthermore, it acts as a link function in probit regression models. The error sigmoid function finds applications similar to other sigmoid functions across various domains, including machine learning, neural networks, control systems, and signal processing. In machine learning, it is particularly valued as a smooth activation function, especially in contexts where a probabilistic interpretation of outputs is desired. For more details on this function, one may refer to Andrews (1998). To reduce the range to $(0, 1)$, we considered the scaled transform of $f(x)$ as follows

$$f(x) = \frac{1}{2}\big(1 + erf(x)\big). \tag{4.1}$$

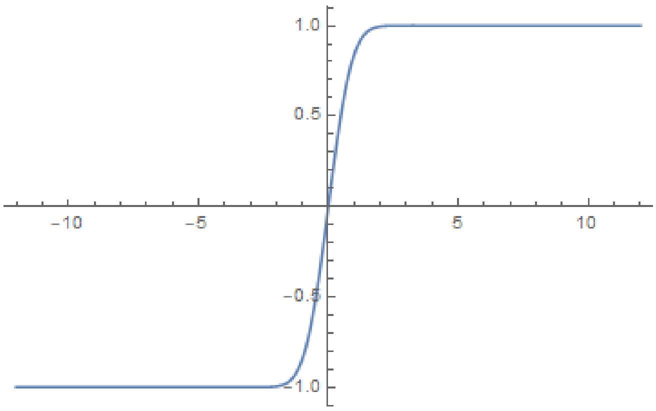

Figure 4.3: Plot of error function over real line

Since the sigmoid functions satisfy all the required properties of $\tau(x)$, defined in **Definition 3.3.1**, we now introduce three families of distributions using these sigmoid functions in the following section.

Notes 3. *From the **Definition** 3.3.1 of QT-transformation, $T(\cdot)$ and $Q(\cdot)$ must share the same support. Since $\tau(x)$ is considered to be a sigmoid function defined on $(-\infty, \infty)$, we arbitrarily choose $Q(\cdot)$ as the quantile function of the Gumbel distribution, characterized by the location parameter μ and the scale parameter β.*

4.3 Logistic sigmoid {Gumbel} family

Consider the non-decreasing continuous function $T(x)$ as the logistic sigmoid function and the $Q(\cdot)$ as the quantile function of the Gumbel distribution, as mentioned earlier. Then

$$\begin{aligned} T(x) &= \frac{1}{1+\exp(-x)}, \quad x \in \mathbb{R}, \\ Q(u) &= \mu - \beta(\log(-\log(u))), \quad 0 < u < 1,\ \mu \in \mathbb{R},\ \beta > 0. \end{aligned}$$

Using the Q-transformation rule, we obtain the quantile function $Q_Y(\cdot)$ as

$$\begin{aligned} Q_Y(u) = T(Q(u)) &= \frac{1}{1+e^{-\mu}(-\log(u))^{\beta}} \\ &= \frac{e^{\mu}}{e^{\mu}+(-\log(u))^{\beta}}. \end{aligned}$$

Now, using the **Definition 3.3.1**, we define a new class of distribution called logistic sigmoid-{Gumbel} transformed family as follows.

Definition 4.3.1. *Let X and Y be any two continuous random variables with CDF $F_X(\cdot)$ and $F_Y(\cdot)$ respectively. Then Y is said to be the logistic sigmoid {Gumbel} (LSG) transformed random variable of X if $F_Y(\cdot)$ is defined as follows:*

$$F_Y(x) = \frac{e^{\mu}}{e^{\mu}+(-\log(F_X(x)))^{\beta}}, \quad x \in \mathbb{R},\ \mu \in \mathbb{R},\ \beta > 0. \tag{4.2}$$

The corresponding PDF is defined as

$$f_Y(x) = -\frac{\beta}{F_X(x)\log(F_X(x))\sqrt{\pi}} \exp\left\{-[\mu-\beta\log(-\log(F_X(x)))]^2\right\} f_X(x), \tag{4.3}$$

where $f_X(x)$ is the PDF of baseline random variable X. Also from equation (4.3), it is obvious that $f_Y(x)$ is a weighted form of $f_X(x)$, with weight function given as

$$w(x) = -\frac{1}{F_X(x)\log(F_X(x))} \exp\left\{-[\mu-\beta\log(-\log(F_X(x)))]^2\right\}.$$

Thus the PDF in (4.3) can be written as

$$f_Y(x) = \frac{w(x) f_X(x)}{c},$$

where $c = E(w(x))$ is the normalizing constant. If $F_X^{-1}(x)$ exists in explicit form, a random sample from the LSG family can be obtained from

$$x = F_X^{-1}\left\{\exp\left[-\left(\frac{e^{\mu}}{U} - e^{\mu}\right)^{1/\beta}\right]\right\},$$

where U is the standard uniform random variable. And if $F_X^{-1}(x)$ does not exist in explicit form, the acceptance-rejection method can be used. The survival function, hazard rate (HR) and reverse hazard function (RHF), of the LSG transformed random variable are respectively given as

$$\bar{F}_Y(x) = \frac{(-\log(F_X(x)))^{\beta}}{e^{\mu} + (-\log(F(x)))^{\beta}}, \tag{4.4}$$

$$\begin{aligned} H_Y(x) &= -\frac{\beta e^{\mu} f_X(x)}{F_X(x)\log(F_X(x))[e^{\mu} + (-\log(F_X(x)))^{\beta}]} \\ &= \left(\frac{\beta e^{\mu} \bar{F}_X(x)}{\Lambda_X(x) F_X(x)[e^{\mu} + (\Lambda_X(x))^{\beta}]}\right) H_X(x), \end{aligned} \tag{4.5}$$

$$\begin{aligned} \lambda_Y(x) &= \frac{\beta(-\log(F_X(x))^{\beta-1}) f_X(x)}{[e^{\mu} + (-\log(F_X(x)))^{\beta}] F_X(x)} \\ &= \left(\frac{\beta(\Lambda_X(x)^{\beta-1})}{[e^{\mu} + (\Lambda_X(x))^{\beta}]}\right)\lambda_X(x), \end{aligned} \tag{4.6}$$

where $H_X(\cdot)$ and $\lambda_X(\cdot)$ are the HR and reverse hazard function (RHF) of baseline random variable X, respectively. And $\Lambda_X(x) = -\log(F_X(x)) = \int_x^{\infty} \lambda_X(t)dt$ is the cumulative reverse hazard function (CRHF) of X. We now proceed to state two theorems concerning the monotonic behavior of the PDF and demonstrate that the LSG family belongs to class $\mathcal{L}$.

Theorem 4.3.1. *If $f_X(x)$ is an increasing function, then for $\beta > 1$, $f_Y(x)$ is also an increasing function.*

Proof. To prove $f_Y(x)$ is increasing, it is enough to show that $\log(f_Y(x))$ is increasing. We have

$$\frac{d}{dx}\log[f_Y(x)] = \left[\frac{(\beta-1)}{-\log[F_X(x)]} - 1\right]\frac{f_X(x)}{F_X(x)} + \frac{2\beta(-\log[F_X(x)])^{\beta-1} f_X(x)}{e^{\mu} + (-\log[F_X(x)])^{\beta} F_X(x)} + \frac{f_X(x)}{f'_X(x)}.$$

Since $f_X(x)$ is increasing and $\beta > 1$, we have $\frac{d}{dx}\log[f_Y(x)] > 0$. This implies

$f_Y(x)$ is an increasing function. □

Theorem 4.3.2. *Let Y be the LSG transformed random variable of X with CDF $F_Y(x)$ and $F_X(x)$, respectively. Then Y belongs to class $\mathcal{L}$ if and only if X belongs to class $\mathcal{L}$.*

Proof. To prove this, from Klüppelberg (1988), we have a distribution $F(\cdot)$ belongs to class $\mathcal{L}$ if and only if its hazard function, $H(x)$, tends to zero as x approaches ∞. Now from (4.5), we have

$$H_Y(x) = H_w(x)H_X(x).$$

where $H_w(x) = \left[-\frac{\beta e^{\mu}\bar{F}_X(x)}{F_X(x)\log(F_X(x))[e^{\mu}+(-\log(F_X(x)))^{\beta}]}\right]$. By Applying L'Hospitals's rule, we get

$$\lim_{x\to\infty} H_w(x) = \beta.$$

Then, we have

$$\begin{aligned}\lim_{x\to\infty} H_Y(x) &= \lim_{x\to\infty} H_w(x)H_X(x)\\ &= \beta \lim_{x\to\infty} H_X(x).\end{aligned}$$

Thus

$$\lim_{x\to\infty} H_Y(x) = 0 \iff \lim_{x\to\infty} H_X(x) = 0,$$

which completes the proof. □

4.3.1 Estimation of model parameters

Let $X_i,\ i = 1, 2, \ldots, n$ be a random sample of size n from the LSG family with parameters (μ, β, θ), and let $x_1, x_2, ..., x_n$ be the observed values. Here, θ denotes the parameter vector of the baseline distribution $F_X(x_i, \theta)$. Then, the log-likelihood function can be written as

$$\begin{aligned} l(\mu,\beta,\theta) &= n\log[\beta]+n\mu+(\beta-1)\sum_{i=1}^{n}\log\left[-\log\left[F(x_i,\theta)\right]\right]+\sum_{i=1}^{n}\log[f(x_i,\theta)] \\ &\quad -\sum_{i=1}^{n}\log[F(x_i,\theta)]-2\sum_{i=1}^{n}\log[e^{\mu}+(-\log[F(x_i,\theta)])^{\beta}]. \end{aligned}$$

The likelihood equation for μ, β, and Θ can be obtained as

$$\frac{\partial l}{\partial \mu} = n-2\sum_{i=1}^{n}\frac{e^{\mu}}{[e^{\mu}+(-\log[F(x_i,\theta)]^{\beta})]}, \tag{4.7}$$

$$\frac{\partial l}{\partial \beta} = \frac{n}{\beta}+\sum_{i=1}^{n}\log\left[\log\left[F(x_i,\theta)\right]\right]-2\sum_{i=1}^{n}\frac{\log[-\log[F(x_i,\theta)]](\log[F(x_i,\theta)])^{\beta}}{e^{\mu}+(-\log[F(x_i,\theta)])^{\beta}}, \tag{4.8}$$

$$\begin{aligned} \frac{\partial l}{\partial \theta} &= -(\beta-1)\sum_{i=1}^{n}\frac{1}{-\log[F(x_i,\theta)]}\left[\frac{\partial F(x_i,\theta)}{\partial\theta}\right]+\sum_{i=1}^{n}\frac{1}{f(x_i,\theta)}\left[\frac{\partial f(x_i,\theta)}{\partial\theta}\right] \\ &- \sum_{i=1}^{n}\frac{1}{F(x_i,\theta)}\left[\frac{\partial F(x_i,\theta)}{\partial\theta}\right]-2\sum_{i=1}^{n}\frac{(-\log[F(x_i,\theta)])^{\beta-1}}{F(x_i,\theta)[e^{\mu}+(-\log[F(x_i,\theta)])^{\beta}]}\left[\frac{\partial F(x_i,\theta)}{\partial\theta}\right]. \end{aligned} \tag{4.9}$$

It is observed from (4.7) and (4.8) that the estimates of the parameters μ and β cannot be obtained analytically. Moreover, the estimate of the parameter vector Θ depends on the choice of the baseline distribution. Therefore, numerical methods such as the Newton-Raphson algorithm must be employed. We now proceed to construct the asymptotic confidence interval (ACI) for the parameters. As discussed in Section 2.3.1 of Chapter 2, under standard regularity conditions, the asymptotic distribution of $\sqrt{n}(\hat{\Theta}-\Theta)$ is multivariate normal with mean vector zero and covariance matrix $I(\Theta)$, where $\Theta=(\mu,\beta,\theta)$ is the vector of parameters, and $I(\cdot)$ denotes the Fisher information matrix. Accordingly, the $100(1-\gamma)\%$ ACI for the parameter Θ_i is given by

$$\hat{\Theta}_i \pm z_{\gamma/2}\sqrt{\frac{I_{ii}^{-1}(\Theta)}{n}},$$

where $z_{\gamma/2}$ is the $\gamma/2^{th}$ percentile of the standard normal distribution and $I_{ii}^{-1}(\Theta)$ denotes the i^{th} diagonal element of the inverse Fisher information matrix. When the Fisher information matrix is not analytically tractable, the observed information matrix, as introduced by Cox and Hinkley (1974), is employed as an alternative.

4.4 Arctangent sigmoid {Gumbel} family

Consider $T(x)$ as the arctangent sigmoid function and $Q(x)$ as the quantile function of the Gumbel distribution. *i.e.*,

$$\begin{aligned} T(x) &= \frac{\arctan(x) + (\pi/2)}{\pi}, \quad x \in (0,1), \\ Q(u) &= \mu - \beta(\log(-\log(u))), \quad 0 < u < 1,\ \mu \in \mathbb{R},\ \beta > 0. \end{aligned}$$

By Q-transformation rule,

$$T(Q(u)) = \frac{\arctan\left(\mu - \beta(\log[-\log(u)])\right) + \frac{\pi}{2}}{\pi}.$$

Using **Definition 3.3.1**, we introduce a new class of distribution called arctangent sigmoid {Gumbel}.

Definition 4.4.1. *Let X and Y be any two continuous random variables with CDF $F_X(\cdot)$ and $F_Y(\cdot)$, respectively. Then Y is said to be the arctangent sigmoid {Gumbel} (ASG) transformed random variable of X if $F_Y(\cdot)$ is defined as follows:*

$$F_Y(x) = \frac{\arctan\left(\mu - \beta(\log[-\log(F_X(x))])\right) + \frac{\pi}{2}}{\pi}, \quad x \in \mathbb{R},\ \mu \in \mathbb{R},\ \beta > 0. \tag{4.10}$$

The corresponding PDF is defined as

$$f_Y(x) = \frac{\beta f_X(x)}{\pi F(x)(-\log[F(x)])\left((\mu - \beta\log(-\log[F(x)]))^2 + 1\right)}, \tag{4.11}$$

where $f_X(x)$ is the PDF of baseline random variable X. Also from (4.11), it is obvious that $f_Y(x)$ is a weighted form of $f_X(x)$, with weight function given as

$$w(x) = \frac{1}{F(x)(-\log[F(x)])\left((\mu - \beta\log(-\log[F(x)]))^2 + 1\right)}.$$

Thus the PDF can be written as

$$f_Y(x) = \frac{w(x) f_X(x)}{c},$$

where $c = E(w(x))$ is the normalizing constant. If $F_X^{-1}(x)$ exists in explicit form, a random sample from the ASG distribution can be obtained from

$$x = F_X^{-1}\left\{\exp\left[-\exp\left(\frac{\mu - \tan\left(\pi U - \frac{\pi}{2}\right)}{\beta}\right)\right]\right\},$$

where U is the standard uniform random variable. And if $F_X^{-1}(x)$ does not exist in explicit form, the acceptance-rejection method can be used. The survival function, HR and RHF, of ASG transformed random variables, respectively, are

$$\begin{aligned}
S(x) &= \frac{1}{2} - \frac{\arctan[\mu - \beta\log(-\log(F_X(x)))]}{\pi}, \\
H(x) &= \frac{-2\beta f_X(x)}{F_X(x)\log(F_X(x))\left((\mu - \beta\log(-\log(F_X(x))))^2 + 1\right)(\pi - 2\arctan(\mu - \beta\log(-\log(F_X(x)))))} \\
&= \left[\frac{2\beta S(x)}{F_X(x)\Lambda_X(x)\left((\mu - \beta\log(\Lambda_X(x)))^2 + 1\right)(\pi - 2\arctan(\mu - \beta\log(\Lambda_X(x)))}\right] h_X(x), \\
\lambda(x) &= -\frac{2\beta f_X(x)}{\log(F_X(x))\left((\mu - \beta\log(-\log(F_X(x))))^2 + 1\right)(2\tan^{-1}(\mu - \beta\log(-\log(F_X(x)))) + \pi)} \\
&= \left[\frac{2\beta}{\Lambda_X(x)\left((\mu - \beta\log(\Lambda_X(x))^2 + 1\right)(2\tan^{-1}(\mu - \beta\log(\Lambda_X(x))) + \pi)}\right]\lambda_X(x).
\end{aligned}$$

4.4.1 Estimation of model parameters

Let $X_i,\ i = 1, 2, \ldots, n$ be a random sample of size n from the ASG family with parameters (μ, β, θ), and let $x_1, x_2, ..., x_n$ be the observed values. Here, θ represents the parameter vector of the baseline distribution $F_X(x_i, \theta)$. Then, the log-likelihood function can be written as

$$\begin{aligned} l(\mu,\beta,\theta) &= n\log(\beta)+\sum_{i=1}^{n}\log[f_X(x_i,\theta)]-\sum_{i=1}^{n}\log[-\log[F_X(x_i,\theta)]] \\ &\quad -\sum_{i=1}^{n}\log[F_X(x_i,\theta)]-\sum_{i=1}^{n}\log\left[\big(\mu-\beta\log[-\log[F_X(x_i,\theta)]]\big)^2+1\right]. \end{aligned}$$

The likelihood equations for μ, β, and θ are obtained as

$$\begin{aligned} \frac{\partial l}{\partial \mu} &= \sum_{i=1}^{n}\frac{-2\big(\mu-\beta\log[-\log[F_X(x_i,\theta)]]\big)}{\big[\big(\mu-\beta\log[-\log[F_X(x_i,\theta)]]\big)^2+1\big]}, \\ \frac{\partial l}{\partial \beta} &= \frac{n}{\beta}+\sum_{i=1}^{n}\frac{2\big(\mu-\beta\log[-\log[F_X(x_i,\theta)]]\big)\log[-\log[F_X(x_i,\theta)]]}{2\big[\big(\mu-\beta\log[-\log[F_X(x_i,\theta)]]\big)^2+1\big]}, \\ \frac{\partial l}{\partial \theta} &= \sum_{i=1}^{n}\frac{1}{f_X(x_i,\theta)}\left[\frac{\partial f_X(x_i,\theta)}{\partial\theta}\right]-\sum_{i=1}^{n}\frac{1}{F_X(x_i,\theta)\log[F_X(x_i,\theta)]}\left[\frac{\partial F_X(x_i,\theta)}{\partial\theta}\right] \\ &\quad -\sum_{i=1}^{n}\frac{1}{F_X(x_i,\theta)}\left[\frac{\partial F_X(x_i,\theta)}{\partial\theta}\right]-\sum_{i=1}^{n}\frac{2\beta\big(\mu-\beta\log[-\log[F_X(x_i,\theta)]]\big)(\log[-\log[F_X(x_i,\theta)]])}{F_X(x_i,\theta)\big[\big(\mu-\beta\log[-\log[F_X(x_i,\theta)]]\big)^2+1\big]}. \end{aligned}$$

In this case also, the estimates of the parameters μ and β cannot be obtained analytically. Therefore, numerical methods such as the Newton-Raphson algorithm must be employed. Similarly, the ACI for the parameters is constructed following the same steps outlined for the LSG model.

4.5 Error sigmoid {Gumbel} family

Let us consider $T(x)$ as the error sigmoid function and $Q(x)$ as the quantile function of Gumbel distribution. *i.e.*,

$$T(x)=\frac{1}{2}\big(1+erf(x)\big),$$

$$Q(u)=\mu-\beta(\log(-\log(u))),\quad 0<u<1,\ \mu\in\mathbb{R},\beta>0,$$

Then by Q-transformation rule

$$T(Q(u))=\frac{1}{2}\bigg(1+erf\big[\mu-\beta(\log(-\log(F_X(x))))\big]\bigg).$$

Using **Definition 3.3.1**, we construct a new family of distribution known as error sigmoid {Gumbel} transformation.

Definition 4.5.1. *Let X and Y be any two continuous random variables with CDF $F_X(\cdot)$ and $F_Y(\cdot)$, respectively. Then Y is said to be the error sigmoid {Gumbel} (ESG) transformed random variable of X if $F_Y(\cdot)$ is defined as follows:*

$$F_Y(x) = \frac{1}{2}\bigg(1 + erf\big(\mu - \beta(\log(-\log(F_X(x))))\bigg) \quad x \in \mathbb{R},\ \mu \in \mathbb{R},\ \beta > 0.$$

The corresponding PDF is defined as

$$f_Y(x) = -\frac{\beta}{F_X(x)\log[F_X(x)]\sqrt{\pi}} \exp\bigg\{-[\mu - \beta\log(-\log(F_X(x)))]^2\bigg\} f_X(x), \tag{4.12}$$

where $f_X(x)$ is the PDF of baseline random variable X. Also from equation (4.12), it is obvious that $f_Y(x)$ is a weighted form of $f_X(x)$, with weight function given as

$$w(x) = -\frac{1}{F_X(x)\log[F_X(x)]} \exp\bigg\{-[\mu - \beta\log(-\log(F_X(x)))]^2\bigg\}.$$

Thus the PDF in (4.12) can be written as

$$f_Y(x) = \frac{w(x)f_X(x)}{c},$$

where $c = E(w(x))$, the normalizing constant. If $F_X^{-1}(x)$ exists in explicit form, a random sample from the ESG family can be obtained from

$$x = F^{-1}\bigg\{\exp\bigg\{-\exp\bigg\{\frac{\mu - erf^{-1}(1-2U)}{\beta}\bigg\}\bigg\}\bigg\},$$

where U is a standard uniform random variable. And if $F_X^{-1}(x)$ does not exist in explicit form, the acceptance-rejection method can be used. The survival function, HR and RHF, of the ESG transformed random variable are, respectively,

$$\bar{F}_Y(x) = \frac{1}{2}\big(1 - erf\big[\mu - \beta(\log(-\log(F_X(x))))\big]\big),$$

$$\begin{aligned}
H_Y(x) &= \frac{2\beta e^{-(\mu-\beta\log[-\log[F_X(x)]])^2} f_X(x)}{\sqrt{\pi}F_X(x)\log[F_X(x)]\left(erf\left(\mu-\beta\log(-\log(F_X(x)))\right)-1\right)}\\
&= \left[-\frac{2\beta e^{-(\mu-\beta\log[\Lambda_X(x)])^2}\bar{F}_X(x)}{\sqrt{\pi}F_X(x)\Lambda_X(x)\left(erf\left(\mu-\beta\log[\Lambda_X(x)]\right)-1\right)}\right]h_X(x),\\
\lambda_Y(x) &= -\frac{2\beta e^{-(\mu-\beta\log[-\log[F_X(x)]])^2} f_X(x)}{\sqrt{\pi}F_X(x)\log[F_X(x)]\left(erf\left(\mu-\beta\log(-\log(F_X(x)))\right)+1\right)}\\
&= \left[\frac{2\beta e^{-(\mu-\beta\log[\Lambda_X(x)])^2}\bar{F}_X(x)}{\sqrt{\pi}F_X(x)\Lambda_X(x)\left(erf\left(\mu-\beta\log[\Lambda_X(x)]\right)+1\right)}\right]\lambda_X(x).
\end{aligned}$$

4.5.1 Estimation of model parameters

Let $X_i,\ i=1,2,\ldots,n$ be a random sample of size n from the LSG family variable with parameters (μ,β,θ), and let $x_1,x_2,...,x_n$ be the observed values. Here, θ is the parameter vector of the baseline distribution $F(x_i,\theta)$. Then, the log-likelihood function can be written as

$$\begin{aligned}
l(\mu,\beta,\theta) &= n\log\beta-\sum_{i=1}^{n}(\mu-\beta\log[\log[F_X(x_i,\theta)]])^2+\sum_{i=1}^{n}\log[f_X(x_i,\theta)]\\
&- \sum_{i=1}^{n}\log[F_X(x_i,\theta)]-\sum_{i=1}^{n}\log[-\log[F_X(x_i,\theta)]].
\end{aligned}$$

The likelihood equation for μ, β and θ are given as

$$\begin{aligned}
\frac{\partial l}{\partial\mu} &= -2n\mu+2\beta\sum_{i=1}^{n}\log[\log[F_X(x_i,\theta)]],\\
\frac{\partial l}{\partial\beta} &= \frac{n}{\beta}-2\mu\sum_{i=1}^{n}\log[-\log[F_X(x_i,\theta)]]+2\beta\sum_{i=1}^{n}(\log[-\log[F_X(x_i,\theta)]])^2,\\
\frac{\partial l}{\partial\theta} &= 2\sum_{i=1}^{n}\frac{(\mu-\beta\log[-\log[F_X(x_i,\theta)]])}{F_X(x_i,\Theta)\log[F_X(x_i,\theta)]}\left[\frac{\partial F_X(x_i,\theta)}{\partial\theta}\right]+\sum_{i=1}^{n}\frac{1}{f_X(x_i,\theta)}\left[\frac{\partial f_X(x_i,\theta)}{\partial\theta}\right]\\
&\quad-\sum_{i=1}^{n}\frac{1}{F_X(x_i,\theta)}\left[\frac{\partial F_X(x_i,\theta)}{\partial\theta}\right]-\sum_{i=1}^{n}\frac{1}{F_X(x_i,\theta)\log[F_X(x_i,\theta)]}\left[\frac{\partial F_X(x_i,\theta)}{\partial\theta}\right].
\end{aligned}$$

From the above equations, we can compute the ML estimates of μ and β as

$$\hat{\mu} = \beta \sum_{i=1}^{n} \frac{\log[-\log[F_X(x_i,\theta)]]}{n},$$

$$\hat{\beta} = \frac{\mu \sum\limits_{i=1}^{n} \log[-\log[F_X(x_i,\Theta)]] + \sqrt{\mu^2 (\sum\limits_{i=1}^{n} \log[-\log[F_X(x_i,\theta)]])^2 + 2n \sum\limits_{i=1}^{n} (\log[-\log[F_X(x_i,\theta)]])^2}}{2 \sum\limits_{i=1}^{n} (\log[-\log[F_X(x_i,\theta)]])^2}.$$

The estimate of θ depends on the specific baseline distribution. The ACI for the parameters is derived using the same methodology outlined for the LSG model.

4.6 Some modified exponential distributions using QT-Transformation

In this section, we develop generalizations of the exponential distribution by considering the standard exponential distribution as the baseline for the families introduced earlier and explore their key properties.

4.6.1 Logistic sigmoid {Gumbel} - exponential distribution

Definition 4.6.1. *The random variable, X, has the LSG-exponential distribution with parameters μ and β, denoted by LSGE (μ, β), if X has the CDF*

$$F(x) = \frac{e^{\mu}}{e^{\mu} + (-\log(1-e^{-x}))^{\beta}}, \quad x > 0,\ \mu \in R,\ \beta > 0.$$

The corresponding PDF is

$$f(x) = \frac{\beta e^{\mu}[-\log(1-e^{-x})^{\beta-1}]}{(e^{x}-1)[e^{\mu} + (-\log(1-e^{-x}))^{\beta}]^2}.$$

The density plot of LSGE for various values of the parameters is depicted in Figure 4.4.

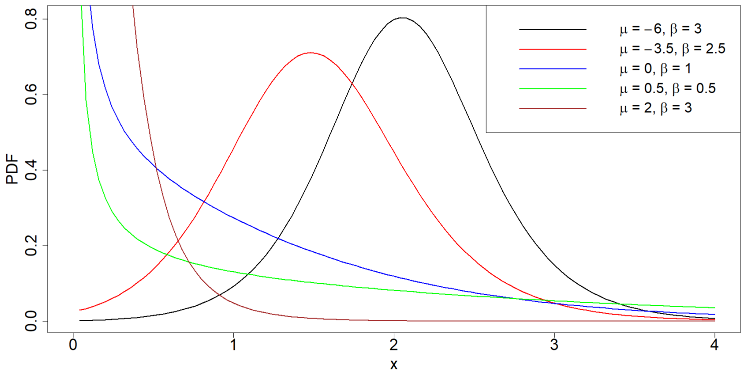

Figure 4.4: Density plots of LSGE distribution.

The survival function and hazard function of LSGE distribution are, respectively, given as

$$\bar{F}(x) = \frac{(-\log 1 - e^{-x})^{\beta}}{e^{\mu} + (-\log(1-e^{-x}))^{\beta}}, \tag{4.13}$$

$$H(x) = \frac{\beta e^{\mu}}{(1-e^{x})\log[1-e^{-x}][e^{\mu} + (-\log[1-e^{-x}])]}. \tag{4.14}$$

Further, the quantile function of LSGE distribution takes the form

$$Q(u) = -\log\left[1 - \exp\left\{-\left(\frac{e^{\mu}(1-U)}{U}\right)^{1/\beta}\right\}\right].$$

We now present a theorem that characterizes the tail behavior of the LSGE random variable.

Theorem 4.6.1. *The LSGE belongs to the class* $\mathcal{L}(\beta)$ *with* $\beta > 0$.

Proof. From **Definition 2.2.2** and (4.13), we have

$$\lim_{x\to\infty}\frac{\bar{F}(x+y)}{\bar{F}(x)} = \lim_{x\to\infty}\left(e^{\mu}\left(-\log\left(1-e^{-x}\right)\right)^{-\beta}+1\right)\left(1 - \frac{e^{\mu}}{e^{\mu} + (-\log(1-e^{-x-y}))^{\beta}}\right).$$

Upon simplification

$$\lim_{x\to\infty}\frac{\bar{F}(x+y)}{\bar{F}(x)} = e^{-\beta y}.$$

Since $\beta > 0$, LSGE belongs to the class $\mathcal{L}(\beta)$ with $\beta > 0$. $\square$

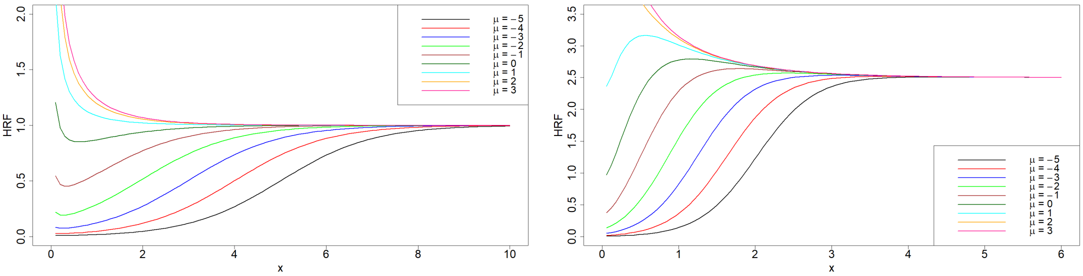

Figure 4.5: Hazard plots of LSGE distribution

Figure 4.5 shows the HR plot of LSGE distribution for a specific value of β and various values of μ. From this, we can observe that the curve tends towards the value of β as x approaches infinity. This serves as an emphasis for the above theorem. Also, we can say that the HR curve shows the non-monotonic behavior such as increasing hazard rate (IHR), decreasing hazard rate (DHR), bathtub (BT), and upside down bathtub (UBT) shapes.

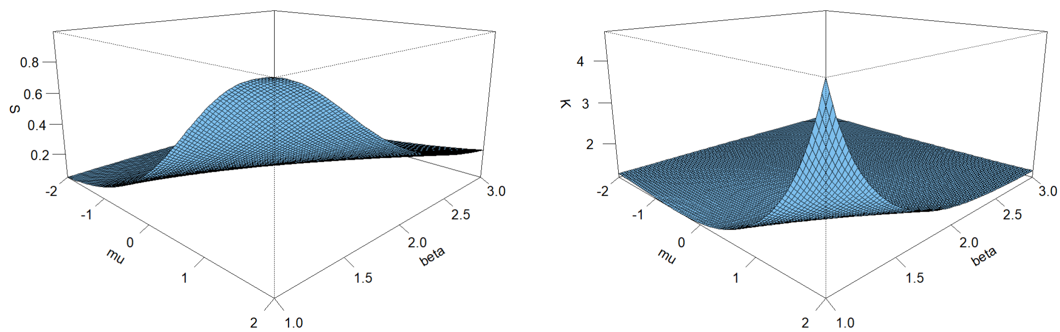

Figure 4.6: 3D-Plot of Galton's skewness (S) and Moor's kurtosis (K) for LSGE distribution.

Figure 4.6 presents the 3D plots of Galton's skewness and Moor's kurtosis for the LSGE distribution over the parameter ranges $\mu \in (-2, 2)$ and $\beta \in (1, 3)$. Throughout this domain, the Galton skewness remains strictly positive, indicating that the LSGE distribution exhibits right skewness. Furthermore, the kurtosis surface shows a sharp peak around $\mu \approx 2$ and $\beta \approx 1$, suggesting high peakedness or leptokurtic behavior, in that region. As either parameter deviates from this region, the kurtosis decreases, implying that the distribution becomes flatter and more platykurtic.

4.6.2 Arctangent sigmoid {Gumbel} - exponential distribution

Definition 4.6.2. *The random variable, X, has the LSG-exponential distribution with parameters μ and β, denoted by ASGE(μ, β), if X has the distribution function*

$$F(x) = \frac{\arctan\left(\mu - \beta \log\left(-\log\left(1 - e^{-x}\right)\right)\right) + \frac{\pi}{2}}{\pi}, \quad x > 0 \mu \in R,\ \beta > 0.$$

The corresponding density function is

$$f(x) = -\frac{\beta e^{-x}}{\pi\left(1 - e^{-x}\right)\log\left(1 - e^{-x}\right)\left(\left(\mu - \beta\log\left(-\log\left(1 - e^{-x}\right)\right)\right)^2 + 1\right)}.$$

The density plots of ASGE distribution for various values of the parameters are depicted in Figure 4.7.

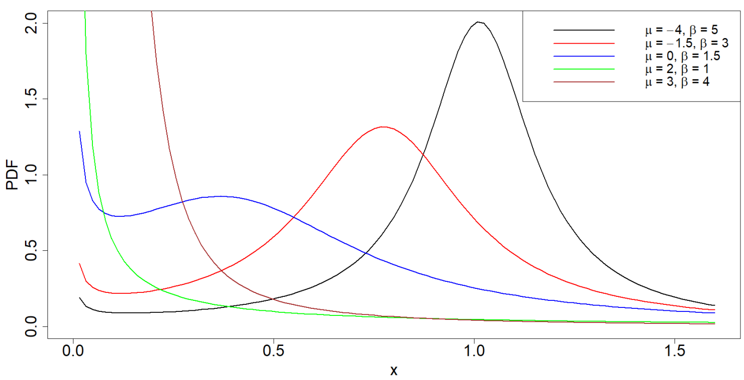

Figure 4.7: Density plots of ASGE distribution.

The survival function and HR of ASGE distribution are respectively given as

$$\bar{F}(x) = \frac{\tan^{-1}\left(\mu - \beta\log\left(-\log\left(1-e^{-x}\right)\right)\right) + \frac{\pi}{2}}{\pi}, \tag{4.15}$$

$$H(x) = \frac{2\beta}{(1-e^{x})\big(\pi - 2\arctan[\mu - \beta\log(-\log[1-e^{-x}])]\big)\log(1-e^{-x})(1+(\mu-\beta\log(-\log(1-e^{-x})))^{2})}.$$

The hazard plots for different parameter values are shown in Figure 4.8. From the figure, we observe that the ASGE model exhibits both decreasing and non-monotonic hazard rates.

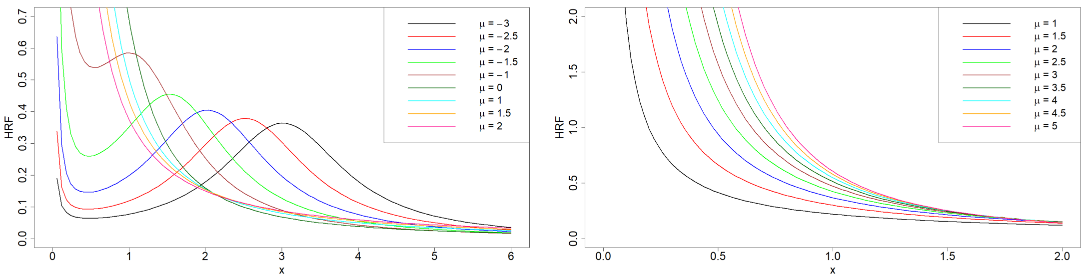

Figure 4.8: Hazard plots of ASGE distribution for different value of μ with $\beta = 1$ and $\beta = 4.5$

Moreover, the quantile function of ASGE distribution is given as

$$Q(u) = -\log\left[1 - \exp\left\{-\exp\left(\frac{\mu - \tan(\pi u - (\pi/2))}{\beta}\right)\right\}\right].$$

Using the quantile function, the 3D plots of Galton's skewness and Moor's kurtosis for the ASGE distribution are presented in Figure 4.9, over the domain $\mu \in (-2.5, 2.5)$ and $\beta \in (1, 4)$. It is evident from the plot that the skewness is consistently positive, indicating the ASGE distribution is right-skewed throughout the considered parameter space. Furthermore, kurtosis is observed to be high near $\mu \approx 2.5$ and $\beta \approx 1$, suggesting significant peakedness or leptokurtic behavior in that region. As either parameter deviates from this point, the kurtosis gradually decreases, implying that the distribution becomes flatter or more platykurtic. Notably, the value of K increases rapidly as μ approaches its upper bound and β approaches its lower bound, reflecting the formation of a sharper and more concentrated peak.

We now discuss some results related to certain classes of distributions and the

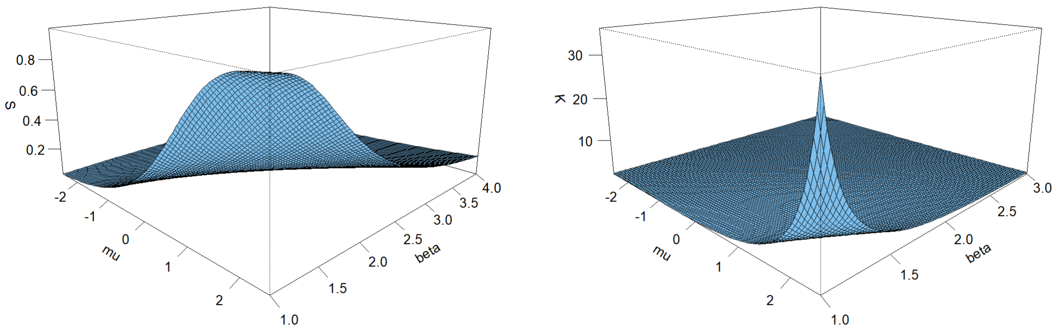

Figure 4.9: 3D-Plot of Galton's skewness (S) and Moor's kurtosis (K) for ASGE distribution.

tail properties of the ASGE distribution.

Theorem 4.6.2. *The ASGE distribution belongs to the class $\mathcal{L}$.*

Proof. From **Definition 2.2.1** and (4.15), we have

$$\lim_{x\to\infty} \frac{\bar{F}(x-y)}{\bar{F}(x)} = \lim_{x\to\infty} \frac{\frac{1}{2} - \frac{\arctan(\mu-\beta\log[-\log[1-e^{-(x-y)}]])}{\pi}}{\frac{1}{2} - \frac{\arctan(\mu-\beta\log[-\log[1-e^{-}x]])}{\pi}}.$$

Applying L'Hospital's rule, we get

$$\lim_{x\to\infty} \frac{\bar{F}(x-y)}{\bar{F}(x)} = 1,$$

which completes the proof. □

Theorem 4.6.3. *The ASGE distribution belongs to the class $\mathcal{D}$ of dominated-variation distributions.*

Proof. From **Definition 2.2.3** and (4.15), we have

$$\lim_{x\to\infty} \frac{\bar{F}(x)}{\bar{F}(2x)} = \lim_{x\to\infty} \frac{\frac{1}{2} - \frac{\arctan(\mu-\beta\log[-\log[1-e^{-x}])}{\pi}}{\frac{1}{2} - \frac{\arctan(\mu-\beta\log[-\log[1-e^{-2x}]])}{\pi}}.$$

Applying L'Hospital rule, we get

$$\lim_{x\to\infty} \frac{\bar{F}(x)}{\bar{F}(2x)} = 2.$$

Since the above limit is finite, ASGE belongs to the class $\mathcal{D}$ of dominated-variation distributions. □

Theorem 4.6.4. *The ASGE distribution belongs to the class $\mathcal{S}$ of sub-exponential distributions.*

Proof. From Klüppelberg (1988) we have that if a distribution F belongs to $(\mathcal{D} \cap \mathcal{L})$, then F belongs to the class of sub-exponential. Now, from **Theorem 4.6.2** and **Theorem 4.6.3**, ASGE belongs to $(\mathcal{D} \cap \mathcal{L}) \subset \mathcal{S}$. □

Theorem 4.6.5. *The ASGE distribution has the following tail properties:*

(i) It is a heavy-tailed distribution.

(ii) Its survival function is a function with regularly varying tails.

Proof. (i) From (2.2) and (4.15), we have

$$\lim_{x\to\infty} e^{sx}\bar{F}(x) = \lim_{x\to\infty} e^{sx}\left(\frac{1}{2} - \frac{\arctan(\mu - \beta\log[-\log[1-e^{-x}]])}{\pi}\right) = \infty.$$

(ii) Similarly, from (2.4), we have

$$\lim_{x\to\infty} \frac{\bar{F}(tx)}{\bar{F}(x)} = \lim_{x\to\infty} \frac{\frac{1}{2} - \frac{\arctan(\mu-\beta\log[-\log[1-e^{-tx}])}{\pi}}{\frac{1}{2} - \frac{\arctan(\mu-\beta\log[-\log[1-e^{-x}]])}{\pi}}, \quad t > 0.$$

Applying L'Hospital rule, we get

$$\lim_{x\to\infty} \frac{\bar{F}(tx)}{\bar{F}(x)} = \frac{1}{t}, \quad t > 0.$$

This completes the proof. □

4.6.3 Error sigmoid {Gumbel} - exponential distribution

Definition 4.6.3. *The random variable X has the LSG-Exponential distribution with parameters μ and β, denoted by ESGE (μ, β), if X has the CDF*

$$F(x) = \frac{1}{2}\Big(1 + erf\big(\mu - \beta \log[-\log[1-e^{-x}]]\big)\Big), \quad x > 0,\ \mu \in R,\ \beta > 0.$$

The corresponding PDF is

$$f(x) = \frac{\beta}{\sqrt{\pi}}\left(\frac{\exp -\left\{x + \big(\mu - \beta \log[-\log[1-e^{-x}]]\big)^2\right\}}{(1-e^{-x})\log[1-e^{-x}]}\right).$$

The HR of ESGE distribution is given as

$$H(x) = \frac{2\beta e^{-\left(\mu - \beta\log\left(-\log\left(1-e^{-x}\right)\right)\right)^2}}{\sqrt{\pi}\,(e^{x}-1)\log(1-e^{-x})\,(erf\,(\mu - \beta\log(-\log(1-e^{-x}))) - 1)}. \quad (4.16)$$

The plots of the PDF and HR of the ESGE distribution for various parameter values are shown in Figures 4.10 and 4.11, respectively. It is observed that the HR exhibits both IHR and BT shapes.

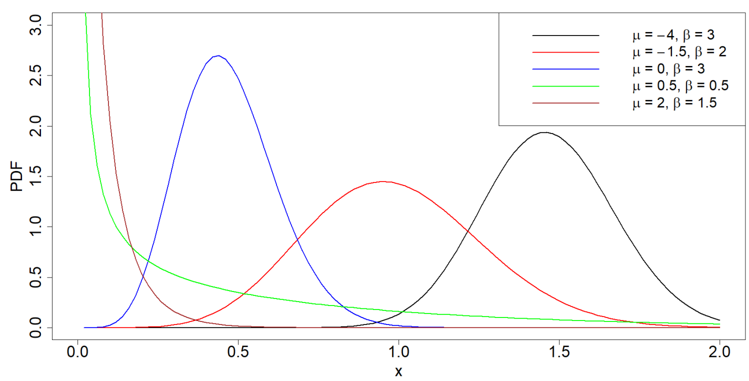

Figure 4.10: The density plot of ESGE distribution.

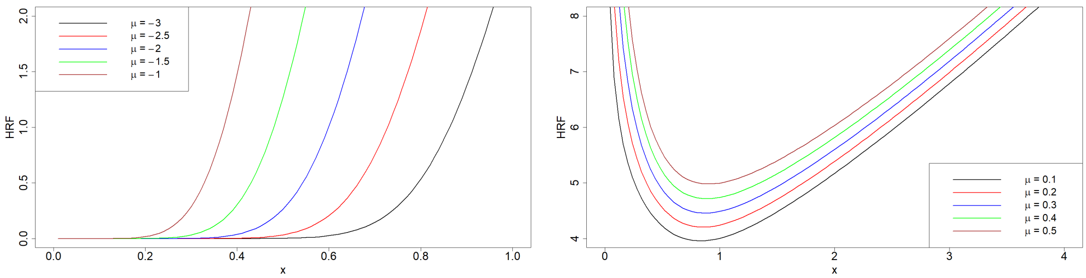

Figure 4.11: Hazard plots of ESGE distribution.

The ESGE distribution does not possess a closed-form expression for its quantile function. Therefore, the inverse error function is employed to compute Galton's skewness and Moor's kurtosis. The resulting 3D plots over the parameter space $\mu \in (-2, 2)$ and $\beta \in (1, 3)$ are presented in Figure 4.12. It is evident from the plots that the skewness remains consistently positive throughout the domain, indicating that the ESGE distribution is inherently right-skewed. Additionally, the kurtosis surface exhibits a sharp peak as μ approaches its upper bound and β approaches its lower bound, reflecting high peakedness or leptokurtic behavior in that region.

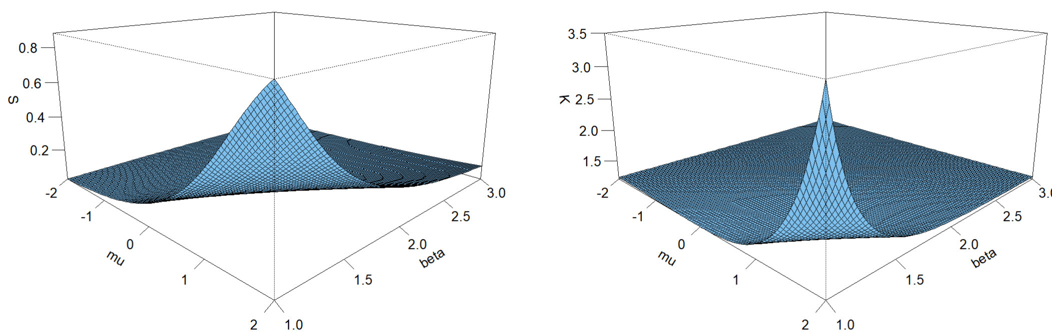

Figure 4.12: 3D-Plot of Galton's skewness (S) and Moor's kurtosis (K) for ESGE distribution.

4.7 Simulation study

To evaluate the performance of the parameter estimates for the proposed distributions, an extensive simulation study is carried out. The performance is assessed based on the absolute bias (AB) and mean square error (MSE) of the parameter estimates. For computational purposes, the R statistical software is used. The results are based on 1,000 replications across various sample sizes and under different parameter combinations. Samples from the LSGE and ASGE distributions are simulated using the inverse transformation technique, while random samples from the ESGE distribution are generated using the acceptance-rejection method.Tables 4.1, 4.2, and 4.3 show the AB, MSE, and the corresponding ACI ($\gamma = 0.05$) for the LSGE, ASGE, and ESGE models, respectively.

Table 4.1: AB, MSE and ACI for ML estimates of the LSGE model

Parameter	n	μ			β		
Value		AB	MSE	ACI	AB	MSE	ACI
	50	0.24950	0.10106	(-2.15275, -0.94699)	0.19724	0.06302	(1.58782, 2.54536)
μ=-1.5	100	0.18107	0.05092	(-1.94846, -1.10282)	0.14370	0.03286	(1.70224, 2.36942)
β=0.25	250	0.10419	0.01713	(-1.77463, -1.24266)	0.08322	0.01115	(1.80493, 2.22240)
	500	0.07881	0.00994	(-1.69431, -1.31868)	0.05876	0.00553	(1.86032, 2.15464)
	50	0.28327	0.12655	(1.38699, 2.74961)	0.30000	0.14560	(2.37585, 3.80955)
μ=2	100	0.20099	0.07152	(1.54449, 2.49638)	0.20913	0.07228	(2.53768, 3.53324)
β=3	250	0.12249	0.02332	(1.72759, 2.32857)	0.12246	0.02306	(2.68106, 3.30153)
	500	0.08479	0.01124	(1.79315, 2.21589)	0.08834	0.01206	(2.79084, 3.23224)

Table 4.2: AB, MSE and ACI for ML estimates of the ASGE model

Parameter Value	n	μ AB	μ MSE	μ ACI	β AB	β MSE	β ACI
	50	0.37016	0.22824	(-3.13896, -1.24524)	0.50463	0.41764	(2.01456, 4.58581)
μ=-2	100	0.25687	0.10664	(-2.80914, -1.49715)	0.35209	0.19506	(2.34161, 4.11653)
β=3	250	0.16593	0.04259	(-2.54423, -1.72464)	0.21814	0.07509	(2.64330, 3.75364)
	500	0.11490	0.02068	(-2.41342, -1.83649)	0.15674	0.03802	(2.78978, 3.56752)
	50	0.26282	0.11466	(0.53692, 1.76797)	0.35939	0.21555	(1.42501, 3.22446)
μ=1	100	0.17716	0.04939	(0.69866, 1.54495)	0.23246	0.08740	(1.65112, 2.88190)
β=2	250	0.11314	0.01961	(0.84667, 1.37615)	0.15413	0.03735	(1.86278, 2.63318)
	500	0.07461	0.00860	(0.91506, 1.28682)	0.10344	0.01702	(1.96248, 2.50250)

Table 4.3: AB, MSE and ACI for ML estimates of the ESGE model

Parameter Value	n	μ AB	μ MSE	μ ACI	β AB	β MSE	β ACI
	50	0.11680	0.02102	(-1.29640, -0.73611)	0.12500	0.02380	(1.22349, 1.82001)
μ=-1	100	0.08400	0.01125	(-1.21113, -0.81594)	0.08886	0.01242	(1.31150, 1.73351)
β=1.5	250	0.05062	0.00413	(-1.13033, -0.88154)	0.05447	0.00470	(1.37437, 1.63845)
	500	0.03590	0.00205	(-1.09160, -0.91592)	0.03871	0.00238	(1.41205, 1.59865)
	50	0.15287	0.03715	(1.17938, 1.90026)	0.25712	0.10359	(2.47575, 3.68280)
μ=1.5	100	0.10571	0.01786	(1.26992, 1.77524)	0.17690	0.04973	(2.62530, 3.47006)
β=3	250	0.06164	0.00612	(1.35136, 1.66897)	0.10690	0.01775	(2.75112, 3.27973)
	500	0.04927	0.00392	(1.38106, 1.62528)	0.08379	0.01121	(2.80479, 3.21166)

It is observed in all cases that, as the sample size increases, both the AB and MSE decrease, and the ACI becomes narrower, indicating that the ML estimates of the proposed model are consistent.

4.8 Real data analysis

In this section, we demonstrate the versatility of the proposed model by applying it to real-world datasets. Three different datasets are used, corresponding to each of the three proposed models. The characteristics of these datasets are summarized in Table 4.4. To assess the goodness of fit, we employ the K-S test. The results are compared against several competing models, specifically chosen as generalizations of the exponential distribution namely generalized exponential (GE) (Gupta and Kundu (1999)), sine-exponential (SinE) (Isa et al. (2022)), beta exponential (BE) (Nadarajah and Kotz (2006a)), modified Kies exponential (MKE) (Aljohani et al. (2021)), and exponential distribution. The CDF of the competing distributions are given as follows:

- The CDF of generalized exponential (GE) is

$$F(x;\alpha,\lambda,\mu)=\left(1-\exp\left\{-\frac{x}{\alpha}\right\}\right)^{\beta},\quad x>0,\ \alpha,\ \beta>0.$$

- The CDF of sine-exponential (SinE) is

$$F(x;\lambda)=\sin\left(\frac{\pi(1-e^{-\lambda x})}{2}\right),\quad x>0,\ \lambda>0.$$

- The CDF of modified Kies exponential (MKE) is

$$F(x;\alpha,\beta)=1-e^{-\left(e^{\beta x}\right)^{\alpha}},\quad x>0,\ \alpha\ \beta>0.$$

- The CDF of exponential distribution is

$$F(x;\lambda)=1-\exp\left\{-\lambda x\right\},\quad x>0,\ \lambda>0.$$

Table 4.4: Summary of Datasets

Data set	Number of observations	Minimum value	First quantile	Median	Mean	Third quantile	Maximum value
I	69	1.312	2.150	2.513	2.477	2.816	3.585
II	43	0.440	0.711	0.778	0.805	0.849	1.444
III	30	0.024	0.065	0.097	0.106	0.140	0.240

4.8.1 Dataset I

We consider the tensile strength dataset reported by Bader and Priest (1982), which represents the tensile strength of carbon fibers measured in gigapascals (GPa). The fibers were tested under a tension gauge length of 20 mm, with a sample size of $n = 69$. The dataset is presented in Table 4.5.

Table 4.5: Tensile strength of carbon fibers

.

1.312	1.314	1.479	1.552	1.700	1.803	1.861	1.865	1.944	1.958
1.966	1.997	2.006	2.021	2.027	2.055	2.063	2.098	2.140	2.179
2.224	2.240	2.253	2.270	2.272	2.274	2.301	2.301	2.359	2.382
2.382	2.426	2.434	2.435	2.478	2.490	2.511	2.514	2.535	2.554
2.566	2.570	2.586	2.629	2.633	2.642	2.648	2.684	2.697	2.726
2.770	2.773	2.800	2.809	2.818	2.821	2.848	2.880	2.954	3.012
3.067	3.084	3.090	3.096	3.128	3.233	3.433	3.585	3.585	

Table 4.6: The ML estimates (with standard errors in bracket), KS statistics and P-value for dataset I

Model	Parameter estimates		KS Statistics	P-value
E	λ=0.40794 (0.04911)	-	0.4482	1.8×10^{-12}
SinE	λ=0.23560 (0.02602)	-	0.4447	2.77×10^{-12}
GE	α=88.2261 (33.3447)	β=2.03748 (0.18066)	0.0949	0.5624
MKE	α=3.97694 (0.36635)	β=0.26001 (0.00597)	0.0657	0.9268
LSGE	μ=-8.17741 (0.84694)	β=3.39897 (0.34029)	0.0475	0.9977

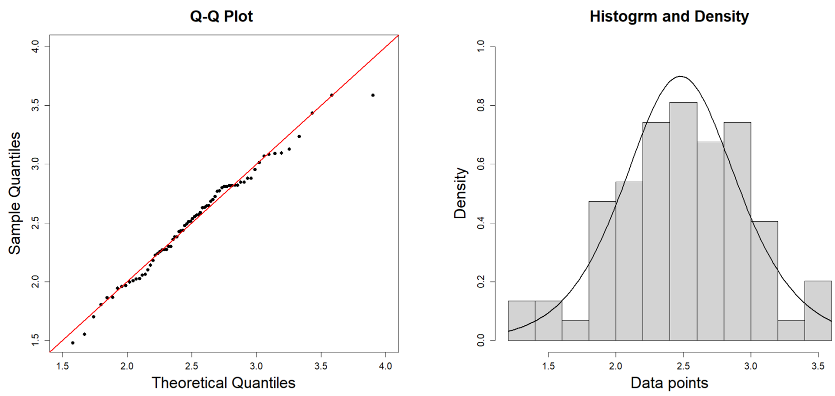

Figure 4.13: Q-Q plot and histogram for LSGE distribution.

The ML estimates, K-S statistic, and P-values for the competing models and the LSGE distribution are summarized in Table 4.6. The relative histogram and Q-Q plot for the fitted LSGE model are shown in Figure 4.13, respectively. The analysis reveals that the LSGE distribution has the lowest K-S statistic and the highest P-value among all the models considered. Therefore, we can conclude that the LSGE distribution provides a better fit to the dataset I compared to the other models.

4.8.2 Dataset II

We consider a dataset of assembled claims for occupational illness provided by the New York State Workers' Compensation Board, available at https://data.ny.gov/Government-Finance/Assembled-Claims-by-OIICS-Part-of-Body/ywkq-zcxe. The dataset consists of 43 observations of average weekly wages, expressed in thousands of dollars, starting from the beginning of the year 2000. The ML estimates, K-S statistic, and P-values for the competing models and ASGE are presented in Table 4.7. Figure 4.14 displays the relative histogram and Q-Q plot for the fitted ASGE distribution.

Table 4.7: The ML estimates (with standard errors in bracket), KS statistics and P-value for dataset II

Model	Parameter estimates		KS Statistics	P-value
E	λ=1.24112 (0.18926)	-	0.4870	6.39×10^{-10}
SinE	λ=0.71698 (0.10033)	-	0.4830	9.33×10^{-10}
MKE	α=3.02792 (0.31887)	β=0.78013 (0.02995)	0.2271	0.0197
GE	α=171.484 (94.3536)	β=7.05922 (0.79145)	0.1387	0.3469
ASGE	μ=-5.09944 (0.10574)	β=10.5067 (0.21180)	0.0760	0.9489

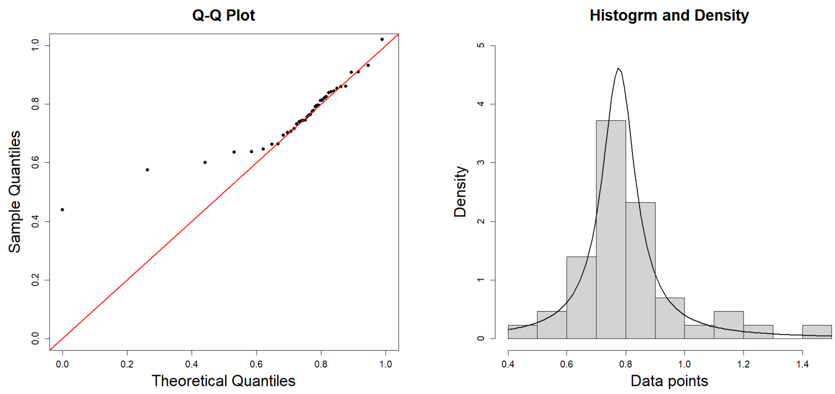

Figure 4.14: Q-Q plot and histogram for ASGE distribution.

The analysis indicates that the ASGE distribution has the lowest K-S statistic and the highest P-value among all the considered models. Thus, we can say that the ASGE distribution offers a better fit to the dataset II compared to the other competing models.

4.8.3 Dataset III

We consider the stock market index data available at https://data.world/chasewillden/stock-market-from-a-high-level. The data consists of the Don Jones stock market price of 30 companies in thousand dollar. The ML estimates, K-S statistic, and P-values for the competing models and the ESGE distribution are shown in Table 4.8. Figure 4.15 presents the histogram and Q-Q plot for the fitted ESGE distribution.

Table 4.8: The ML estimates (with standard errors in bracket), KS statistics and P-value for dataset III

Model	Parameter estimates		KS Statistics	P-value
E	λ=9.39611 (1.71548)	-	0.2299	0.0707
SinE	λ=5.35007 (0.90658)	-	0.2199	0.0938
MKE	α=1.44941 (0.21633)	β=5.50488 (0.50988)	0.0850	0.9688
GE	α=3.79954 (1.18129)	β=7.05922 (3.43392)	0.0714	0.9950
ESGE	μ=2.66950 (0.36801)	β=3.06456 (0.39562)	0.0664	0.9981

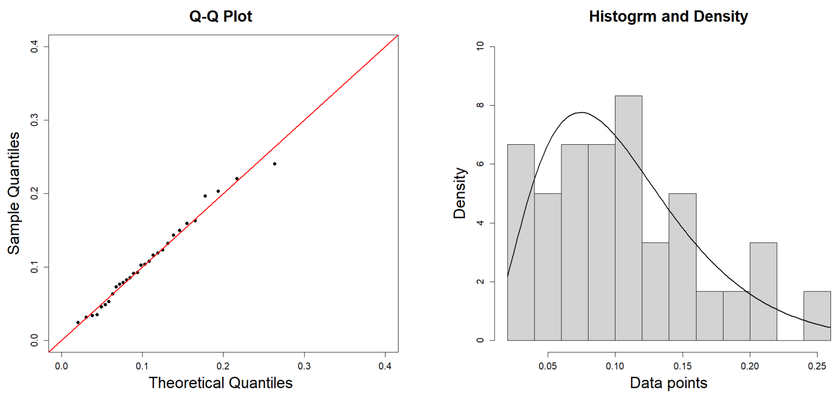

Figure 4.15: Q-Q plot and histogram for ESGE distribution.

The results indicate that the ESGE distribution has the lowest K-S statistic and the highest P-value among all the models considered. Therefore, we conclude that the ESGE distribution provides the best fit to the dataset compared to the other models.

4.9 Summary of the chapter

In this chapter, we proposed three families of distributions: LSG, ASG, and ESG by incorporating three types of sigmoid functions within the QT-transformation framework. Their properties, including estimation of parameters using the MLE method, are thoroughly explored. Sub-models LSGE, ASGE, and ESGE are derived by considering the exponential distribution as the baseline, and their structural properties and tail behavior are analyzed. An extensive simulation study is conducted to assess the performance of the ML estimates based on AB and MSE. To demonstrate the applicability of the proposed distributions, real data analyses are performed, and the results are compared with some generalizations of the exponential distribution, showing that the proposed models provide a superior fit for the considered datasets.

Chapter 5

Application of QT-transformation using some well-known transformations

5.1 Introduction

In the previous chapter, we explored the application of the QT-transformation using the sigmoid function as the core function. Building on this foundation, the current chapter delves into the application of the QT-transformation by incorporating two versatile transformations: Yun transformation and sigmoidal transformation.

The Yun transformation, introduced by Chesneau et al. (2021), is a technique for constructing a family of distributions. Chesneau et al. (2021) developed this transformation based on the work of Yun (2014), which was originally formulated as an approximation to the Gaussian error function. Another transformation closely related to the Yun transformation is the sigmoidal transformation introduced by Prössdorf and Rathsfeld (1991). Similar to Yun transformation, it possesses great flexibility and desirable mathematical properties, making it a suitable tool for modeling complex distributions. In this chapter, we demonstrate the application of QT-transformation using these transformations to generate new families of distributions and analyze their structural properties, tail behavior, and suitability for real-world data modeling.

The chapter is organized as follows: We begin by discussing the mathematical formulation and key characteristics of the Yun and sigmoidal transformations, presented in Section 5.2 and Section 5.3, respectively. In the following sections, Section 5.4 and Section 5.5, we introduce two families of distributions, namely the Yun {unit Gumbel} (YUG) and sigmoidal type-I {unit exponential} (SUE) families, along with their corresponding sub models. Additionally, we explore their properties and carry out parameter estimation. In Section 5.6, an extensive simulation study is conducted to assess the performance of the proposed models. Section 5.7 presents the analysis of two real datasets for illustrative purposes. Finally, the chapter concludes with a summary in Section 5.8.

5.2 Yun transformation

The Gauss error function, commonly denoted as $erf(x)$, is a fundamental tool in statistics and various fields of mathematics. It is defined as

$$erf(x) = \frac{2}{\sqrt{\pi}} \int_0^x e^{-t^2} dt.$$

Since it is impossible to express this integral in a closed form, numerous approximations have been proposed by researchers. However, many of these approximations are only valid within limited ranges and are not invertible. To address these limitations, Yun (2014) introduced a simple, algebraic approximation for the error function that is invertible and also has a wide range. The approximation is defined using the signum function ($sgn(x)$) as follows:

$$\tau_r(x) = \begin{cases} f_r(x), & -r \leq x \leq r \\ sgn(x), & |x| > r, \end{cases}$$

where

$$
\begin{aligned}
sgn(x) &= \begin{cases} -1, & \text{if } x < 0 \\ 0, & \text{if } x = 0 \\ 1, & \text{if } x > 0 \end{cases}, \\
f_r(x) &= \frac{(\alpha + x)^r - (\alpha - x)^r}{(\alpha + x)^r + (\alpha - x)^r}, \quad r > 1,\ \alpha > 0,\ x \in [-\alpha, \alpha].
\end{aligned}
$$

The inverse function of τ_r is

$$\tau_r^{-1}(y) = \alpha \frac{(1 + y)^{1/r} - (1 - y)^{1/r}}{(1 + y)^{1/r} + (1 - y)^{1/r}}, \quad -1 \leq y \leq 1. \tag{5.1}$$

Recognizing the flexibility and desirable mathematical properties of the function $f_r(x)$, Chesneau et al. (2021) introduced a new family of distributions by considering $\alpha = 1$ and referred to it as the Yun transformation. Also, Chesneau et al. (2021) proposed a three-parameter distribution from this family, named the Yun-Weibull distribution. This distribution is derived by applying the Yun transformation to the Weibull distribution. Another work based on the Yun transformation is Akhila et al. (2023), which proposed the Yun-Frechet distribution. We considered the following particular case of the Yun transform defined as

$$T_r(x) = \frac{(1 + x)^r - (1 - x)^r}{(1 + x)^r + (1 - x)^r}, \quad x \in (0, 1), \tag{5.2}$$

with $T_r(x) = 0$ for $x \leq 0$ and $T_r(x) = 1$ for $x \geq 1$.

5.3 Sigmoidal transformation

Another transformation with properties similar to the Yun transformation is the sigmoidal transformation, introduced by Prössdorf and Rathsfeld (1991). This transformation maps the interval $[0, 1]$ onto itself, forming an elongated 'S'-shaped curve. A more formal definition can be found in Elliott (1998) as follows:

Definition 5.3.1. *A real-valued function $\gamma(\cdot)$ is said to be a sigmoidal transformation if the following conditions are satisfied:*

(i) $\gamma(\cdot) \in C^1[0,1] \cap C^\infty(0,1)$ *with* $\gamma(0) = 0$.

(ii) $\gamma(x) + \gamma(1-x) = 1,\ 0 \leq x \leq 1$.

(iii) $\gamma(\cdot)$ *is strictly increasing on* $[0,1]$.

(iv) $\gamma'(x)$ *is strictly increasing on* $[\frac{1}{2}]$ *with* $\gamma'(0) = 0$.

From **Definition 5.3.1**, we observe that the sigmoidal transformation satisfies all the desired properties of the function $T(\cdot)$, defined in the QT-transformation. Now, to generate sigmoidal transformation, consider the following theorem addressed in Elliott (1998) as follows:

Theorem 5.3.1. *Suppose a real-valued function $f(\cdot)$, defined on $[0,1]$, has the following properties:*

(i) $f \in C^1[0,1] \cap C^\infty(0,1)$ *with* $f(0) = f'(0) = 0$, *and* $f(x) > 0$ *for* $0 < x \leq 1$.

(ii) $\frac{f'(x)}{f(x)} + \frac{f'(1-x)}{f(1-x)} > 0$, *for* $0 < x < 1$.

(iii) $\frac{f''(x)}{f(x)} - \frac{f''(1-x)}{f(1-x)} > 2\Big(\frac{f'(x)-f'(1-x)}{f(x)+f(1-x)}\Big)\Big(\frac{f'(x)}{f(x)} + \frac{f'(1-x)}{f(1-x)}\Big)$, *for* $0 < x \leq \frac{1}{2}$.

Then the function γ defined on $[0,1]$ by

$$\gamma(x) = \frac{f(x)}{f(x) + f(1-x)}, \tag{5.3}$$

is sigmoidal.

Many sigmoidal transformations, though not explicitly named as such, have already appeared in the literature. Here, we examine one of these transformations and use it as the foundation for constructing a new family of distributions.

5.3.1 Sigmoidal type-I transformation

The algebraically simplest and most widely used sigmoidal transformations can be achieved by choosing

$$f(x) = x^r, \quad r > 1,$$

in (5.3). This transformation has been used in various contexts; for instance, one may refer to Johnson (1949) and Elliot and Prössdorf (1995). For the purpose of this study, and since we consider one form of sigmoidal transformation, we refer to it as the sigmoidal type-I transformation, denoted as $\gamma_1(x)$ given by

$$\gamma_1(x) = \frac{x^r}{x^r + (1-x)^r}, \quad 0 \leq x < 1, \tag{5.4}$$

and $\gamma_1(1) = 1$. In the upcoming sections, we propose new models based on these transformations and conduct a detailed study of their structural and statistical properties.

5.4 Yun {unit Gumbel} family

From (5.2), it is observed that the Yun transformation, $T_r(x)$, is an increasing and continuous function, satisfying the boundary conditions $T_r(0) = 0$ and $T_r(1) = 1$. Thus, it meets the desired properties of $T(x)$, defined in the **Definition 3.1** of QT-transformation. To proceed, it is necessary to select a quantile function, $Q(\cdot)$, that shares the same support as $T(x)$; that is, we must choose a quantile function of a random variable supported on $(0, 1)$. For this purpose, we consider the unit Gumbel (UG) distribution proposed by Arslan (2023), whose CDF, PDF, and quantile function are given, respectively, as follows:

$$F(x) \;=\; \exp(-(x^{-\alpha} - 1)), \quad x \in (0,1),\ \alpha > 0$$

$$\begin{aligned} f(x) &= \alpha x^{-(\alpha+1)} exp(-(x^{-\alpha}-1)) \\ Q(u) &= (1-\log(u))^{-\frac{1}{\alpha}}, \quad 0<u<1. \end{aligned}$$

Now, we define a new class of distribution called Yun {Unit Gumbel} transformed family as follows.

Definition 5.4.1. *Let X and Y be any two continuous random variables with CDF $F_X(\cdot)$ and $F_Y(\cdot)$ respectively. Then Y is said to be the Yun {unit Gumbel} (YUG) transformed random variable of X, if $F_Y(\cdot)$ is defined as follows:*

$$F_Y(x) = \frac{\left(1+(1-\log(F_X(x)))^{-1/a}\right)^r - \left(1-(1-\log(F_X(x)))^{-1/a}\right)^r}{\left(1+(1-\log(F_X(x)))^{-1/a}\right)^r + \left(1-(1-\log(F_X(x)))^{-1/a}\right)^r}, \quad x \in (0,1),\ \alpha>0,\ r>1. \tag{5.5}$$

The corresponding PDF is

$$f_Y(x) = \frac{4r(1-\log(F_X(x)))^{-\left(\frac{1}{\alpha}+1\right)}\left(3(1-\log(F_X(x)))^{\frac{2}{\alpha}}-1\right)^{r-1} f_X(x)}{\alpha F_Y(x)\left(\left(1-(1-\log(F_Y(x)))^{1/\alpha}\right)^r + \left((1-\log(F_Y(x)))^{1/\alpha}+1\right)^r\right)^2}, \tag{5.6}$$

where $f_X(x)$ is the PDF of the baseline random variable X. From (5.6), we can say that $f_Y(x)$ is a weighted distribution of $f_X(x)$, with the weight function of form

$$w(x) = \frac{(1-\log(F_X(x)))^{-\left(\frac{1}{\alpha}+1\right)}\left((1-\log(F_X(x)))^{\frac{2}{\alpha}}-1\right)^{r-1}}{F_X(x)\left(\left(1-(1-\log(F_X(x)))^{1/\alpha}\right)^r + \left((1-\log(F_X(x)))^{1/\alpha}+1\right)^r\right)^2}.$$

Thus, the PDF $f_Y(x)$ can be written as

$$f_Y(x) = \frac{w(x) f_X(x)}{c},$$

where $c = E(w(x))$ is the normalizing constant. If $F_X^{-1}(x)$ exists in explicit form, the random sample from YUG transformation can be obtained from

$$x = F_X^{-1}\left[\exp\left(1-\left(\frac{(U+1)^{1/r}-(1-U)^{1/r}}{(1-U)^{1/r}+(U+1)^{1/r}}\right)^{-\alpha}\right)\right].$$

where U is the standard uniform random variable. And if $F_X^{-1}(x)$ does not exist in explicit form, the acceptance-rejection method can be used. The survival function and HR of the YUG transformed random variable are, respectively, given as

$$
\begin{aligned}
\bar{F}_Y(x) &= \frac{2\left(1-(1-\log(F_X(x)))^{-1/\alpha}\right)^r}{\left(1-(1-\log(F_X(x)))^{-1/\alpha}\right)^r+\left((1-\log(F_X(x)))^{-1/\alpha}+1\right)^r}, \qquad (5.7)\\
H_Y(x) &= \frac{2r(1-\log(F_X(x)))^{-\left(\frac{1}{\alpha}+1\right)}\left((1-\log(F_X(x)))^{2/a}-1\right)^{r-1} f_X(x)}{\alpha F_X(x)\left(\left(1-(1-\log(F_X(x)))^{-1/\alpha}\right)^r+\left((1-\log(F_X(x)))^{-1/\alpha}+1\right)^r\right)\left(1-(1-\log(F_X(x)))^{-1/\alpha}\right)^r}.
\end{aligned}
$$

In the next section, we introduce a submodel of the YUG family by using the standard exponential distribution as the baseline and analyze its properties.

5.4.1 Yun {unit Gumbel}-exponential distribution

Definition 5.4.2. *The random variable X has the Yun {unit Gumbel}-exponential distribution with parameters α and r denoted by YUGE(α, r) if X has the CDF*

$$
F(x)=\frac{\left(1+\left(1-\log\left(1-e^{-x}\right)\right)^{-1/\alpha}\right)^r-\left(1-\left(1-\log\left(1-e^{-x}\right)\right)^{-1/\alpha}\right)^r}{\left(1+\left(1-\log\left(1-e^{-x}\right)\right)^{-1/\alpha}\right)^r+\left(1-\left(1-\log\left(1-e^{-x}\right)\right)^{-1/\alpha}\right)^r}.
$$

The PDF is given as

$$
f(x)=\frac{4r\left(\left(1-\log\left(1-e^{-x}\right)\right)^{\frac{2}{\alpha}}-1\right)^{r-1}\left(1-\log\left(1-e^{-x}\right)\right)^{\left(\frac{1-2r}{\alpha}\right)-1}}{\alpha\left(e^x-1\right)\left(\left(1+\left(1-\log\left(1-e^{-x}\right)\right)^{1/a}\right)^r+\left(1-\left(1-\log\left(1-e^{-x}\right)\right)^{-1/\alpha}\right)^r\right)^2}.
$$

The survival and HR are respectively given as

$$
\bar{F}(x)=\frac{2\left(1-\left(1-\log\left(1-e^{-x}\right)\right)^{-1/a}\right)^r}{\left(1-\left(1-\log\left(1-e^{-x}\right)\right)^{-1/a}\right)^r+\left(\left(1-\log\left(1-e^{-x}\right)\right)^{-1/a}+1\right)^r}, \qquad (5.8)
$$

$$H(x)=\frac{2r\left(\left(1-\log\left(1-e^{-x}\right)\right)^{1/a}-1\right)^{-r}\left(\left(1-\log\left(1-e^{-x}\right)\right)^{2/a}-1\right)^{r-1}\left(1-\log\left(1-e^{-x}\right)\right)^{\frac{1-r}{a}-1}}{a\left(e^{x}-1\right)\left(\left(1-\left(1-\log\left(1-e^{-x}\right)\right)^{-1/a}\right)^{r}+\left(\left(1-\log\left(1-e^{-x}\right)\right)^{-1/a}+1\right)^{r}\right)}.$$

The density and HR plots of the YUGE distribution for different parameter values are presented in Figure 5.1 and 5.2, respectively. The quantile function takes the form

$$Q(u)=-\log\left(1-\exp\left(1-\left(\frac{(u+1)^{1/r}-(1-u)^{1/r}}{(1-u)^{1/r}+(u+1)^{1/r}}\right)^{-\alpha}\right)\right),\ 0<u<1.$$

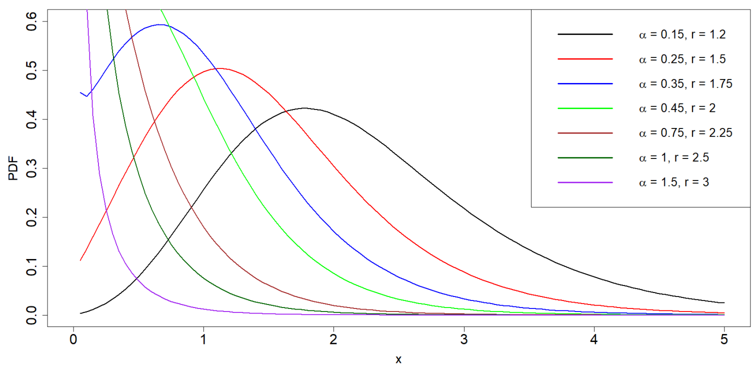

Figure 5.1: Density plot of YUGE distribution

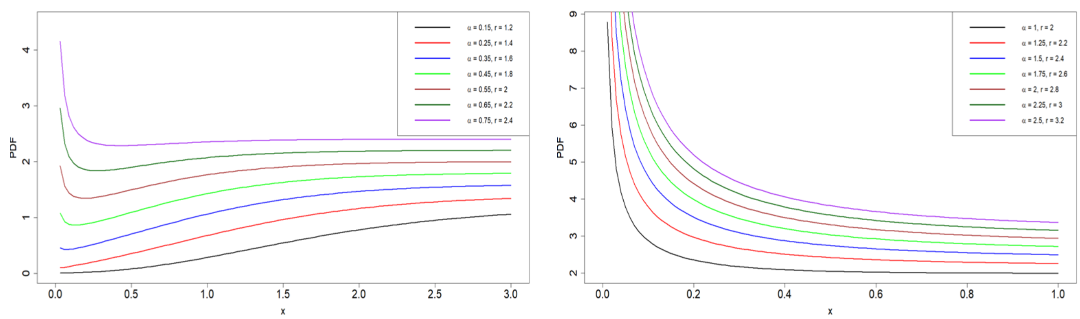

Figure 5.2: Hazard plots of YUGE distribution

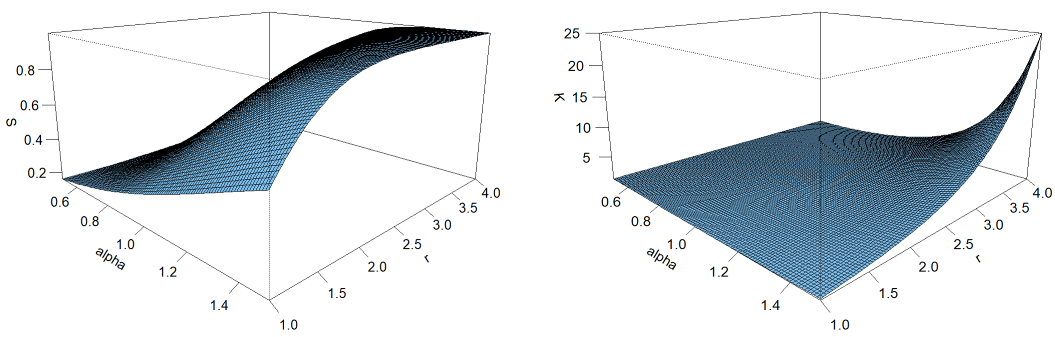

Figure 5.3: 3D-Plot of Galton's skewness (S) and Moor's kurtosis (K) for YUGE distribution.

Figure 5.3 illustrates the 3D plot of Galton's skewness and Moor's kurtosis for the YUGE distribution over the domain $\mu \in (0.5, 1.5)$ and $r \in (1, 4)$. The plot reveals that skewness is positive throughout, indicating a right-skewed nature of the YUGE distribution in this region. Additionally, for smaller values of μ and r, the skewness approaches zero ($S \approx 0$), suggesting near symmetry. The kurtosis surface exhibits a pronounced peak near the corner where both μ and r approach their lower bounds, reflecting high peakedness or leptokurtic behavior. Now, we discuss some results related to certain classes of distributions and the tail properties of the YUGE distribution.

Theorem 5.4.1. *The YUGE belongs to the class $\mathcal{L}(r)$ with $r > 0$.*

Proof. From **Definition 2.2.2** and (5.8), we have,

$$\frac{\bar{F}(x+y)}{\bar{F}(x)} = \frac{\left(1-\left(1-\log\left(1-e^{-(x+y)}\right)\right)^{\frac{-1}{\alpha}}\right)^{r}\left(\left(1-\left(1-\log\left(1-e^{-x}\right)\right)^{\frac{-1}{\alpha}}\right)^{r}+\left(\left(1-\log\left(1-e^{-x}\right)\right)^{\frac{-1}{\alpha}}+1\right)^{r}\right)}{\left(1-\left(1-\log\left(1-e^{-x}\right)\right)^{\frac{-1}{\alpha}}\right)^{r}\left(\left(1-\left(1-\log\left(1-e^{-(x+y)}\right)\right)^{\frac{-1}{\alpha}}\right)^{r}+\left(\left(1-\log\left(1-e^{-(x+y)}\right)\right)^{-1/\alpha}+1\right)^{r}\right)}$$

$$\implies \lim_{x\to\infty} \frac{\bar{F}(x+y)}{\bar{F}(x)} = e^{-yr}.$$

Since $r > 1$, YUGE belongs to the class $\mathcal{L}(r)$ with $r > 0$. $\square$

Notes 4. *From Figure 5.2, we can observe that the hazard curve tends towards the value of r as x approaches infinity, supporting the validity of the above theorem.*

Furthermore, the hazard function exhibits non-monotonic behavior, including IHR, DHR, and BT shapes.

5.4.2 Estimation of parameters

Let $X_i,\ i = 1, 2, \ldots, n$ be a random sample of size n from the YUGE distribution with parameters (α, r) and $x_1, x_2, ..., x_n$ be the observed values. Then, the log-likelihood function can be written as

$$\begin{aligned} l(\alpha, r) &= \log(4r) - \log\alpha + (r-1)\sum_{1=1}^{n}\log\Big(1-\log\left(1-\exp(-x_i)\right)^{\frac{2}{\alpha}}-1\Big) + \\ &\quad \left(\frac{1-2r}{\alpha}-1\right)\sum_{i=1}^{n}\log\left(1-\log\left(1-\exp(-x_i)\right)\right) - \sum_{i=1}^{n}\log\left(\exp(x_i-1)\right) - \\ &\quad 2\sum_{i=1}^{n}\log\left(\left(1+\left(1-\log\left(1-e^{-x}\right)\right)^{1/a}\right)^{r} + \left(1-\left(1-\log\left(1-e^{-x}\right)\right)^{\frac{-1}{\alpha}}\right)^{r}\right). \end{aligned}$$

The maximum likelihood equations are

$$\begin{aligned} \frac{\partial l}{\partial \alpha} &= \frac{1}{\alpha} + \frac{2r}{\alpha^2}\sum_{i=1}^{n}\log\left(1-\log\left(1-e^{-x_i}\right)\right) + (r-1)\sum_{i=1}^{n}\frac{\left(1-\log\left(1-e^{-x_i}\right)^{\frac{2}{\alpha}}\log\left(1-\log(1-e^{-x_i})\right)\right)}{\left(1-\log\left(1-e^{-x_i}\right)\right)^{\frac{2}{\alpha}}-1} \\ &\quad -2r\sum_{i=1}^{n}\left(1-\log\left(1-e^{-x_i}\right)\right)^{\frac{-1}{\alpha}}\log\left(1-\log\left(1-e^{-x_i}\right)\right) \times \\ &\quad \frac{\left(1+\left(1-\log\left(1-e^{-x_i}\right)\right)^{\frac{-1}{\alpha}}\right)^{r-1} + \left(1-\left(1-\log\left(1-e^{-x_i}\right)\right)^{\frac{-1}{\alpha}}\right)^{r-1}}{\left(1+\left(1-\log\left(1-e^{-x_i}\right)\right)^{\frac{-1}{\alpha}}\right)^{r} + \left(1-\left(1-\log\left(1-e^{-x_i}\right)\right)^{\frac{-1}{\alpha}}\right)^{r}} = 0, \qquad (5.9) \\ \frac{\partial l}{\partial r} &= \frac{1}{4r} + \sum_{i=1}^{n}\log\left(\left(1-\log\left(1-e^{x_i}\right)\right)^{\frac{2}{\alpha}}-1\right) \\ &\quad -2\sum_{i=1}^{n}\frac{\left(1+\left(1-\log\left(1-e^{-x_i}\right)\right)^{\frac{-1}{\alpha}}\right)^{r}\log\left(1+\left(1-\log\left(1-e^{x_i}\right)\right)^{\frac{-1}{\alpha}}\right)}{\left(1+\left(1-\log\left(1-e^{-x_i}\right)\right)^{\frac{-1}{\alpha}}\right)^{r} + \left(1-\left(1-\log\left(1-e^{-x_i}\right)\right)^{\frac{-1}{\alpha}}\right)^{r}} \\ &\quad -2\sum_{i=1}^{n}\frac{\left(1-\left(1-\log\left(1-e^{-x_i}\right)\right)^{\frac{-1}{\alpha}}\right)^{r}\log\left(1-\left(1-\log\left(1-e^{x_i}\right)\right)^{\frac{-1}{\alpha}}\right)}{\left(1+\left(1-\log\left(1-e^{-x_i}\right)\right)^{\frac{-1}{\alpha}}\right)^{r} + \left(1-\left(1-\log\left(1-e^{-x_i}\right)\right)^{\frac{-1}{\alpha}}\right)^{r}} = 0. \qquad (5.10) \end{aligned}$$

By solving (5.9) and (5.10), estimators for α and r can be obtained. However, these equations cannot be solved explicitly. Therefore, numerical iterative methods, such as the Newton-Raphson method are employed to obtain the estimates.

We now construct the asymptotic confidence interval (ACI) for the parameters. Under standard regularity conditions, $\sqrt{n}(\hat{\Theta} - \Theta)$ follows a multivariate normal distribution with mean 0 and covariance matrix $I(\Theta)$, where $\Theta = (\alpha, r)$ is the parameter vector and $I(\cdot)$ is the Fisher information matrix. Then the $100(1-\gamma)\%$ confidence interval for the parameters can be obtained as

$$\hat{\Theta}_i \pm z_{\gamma/2}\sqrt{I_{ii}^{-1}(\Theta)},$$

where $z_{\gamma/2}$ is the $\gamma/2^{th}$ percentile of the standard normal distribution and $I_{ii}^{-1}(\Theta)$ denotes the i^{th} diagonal element of the inverse Fisher information matrix. When the Fisher information cannot be obtained analytically, we use the observed information matrix, introduced by Cox and Hinkley (1974).

5.5 Sigmoidal type-I {unit exponential} family

Consider the sigmoidal type-I transformation, $\gamma_1(x)$ defined in (5.4), as $T(x)$. Since the domain is $[0, 1)$, it is necessary to select a quantile function, $Q(\cdot)$ of a random variable supported on $[0, 1)$. For this purpose, we consider a special distribution known as unit exponential distribution proposed by Bakouch et al. (2023), whose CDF, PDF, and quantile function are defined as

$$\begin{aligned}
F(x) &= 1 - \exp\left\{\alpha\left(1 - \left(\frac{x+1}{1-x}\right)^{\beta}\right)\right\}, \quad 0 \le x < 1,\ \alpha > 0,\ \beta > 0, \\
f(x) &= \frac{2\alpha\beta\left(\frac{1+x}{1-x}\right)^{\beta} e^{\alpha\left(1-\left(\frac{x+1}{1-x}\right)\right)^{\beta}}}{1-x^2}, \\
Q(u) &= \frac{\left(1 - \frac{\log(1-u)}{\alpha}\right)^{1/\beta} - 1}{\left(1 - \frac{\log(1-u)}{\alpha}\right)^{1/\beta} + 1}, \quad 0 < u < 1.
\end{aligned}$$

Now, we define a family of distributions called the sigmoidal type-I {unit exponential} family, as follows:

Definition 5.5.1. *Let X and Y be any two continuous random variables with CDF $F_X(\cdot)$ and $F_Y(\cdot)$, respectively. Then Y is said to be the sigmoidal type-I* *{unit exponential} (SUE) transformed random variable of X, if $F_Y(\cdot)$ is defined as follows:*

$$F_Y(x) = \left[2^r \left(\frac{1}{\left(1 - \frac{\log(1-F_X(x))}{\alpha}\right)^{1/\beta} - 1} \right)^r + 1 \right]^{-1}, \quad x > 0,\ \alpha > 0,\ \beta > 0\ r > 1,$$

and the corresponding PDF is

$$f_Y(x) = \frac{2^r r \left(1 - \frac{\log(1-F_X(x))}{\alpha}\right)^{\frac{1}{\beta}-1} \left(\frac{1}{\left(1 - \frac{\log(1-F_X(x))}{\alpha}\right)^{1/\beta} - 1} \right)^{r+1} f_X(x)}{\alpha\beta(1-F_X(x)) \left(2^r \left(\frac{1}{\left(1 - \frac{\log(1-F_X(x))}{\alpha}\right)^{1/\beta} - 1} \right)^r + 1 \right)^2}, \qquad (5.11)$$

where $f_X(x)$ is the PDF of the baseline random variable X. Also, from (5.11), it is clear that $f_Y(x)$ represents a weighted form of $f_X(x)$, where the weight function is given by

$$w(x) = \frac{\left(1 - \frac{\log(1-F_X(x))}{\alpha}\right)^{\frac{1}{\beta}-1} \left(\frac{1}{\left(1 - \frac{\log(1-F_X(x))}{\alpha}\right)^{1/\beta} - 1} \right)^{r+1}}{(1-F_X(x)) \left(2^r \left(\frac{1}{\left(1 - \frac{\log(1-F_X(x))}{\alpha}\right)^{1/\beta} - 1} \right)^r + 1 \right)^2}. \qquad (5.12)$$

Also, provided that $F_X^{-1}(\cdot)$ exists in an explicit form, a random sample from the SUE type-I family can be generated using

$$x = F_X^{-1} \left[1 - \exp\left\{ \alpha \left(1 - \left(2 \left(\frac{U}{1-U} \right)^{\frac{1}{r}} + 1 \right)^{\beta} \right) \right\} \right],$$

where U is the standard uniform random variable. Otherwise, methods such as the acceptance-rejection can be employed. The survival function and HR of the SUE transformed random variable are, respectively, given as

$$\begin{aligned}
\bar{F}_Y(x) &= \frac{2^r\left(\left(\frac{1-\log(1-F_X(x))}{\alpha}\right)^{1/\beta}-1\right)^{-r}}{2^r\left(\left(\frac{1-\log(1-F_X(x))}{\alpha}\right)^{1/\beta}-1\right)^{-r}+1},\\
H_Y(x) &= \frac{r(\alpha-\log(1-F_X(x)))^{\frac{1}{\beta}-1}(\alpha-\log(1-F_X(x)))^{\frac{1}{\beta}-1}\left((\alpha-\log(1-F_X(x)))^{1/\beta}-\alpha^{1/\beta}\right)^{r-1}}{\beta(1-F_X(x))\left(((\alpha-\log(1-F_X(x)))^{1/\beta}-\alpha^{1/\beta})^r+(2\alpha^{1/\beta})^r\right)}.
\end{aligned}$$

Now, we consider the standard exponential distribution as the baseline to introduce a submodel for the SUE family and analyze its properties.

5.5.1 Sigmoidal type-I {unit exponential}-exponential distribution

Definition 5.5.2. *The random variable X has the sigmoidal type-I {unit exponential}-exponential distribution with parameters α, β and r denoted by $SUEE(\alpha,\beta,r)$, if X has the CDF*

$$F(x)=\left[\left(\frac{2}{\left(1+\frac{x}{\alpha}\right)^{1/\beta}-1}\right)^r+1\right]^{-1},\quad x>0,\ \alpha>0,\ \beta>0.$$

The corresponding PDF is given as

$$f(x)=\frac{2^r r\left(1+\frac{x}{\alpha}\right)^{\frac{1}{\beta}-1}\left(\left(1+\frac{x}{\alpha}\right)^{1/\beta}-1\right)^{-(r+1)}}{\alpha\beta\left(2^r\left(\left(1+\frac{x}{\alpha}\right)^{1/\beta}-1\right)^{-r}+1\right)^2}.$$

The survival and HR are respectively given as

$$\begin{aligned}
\bar{F}(x) &= \frac{2^r}{2^r+\left(\left(\frac{x}{\alpha}+1\right)^{1/\beta}-1\right)^r}, &(5.13)\\
H(x) &= \frac{r\left(\frac{x}{\alpha}+1\right)^{\frac{1}{\beta}-1}}{\alpha\beta\left(\left(\frac{x}{\alpha}+1\right)^{1/\beta}-1\right)\left(2^r\left(\left(\frac{x}{\alpha}+1\right)^{1/\beta}-1\right)^{-r}+1\right)}. &(5.14)
\end{aligned}$$

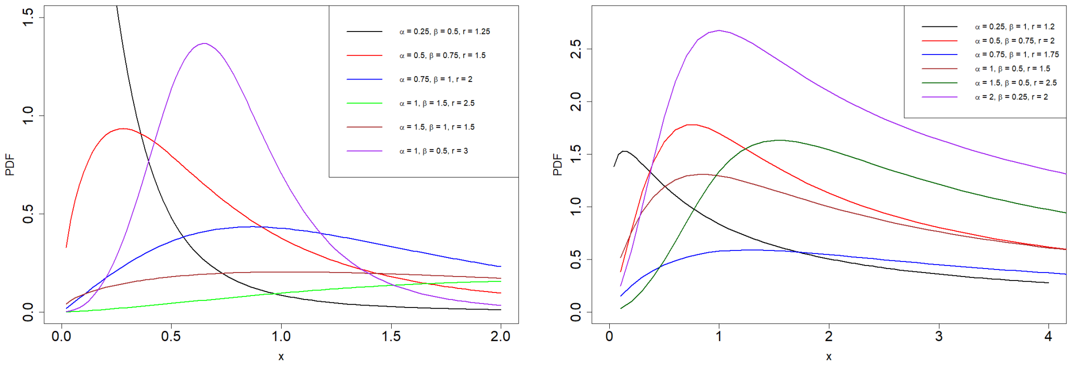

(a) Density plot of SUEE distribution **(b)** Hazard plot of SUEE distribution

Figure 5.4: Hazard and density plots

The density plot and HR plot for different parameter values are given in Figure 5.4a and Figure 5.4b, respectively. Further, the quantile function is given by

$$Q(u) = \alpha \left[\left(2 \left(\frac{u}{1-u} \right)^{\frac{1}{r}} + 1 \right)^{\beta} - 1 \right], \quad 0 < u < 1.$$

Using the quantile function, the 3D plots of Galton's skewness and Moor's kurtosis for the SUEE distribution are presented in Figure 5.5, considering a fixed value of $\alpha = 0.5$ and varying parameters $\beta \in (0, 5)$ and $r \in (1, 6)$.

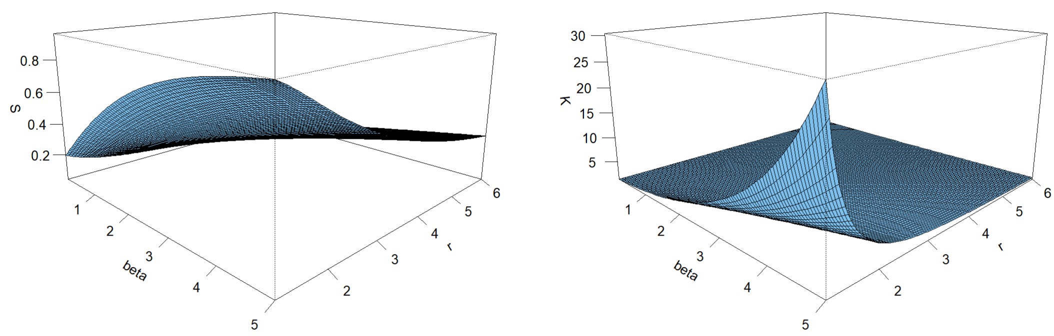

Figure 5.5: 3D-Plot of Galton's skewness (S) and Moor's kurtosis (K) for SUEE distribution.

From the figure, it is observed that in the considered parameter space $S > 0$, indicating that the SUEE distribution is positively skewed. Additionally, for smaller values of β and r, $S \approx 0$, suggesting near symmetry. The kurtosis surface shows a sharp peak when β is large and r is small, reflecting high peakedness or leptokurtic behavior in that region. We now discuss some results related to certain classes of distributions and the tail properties of the SUEE distribution.

Theorem 5.5.1. *The SUEE distributions belongs to the class $\mathcal{L}$.*

Proof. From the survival function (5.13) and **Definition 2.2.1**, we have

$$\lim_{x\to\infty} \frac{\bar{F}(x-y)}{\bar{F}(x)} = \lim_{x\to\infty} \frac{2^r + \left(\left(\frac{x}{\alpha}+1\right)^{\frac{1}{\beta}}-1\right)^r}{2^r + \left(\left(\frac{x-y}{\alpha}+1\right)^{\frac{1}{\beta}}-1\right)^r}.$$

On simplification

$$\lim_{x\to\infty} \frac{\bar{F}(x-y)}{\bar{F}(x)} = 1,$$

which completes the proof. □

Theorem 5.5.2. *The SUEE distribution belongs to the class $\mathcal{D}$ of dominated variation.*

Proof. From the survival function (5.13) and **Definition 2.2.3**, we have

$$\lim_{x\to\infty} \frac{\bar{F}(x)}{\bar{F}(2x)} = \lim_{x\to\infty} \frac{2^r + \left(\left(\frac{2x}{\alpha}+1\right)^{\frac{1}{\beta}}-1\right)^r}{2^r + \left(\left(\frac{x}{\alpha}+1\right)^{\frac{1}{\beta}}-1\right)^r}.$$

Applying L'Hospital rule, we get

$$\lim_{x\to\infty} \frac{\bar{F}(x)}{\bar{F}(2x)} = 2^{\frac{r}{\beta}} < \infty.$$

Since the above limit is finite, SUEE belongs the class $\mathcal{D}$ of dominated-variation. □

Theorem 5.5.3. *The SUEE distribution belongs to the class $\mathcal{S}$ of sub-exponential distributions.*

Proof. From Klüppelberg (1988), a distribution F belongs to $(\mathcal{D} \cap \mathcal{L})$, then

F belongs to the class of sub-exponential. Then from **Theorem 5.5.1** and **Theorem 5.5.2**, SUEE belongs to $(\mathcal{D} \cap \mathcal{L}) \subset \mathcal{S}$. □

Theorem 5.5.4. *The SUEE distribution has the following tail properties:*

(i) It is a heavy tailed distribution.

(ii) It has regularly varying tails.

Proof. (i) From (5.13) and (2.2), we have

$$\lim_{x\to\infty} e^{sx}\bar{F}(x) = \lim_{x\to\infty} e^{sx}\left(\frac{2^r}{2^r + \left(\left(\frac{x}{\alpha}+1\right)^{1/\beta} - 1\right)^r}\right) = \infty.$$

(ii) Similarly, from (2.4), we have

$$\lim_{x\to\infty} \frac{\bar{F}_X(tx)}{\bar{F}_X(x)} = \lim_{x\to\infty} \frac{2^r + \left(\left(\frac{x}{\alpha}+1\right)^{\frac{1}{\beta}} - 1\right)^r}{2^r + \left(\left(\frac{tx}{\alpha}+1\right)^{\frac{1}{\beta}} - 1\right)^r}.$$

Applying L'Hospital rule, we get

$$\lim_{x\to\infty} \frac{\bar{F}(tx)}{\bar{F}(x)} = t^{-\frac{r}{\beta}}, \quad t > 0.$$

This completes the proof. □

5.5.2 Estimation of parameter

Let $X_i,\ i = 1, 2, \ldots, n$ be a random sample of size n from the SUEE distribution with parameters (α, β, r) and $x_1, x_2, ..., x_n$ be the observed values. Then, the log-likelihood function can be written as

$$\begin{aligned} l(\alpha,\beta,r) &= r\log 2 + \log r - \log(\alpha\beta) + \left(\frac{1-\beta}{\beta}\right)\sum_{i=1}^{n}\log\left(1+\frac{x_i}{\alpha}\right) - \\ &\quad (r+1)\sum_{i=1}^{n}\log\left(\left(1+\frac{x_i}{\alpha}\right)^{\frac{1}{\beta}} - 1\right) - 2\sum_{i=1}^{n}\log\left(2^r\left(\left(1+\frac{x}{\alpha}\right)^{\frac{1}{\beta}} - 1\right)^{-r} + 1\right)^2. \end{aligned}$$

Then the corresponding likelihood equations are

$$\begin{aligned}
\frac{\partial l}{\partial \alpha} &= -\frac{1}{\alpha}-\left(\frac{1-\beta}{\alpha^2\beta}\right)\sum_{i=1}^{n}x_i\left(1+\frac{x_i}{\alpha}\right)^{-1}+\left(\frac{r+1}{\alpha^2\beta}\right)\sum_{i=1}^{n}x_i\left(1+\frac{x_i}{\alpha}\right)^{\frac{1}{\beta}-1}\left(\left(1+\frac{x_i}{\alpha}\right)^{\frac{1}{\beta}}-1\right)^{-1}\\
&\quad -\frac{2^{r+2}r}{\alpha^2\beta}\sum_{i=1}^{n}x_i\left(1+\frac{x_i}{\alpha}\right)^{\frac{1}{\beta}-1}\left(\left(1+\frac{x_i}{\alpha}\right)^{\frac{1}{\beta}}-1\right)^{-(r+1)}\left(2^r\left(\left(1+\frac{x_i}{\alpha}\right)^{\frac{1}{\beta}}-1\right)^{-r}+1\right)^{-1}=0\\
\frac{\partial l}{\partial \beta} &= \frac{1}{\beta}-\frac{1}{\beta^2}\sum_{i=1}^{n}\log\left(1+\frac{x_i}{\alpha}\right)-(r+1)\sum_{i=1}^{n}\left(1+\frac{x_i}{\alpha}\right)^{\frac{1}{\beta}}\log\left(1+\frac{x_i}{\alpha}\right)\left(\left(1+\frac{x_i}{\alpha}\right)^{\frac{1}{\beta}}-1\right)^{-1}+\\
&\quad 2^{r+2}r\sum_{i=1}^{n}\left(2^r\left(\left(1+\frac{x_i}{\alpha}\right)^{\frac{1}{\beta}}-1\right)^{-r}+1\right)^{-1}\left(\left(1+\frac{x_i}{\alpha}\right)^{\frac{1}{\beta}}-1\right)^{-(r+1)}\left(1+\frac{x_i}{\alpha}\right)^{\frac{1}{\beta}}\log\left(1+\frac{x_i}{\alpha}\right)=0\\
\frac{\partial l}{\partial r} &= \log 2+\frac{1}{r}-\sum_{i=1}^{n}\log\left(\left(1+\frac{x_i}{\alpha}\right)^{\frac{1}{\beta}}-1\right)-2^{r+1}\sum_{i=1}^{n}\left(2^r\left(\left(1+\frac{x_i}{\alpha}\right)^{\frac{1}{\beta}}-1\right)^{-r}+1\right)^{-1}\times\\
&\quad \left(\left(1+\frac{x_i}{\alpha}\right)^{\frac{1}{\beta}}-1\right)^{-r}\left(\log 2-\log\left(\left(1+\frac{x_i}{\alpha}\right)^{\frac{1}{\beta}}-1\right)\right)=0.
\end{aligned}$$

By solving the above likelihood equations, estimators for α, β, and r can be obtained. Although these equations are not explicitly solvable, numerical iterative methods such as the Newton-Raphson method are employed to compute the estimates efficiently. Also, we construct the ACI for the parameters following similar steps as discussed for the YUGE model.

5.6 Simulation study

To assess the performance of the ML estimates and the ACI of the parameters in the proposed models, we conduct a comprehensive simulation study using R statistical software. The performance is evaluated based on the AB and MSE of the parameter estimates. The results are based on 1000 replications, with varying sample sizes and different parameter combinations. Samples are simulated from the YUGE and SUEE distributions using the inverse transformation technique.

Table 5.1: AB,MSE and ACI for ML estimates of the YUGE model

Parameter Value	n	μ			β		
		AB	MSE	ACI	AB	MSE	ACI
	50	0.03199	0.00160	(0.17054, 0.32221)	0.21511	0.08177	(1.06391, 2.10015)
μ=0.25	100	0.02294	0.00080	(0.19471, 0.30321)	0.14769	0.03669	(1.18427, 1.88824)
β=1.5	250	0.01429	0.00032	(0.21595, 0.28509)	0.08950	0.01244	(1.29031, 1.72412)
	500	0.00974	0.00015	(0.22569, 0.27441)	0.06222	0.00609	(1.35412, 1.66075)
	50	0.05370	0.00448	(0.35128, 0.63158)	0.29833	0.16928	(1.36716, 2.87048)
μ=0.5	100	0.04013	0.00254	(0.39240, 0.59071)	0.21472	0.07816	(1.55804, 2.58698)
β=2	250	0.02514	0.00098	(0.43111, 0.55724)	0.12572	0.02653	(1.71853, 2.35310)
	500	0.01796	0.00050	(0.45071, 054009)	0.09258	0.01368	(1.80414, 2.24982)

The average estimated values along with their corresponding AB, MSE and ACI ($\gamma = 0.05$) for the parameters of the YUGE distribution are shown in Table 5.1. The results indicate that, in all cases, as the sample size increases, both the AB and MSE decrease, and the length of the confidence interval becomes smaller.

Table 5.2: AB,MSE and ACI for ML estimates of the SUEE model

Parameter Value	n	μ AB	μ MSE	μ ACI	β AB	β MSE	β ACI	r AB	r MSE	r ACI
μ=0.5 β=0.75 r=1.5	50	0.08569	0.01575	(0.27571, 0.86893)	0.15356	0.03791	(0.39139, 1.22758)	0.25585	0.07203	(1.07441, 2.24860)
	100	0.06802	0.00992	(0.29961, 0.76370)	0.10770	0.02415	(0.44274, 1.09987)	0.21539	0.05168	(1.16507, 2.06901)
	250	0.04807	0.00418	(0.33879, 0.64219)	0.07359	0.01053	(0.51369, 0.97775)	0.15613	0.02618	(1.27419, 1.84889)
	500	0.03653	0.00198	(0.36897, 0.61826)	0.02251	0.00084	(0.57734, 0.94231)	0.07052	0.00696	(1.26727, 1.74405)
μ=1 β=1.5 r=2	50	0.11806	0.01939	(0.40113, 1.53219)	0.07084	0.01166	(1.00289, 1.92570)	0.16662	0.03992	(1.42645, 2.79686)
	100	0.07689	0.01113	(0.47670, 1.48706)	0.05648	0.00583	(1.08842, 1.86249)	0.11827	0.01164	(1.58623, 2.55937)
	250	0.05665	0.00461	(0.55439, 1.41043)	0.04238	0.00277	(1.18806, 1.82876)	0.06366	0.00777	(1.68628, 2.36943)
	500	0.05436	0.00412	(0.60711, 1.40016)	0.03227	0.00144	(1.126771, 1.74785)	0.04152	0.00386	(1.75292, 2.25117)

Similarly, Table 5.2 presents the average ML estimates of the SUEE distribution, along with their corresponding AB, MSE, and ACI ($\gamma = 0.05$). In this case as well, we observe that as the sample size increases, the AB and MSE decrease, and the ACIs become narrower. These results indicate the consistency of the MLE for the parameters of both models.

5.7 Real data analysis

In this section, we illustrate the versatility of the proposed model by applying it to real-world datasets. We use two different datasets for the proposed models. The characteristics of these datasets are summarized in Table 5.3. To evaluate the fit of the proposed model to the considered datasets, we employ the K-S goodness-of-fit test. The results are then compared with some competing models, including generalized exponential (GE) (Gupta and Kundu (1999)), Weibul exponential

(WE)(Oguntunde et al. (2015)), exponentiated generalized inverted exponential (EGIE) (Oguntunde et al. (2014)) inverse Weibull (IW), Weibull and exponential distribution. The CDF of the competing distributions are given as follows:

- The CDF of generalized exponential (GE) is

$$F(x;\alpha,\lambda,\mu)=\left(1-\exp\left\{-\frac{x}{\alpha}\right\}\right)^{\beta},\quad x>0,\ \alpha,\ \beta>0.$$

- The CDF of Weibull exponential (WE) is

$$F(x;\alpha,\beta,\lambda)=1-\exp\left\{-\alpha\left(e^{\lambda x}-1\right)^{\beta}\right\},\quad x>0,\alpha,\ \beta,\ \lambda>0.$$

- The CDF of inverse Weibull (IW) is

$$F(x;\alpha,\beta)=\exp\left\{-\frac{\alpha}{x}\right\}^{\beta},\quad x>0,\ \alpha\ \beta>0.$$

- The CDF of Weibull is

$$F(x;\alpha,\beta)=1-\exp\left\{\frac{x}{\alpha}\right\}^{\beta},\quad x>0,\ \alpha,\ \beta>0.$$

- The CDF of exponential distribution is

$$F(x;\lambda)=1-\exp\left\{-\lambda x\right\},\quad x>0,\ \lambda>0.$$

Table 5.3: Summary of Datasets

Dataset	Minimum value	First quantile	Median	Mean	Third quantile	Maximum value
I	0.008	0.505	1.334	1.673	2.315	8.596
II	49.26	70.23	81.60	83.65	95.92	146.79

5.7.1 Dataset I

We consider the dataset comprising the failure times (in years) of 50 components, originally reported in Murthy et al. (2004). This dataset has also been utilized in subsequent studies such as Hashempour and Alizadeh (2023) and Hashempour and Alizadeh (2024), and is presented in Table 5.4.

Table 5.4: Failure time of 50 components (in years)

0.008	0.017	0.058	0.061	0.084	0.090	0.134	0.238	0.245	0.353
0.374	0.480	0.495	0.535	0.564	0.681	0.686	0.688	0.921	0.959
1.022	1.092	1.260	1.284	1.295	1.373	1.395	1.414	1.760	1.858
1.892	1.921	1.926	1.933	2.135	2.169	2.301	2.320	2.405	2.506
2.598	2.808	2.971	3.087	3.492	3.669	3.926	4.446	5.119	8.596

Table 5.5: The ML estimates (with standard errors in bracket), KS statistics and P-value for dataset I

Model	Parameter estimates			KS Statistics	P-value
IW	α=0.39540	β=0.55232	-	0.1957	0.765
	(0.10794)	(0.05200)	-		
GE	α=0.56015	β=0.90390	-	0.1005	0.922
	(0.10556)	(0.16281)	-		
Weibull	α=1.65759	β=0.97684	-	0.0947	0.929
	(0.25142)	(0.11152)	-		
E	λ=0.59777	-	-	0.0907	0.935
	(0.08453)	-	-		
WE	α=3.51562	β=0.86907	λ=0.12181	0.0818	0.982
	(4.84144)	(0.15824)	(0.14486)		
YUGE	α=0.53177	r=0.79034	-	0.06284	0.996
	(0.10294)	(0.11276)	-		

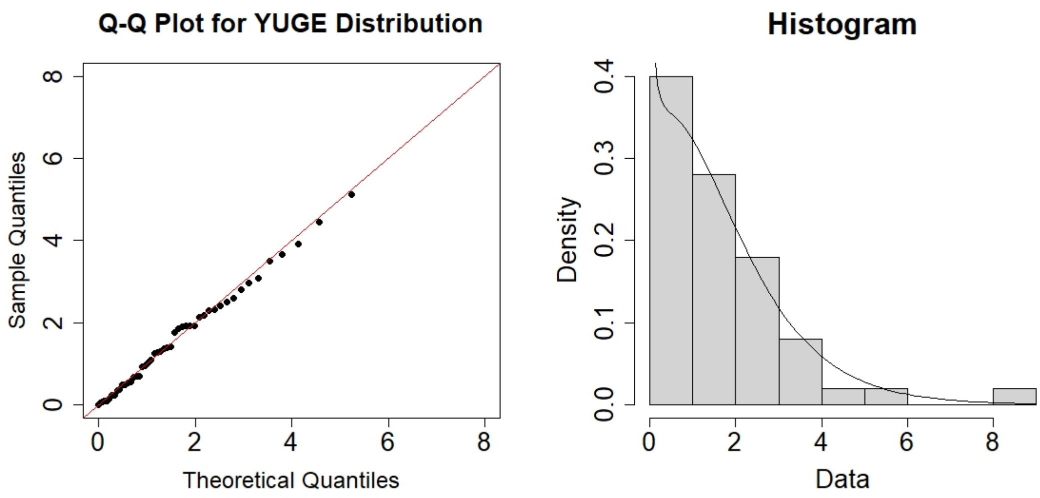

Figure 5.6: Q-Q plot and histogram for YUGE distribution

The ML estimates, K-S statistic, and P-values for the YUGE distribution and competing models are summarized in Table 5.5. The relative histogram and Q-Q plot for the fitted YUGE distribution are presented in Figure 5.6. From Table 5.5, it is observed that the YUGE distribution has the lowest K-S statistic and the highest P-value among all the other models. Therefore, we conclude that the YUGE distribution provides a better fit to the dataset I compared to the other considered models.

5.7.2 Dataset II

We consider the unemployment insurance dataset, which records monthly initial claims for regular unemployment insurance benefits in New York. The dataset consists of initial claims for the years 2013 to 2018, and it is available at https://data.ny.gov/d/ns8z-xewg.

Table 5.6: The ML estimates (with standard errors in bracket), KS statistics and P-value for dataset II

Model	Parameter estimates			KS Statistics	P-value
E	λ=0.01198	-	-	0.4681	0.595
	(0.00142)	-	-		
WE	α=0.01391	β=0.21813	λ=0.20974	0.1440	0.614
	(0.00551)	(0.47944)	(0.46102)		
IW	α=4.77369	β=73.3306	-	0.1025	0.736
	(0.41398)	(1.93371)	-		
Weibull	α=4.56626	β=91.0880	-	0.0888	0.873
	(0.38221)	(2.51198)	-		
GE	α=0.06408	β=121.426	-	0.0724	0.876
	(1.66×10^{-3})	(1.83×10^{-7})	-		
SUEE	α=21.0679	β=1.44254	r=9.77057	0.0465	0.998
	(0.12967)	(0.01875)	(0.94961)		

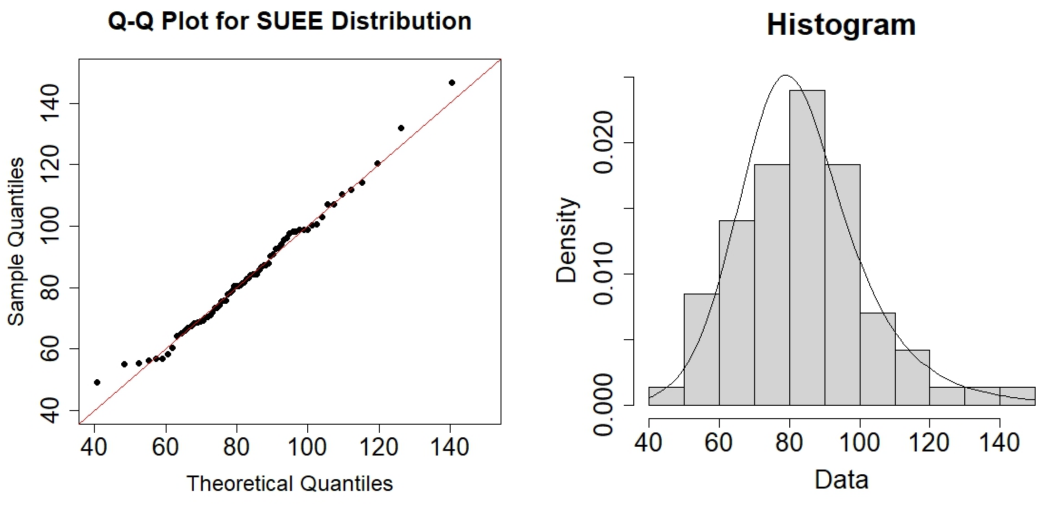

Figure 5.7: Q-Q plot and histogram for SUEE distribution

The ML estimates, K-S statistic, and P-values for the SUEE distribution and competing models are summarized in Table 5.6. The relative histogram and Q-Q plot for the fitted SUEE distribution are presented in Figure 5.7. From

Table 5.6, it is observed that the SUEE distribution has the lowest K-S statistic and the highest P-value among all the other models. This suggests that the SUEE distribution provides the best fit to dataset II when compared to the other considered models.

5.8 Summary of the chapter

This chapter introduced two new families of distributions, the YUG and SUE families—formulated using the QT-transformation. These were developed by incorporating the Yun transformation and the sigmoidal transformation as the core functions. The corresponding sub-models, YUGE and SUEE, were obtained by using the exponential distribution as the baseline. Their structural properties and tail behavior were analyzed, revealing that both belonged to certain significant classes of distributions. Furthermore, the parameters were estimated using the MLE, and ACI were constructed to evaluate the precision of the estimates. Their performance was assessed through extensive simulation studies based on AB and MSE. The results showed that with increasing sample size, both the AB and MSE decreased, and the lengths of the confidence intervals became shorter, confirming the consistency of the ML estimates for both models. Additionally, the applicability of the proposed models was demonstrated using two real-life datasets. Comparative goodness-of-fit analyses showed that the proposed distributions provided a better fit than several existing generalizations of the exponential distribution.

Chapter 6

Application of QT-transformation using an arbitrary function

6.1 Introduction

In earlier discussions, we examined different existing functional forms for the function $T(\cdot)$, a key component in defining the QT-transformation. This approach led to the development of more generalized and flexible models. Specifically, Chapter 4 explored three forms of the sigmoid function as $T(\cdot)$, while Chapter 5 introduced the Yun transformation and the sigmoidal transformation as alternative choices. These transformations provided a robust foundation for constructing models capable of capturing diverse real-world phenomena, including skewed distributions, varying tail behaviors, and complex failure patterns.

Beyond these well-established functional forms, this chapter considers a simple arbitrary function that satisfies the necessary assumptions for $T(\cdot)$. The primary objective is to explore the properties of the models derived from this function and systematically analyze their structural behavior, statistical characteristics, and adaptability to different data patterns.

The chapter is structured as follows: In Section 6.2, we introduce a new transformation for constructing a flexible class of distributions, termed the alpha gamma power transformation (AGPT), and discuss its fundamental properties. Section 6.3 develops the linear representation of the AGPT family using certain series expansions, which enables the derivation of expressions for various statistical measures. Section 6.4 presents the parameter estimation procedure using the MLE method. In Section 6.5, we establish characterization results for the AGPT family. Section 6.6 introduces a specific submodel of the AGPT family, namely the AGPT-exponential distribution, and examines its key properties. Section 6.7 is dedicated to a simulation study evaluating the performance of the proposed models, while Section 6.8 presents a real data analysis to demonstrate their practical applicability. Finally, the chapter concludes with a summary in Section 6.9.

6.2 The proposed model

Recall the definition of QT-transformation (see **Definition 3.3.1**), where the function $T(x) : (x_L, x_R) \to (0, 1)$ is a non-decreasing continuous function such that $T(x_L) = 0$ and $T(x_R) = 1$. We choose $T(\cdot)$ as follows:

$$T(x) = 1 - \alpha^{-x^{\beta}}, \quad x > 0,\ \alpha > 1,\ \beta > 0.$$

Also, choose $Q(\cdot)$ as the quantile function of log-logistic distribution, *i.e.*,

$$Q(u) = \left(\frac{u}{1-u}\right)^{1/\lambda}, \quad \lambda > 0.$$

Then from **Definition 3.3.1**, we have the quantile function $Q_T(\cdot)$, which is obtained as

$$\begin{aligned} Q_T(u) = T(Q(u)) &= 1 - \alpha^{-\left(\frac{u}{1-u}\right)^{\frac{\beta}{\lambda}}} \\ &= 1 - \alpha^{-\left(\frac{u}{1-u}\right)^{\gamma}}, \quad \text{where } \gamma = \frac{\beta}{\lambda} > 0. \end{aligned}$$

Now based on these, we define a new class of distributions referred as the alpha gamma power transformation (AGPT).

Definition 6.2.1. *Let X and Y be any two continuous random variables with CDF $F_X(\cdot)$ and $F_Y(\cdot)$, respectively. Then, Y is the alpha gamma power transformed random variable of X, if $F_Y(\cdot)$ is defined as follows:*

$$F_Y(x) = 1 - \alpha^{-\left(\frac{F_X(x)}{1-F_X(x)}\right)^{\gamma}}, \quad x > 0,\ \alpha > 1,\ \gamma > 0. \tag{6.1}$$

The corresponding PDF is given as

$$f_Y(x) = \gamma \log(\alpha)\ \alpha^{-\left(\frac{F_X(x)}{1-F_X(x)}\right)^{\gamma}} \frac{\big(F_X(x)\big)^{\gamma-1}}{\big(1-F_X(x)\big)^{\gamma+1}}\ f_X(x), \quad x > 0,\ \alpha > 1,\ \gamma > 0, \tag{6.2}$$

where $f_X(x)$ is the PDF of X. From (6.2), it is clear that $f_Y(x)$ is a weighted form of $f_X(x)$, where the weight function $w(x)$ has the form

$$w(x) = \alpha^{-\left(\frac{F_X(x)}{1-F_X(x)}\right)^{\gamma}} \frac{\big(F_X(x)\big)^{\gamma-1}}{\big(1-F_X(x)\big)^{\gamma+1}}.$$

Thus $f_Y(x)$ can be written as

$$f_Y(x) = \frac{w(x) f_X(x)}{c}.$$

where $c = E(w(x))$, the normalizing constant. If $F_X^{-1}(x)$ exist in explicit form, a random sample from AGPT distribution can be obtained from

$$x = F_X^{-1}\left\{\left[\left(\frac{-\log(1-U)}{\log\alpha}\right)^{-\frac{1}{\gamma}} + 1\right]^{-1}\right\},$$

where U is a $U(0,1)$. And if $F_X^{-1}(x)$ does not exist in explicit form, acceptance rejection method can be used. Now, we move on to some reliability measures of the AGPT random variable Y. The survival function and HR of AGPT family are given as

$$\begin{aligned} S_Y(x) &= \alpha^{-\left(\frac{F_X(x)}{1-F_X(x)}\right)^{\gamma}} \\ H_Y(x) &= \gamma\log(\alpha)\frac{\big(F_X(x)\big)^{\gamma-1} f_X(x)}{\big(1-F_X(x)\big)^{\gamma+1}} \\ &= \gamma\log(\alpha)\frac{\big(F_X(x)\big)^{\gamma-1}}{\big(1-F_X(x)\big)^{\gamma}}\ H_X(x), \end{aligned} \tag{6.3}$$

respectively, where $H_X(\cdot)$ is the HR of baseline random variable X. Another measure of aging is the aging intensity (AI) function proposed by Jiang et al. (2003). AI of a random variable X is defined as

$$L_X(x) = \frac{-x f_X(x)}{S_X(x)\log S_X(x)}. \tag{6.4}$$

AI function of AGPT family is given as

$$L_Y(t) = \frac{-x f_Y(x)}{S_Y(x)\log S_Y(x)} = \frac{-\gamma\log S_X(x)}{F_X(x)} L_X(x). \tag{6.5}$$

Now, some results based on general baseline distribution are given below.

Result 1. *If $f_X(x)$ is an increasing function, then for $\gamma > 1$, $f_Y(x)$ is also an increasing function.*

Proof. To prove $f_Y(x)$ is increasing, it is enough to show that $\log f_Y(x)$ is increasing. We have

$$\frac{d}{dx}\log\big(f_Y(x)\big) = \gamma\log(\alpha)\frac{\big(F_X(x)\big)^{\gamma-1}}{\big(1-F_X(x)\big)^{\gamma+1}} f_X(x) + (\gamma-1)\frac{f_X(x)}{F_X(x)} + \frac{f'_X(x)}{f_X(x)} + (\gamma+1)\frac{f_X(x)}{1-F_X(x)}.$$

Since $f_X(x)$ is increasing and $\gamma > 1$, we have $\frac{d}{dx}\log\big(f_Y(x)\big) > 0$. This implies that $f_Y(x)$ is an increasing function. □

Result 2. *If the baseline random variable X has IHR, then for $\gamma > 1$, the AGPT family also has IHR.*

Proof. From (6.3) we have,

$$\frac{d}{dx}H_Y(x) = \frac{\big(F_X(x)\big)^{\gamma-1}}{\big(1-F_X(x)\big)^{\gamma}}\big[H_X(x)(\gamma-1)\big(F_X(x)\big)^{-1} + H'_X(x) + H_X(x)\gamma f_X(x)\big]. \tag{6.6}$$

Since $h_X(\cdot)$ is increasing and $\gamma > 1$, we have $\frac{d}{dx}H_Y(x) > 0$. Thus AGPT family has IHR. □

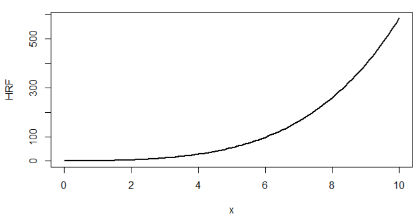

(a) $\alpha = 1.5, \gamma = 2, \lambda = 3, \beta = 3.5$

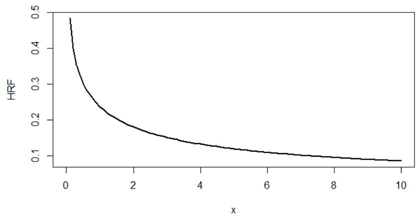

(b) $\alpha = 2, \gamma = 0.75, \lambda = 0.65, \beta = 1.5$

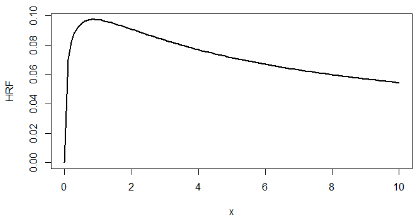

(c) $\alpha = 2.5, \gamma = 1.3, \lambda = 0.3, \beta = 1.5$

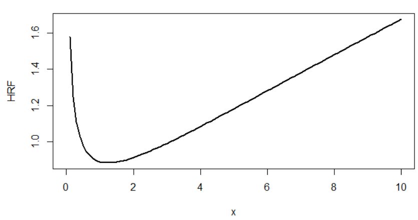

(d) $\alpha = 3, \gamma = 0.6, \lambda = 3, \beta = 3.5$

Figure 6.1: The shapes of HR of AGPT - Pareto for different parameter combinations.

Notes 5. *The effects of the additional parameters on the HR of some parent distribution make the distribution more flexible. For example, the Pareto II distribution, with CDF* $F(x) = 1 - \big(1 + \frac{x}{\beta}\big)^{-\lambda}$, $\beta, \lambda > 0$, *exhibits a DHR, whereas the AGPT-Pareto distribution, as derived from (6.3), has HR.*

$$H(x) = \frac{\gamma\lambda\log\alpha}{\beta}\left(\left[\frac{x+\beta}{\beta}\right]^{\lambda} - 1\right)^{\gamma-1}\left(\frac{x+\beta}{\beta}\right)^{\lambda-1},$$

that demonstrates IHR, DHR, BT, and UBT shapes, as illustrated in Figure 6.1.

6.3 Linear representation of AGPT family

In this section, we discuss the linear representation of PDF of the AGPT family using the series representation given below:

$$\alpha^v = \sum_{i=0}^{\infty} \frac{(\log \alpha)^i}{i!} v^i, \tag{6.7}$$

The PDF of AGPT family can be expressed as

$$\begin{aligned} f_Y(x) &= \gamma \log \alpha \frac{\big(F_X(x)\big)^{\gamma-1} f_X(x)}{\big(1-F_X(x)\big)^{\gamma+1}} \sum_{i=0}^{\infty} \frac{(\log \alpha)^i}{i!} \left[-\left(\frac{F_X(x)}{1-F_X(x)} \right)^{\gamma} \right]^i \\ &= \sum_{i=0}^{\infty} \eta_i f_X(x) \big(F_X(x)\big)^{\gamma(i+1)-1} \big(1-F_X(x)\big)^{-\gamma(i+1)+1}, \end{aligned}$$

where $\eta_i = \frac{\gamma(\log \alpha)^{i+1}(-1)^i}{i!}$. Now, consider the binomial expansion

$$(1-z)^{-k} = \sum_{j=0}^{\infty} \binom{k+j-1}{j} z^j, \tag{6.8}$$

and

$$(1-z)^{k} = \sum_{j=0}^{\infty} \binom{k}{j} z^j, \tag{6.9}$$

for $|z| < 1$ and $k > 0$. Then

$$\begin{aligned} f_Y(x) &= \sum_{i,j=0} \eta_i \binom{\gamma(i+1)+j}{j} f_X(x) \big(F_X(x)\big)^{\gamma(i+1)+j-1} \\ &= \sum_{i,j=0}^{\infty} \eta_{i,j}\ \pi_{\gamma(i+1)+j}(x), \end{aligned} \tag{6.10}$$

where $\eta_{i,j} = \frac{\eta_i}{\gamma(i+1)+j} \binom{\gamma(i+1)+j}{j}$ and $\pi_a(x) = a f_X(x)\big(F_X(x)\big)^{a-1}$, which is the exponentiated generated (Exp-G) density with power parameter a. Thus, from (6.10), it is observed that the AGPT family can be expressed as infinite linear combinations of the exponentiated-g family.This representation enables the derivation of several mathematical properties of the AGPT family using the properties of the exponentiated-g class.

6.3.1 Ordinary moments

The ordinary moments can be used to evaluate a variety of measures, such as measures of central tendency, dispersion, skewness, and kurtosis. Suppose Y is the AGPT random variable. Then the r^{th} ordinary moment of Y can be obtained from (6.10) as

$$\begin{aligned}\mu_r' = E(Y^r) &= \int_{-\infty}^{\infty} \sum_{i,j=0}^{\infty} x^r \eta_{i,j} f_X(x)\big(F_X(x)\big)^{\gamma(i+1)+j-1}\, dx \\ &= \sum_{i,j=0}^{\infty} \eta_{i,j}\ v_{i,j,r},\end{aligned}$$

where $v_{i,j,r} = \int_{-\infty}^{\infty} x^r f_X(x)\big(F_X(x)\big)^{\gamma(i+1)+j-1}\, dx.$

6.3.2 Incomplete moments

The incomplete moments of a distribution are used for measuring inequalities such as the Lorenz curve, Gini measures, and Bonferroni curves. The r^{th} incomplete moment of Y, using (6.10) is

$$\begin{aligned}u_r(x) = E(Y^r|Y < x) &= \int_{-\infty}^{x} \sum_{i,j=0}^{\infty} t^r \eta_{i,j} f_X(t)\big(F_X(t)\big)^{\gamma(i+1)+j-1}\, dt \\ &= \sum_{i,j=0}^{\infty} \eta_{i,j}\ b_{i,j,r},\end{aligned}$$

where $b_{i,j,r} = \int_{-\infty}^{t} t^r f_X(t)\big(F_X(t)\big)^{\gamma(i+1)+j-1}\, dt$. Further, the conditional measure is derived as

$$
\begin{aligned}
E(Y^r|Y>x) &= \frac{1}{S_Y(x)} \int\limits_x^\infty \sum_{i,j=0}^\infty t^r \eta_{i,j} f_X(t)\big(F_X(t)\big)^{\gamma(i+1)+j-1}\, dt \\
&= \frac{1}{S_Y(x)} \sum_{i,j=0}^\infty \eta_{i,j}\ c_{i,j,r},
\end{aligned}
$$

where $c_{i,j,r} = \int\limits_t^\infty t^r f_X(t)\big(F_X(t)\big)^{\gamma(i+1)+j-1}\, dt.$

6.3.3 Moment generating function

The moment generating function of the AGPT random variable is given as

$$M_Y(t) = \int\limits_{-\infty}^{\infty} e^{tx} g(x)\ dx = \sum_{r=0}^\infty \frac{t_r}{r!}\mu'_r = \sum_{i,j,r=0}^\infty \frac{t_r}{r!}\ \eta_{i,j}\ v_{i,j,r}.$$

6.3.4 Mean Residual Life and Mean Waiting Time

The MRL function, $\mu(x)$ of a random variable X is defined as

$$\mu(x) = \frac{1}{S_X(x)} \int_x^\infty S_X(t)\ dt.$$

Using the series representation given in (6.7) and (6.8), the survival function of Y can be expressed as

$$S_Y(x) = \sum_{i,j=0}^\infty a_{i,j}(F_X(x))^{\gamma i+j},$$

where $a_{i,j} = \frac{(\log\alpha)^i(-1)^i}{i!}\binom{\gamma i+j-1}{j}$. Hence the MRL function of Y is obtained as

$$\mu_Y(x) = \alpha^{-(\frac{F_X(x)}{1-F_X(x)})^\gamma} \sum_{i,j=0}^\infty \int_x^\infty a_{i,j}(F_X(t))^{\gamma i+j}\, dt.$$

The MWT, $\bar{\mu}_X(x)$ of a random variable X is defined as

$$\bar{\mu}_X(x) = x - \frac{1}{F_X(x)} \int_0^x t f_X(t)\ dt.$$

Then, the MWT of the AGPT random variable Y can be expressed as

$$\bar{\mu_Y}(x) = x - \left(1 - \alpha^{-\frac{F_X(x)}{1-F_X(x)}^{\gamma}}\right)^{-1} \sum_{i,j=0}^{\infty} \int_0^x \eta_{i,j} t f_X(t) \big(F_X(t)\big)^{\gamma(i+1)+j-1}\ dt.$$

6.3.5 Renyi Entropy and q - entropy

Renyi entropy of a random variable X is defined as,

$$H_{\delta,X} = \frac{1}{1-\delta} \log \int\limits_{-\infty}^{\infty} (f(x))^{\delta}\ dx, \delta > 0.$$

Using the series expansion given in (6.7) and (6.8), we have

$$\big(f_Y(x)\big)^{\delta} = \sum_{i,j=0}^{\infty} d_{i,j} \big(f_X(x)\big)^{\delta} \big(F_X(x)\big)^{\delta(\gamma(i+1)-1)+j},$$

where $d_{i,j} = \frac{\gamma^{\delta} (\log \alpha)^{\delta+i} (-1)^{\delta\gamma i}}{i!} \binom{\delta(\gamma(i+1)-1)+j-1}{j}$. Therefore from the above equation, the Renyi entropy of the AGPT random variable Y is

$$H_{\delta,Y} = \frac{1}{1-\delta} \log \sum_{i,j=0}^{\infty} \int\limits_{-\infty}^{\infty} d_{i,j} \big(f_X(x)\big)^{\delta} \big(F_X(x)\big)^{\delta(\gamma(i+1)-1)+j}\ dx.$$

Similarly, the q - entropy of the AGPT random variable Y can be obtained as

$$\begin{aligned} H_{q,Y} &= \frac{1}{1-q} \log \left(1 - \int\limits_{-\infty}^{\infty} (f_Y(x))^q\ dx\right), \quad q \in \mathbb{R} \\ &= \frac{1}{1-q} \log \left[\sum_{i,j=0}^{\infty} 1 - \int\limits_{-\infty}^{\infty} d_{i,j} \big(f_X(x)\big)^q \big(F_X(x)\big)^{q(\gamma(i+1)-1)+j}\ dx\right]. \end{aligned}$$

6.3.6 Order statistics

The PDF of s^{th} order statistics of a random variable X is defined as

$$f_{(s),X}(x) = \frac{f_X(x)}{B(s, n-s+1)} \sum_{k=0}^{n-s} (-1)^k \binom{n-s}{k} \big(F_X(x)\big)^{k+s-1},$$

where $B(\cdot,\cdot)$ is the beta function. Let $X_i, i = 1, 2, \ldots, n$ be the random variables form AGPT family and $X_{(i)}$ be the corresponding order statistics. Using the series expansion given in (6.7), (6.8), and (6.9), we have

$$\big(F_Y(x)\big)^u = \sum_{i,j,v=0}^{\infty} \epsilon_{i,j,v} \big(F_X(x)\big)^{\gamma i+j},$$

where $\epsilon_{i,j,v} = \frac{(-1)^j (\log\alpha) j^i}{i!} \binom{u}{j} \binom{\gamma i+v-1}{v}$. Now, by replacing u by $k+s-1$ in the above equation, the PDF of s^{th} order statistics of the AGPT random variable Y is found to be

$$f_{(s),Y}(x) = \frac{f_X(x)}{B(s, n-s+1)} \sum_{i,j,v=0}^{\infty} \sum_{k=0}^{n-s} (-1)^k \binom{n-s}{k} \epsilon_{i,j,v} \big(F_X(x)\big)^{\gamma i+j}.$$

Furthermore, the r^{th} moment of s^{th} order statistics is

$$\begin{aligned} E(Y^r_{(s)}) &= \int_{-\infty}^{\infty} x^r f_{(s),Y}(x)\, dx \\ &= \frac{1}{B(s, n-s+1)} \sum_{i,j,v=0}^{\infty} \sum_{k=0}^{n-s} (-1)^k \binom{n-s}{k} \epsilon_{i,j,v} \int_{-\infty}^{\infty} x^r f_X(x) \big(F_X(x)\big)^{\gamma i+j}\, dx. \end{aligned}$$

6.4 Estimation of parameters

Let $X_i, i = 1, 2, \ldots, n$ be a random sample of size n from the AGPT family with parameters (α, γ, Θ) and observed values $x_1, x_2, ..., x_n$. Here, Θ denotes the parameter vector of the baseline distribution $F_X(x_i, \Theta)$. The log-likelihood function can be written as

$$\begin{aligned} l(\alpha,\gamma,\Theta) &= n\log\gamma + n\log(\log\alpha) + (\gamma-1)\sum_{i=1}^{n}\log F_X(x_i,\Theta) + \sum_{i=1}^{n}\log f_X(x_i,\Theta) \\ &- \left[\sum_{i=1}^{n}\frac{F_X(x_i,\Theta)}{1-F_X(x_i,\Theta)}\right]^{\gamma}\log\alpha - (\gamma+1)\sum_{i=1}^{n}\log\big(1-F_X(x_i,\Theta)\big). \end{aligned}$$

The likelihood equation for α, γ and λ are given below

$$\begin{aligned} \frac{\partial l}{\partial\alpha} &= \frac{n}{\alpha\log\alpha} - \frac{1}{\alpha}\sum_{i=1}^{n}\left[\frac{F_X(x_i,\Theta)}{1-F_X(x_i,\Theta)}\right]^{\gamma}, \\ \frac{\partial l}{\partial\gamma} &= \frac{n}{\gamma} + \sum_{i=1}^{n}\log F_X(x_i,\Theta) - \sum_{i=1}^{n}\left[\frac{F_X(x_i,\Theta)}{1-F_X(x_i,\Theta)}\right]^{\gamma}\log\left[\frac{F_X(x_i,\Theta)}{1-F_X(x_i,\Theta)}\right] \qquad (6.11) \\ &\quad -\sum_{i=1}^{n}\log\big(1-F_X(x_i,\Theta)\big), \\ \frac{\partial l}{\partial\theta} &= \sum_{i=1}^{n}\left(\frac{(\gamma-1)}{F_X(x_i,\Theta)} - \gamma\log\alpha\left[\frac{F_X(x_i,\Theta)}{1-F_X(x_i,\Theta)}\right]^{\gamma-1} - \frac{(\gamma+1)}{1-F_X(x_i,\Theta)}\right)\frac{\partial F_X(x_i,\Theta)}{\partial\theta} \\ &\quad +\sum_{i=1}^{n}\frac{1}{f_X(x_i,\Theta)}\frac{\partial f_X(x_i,\Theta)}{\partial\theta}. \qquad (6.12) \end{aligned}$$

From (6.11), we can obtain the MLE of α, say $\hat{\alpha}$ as

$$\hat{\alpha} = e^{n\sum_{i=1}^{n}\left[\frac{F_X(x_i,\hat{\Theta})}{1-F_X(x_i,\hat{\Theta})}\right]^{\gamma}}.$$

Since the estimate of γ and Θ cannot be solved analytically, numerical methods such as Newton-Raphson algorithm are employed.

6.5 Characterization results

Characterization results in the context of probability distributions typically involve identifying distributions based on specific properties or relationships they demonstrate. This section explores two characterizations of the AGPT family, which are based on (i) the ratio of two truncated moments and (ii) the HR.

6.5.1 Characterization based on truncated moments

Here, we examine the characterization of the AGPT family through the ratio of two truncated moments. To accomplish this, we utilize a theorem outlined by Glänzel (1987) as described below:

Theorem 6.5.1. *(Glänzel (1987)) Let $(\Omega, \mathcal{F}, \boldsymbol{P})$ be a given probability space and let $H = [a, b]$ be an interval for some $a < b$ ($a = -\infty, b = \infty$ might as well be allowed). Let $X : \Omega \to H$ be a continuous random variable with the distribution function $F(\cdot)$ and let $q_1(x)$ and $q_2(x)$ be two real function defined on H such that*

$$E(q_1(X)|X \geq x) = E(q_2(X)|X \geq x)\epsilon(x), \quad x \in H, \tag{6.13}$$

is defined with some real function $\epsilon(x)$. Assume that $q_1, q_2 \in C^1(H), \epsilon\ inC^2(H)$ and F is twice continuously differentiable and strictly monotone function on the set H. Finally, assume that the equation $\epsilon q_1 = q_2$ has no real solution in the interior of H. Then F is uniquely determined by the functions q_1, q_2, and ϵ, particularly

$$F(x) = \int_a^x C \left| \frac{\epsilon'(u)}{\epsilon'(u)q_1(u) - q_2(u)} \right| \exp(-s(u))\ du, \tag{6.14}$$

where the function s is a solution of the differential equation $s' = \frac{\epsilon' q_1}{\epsilon' q_1 - q_2}$ and C is the normalization constant, such that $\int_H dF = 1$.

Proposition 6.5.1. *Let $X : \Omega \to (0, \infty)$ be a continuous random variable and let $q_1(x) = \alpha^{\frac{F_X(x)}{1-F_X(x)}}(1 - F_X(x)^{\gamma+1})$ and $q_2(x) = q_1(x)(F_X(x))^{1-\gamma}$, for $x > 0$. The random variable X belongs to AGPT family if and only if $\epsilon(\cdot)$ defined in **Theorem 6.5.1** has the form*

$$\epsilon(x) = \frac{\gamma \bar{F}(x)}{(1 - (F_X(x))^\gamma)}, \quad x > 0. \tag{6.15}$$

Proof. Let X be a random variable with PDF (6.2), then

$$(1 - F_X(x))\mathrm{E}(q_1(x)|X \geq x) = (1 - (F_X(x)^\gamma))\log(\alpha), \quad x > 0,$$

and

$$(1 - F_X(x))\mathrm{E}(q_2(x)|X \geq x) = \gamma\log(\alpha)\bar{F}(x), \quad x > 0.$$

Further

$$\epsilon(x)q_1(x) - q_2(x) = \frac{q_1(x)}{1 - (F_X(x))^(\gamma)}(\gamma\bar{F}(x) - (F_X(x))^\gamma + F_X(x)).$$

Conversely, if $\epsilon(x)$ is of the form in (6.15), then

$$s'(x) = \frac{\epsilon'(x)q_1(x)}{\epsilon(x)q_1(x) - q_2(x)} = \frac{\gamma(F_X(x))^{\gamma-1}f_X(x)}{1 - (F_X(x))^\gamma}, \tag{6.16}$$

and hence $s(x) = -\log(1 - (F_X(x))^\gamma), \quad x > 0$. Now, in view of **Theorem 6.5.1**, X has CDF (6.1). $\square$

Corollary 6.5.2. *Let $X : \Omega \to (0, \infty)$ be a continuous random variable and let $q_1(x)$ be defined as in **Proposition 6.5.1**. The PDF of X is (6.2) if and only if there exist functions q_2 and ϵ defined in **Theorem 6.5.1** satisfying the differential equation*

$$\frac{\epsilon'(x)q_1(x)}{\epsilon(x)q_1(x) - q_2(x)} = \frac{\gamma(F_X(x))^{\gamma-1}f_X(x)}{1 - (F_X(x))^\gamma}, \quad x > 0.$$

The general solution of the differential equation given in **Corollary 6.5.2** is

$$\epsilon(x) = \frac{1}{1 - (F_X(x))^\gamma}\int \gamma(F_X(x))^{\gamma-1}q_2(x)(q_1(x))^{-1}f_X(x)dx + C,$$

where C is a constant. Note that a set of functions satisfying the above differential equation is given in **Proposition 6.5.1** with $C = 1$. However, it should also be noted that there are other triplets (q_1, q_2, ϵ) satisfying the conditions of **Theorem 6.5.1**.

6.5.2 Characterization based on hazard rate

Suppose that we have a random variable X with twice differentiable HR. It is well established that the HR satisfies the following first-order differential equation:

$$\frac{f'(x)}{f(x)} = \frac{H'(x)}{H(x)} - H(x).$$

For numerous univariate continuous distributions, this remains the only characterization concerning the HR. The following proposition gives a non-trivial characterization of the AGPT family based on HR.

Proposition 6.5.2. *Let $Y : \Omega \to (0, \infty)$ be a continuous random variable. Then Y is an AGPT random variable corresponding to the baseline X if and only if its HR, $H_Y(x)$ satisfies the following differential equation:*

$$H'_Y(x) - (\gamma-1)\frac{f_X(x)}{F_X(x)}H_Y(x) = \frac{\gamma \log(\alpha)(F_X(x))^{\gamma-1}\big(f'_X(x)(1-F_X(x)) + (\gamma+1)(f_X(x))^2\big)}{(1-F_X(x))^{\gamma+1}}, \tag{6.17}$$

with the boundary condition $\lim_{x\to 0} H_Y(x) = 0.$

Proof. If Y has PDF (6.2), then the differential equation in (6.17) holds. Conversely, if the differential equation holds, then

$$\frac{d}{dx}\left(\frac{H_Y(x)}{(F_X(x))^{\gamma-1}f_X(x)}\right) = \gamma(\gamma+1)\log(\alpha)\frac{d}{dx}\left(\frac{1}{(\gamma+1)(1-F_X(x))^{\gamma+1}}\right).$$

Equivalently

$$H_Y(x) = \gamma \log(\alpha)\frac{\big(F_X(x)\big)^{\gamma-1} f_X(x)}{\big(1-F_X(x)\big)^{\gamma+1}},$$

which is the HR of AGPT family. $\square$

6.6 Alpha gamma power transformed exponential distribution

In this section, we apply the alpha gamma transformation to an exponential distribution with parameter λ and introduce a novel model called the three parameter alpha gamma power transformed exponential (AGPTE) distribution.

Definition 6.6.1. *(AGPTE distribution): A random variable X is said to follow a three-parameter alpha gamma power transformed exponential distribution denoted by AGPTE (α,γ,λ), if its CDF has the form*

$$F(x) = 1 - \alpha^{-(e^{\lambda x}-1)^{\gamma}}, \quad x > 0,\ \alpha > 1,\ \gamma > 0,\ \lambda > 0.$$

The corresponding PDF is given as

$$f(x) = \gamma\lambda(\log\alpha)e^{\lambda x}(e^{\lambda x} - 1)^{\gamma-1}\alpha^{-(e^{\lambda x}-1)^{\gamma}}.$$

The plots of PDF and HR for different values of parameters are sketched in Figure 6.3 and Figure 6.2 respectively.

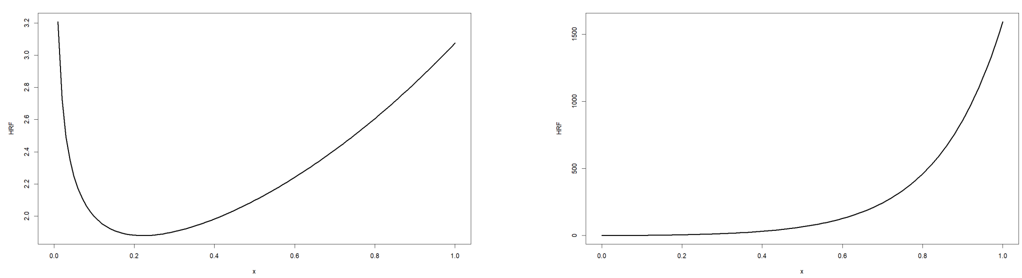

(a) $\alpha = 3$, $\gamma = 0.75$, $\lambda = 1.3$ **(b)** $\alpha = 2$, $\gamma = 2$, $\lambda = 3$

Figure 6.2: The hazard rate plot of AGPTE distribution (a) BT (b) IHR.

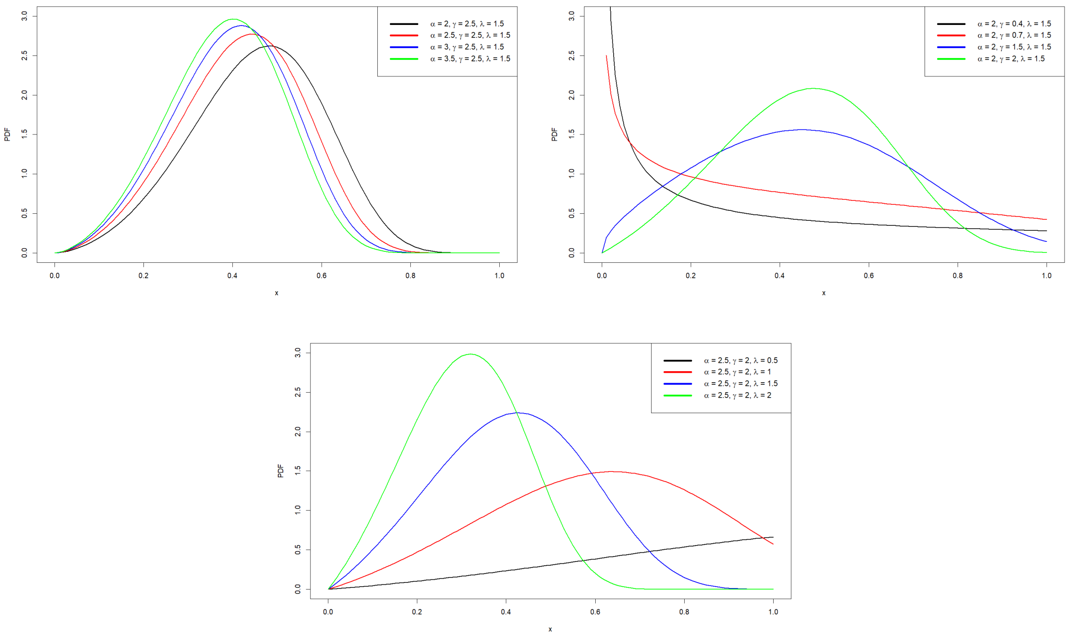

Figure 6.3: Plot of AGPTE density for different values of α, γ and λ.

Further, the survival function and HR of the AGPTE distribution are respectively given as

$$S(x) = \alpha^{-(e^{\lambda x}-1)^{-\gamma}}, \tag{6.18}$$

$$H(x) = \gamma\lambda(\log\alpha)e^{\lambda x}(e^{\lambda x}-1)^{\gamma-1}. \tag{6.19}$$

Furthermore, the quantile function of the AGPTE distribution is given by

$$Q(u) = \frac{1}{\lambda}\log\left\{1+\left(\frac{-\log(1-u)}{\log\alpha}\right)\right\}^{\frac{1}{\gamma}}.$$

Figure 6.4 depicts the three-dimensional plot of Galton's skewness and Moor's kurtosis for $\alpha \in (1,5)$, $\gamma \in (1,5)$, and $\lambda = 1$. From the figure, it is observed that Galton's skewness can take negative, zero, or positive values, indicating that the distribution can be left-skewed, symmetric, or right-skewed within the considered parameter domain. Regarding kurtosis, for small values of γ, the curve initially decreases, attains a minimum point as α increases, and then begins to rise. In contrast, as γ increases, the kurtosis curve increases steadily for all values of α.

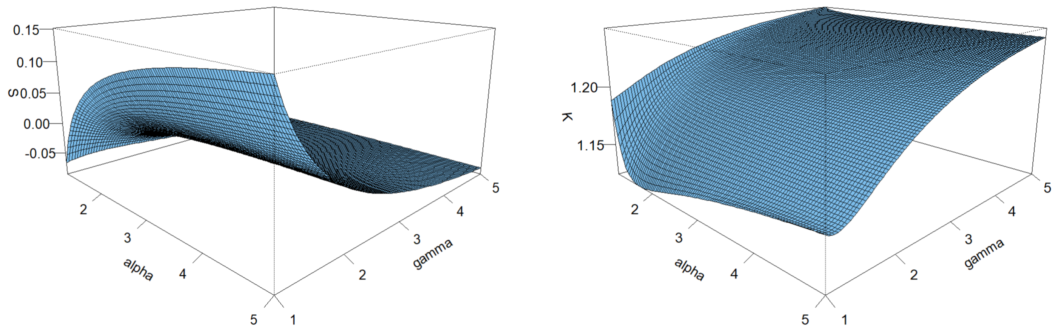

Figure 6.4: 3D-Plot of Galton's skewness (S) and Moor's kurtosis (K) for AGPTE distribution.

Now, we discuss the stress-strength model when the strength and stress variable follows an independent AGPTE distribution, *i.e.*, $X \sim \text{AGPTE}(\alpha_1, \gamma, \lambda)$ and $Y \sim \text{AGPTE}(\alpha_2, \gamma, \lambda)$. Then the stress-strength parameter R is given as

$$\begin{aligned} R &= P(X > Y) = \int_0^\infty f_X(x) F_Y(x)\, dx \\ &= \gamma\lambda \log\alpha_1 \int_0^\infty e^{\lambda x}(e^{\lambda x}-1)^{\gamma-1}\alpha_1^{-(e^{\lambda x}-1)^\gamma}\left(1-\alpha_2^{-(e^{\lambda x}-1)^\gamma}\right) dx \\ &= \frac{\log(\alpha_2)}{\log(\alpha_1\alpha_2)}. \end{aligned}$$

The following proposition states the characterization of AGPTE distribution in terms of AI function and HR.

Proposition 6.6.1. *A random variable $X \sim$ AGPTE (α,γ,λ) if and only if its AI function is given by*

$$L(x) = \frac{x\gamma\lambda e^{\lambda x}}{(e^{\lambda x}-1)}. \tag{6.20}$$

Proof. Generally, AI function of a random variable X is given in (6.4). When $X \sim$ AGPTE (α,γ,λ), from (6.5) we have

$$L(x) = \frac{x\gamma\lambda e^{\lambda x}}{(e^{\lambda x} - 1)}.$$

Conversely, suppose that the AI function is of the form given in (6.20). Then, for $x > 0$ and any $c > 0$, the survival function in terms of the AI function can be expressed as

$$S(x) = \exp\left(\log S(c) \exp\left(\int_c^x \frac{L(u)}{u}\, du\right)\right). \tag{6.21}$$

Then, using equation (6.21), we have

$$S(x) = 1 - \alpha^{-(e^{\lambda x}-1)^{\gamma}},$$

which is the survival function of X. This completes the proof. □

Proposition 6.6.2. *The hazard rate of AGPTE(α,γ,λ) shows*

(i) IHR for $\gamma > 1$ and

(ii) Bathtub shape for $\gamma < 1$.

Proof. From (6.19) we have,

$$\frac{d}{dx}\big(H(x)\big) = \gamma\lambda^2 \log \alpha e^{\lambda x}(e^{\lambda x} - 1)^{\gamma-2}(\gamma e^{\lambda x} - 1).$$

For $\gamma > 1$, it follows that $\frac{d}{dx}\big(H(x)\big) > 0$, for all x. Hence (i) follows. Now, for $\gamma < 1$, $\frac{d}{dx}\big(H(x)\big) = 0$, if and only if $x = x_0 = \frac{-\log\gamma}{\lambda}$. Also, it is easy to verify that $\frac{d^2}{dx^2}\big(H(x)\big) > 0$ at $x = x_0$, implying that $H(x)$ has a minimum at $x = x_0$. This completes the proof. □

Estimation of parameters

Let $X_1, X_2, \ldots, X_n$ be a random sample of size n from the AGPTE distribution with parameter space $\Theta = (\alpha, \gamma, \lambda)$ and observed values $x_1, x_2, \ldots, x_n$.

Then the log-likelihood function is given by

$$\begin{aligned} l(\Theta) &= n\log\gamma + n\log\lambda + n\log(\log\alpha) + \sum_{i=1}^{n}\lambda x_i + (\gamma-1)\sum_{i=1}^{n}\log(e^{\lambda x_i - 1}) \\ &\quad - \log\alpha\sum_{i=1}^{n}(e^{\lambda x_i}-1)^{\gamma}. \end{aligned}$$

The maximum likelihood equations are

$$\frac{\partial l}{\partial\alpha} = \frac{n}{\alpha\log\alpha} - \frac{1}{\alpha}\sum_{i=1}^{n}(e^{\lambda x_i}-1)^{\gamma}, \tag{6.22}$$

$$\frac{\partial l}{\partial\gamma} = \frac{n}{\gamma} + \sum_{i=1}^{n}\log(e^{\lambda x_i}-1) - \log\alpha\sum_{i=1}^{n}(e^{\lambda x_i})^{\gamma}\log(e^{\lambda x_i}-1), \tag{6.23}$$

$$\frac{\partial l}{\partial\lambda} = \frac{n}{\lambda} + \sum_{i=1}^{n}x_i + (\gamma-1)\sum_{i=1}^{n}\frac{x_i e^{\lambda x_i}}{(e^{\lambda x_i}-1)} - \gamma\log\alpha\sum_{i=1}^{n}x_i e^{\lambda x_i}(e^{\lambda x_i}-1). \tag{6.24}$$

From equation (6.22), the MLE of α is given as

$$\hat{\alpha} = \exp\left(\frac{n}{\sum_{i=1}^{n}(e^{\hat{\lambda} x_i}-1)}\right).$$

It is clear from the above two equations that the estimates of γ and λ cannot be solved analytically; hence, we use numerical iterative procedures such as the Newton-Raphson method for this purpose. Now, to construct ACI, consider the matrix.

$$I(\Theta) = \left[-\frac{\partial^2 l(\Theta|x)}{\partial\Theta^2}\right]_{i,j},$$

where $\Theta = (\alpha,\gamma,\lambda)$ and the entries of $I(\hat{\Theta})$ are given by

$$\begin{aligned} I_{11} =& \frac{\partial^2 l}{\partial\alpha^2} = \frac{-n(1+\log\alpha)}{\alpha^2(\log\alpha)^2} + \frac{1}{\alpha^2}\sum_{i=1}^{n}(e^{\lambda x_i}-1)^{\gamma}, \\ I_{12} =& I_{21} = \frac{\partial^2 l}{\partial\alpha\partial\gamma} = \frac{-1}{\alpha}\sum_{i=1}^{n}(e^{\lambda x_i}-1)^{\gamma}\log(e^{\lambda x_i}-1), \\ I_{13} =& I_{31} = \frac{\partial^2 l}{\partial\alpha\partial\lambda} = \frac{-\gamma}{\alpha}\sum_{i=1}^{n}x_i e^{\lambda x_i}(e^{\lambda x_i}-1)^{\gamma-1}, \\ I_{22} =& \frac{\partial^2 l}{\partial\gamma^2} = \frac{-n}{\gamma^2} - \log\alpha\sum_{i=1}^{n}(e^{\lambda x_i}-1)^{\gamma}(\log(e^{\lambda x_i}-1))^2, \end{aligned}$$

$$I_{23} = I_{32} = \frac{\partial^2 l}{\partial\gamma\partial\lambda} = \sum_{i=1}^{n} \frac{x_i e^{\lambda x_i}}{(e^{\lambda x_i}-1)} - \gamma \log\alpha \sum_{i=1}^{n} x_i e^{\lambda x_i}(e^{\lambda x_i}-1)^{\gamma-1}\big[\log(e^{\lambda x_i}-1)+1\big],$$

$$I_{33} = \frac{\partial^2 l}{\partial\lambda^2} = \frac{-n}{\lambda^2} - (\gamma-1)\sum_{i=1}^{n} \frac{x_i^2 e^{\lambda x_i}}{(e^{\lambda x_i}-1)^2} - \gamma\log\alpha \sum_{i=1}^{n} x_i^2 e^{\lambda x_i}(e^{\lambda x_i})^{\gamma-1}\left[1+\frac{(\gamma-1)e^{\lambda x_i}}{(e^{\lambda x_i}-1)}\right].$$

Let $E(I(\hat{\Theta}))$ represent the Fisher information matrix. Since the computation of the expectation is quite challenging, we can employ the observed information matrix, as introduced by Cox and Hinkley (1974), as a consistent estimator of the Fisher information matrix. From the large sample approximation, we have $\sqrt{n}(\hat{\Theta}-\Theta)$ that are asymptotically normally distributed with mean vector $\mathbf{0}$ and variance covariance matrix as the inverse of $I(\hat{\Theta})$. Thus, the $100(1-\beta)\%$ confidence intervals for the model parameters α, γ, and λ are

$$\hat{\alpha} \pm z_{(\beta/2)}\sqrt{I^{-1}_{11(\hat{\Theta})}/n}, \quad \hat{\gamma} \pm z_{(\beta/2)}\sqrt{I^{-1}_{22(\hat{\Theta})}/n} \quad \text{and} \quad \hat{\lambda} \pm z_{(\beta/2)}\sqrt{I^{-1}_{33(\hat{\Theta})}/n}.$$

Stochastic Ordering

The ordering of distributions among lifetime models plays a significant role in literature. Specifically, we consider the likelihood ratio ordering for two independent AGPTE random variables. Also, it should be noted that if a family has a likelihood ratio ordering, it implies that it has the monotone likelihood ratio property and thus there exists a uniformly most powerful test for any one-sided hypothesis when the other parameters are known. Let $X \sim$ AGPTE $(\alpha_1, \gamma_1, \lambda_1)$ and $Y \sim$ AGPTE $(\alpha_2, \gamma_2, \lambda_2)$, then the likelihood ratio is

$$\frac{f_X(x)}{f_Y(x)} = \frac{\gamma_1(\log\alpha_1)\lambda_1\alpha_1^{-(e^{\lambda_1 x}-1)^{\gamma_1}}(e^{\lambda_1 x}-1)^{\gamma_1-1}e^{\lambda_1 x}}{\gamma_2(\log\alpha_2)\lambda_2\alpha_2^{-(e^{\lambda_2 x}-1)^{\gamma_2}}(e^{\lambda_2 x}-1)^{\gamma_2-1}e^{\lambda_2 x}}.$$

Case 1: $\gamma_1=\gamma_2=\gamma$, $\lambda_1=\lambda_2=\lambda$, $\alpha_1<\alpha_2$.

Taking logarithm on both sides and differentiating we get

$$\frac{d}{dx}\left(\log\frac{f_X(x)}{f_Y(x)}\right) = \gamma\lambda(e^{\lambda x}-1)^{\gamma-1}e^{\lambda x}[\log\alpha_2 - \log\alpha_2] \geq 0.$$

$\implies X \geq_{lr} Y$ and thus $X \geq_{hr} Y, X \geq_{mrl} Y, X \geq_{st} Y$.

Case 2: $\alpha_1 = \alpha_2 = \alpha$, $\lambda_1 = \lambda_2 = \lambda$, $\gamma_1 < \gamma_2$.

$$\frac{d}{dx}\left(\log\frac{f_X(x)}{f_Y(x)}\right) = \frac{\lambda e^{\lambda x}}{e^{\lambda x}-1}\left[\gamma_1\big(1-\log\alpha(e^{\lambda x}-1)^{\gamma_1}\big)-\gamma_2\big(1-\log\alpha(e^{\lambda x}-1)^{\gamma_2}\big)\right] \leq 0.$$

$\implies X \leq_{lr} Y$ and thus $X \leq_{hr} Y$, $X \leq_{mrl} Y$, $X \leq_{st} Y$.

6.7 Simulation study

A simulation study has been conducted to evaluate the performance of the MLE for the AGPTE parameters α, γ, and λ, in terms of AB and MSE. Additionally, ACI for each parameter is calculated and assessed based on average interval length (AIL). The analyses have been conducted using the R statistical software. These experiments are replicated 1000 times across various sample sizes ($n = 50, 100, 250, 500$) and under three different parameter scenarios: $\Theta_1 = (2, 3, 1.5)$ and $\Theta_2 = (1.5, 2, 2.5)$. Samples from the AGPTE distribution are created via the inverse transformation technique. Table 6.1 presents the AB and MSE of the ML estimates, while Table 6.2 displays the ACI of the parameters, where LCI and UCI denote the lower and upper confidence limits, respectively. It is observed that as the sample size n increases, the AB and MSE decrease, and the confidence intervals become narrower. This indicates that the ML estimates of the AGPTE distribution are consistent.

Table 6.1: AB and MSE for ML estimates of AGPTE distribution.

Parameter Value	n	α		γ		λ	
		AB	MSE	AB	MSE	AB	MSE
α=2 γ=3 λ=1.5	50	0.16891	0.05064	0.28704	0.13663	0.02398	0.00094
	100	0.11413	0.02097	0.20297	0.06541	0.01747	0.00047
	250	0.06694	0.00719	0.13022	0.02670	0.01148	0.00020
	500	0.05045	0.00412	0.08671	0.01195	7.67×10^{-3}	9.4×10^{-5}
α=1.5 γ=2 λ=2.5	50	0.07144	0.00888	0.22202	0.08107	0.10599	0.01787
	100	0.04909	0.00395	0.15169	0.03741	0.07317	0.00848
	250	0.03086	0.00151	0.09755	0.01488	0.04812	0.00356
	500	0.02163	0.00073	0.06478	0.00666	0.03247	0.00167

Table 6.2: ACI of AGPTE distribution.

Parameter Value	n	α		γ		λ	
		LCI	UCI	LCI	UCI	LCI	UCI
α=2 γ=3 $\lambda = 1.5$	50	1.89139	2.19467	2.98126	3.17085	1.45812	1.53846
	100	1.93606	2.09979	2.99398	3.09056	1.47730	1.52057
	250	1.94225	2.07249	2.99137	3.03374	1.48306	1.51697
	500	1.96388	2.05092	2.99062	3.01389	1.48903	1.51153
α=1.5 γ=2 λ=2.5	50	1.40884	1.61460	1.97888	2.13397	2.34265	2.64688
	100	1.45230	1.56412	1.99725	2.07882	2.40950	2.57492
	250	1.49004	1.51658	2.00183	2.02896	2.47758	2.51602
	500	1.49056	1.51192	1.99623	2.01180	2.48456	2.51562

6.8 Real data analysis

This section demonstrates the versatility of the AGPTE distribution by applying it to a real-world dataset. For this, we employ the AGPTE distribution to model the breaking stress of carbon fibers, measured in gigapascals (GPa), based on a sample of 100 observations provided in Table 6.3. The characteristics of this data set are summarized in Table 6.4. Furthermore, the analysis includes a scaled TTT plot, presented in Figure 6.5, which indicates that the data has an IHR. Our objective is to fit the AGPTE distribution to this data and compare the outcomes with those obtained from fitting generalized versions of the exponential distribution, thereby illustrating the proposed distribution's effectiveness and flexibility in handling real data scenarios.

Table 6.3: Breaking stress of carbon fibers (100 observations)

3.70	2.74	2.73	2.50	3.60	3.11	3.27	2.87	1.47	3.11
4.42	2.41	3.19	3.22	1.69	3.28	3.09	1.87	3.15	4.90
3.75	2.43	2.95	2.97	3.39	2.96	2.53	2.67	2.93	3.22
3.39	2.81	4.20	3.33	2.55	3.31	3.31	2.85	2.56	3.56
3.15	2.35	2.55	2.59	2.38	2.81	2.77	2.17	2.83	1.92
1.41	3.68	2.97	1.36	0.98	2.76	4.91	3.68	1.84	1.59
3.19	1.57	0.81	5.56	1.73	1.59	2.00	1.22	1.12	1.71
2.17	1.17	5.08	2.48	1.18	3.51	2.17	1.69	1.25	4.38
1.84	0.39	3.68	2.48	0.85	1.61	2.79	4.70	2.03	1.80
1.57	1.08	2.03	1.61	2.12	1.89	2.88	2.82	2.05	3.65

Table 6.4: Summary of breaking stress data

Minimum Value	First Quantile	Median	Mean	Third Quantile	Maximum Value
0.390	1.840	2.700	2.621	3.220	5.560

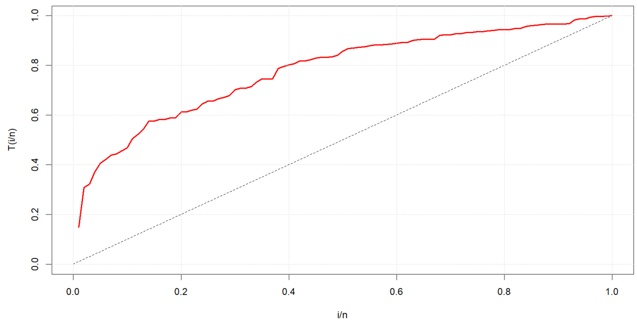

Figure 6.5: TTT plot of Breaking stress data

We fit the data set to the proposed model and compared the result with some competitive models namely: Generalized exponential (GE)(Gupta and Kundu (1999)), Weibul exponential (WE) (Oguntunde et al. (2015)), exponentiated generalized inverted exponential (EGIE) (Oguntunde et al. (2014)), alpha power within Weibul quantile (APWQ) (Nassar et al. (2018)), exponentiated Weibul (EW) (Mudholkar and Srivastava (1993)). The CDF of the competing distributions are given as follows:

- The CDF of generalized exponential (GE) is

$$F(x;\alpha,\lambda,\mu) = \left(1 - \exp\left\{-\frac{x}{\alpha}\right\}\right)^{\beta}, \quad x > 0,\ \alpha,\ \beta > 0.$$

- The CDF of Weibull exponential (WE) is

$$F(x;\alpha,\beta,\lambda) = 1 - \exp\left\{-\alpha\left(e^{\lambda x} - 1\right)^{\beta}\right\}, \quad x > 0, \alpha,\ \beta,\ \lambda > 0.$$

- The CDF of exponentiated generalized inverted exponential (EGIE) is

$$F(x;\alpha,\beta,\lambda) = \left(1 - \left(1 - e^{-\frac{\lambda}{x}}\right)^{\alpha}\right)^{\beta}, \quad x > 0,\ \alpha\ \beta > 0\ \lambda > 0.$$

- The CDF of exponentiated Weibul (EW) is

$$F(x;\alpha,\beta,\lambda) = \left(1 - e^{-\lambda x^{\beta}}\right)^{\alpha}, \quad x > 0,\ \alpha\ \beta > 0\ \lambda > 0.$$

- The CDF of alpha power within Weibul quantile (APWQ) is

$$F(x;\alpha,\beta,\lambda) = \frac{\log\left(1+(\alpha-1)(1-e^{-\lambda x^{\beta}})\right)}{\log\alpha}, \quad x>0,\ \alpha\,\beta>0.$$

We have evaluated the ML estimates of the parameters with respect to these models. To measure the goodness of fit, the K-S test is performed. The corresponding ML estimates, K-S statistic, and the P-value for the above models are tabulated in Table 6.5.

Table 6.5: The ML estimates (with standard errors in bracket), KS statistics and P-value for breaking stress data

Model	Parameter estimates			KS Statistics	P-value
GE	α=7.78820 (1.49619)	β=1.01317 (0.08747)	-	0.1077	0.1962
EGIE	α=41.33877 (7.70079)	β=0.33264 (0.03740)	λ=14.16922 (0.00291)	0.0943	0.3351
WE	α=1.56648 (1.67475)	β=2.11302 (0.25536)	λ=0.19743 (0.07128)	0.0730	0.6605
EW	α=1.31622 (0.58908)	β=2.40967 (0.59766)	λ=0.09272 (0.09060)	0.06440	0.8011
APWQ	α=1.47428 (2.48338)	β=2.91140 (0.56818)	λ=0.03831 (0.04299)	0.06152	0.8435
AGPTE	α=1.58685 (0.55379)	γ=0.30587 (0.07983)	$\lambda = 2.00687$ (0.20882)	0.04510	0.9871

The analysis indicates that the proposed model exhibits the lowest K-S statistic and the highest P-value among all other models, even though the difference between the WE model and the proposed model is negligible. Therefore, we can conclude that the AGPTE distribution offers a better fit to this data set compared to the other models considered. The relative histogram and P-P plot for the fitted AGPTE are displayed in Figures 6.6.

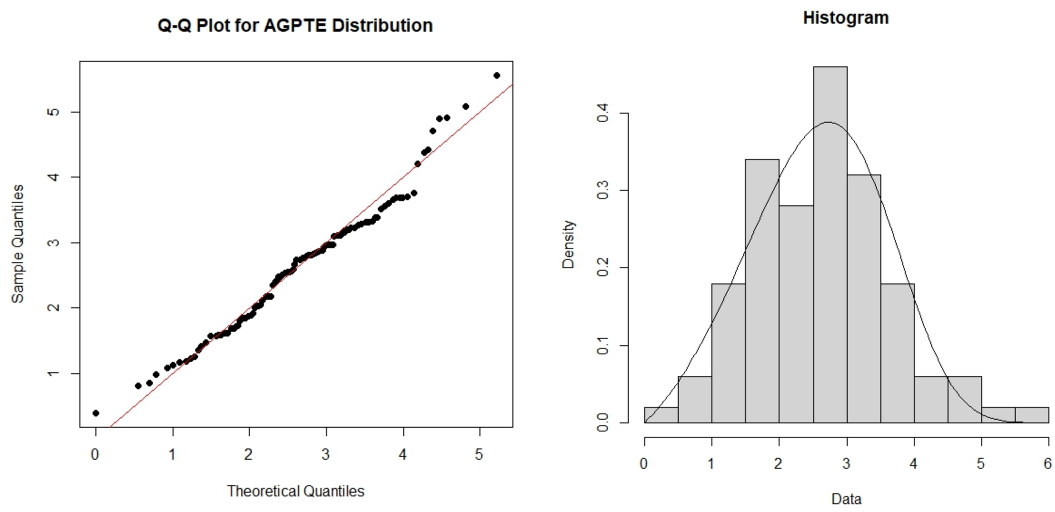

Figure 6.6: P-P plot and histogram for the fitted AGPTE distribution

6.9 Summary of the chapter

This chapter introduced a new class of distributions by selecting an arbitrary simple function as $T(\cdot)$ in the definition of the QT-transformation. Since the resulting model can be viewed as a modified version of the APT family proposed by Mahdavi and Kundu (2017a), it is termed the AGPT family. Various statistical properties of the proposed model were explored in detail. Parameter estimation was performed using the method of MLE, and characterization results were also established. A specific submodel, AGPTE, was constructed by considering the exponential distribution as the baseline, and its reliability properties were examined. A simulation study was conducted to evaluate the efficiency of the estimators; the results indicate that the ML estimates are consistent and efficient, and the ACI exhibit satisfactory coverage probabilities across various parameter settings. To illustrate the practical utility of the proposed model, real data analyses were carried out. The results revealed that the proposed model offers a superior fit to the considered datasets when compared with several existing generalizations of the exponential distribution, highlighting their flexibility and effectiveness.

Chapter 7

Stress-strength reliability based on AGPT family

7.1 Introduction

Reliability analysis is fundamental in various scientific and engineering disciplines, particularly for evaluating system performance under uncertain conditions. One of the widely used measures in reliability theory is the stress-strength reliability, R, which represents the probability that the system's strength (Y) exceeds the applied stress (X).

This modeling is particularly important in engineering, communication networks, and defense applications, where systems are designed to tolerate failures in some components while maintaining overall functionality. As reliability demands increase in complex applications, the need for advanced statistical inference methods to estimate R has grown significantly.

Researchers have explored various approaches to estimate R under different combinations of stress and strength distributions, addressing the diverse requirements of real-world applications. This chapter focuses on the statistical inference of stress-strength reliability in a system where both the stress and strength variables follow a distribution from the AGPT family. Both point and interval estimations are performed using classical and Bayesian approaches, and their performance is assessed through a simulation study and real data analysis.

The rest of the chapter is structured as follows: Section 7.2 presents some basic concepts essential for understanding the subsequent developments, followed by a review of relevant literature in the Section 7.3. The expression for R is derived in Section 7.2 under the assumption that both the stress and strength variables follow the general CDF of the AGPT family, sharing a common parameter γ. Section 7.3 focuses on both point and interval estimation of R when γ is unknown, using MLE and Bayesian methods. Furthermore, interval estimates are obtained using ACI, BCI, and HPD credible intervals. Section 7.4 extends these estimation techniques to the case where γ is known. To assess the performance of the proposed estimation methods, a comprehensive simulation study is carried out in Section 7.5, followed by a real data analysis in Section 7.6. Finally, the chapter concludes with a summary in Section 7.7.

7.2 Some basic concepts

Before delving into the details, we discuss some fundamental preliminaries essential for this chapter.

7.2.1 System

A system refers to a collection of components or subsystems arranged in a specific configuration, working together to perform a desired function. The types of components, their quantities, their qualities, and the way they are arranged within the system directly influence the system's overall reliability and performance. Systems can be classified based on various factors. One such classification is based on the number of components, which divides systems into the following categories:

- **Single-component systems:** These systems consist of a single component responsible for the system's overall functioning. The reliability of such systems entirely depends on the performance and behavior of this component.
- **Multi-component systems:** These systems consist of two or more components working together in order to run the system. The reliability of such systems is influenced by the interactions between the components and their configuration.

7.2.2 Stress-strength reliability

Stress-strength reliability is a valuable tool in reliability analysis used to assess the probability that a system's strength exceeds the applied stress, ensuring that the system does not fail. This is especially useful when evaluating systems where the applied stress (load) and the inherent strength (capacity) of components are key factors. In this context, stress and strength can be described as:

- **Stress :** Stress refers to the external force or load exerted on a system or its components. It can represent any kind of demand or challenge the system must withstand, such as pressure, weight, or environmental conditions. It is typically considered a random variable, as it can vary depending on different operating conditions or external factors.
- **Strength :** Strength represents the capacity of the system or its components to withstand the applied stress. It is a measure of the inherent reliability and durability of the components. Similar to stress, strength is also considered a random variable because the capacity of a system or component (such as tensile strength or durability) can vary due to factors like manufacturing inconsistencies, wear and tear, or environmental influences. These variations lead to a range of possible strength values for a given system or component.

Now, we discuss the definition of stress-strength reliability in both single and multi-component systems.

- **Stress-strength reliability in single-component Systems:**
  Stress-strength reliability, R, of a single-component system having a strength variable Y subject to a stress X is defined as the probability that the strength Y of the component exceeds the applied stress X. Mathematically,
  $$R = P(X < Y).$$
- **Stress-strength reliability in multi-component systems:**
  Stress-strength reliability, R_s of a multi-component system that consists of s independent components subject to a common stress X is defined as
  $$\begin{aligned} R_s &= P(X < \min(Y_1, Y_2, \ldots, Y_s)) \\ &= P(X < Y_1, X < Y_2, \ldots, X < Y_s), \end{aligned}$$
  where $(Y_1, Y_2, \ldots, Y_s)$ represents the strength variables of the s components.

7.3 Review of literature

Birnbaum et al. (1956) introduced the concept of stress-strength reliability and provided a non-parametric inference for it. Subsequently, Birnbaum and McCarty (1958) and Govindarajulu (1968) explored procedures for constructing distribution-free confidence intervals for stress-strength reliability. Later, Church and Harris (1970) constructed confidence intervals under the assumption that stress and strength variables follow normal distributions and compared the results with those of Govindarajulu (1968). Furthermore, Cheng and Chao (1984) examined the performance of various methods for constructing confidence intervals and proposed a new approach for obtaining s-confidence intervals for the stress-strength reliability measure.

From a practical perspective, the stress-strength reliability of a system is inherently dynamic, changing over time due to varying operational conditions. The dynamic approach to modeling stress-strength systems considers stress and strength as time-dependent processes, denoted by $X(t)$ and $Y(t)$, respectively. Basu and Ebrahimi (1983) examined such a dynamic model by treating $X(t)$ and $Y(t)$ as stochastic processes. Ebrahimi and Ramallingam (1993) extended this model by considering $X(t)$ and $Y(t)$ as independent Brownian motions. Later, Basu and Lingham (2003) further explored Bayesian estimation in the Brownian stress-strength model proposed by Ebrahimi and Ramallingam (1993).

In many real-life scenarios, system reliability is influenced by dynamic stress–strength interaction, where the system's strength deteriorates while stress accumulates over time. To address these situations, Bhuyan and Dewanji (2014), Bhuyan and Dewanji (2017a), and Bhuyan and Dewanji (2017b) considered the estimation of reliability under cumulative stress and strength degradation.

In the aforementioned studies, researchers focused on assessing system reliability over time. However, such approaches may not be ideal for monitoring reliability in a production line. To address this limitation, Xu et al. (2019) tackled the statistical challenge of identifying change points in stress-strength reliability.

Researchers have developed various stress-strength models by assuming different lifetime distributions for the stress and strength variables. Examples include the exponential distribution (Baklizi (2014)), Weibull distribution (Kundu and Gupta (2006)), normal distribution (Weerahandi and Johnson (1992)), uniform distribution (Ivshin (1996)), gamma distribution (Ismail et al. (1986)), beta distribution (Nadarajah (2002)), Lindley distribution (Al-Mutairi et al. (2013)), Burr XII distribution (Lio and and (2012)), Kumaraswamy distribution (Nadar et al. (2014)), and generalized exponential distribution (Kundu and Gupta (2005)). Similarly, Kundu and Raqab (2009, 2015) evaluated inference procedures for stress-strength reliability for the three-parameter Weibull distribution and the three-parameter generalized Rayleigh distribution, respectively. In addition to classical distributions, two-piece distributions such as the Laplace distribution (Nadarajah (2004)) and the double Lomax distribution (Punathumparambath (2011)) have also been explored in the context of stress-strength reliability. Furthermore, Khan and Jan (2015) addressed stress-strength modeling using a finite mixture of two-parameter Lindley distributions. A comprehensive review of stress-strength reliability is available in Kotz et al. (2003).

Recently, Mokhlis et al. (2017) presented characterizations related to stress-strength reliability for distributions belonging to the generalized exponential and generalized inverse exponential families. Motivated by this line of work, the present chapter focuses on estimating stress-strength reliability based on the AGPT family, offering a broader and more flexible framework through the incorporation of a general baseline distribution.

7.4 System reliability, R

Let $X \sim AGPT(\alpha_1, \gamma, F(x))$ and $Y \sim AGPT(\alpha_2, \gamma, F(y))$, be two independent random variables from the AGPT family sharing the same baseline CDF $F(\cdot)$. Then the stress-strength reliability, R, is given by

$$\begin{aligned} R &= P(X < Y) = \int_0^\infty P(Y > X|X = x) f_X(x) dx \\ &= \int_0^\infty \gamma \log(\alpha_1) \left(1 - \alpha_2^{\left(\frac{F(x)}{1-F(x)}\right)^\gamma}\right) \alpha_1^{-\left(\frac{F(x)}{1-F(x)}\right)^\gamma} \frac{F(x)^{\gamma-1}}{(1-F(x))^{\gamma+1}} f(x) dx. \end{aligned}$$

Let $t = 1 - \alpha_2^{\left(\frac{F(y)}{1-F(y)}\right)^\gamma}$. Upon simplification, we get

$$R = \frac{\log(\alpha_1)}{\log \alpha_2} \int_0^1 t(1-t)^{\frac{\log(\alpha_1)}{\log(\alpha_2)} - 1} dt \tag{7.1}$$

$$= \frac{\log(\alpha_2)}{\log(\alpha_1) + \log(\alpha_2)}. \tag{7.2}$$

In the upcoming section, we discuss the classical and Bayesian estimation of R, considering both cases where γ is known and unknown.

7.5 Estimation of R, when γ is unknown

7.5.1 Maximum likelihood estimation

To compute MLE of R, we first compute the MLE of α_1, α_2, and γ. Let $X_i,\ i = 1, 2, \ldots, n$ and $Y_i,\ i = 1, 2, \ldots, m$ be two independent random samples from the $AGPT$ family with parameters (α_1,γ) and (α_2,γ) respectively. Then the likelihood function is given by

$$\begin{aligned} L(\alpha_1, \alpha_2, \gamma|data) &= \prod_{i=1}^{n} f(x_i) \prod_{i=1}^{m} f(y_i) \\ &= \gamma^{n+m} (\log(\alpha_1))^n \alpha_1^{-\sum_{1=1}^{n}\left(\frac{F(x_i)}{1-F(x_i)}\right)^{\gamma}} \prod_{i=1}^{n} \frac{F(x_i)^{r-1}}{(1-F(x_i))^{r+1}} \\ &\quad \alpha_2^{-\sum_{1=1}^{m}\left(\frac{F(y_i)}{1-F(y_i)}\right)^{\gamma}} \prod_{i=1}^{m} \frac{F(y_i)^{r-1}}{(1-F(y_i))^{r+1}}. \end{aligned}$$

Then the corresponding log likelihood function is

$$\begin{aligned} l(\alpha_1, \alpha_2, \gamma|data) &= (n+m)\log\gamma + n\log(\log(\alpha_1)) + m\log(\log(\alpha_2)) - \log(\alpha_1)\sum_{i=1}^{n}\left(\frac{F(x_i)}{1-F(x_i)}\right)^{\gamma} \\ &\quad -\log(\alpha_2)\sum_{i=1}^{m}\left(\frac{F(y_i)}{1-F(y_i)}\right)^{\gamma} + (\gamma-1)\left[\sum_{i=1}^{n}\log F(x_i) + \sum_{i=1}^{m}\log F(y_i)\right] \\ &\quad -(\gamma+1)\left[\sum_{i=1}^{n}\log(1-F(x_i)) + \sum_{i=1}^{m}\log(1-F(y_i))\right]. \end{aligned}$$

From the likelihood equations, we obtain the ML estimates of α_1, α_2, and γ, say $\hat{\alpha}_1$, $\hat{\alpha}_2$, and $\hat{\gamma}$ as follows:

$$\frac{\partial l}{\partial \alpha_1} = \frac{n}{\alpha_1 \log\alpha_1} - \frac{1}{\alpha_1}\sum_{i=1}^{n}\left(\frac{F(x_i)}{1-F(x_i)}\right)^{\gamma} = 0, \tag{7.3}$$

$$
\begin{aligned}
\frac{\partial l}{\partial \alpha_2} &= \frac{n}{\alpha_2 \log \alpha_2} - \frac{1}{\alpha_2} \sum_{i=1}^{m} \left(\frac{F(y_i)}{1 - F(y_i)} \right)^{\gamma} = 0, \qquad (7.4) \\
\frac{\partial l}{\partial \gamma} &= \frac{n+m}{\gamma} - \log \alpha_1 \sum_{i=1}^{n} \left(\frac{F(x_i)}{1 - F(x_i)} \right)^{\gamma} \log \left[\frac{F(x_i)}{1 - F(x_i)} \right] - \\
& \log \alpha_2 \sum_{i=1}^{m} \left(\frac{F(y_i)}{1 - F(y_i)} \right)^{\gamma} \log \left[\frac{F(y_i)}{1 - F(y_i)} \right] + \sum_{i=1}^{n} \log F(x_i) + \\
& \sum_{i=1}^{n} \log F(y_i) - \sum_{i=1}^{n} \log(1 - F(x_i)) - \sum_{i=1}^{m} \log F(y_i) = 0. \qquad (7.5)
\end{aligned}
$$

From (7.3) and (7.4), we get

$$
\hat{\alpha}_1 = \exp \left\{ \frac{n}{\sum_{i=1}^{n} \left(\frac{F(x_i)}{1-F(x_i)} \right)^{\hat{\gamma}}} \right\} \quad \text{and} \quad \hat{\alpha}_2 = \exp \left\{ \frac{m}{\sum_{i=1}^{n} \left(\frac{F(y_i)}{1-F(y_i)} \right)^{\hat{\gamma}}} \right\}.
$$

From (7.5), it is evident that γ cannot be solved analytically. Therefore, we employ the Newton-Raphson method to obtain $\hat{\gamma}$. Once $\hat{\alpha}_1$, $\hat{\alpha}_2$, and $\hat{\gamma}$ are obtained, the MLE of R, say, $\hat{R}_{MLE}$, is determined using the invariance property of maximum likelihood estimators as

$$
\hat{R} = \frac{\log(\hat{\alpha}_2)}{\log(\hat{\alpha}_1) + \log(\hat{\alpha}_2)}.
$$

7.5.2 Asymptotic confidence interval

To construct the ACI for R, we utilize the asymptotic distribution of $\hat{R}$. For this purpose, consider the following matrix:

$$
I(\Theta) = [I_{ij}] = \left[-\frac{\partial^2 l}{\partial \theta_i \partial \theta_j} \right], \quad i, j = 1, 2, 3,
$$

where $\Theta = (\alpha_1, \alpha_2, \gamma)$. Then expectation of $I(\theta)$, $E(I(\theta))$ gives the Fisher information matrix. Since the evaluation of the expectation is quite difficult, we can use the observed information matrix, $I(\Theta)$, as mentioned in Cox and Hinkley (1974), which serves as a consistent estimator of the Fisher information matrix. Thus the asymptotic variance-covariance matrix of Θ is $I^{-1}(\Theta)$. Suppose $R^T = \left(\frac{\partial R}{\partial \alpha_1}, \frac{\partial R}{\partial \alpha_2}, \frac{\partial R}{\partial \gamma}\right)$, where

$$\begin{aligned}\frac{\partial R}{\partial \alpha_1} &= \frac{-\log \alpha_2}{\alpha_1(\log \alpha_1 + \log \alpha_2)^2},\\ \frac{\partial R}{\partial \alpha_2} &= \frac{\log \alpha_1}{\alpha_2(\log \alpha_1 + \log \alpha_2)^2}.\end{aligned}$$

As R does not depend on γ, $\frac{\partial R}{\partial \gamma} = 0$. From Cox and Hinkley (1974), we have $\hat{R}$ is asymptotically normal with mean R and the variance, $Var(R) = R^T I^{-1} R$. Thus the $100(1-\alpha)\%$ confidence interval of R is given as

$$\hat{R} \pm z_{\alpha/2} \hat{V}(\hat{R}),$$

where $z_{\alpha/2}$ is the upper $(\alpha/2)$ percentile of the standard normal distribution and $\hat{V}(\hat{R})$ is the estimate of $V(\hat{R})$, obtained by substituting $\Theta = \hat{\Theta}$, where $\hat{\Theta} = (\hat{\alpha}_1, \hat{\alpha}_2, \hat{\gamma})$.

7.5.3 Bayesian estimation

In this section, we derive the Bayes estimate of R based on the squared error loss function, assuming that the parameters α_1, α_2, and γ are independent random variables with non-informative uniform priors. The joint prior density function of α_1, α_2, and γ is of the form

$$g(\alpha_1, \alpha_2, \gamma) \propto \frac{1}{\alpha_1 \alpha_2 \gamma}, \quad \alpha_1,\ \alpha_2 > 1, \gamma > 0.$$

Based on observed data, the joint posterior density function of α_1, α_2, and γ is given by

$$\pi(\alpha_1, \alpha_2, \gamma | data) = \gamma^{n+m-1} (\log(\alpha_1))^n \alpha_1^{-\left(\sum_{i=1}^n \left(\frac{F(x_i)}{1-F(x_i)}\right)^\gamma + 1\right)} \prod_{i=1}^n \frac{F(x_i)^{r-1}}{(1-F(x_i))^{r+1}}$$

$$\alpha_2^{-\left(\sum_{i=1}^{m}\left(\frac{F(y_i)}{1-F(y_i)}\right)^{\gamma}+1\right)} \prod_{i=1}^{m} \frac{F(y_i)^{r-1}}{(1-F(y_i))^{r+1}}. \tag{7.6}$$

From (7.6), we get

$$\log \alpha_1 \sim gamma\left(n+1, \sum_{i=1}^{n}\left(\frac{F(x_i)}{1-F(x_i)}\right)^{\gamma}+1\right), \tag{7.7}$$

$$\log \alpha_2 \sim gamma\left(m+1, \sum_{i=1}^{m}\left(\frac{F(y_i)}{1-F(y_i)}\right)^{\gamma}+1\right), \tag{7.8}$$

and

$$\begin{aligned}\pi(\gamma|\alpha_1, \alpha_2, data) \propto\ & \gamma^{n+m-1}\alpha_1^{-\sum_{i=1}^{n}\left(\frac{F(x_i)}{1-F(x_i)}\right)^{\gamma}} \prod_{i=1}^{n} \frac{F(x_i)^{r-1}}{(1-F(x_i))^{r+1}} \\ & \alpha_2^{-\sum_{i=1}^{m}\left(\frac{F(y_i)}{1-F(y_i)}\right)^{\gamma}} \prod_{i=1}^{m} \frac{F(y_i)^{r-1}}{(1-F(y_i))^{r+1}}.\end{aligned} \tag{7.9}$$

From (7.7) and (7.8), we observe that the marginal posterior distributions of α_1 and α_2 follow a log-gamma distribution. Therefore, samples of α_1 and α_2 can be easily generated using the log-gamma distribution. However, from (7.9), it is evident that the posterior distribution of γ cannot be analytically reduced to a well-known distribution, making direct sampling using standard methods infeasible. Hence, we use the Metropolis-Hastings (MH) algorithm to generate random sample from the posterior density of γ. Then the Bayes estimator of R under squared error loss function is given by

$$\hat{R}_B = \int_0^{\infty}\int_0^{\infty}\int_0^{\infty} R\ \pi(\alpha_1, \alpha_2, \gamma|data)\ d\alpha_1\ d\alpha_2\ d\gamma. \tag{7.10}$$

Since the integral in (7.10) is challenging to solve analytically, we employ the MCMC method to compute the Bayesian estimate of R. For this purpose, we implement the following steps:

1. Choose the initial guess $\alpha_1^{(0)}$, $\alpha_2^{(0)}$ and $\gamma^{(0)}$.

2. Initialize $t = 1$.

3. Generate $\alpha_1^{(t)}$ from $log-gamma\left(n+1, \sum_{i=1}^{n}\left(\frac{F(x_i)}{1-F(x_i)}\right)^{\gamma}+1\right)$.

4. Generate $\alpha_2^{(t)}$ from $log-gamma\left(m+1, \sum_{i=1}^{m}\left(\frac{F(y_i)}{1-F(y_i)}\right)^{\gamma}+1\right)$.

5. Using the following MH algorithm generate $\gamma^{(t)}$ from $\pi(\gamma|\alpha_1, \alpha_2, data)$ with $N(\gamma^{(t-1)}, Var(\gamma^{(t-1)}))$ as the proposal distribution, where $Var(\gamma)$ is obtained from observed information matrix.

   - Generate a proposal γ^* from $N(\gamma^{(t-1)}, Var(\gamma^{(t-1)}))$.
   - Compute the acceptance probability

$$\eta_\gamma = min\left\{1, \frac{\pi(\gamma^*|\alpha_1^{(t-1)}, \alpha_2^{(t-1)}, data)}{\pi(\gamma|\alpha_1^{(t-1)}, \alpha_2^{(t-1)}, data)}\right\}.$$

   - Generate U from $U(0,1)$.
   - If $U < \eta_\gamma$, accept the proposal and set $\gamma^{(t)} = \gamma^*$, else set $\gamma^{(t)} = \gamma^{(t-1)}$.

6. Compute $R^{(t)} = \frac{\log \alpha_2^{(t)}}{\log \alpha_1^{(t)} + \log \alpha_2^{(t)}}$.

7. Set $t = t+1$.

8. Repeat step 3-7, T times. Then the Bayes estimate of R is given by

$$\hat{R}_{MCMC} = \frac{1}{T}\sum_{i=1}^{T} R^{(t)}.$$

7.5.4 Bayesian credible interval and highest posterior density credible interval

The BCI and HPD of R are constructed using the method suggested by Chen and Shao (1999). Once we compute $R^{(t)}$, $t = 1, 2, \ldots, T$, we obtain the ordered values as $R_{(1)} \le R_{(2)} \le \cdots \le R_{(T)}$. Then the $100(1-\alpha)\%$ BCI for R is given by

$$(R_{([\alpha/2]T)}, R_{([1-\alpha/2]T)}).$$

Also, a $100(1-\alpha)\%$ HPD credible interval of R is constructed by considering the smallest confidence length among all possible $100(1-\alpha)\%$ credible intervals. *i.e.*, $100(1-\alpha)\%$ HPD credible interval for R is obtained as

$$(R_{(j)}, R_{(j+[(1-\alpha)T])}),$$

where j is chosen in such a way that, $R_{(j+[(1-\alpha)T])} - R_{(j)} = \min\limits_{1\le j\le T}(R_{(j+[(1-\alpha)T])} - R_{(j)}),\ j = 1, 2, \ldots, T$ and $[\cdot]$ is the greatest integer value function.

7.6 Estimation of R, when γ is known

7.6.1 Maximum likelihood estimation

Following the similar procedure as in Section 7.5.1, the ML estimate of R can be obtained as

$$\hat{R}_{MLE} = \frac{\log(\hat{\alpha}_2)}{\log(\hat{\alpha}_1) + \log(\hat{\alpha}_2)},$$

where

$$\hat{\alpha}_1 = \exp\left\{\frac{n}{\sum_{i=1}^{n}\left(\frac{F(x_i)}{1-F(x_i)}\right)^{\gamma}}\right\} \quad \text{and} \quad \hat{\alpha}_2 = \exp\left\{\frac{m}{\sum_{i=1}^{n}\left(\frac{F(y_i)}{1-F(y_i)}\right)^{\gamma}}\right\}.$$

Using the similar procedure as in Section 7.5.2, the ACI of R can also be constructed.

7.6.2 Bayesian estimation

In this section, we obtain the Bayes estimate of R under the squared error loss function, assuming that the parameters α_1 and α_2 are independent random variables following non-informative uniform priors. The joint prior density function of α_1 and α_2 is of the form

$$g(\alpha_1, \alpha_2) \propto \frac{1}{\alpha_1 \alpha_2}, \quad \alpha_1,\ \alpha_2 > 1.$$

Based on observed data the joint posterior density function of α_1 and α_2 is given by

$$\pi(\alpha_1, \alpha_2|data) \quad = \quad \frac{U^{n+1}V^{m+1}}{\Gamma(n+1)\Gamma(m+1)} \frac{(\log\alpha_1)^n}{\alpha_1} \frac{(\log\alpha_2)^m}{\alpha_2} \exp\left\{-\left(U\log\alpha_1 + V\log\alpha_2\right)\right\},$$

where $U = \sum_{i=1}^{n} \left(\frac{F(x_i)}{1-F(x_i)}\right)^{\gamma}$ and $V = \sum_{i=1}^{n} \left(\frac{F(y_i)}{1-F(y_i)}\right)^{\gamma}$. Then the Bayes estimate of R under squared error loss function is given by

$$\hat{R}_B = \int_0^{\infty} \int_0^{\infty} R\ \pi(\alpha_1, \alpha_2|data)\ d\alpha_1\ d\alpha_2. \tag{7.11}$$

Now, consider the one to one transformation $u_1 = \frac{\log(\alpha_2)}{\log(\alpha_1)+\log(\alpha_2)}$ and $u_2 = \log(\alpha_1) + \log(\alpha_2)$. This implies $0 < u_1 < 1$, $0 < u_2 < \infty$, $\alpha_1 = e^{u_2(1-u_1)}$, $\alpha_2 = e^{u_1 u_2}$ and the Jacobian of (u_1, u_2) is $J(u_1, u_2) = u_2 e^{u_2}$. After simplification we get,

$$R = \left(\frac{m+1}{n+m+2}\right) \frac{(1-z)^{m+1}}{\beta(m+2, n+1)} \int_0^1 u_1^{m+1}(1-u_1)^n(1-u_1 z)^{-p} du_1,$$

where $Z = 1 - \frac{V}{U}$ and $p = n+m+2$. Using the integral form of hyper-geometric series given in Gradshteyn and Ryzhik (1994) as

$${}_2F_1(\alpha, \beta, \gamma, z) = \frac{1}{B(\beta, \gamma-\beta)} \int_0^1 t^{\beta-1}(1-t)^{\gamma-\beta-1}(1-tz)^{-\alpha}\ dt,\ Re(\gamma) > 0,\ Re(\beta) > 0, |z| < 1.$$

Thus the Bayes estimate, $\hat{R}_B$ of R is deduced as

$$\hat{R}_B = \begin{cases} \dfrac{(m+1)(1-z)^{m+1}}{p}\ {}_2F_1(p, m+2, m-n+1, z), & \text{if } |z| < 1 \\ \dfrac{(m+1)}{p(1-z)^{n+1}}\ {}_2F_1\left(p, n+1, n+m+1, \dfrac{z}{(1-z)}\right), & \text{if } z < -1. \end{cases}$$

Thus, we derived a closed-form expression for the Bayes estimator of R. However, in situations where obtaining the stress-strength reliability from this expression is challenging, the MCMC method can be utilized to estimate it using simulated random samples. The steps for this procedure are given below.

1. Choose the initial guess $\alpha_1^{(0)}$, $\alpha_2^{(0)}$.
2. Initialize $t = 1$.
3. Generate $\alpha_1^{(t)}$ from $log - gamma\,(n+1, U)$.
4. Generate $\alpha_2^{(t)}$ from $log - gamma\,(m+1, V)$.
5. Compute $R^{(t)} = \frac{\log \alpha_2^{(t)}}{\log \alpha_1^{(t)} + \log \alpha_2^{(t)}}$.
6. Set $t = t + 1$.
7. Repeat step 3-7, T times.

Then the Bayes estimate of R is given by

$$\hat{R}_{MCMC} = \frac{1}{T} \sum_{i=1}^{T} R^{(t)}.$$

Here also, we construct the HPD and BCI of R using the method suggested by Chen and Shao (1999). The steps are similar to those given in Section 7.5.4.

7.7 Simulation study

A simulation study is carried out to evaluate the performance of both point and interval estimators of R. For this purpose, we consider the AGPTE (AGPT-Exponential) distribution, which is derived by using the exponential distribution as the baseline discussed in the previous chapter. Thus the CDF and PDF of AGPTE(α,γ) are given as

$$F(x) = 1 - \alpha^{-(e^x - 1)^\gamma}, \quad x > 0,\ \alpha > 1,\ \gamma > 0, \tag{7.12}$$

$$f(x) = \gamma(\log \alpha) e^x (e^{\lambda x} - 1)^{\gamma - 1} \alpha^{-(e^x - 1)^\gamma}. \tag{7.13}$$

The efficiency of the estimates is evaluated based on AB and MSE, while the efficiency of confidence intervals is assessed in terms of average interval length (AIL) and the corresponding coverage probabilities (CP). These evaluations are performed for various parameter combinations and sample sizes. For computational purposes, we use the R statistical software, and the results are based on 1000 replications. To generate random samples from AGPTE(α_1, γ) and AGPTE(α_2, γ), we employ the inverse transformation method.

In the case when γ is unknown, we consider the sample size $n = m$=20, 30, 50, 80, 120, and two sets of parameter values $\Theta_1 = (\alpha_1, \alpha_2, \gamma) = (1.5, 2, 2.5)$ and $\Theta_2 = (\alpha_1, \alpha_2, \gamma) = (2, 2.5, 3)$. The AB and MSE of the estimates of R obtained using the MLE and MCMC methods are represented in Table 7.1. To assess the convergence of the MCMC algorithm, we examine two diagnostic measures: the trace plot and the ergodic mean plot, which are provided for selected sample sizes and illustrated in Figure 7.1 and Figure 7.2. Moreover, 95% HPD, BCI, and ACI are constructed, and their corresponding AIL along with CP are tabulated in Table 7.2.

Table 7.1: AB and MSE for the estimates of R (γ unknown)

(n,m)	Θ	R	MLE		MCMC	
			AB	MSE	AB	MSE
(20,20)	Θ_1	0.630929	0.059619	0.005831	0.027771	0.000795
(30,30)			0.049483	0.003750	0.026649	0.000729
(50,50)			0.036874	0.002204	0.026385	0.000708
(80,80)			0.027865	0.001201	0.026359	0.000701
(120,120)			0.023527	0.000857	0.026080	0.000683
(20,20)	Θ_2	0.569323	0.060970	0.005742	0.005092	4.228×10^{-5}
(30,30)			0.051091	0.004093	0.003248	1.765×10^{-5}
(50,50)			0.039036	0.002380	0.002514	9.701×10^{-6}
(80,80)			0.030673	0.001473	0.001725	5.138×10^{-6}
(120,120)			0.025033	0.001016	0.001578	4.279×10^{-6}

Table 7.2: AIL and CP for R (γ unknown)($\lambda = 0.05$)

(Θ)	(n,m)	ACI		HPD		BCI	
		AIL	CP	AIL	CP	AIL	CP
Θ_1	(20,20)	0.334804	0.970	0.021534	0.950	0.022460	0.970
	(30,30)	0.276402	0.976	0.016837	0.920	0.017699	0.950
	(50,50)	0.214480	0.970	0.012447	0.960	0.012989	0.950
	(80,80)	0.169930	0.986	0009730	0.920	0.010211	0.920
	(120,120)	0.138829	0.972	0.007945	0.980	0.008285	0.970
Θ_2	(20,20)	0.323284	0.958	0.021765	0.900	0.023097	0.920
	(30,30)	0.266203	0.976	0.016746	0.950	0.017577	0.950
	(50,50)	0.206800	0.972	0.012127	0.950	0.012753	0.970
	(80,80)	0.164038	0.966	0.009611	0.960	0.010053	0.960
	(120,120)	0.134131	0.982	0.007709	0.960	0.008076	0.970

Table 7.3: AB and MSE for the estimates of R (γ known)

(n,m)	Θ	R	MLE		Exact		MCMC	
			AB	MSE	AB	MSE	AB	MSE
(20,20)	Θ_3	0.306762	0.051311	0.004206	0.049364	0.004030	0.003933	2.405×10^{-5}
(30,30)			0.044638	0.003156	0.043114	0.002930	0.003323	1.640×10^{-5}
(50,50)			0.033823	0.001767	0.034445	0.001944	0.002475	9.316×10^{-6}
(80,80)			0.026003	0.001047	0.025719	0.000627	0.001693	4.454×10^{-6}
(120,120)			0.022923	0.000816	0.022427	0.000502	0.001387	2.929×10^{-6}
(20,20)	Θ_4	0.643832	0.059923	0.005525	0.060355	0.005723	0.004368	3.022×10^{-5}
(30,30)			0.046394	0.003380	0.044143	0.003183	0.003574	1.883×10^{-5}
(50,50)			0.037019	0.002125	0.036339	0.002061	0.002390	9.151×10^{-6}
(80,80)			0.029967	0.001393	0.029337	0.001374	0.001949	6.071×10^{-6}
(120,120)			0.023235	0.000876	0.022513	0.000851	0.001581	4.078×10^{-6}

Table 7.4: AIL and CP for R (γ known)($\lambda = 0.05$)

Θ	(n,m)	ACI		HPD		BCI	
		AIL	CP	AIL	CP	AIL	CP
Θ_3	(20,20)	0.260778	0.944	0.013888	0.910	0.014488	0.940
	(30,30)	0.212799	0.936	0.018163	0.920	0.019091	0.940
	(50,50)	0.166370	0.934	0.010586	0.910	0.011143	0.930
	(80,80)	0.131417	0.942	0.008177	0.940	0.008602	0.970
	(120,120)	0.107442	0.916	0.006647	0.960	0.006910	0.950
Θ_4	(20,20)	0.278738	0.938	0.019902	0.950	0.020890	0.980
	(30,30)	0.229130	0.930	0.015148	0.910	0.015989	0.920
	(50,50)	0.177756	0.938	0.011252	0.940	0.011826	0.960
	(80,80)	0.142427	0.948	0.008850	0.920	0.009293	0.920
	(120,120)	0.116004	0.950	0.007091	0.930	0.007516	0.920

Similarly, for the case where γ is known ($\gamma = 2$), we consider the same set of sample sizes and the two sets of parameter values as $\Theta_3 = (\alpha_1, \alpha_2) = (2.5, 1.5)$ and $\Theta_4 = (\alpha_1, \alpha_2) = (1.75, 2.75)$. The AB and MSE of the estimates of R are summarized in Table 7.3. Additionally, the 95% HPD interval, BCI, and ACI are constructed, with their corresponding AIL and CP presented in Table 7.4. The key findings from the simulation study are as follows:

- All the considered estimation techniques perform well, as evidenced by the small AB and MSE values. Furthermore, these values decrease as the sample size increases, demonstrating the consistency of the estimators.
- Table 7.1 shows that the AB and MSE of the Bayes estimates based on the MCMC method are lower than those of the ML estimates when γ is unknown, that Bayesian estimation outperforms MLE in this case.
- When comparing the parameter sets Θ_1 and Θ_2, the ML estimates perform better for Θ_1, while the Bayesian estimates using MCMC perform better for Θ_2.

- Table 7.3 demonstrates that Bayes estimates perform better than ML estimates when γ is known. Additionally, among the Bayesian estimation methods, the MCMC based approach provides more accurate results compared to exact Bayesian estimates.
- When comparing the parameter sets Θ_3 and Θ_4, Θ_3 consistently yields lower AB and MSE values across all cases than Θ_4.
- The ergodic mean plot in Figure left side of 7.1 and Figure 7.2 in respect of two parameter sets Θ_1 and Θ_2, confirms that the system is ergodic, which ensures that the system behaves predictably over time.
- The rapid oscillations around a central value and rapid up and down variation in the trace plot in right side of Figure 7.1 and Figure 7.2 confirm proper convergence and mixing of stages of the MCMC method employed here.
- From Tables 7.2 and 7.4, it is observed that the CP of the HPD interval, BCI, and ACI are satisfactory and close to the nominal level. Additionally, the AIL decreases as the sample size increases.
- In both the known and unknown cases of γ, the AIL of the HPD interval and BCI is smaller compared to that of the ACI. Among the HPD interval and BCI, the HPD interval has the smallest AIL, indicating greater efficiency.

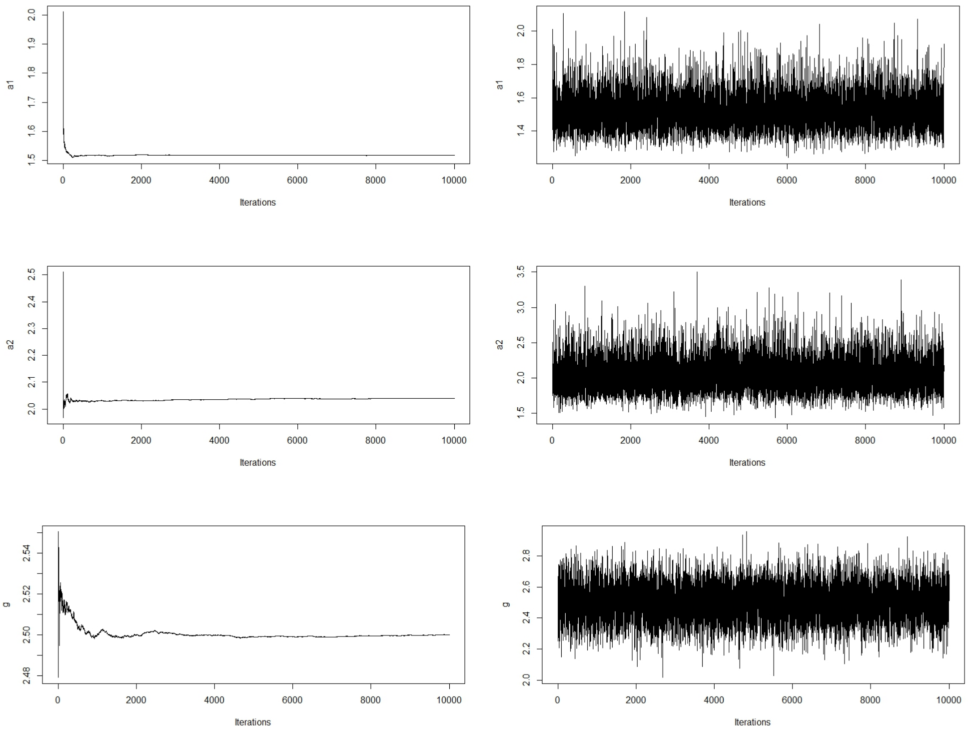

Figure 7.1: Ergodic mean plot and trace plot of Θ_1 for sample size (80,80)

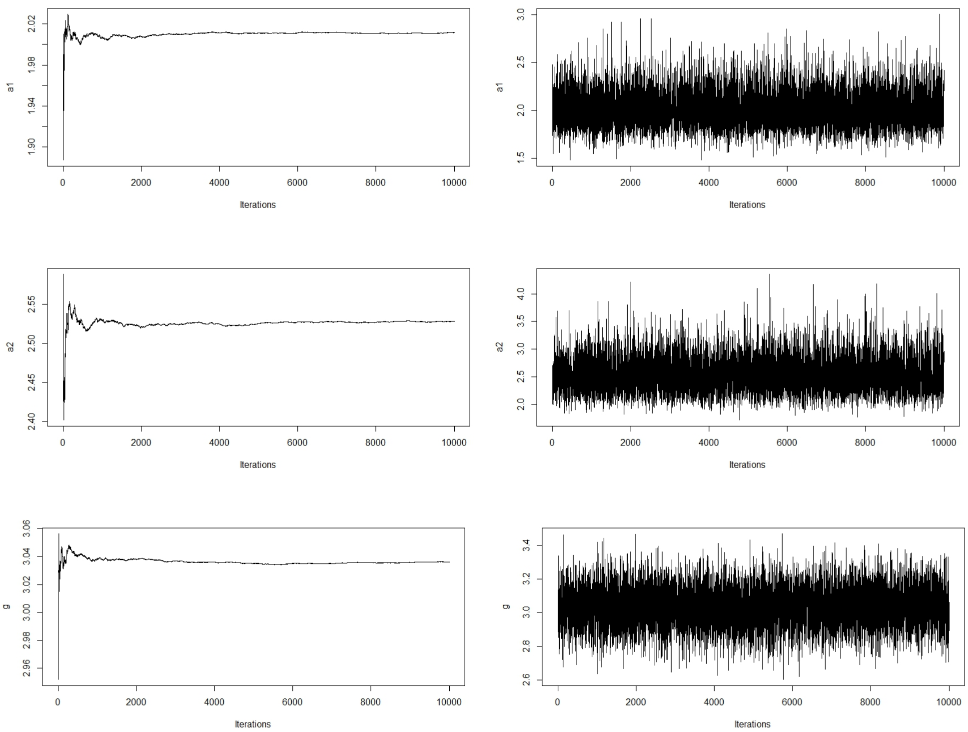

Figure 7.2: Ergodic mean plot and trace plot of Θ_2 for sample size (120,120)

7.8 Data analysis

To illustrate the practical applications, we analyze a real dataset. For this, we consider the failure times of two types of electrical insulation subjected to a continuously increasing voltage stress. This dataset contains 30 recorded failure times for each insulation type as reported in Abd El-Monsef et al. (2022). The failure times of the first type (X) and second type (Y) are given in Table 7.5 and Table 7.6, respectively.

Table 7.5: Failure time of first type (X)

0.097	0.014	0.030	0.134	0.240	0.084
0.146	0.024	0.045	0.004	0.099	0.277
0.472	0.094	0.023	0.146	0.030	0.031
0.104	0.105	0.036	0.065	0.022	0.098
0.178	0.059	0.014	0.007	0.007	0.286

Table 7.6: Failure time of second type (Y)

0.199	0.252	0.103	0.455	0.135	0.348
0.321	0.166	0.040	0.027	0.519	0.270
0.008	0.030	0.084	0.236	0.315	0.177
0.268	0.180	0.796	0.245	0.703	0.045
0.017	0.821	0.942	0.314	0.281	0.652

First, we evaluate the fit of the AGPTE distribution to the given dataset using the K-S goodness-of-fit test. The results are then compared with those of several competing models, including the exponentiated Weibull (EW) (Mudholkar and Srivastava (1993)), the exponentiated generalized inverted exponential (EGIE) (Oguntunde et al. (2014)), Weibull exponential (WE) (Oguntunde et al. (2015)), inverse Weibull (Inv.W.), and exponential distribution. The CDF of the competing distributions are given as follows:

- The CDF of exponential distribution is

$$F(x;\lambda) = 1 - \exp\left\{-\lambda x\right\}, \quad x > 0,\ \lambda > 0.$$

- The CDF of Weibull exponential (WE) is

$$F(x;\alpha,\beta,\lambda) = 1 - \exp\left\{-\alpha\left(e^{\lambda x} - 1\right)^{\beta}\right\}, \quad x > 0, \alpha,\ \beta,\ \lambda > 0.$$

- The CDF of exponentiated generalized inverted exponential (EGIE) is

$$F(x;\alpha,\beta,\lambda) = \left(1 - \left(1 - e^{-\frac{\lambda}{x}}\right)^{\alpha}\right)^{\beta}, \quad x > 0,\ \alpha\ \beta > 0\ \lambda > 0.$$

- The CDF of exponentiated Weibul (EW) is

$$F(x;\alpha,\beta,\lambda) = \left(1 - e^{-\lambda x^{\beta}}\right)^{\alpha}, \quad x > 0,\ \alpha\ \beta > 0\ \lambda > 0.$$

- The CDF of inverse Weibull (IW) is

$$F(x;\alpha,\beta) = \exp\left\{-\frac{\alpha}{x}\right\}^{\beta}, \quad x > 0,\ \alpha\ \beta > 0.$$

Table 7.7: The ML estimates (with standard errors in bracket), KS statistics and P-value for dataset (X)

Model	Parameter estimates			KS Statistics	P-value
EGIE	α=0.50004	β=0.17097	λ=0.14012	0.17368	0.3259
	(0.00390)	(0.03133)	(0.00260)		
IW	α=0.83117	β=0.03064		0.14884	0.5196
	(0.10986)	(0.00714)			
EW	α=2.14890	β=0.66652	λ=8.10348	0.10731	0.8801
	(2.67202)	(0.40697)	(2.56759)		
E	λ=10.0976	-	-	0.09784	0.9363
	(1.84356)				
WE	α=90.2673	β=0.98157	λ=0.10254	0.09315	0.9570
	(0.06067)	(0.14241)	(0.06936)		
AGPTE	α=3010.00	γ=0.92860	-	0.04510	0.9871
	(0.00026)	(0.01284)			

Table 7.8: The ML estimates (with standard errors in bracket), KS statistics and P-value for dataset (Y)

Model	Parameter estimates			KS Statistics	P-value
EGIE	α=0.72393	β=7.14996	λ=0.00556	0.23163	0.0673
	(0.10913)	(8.84909)	(0.00878)		
IW	α=0.74394	β=0.09561		0.21511	0.1068
	(0.09481)	(0.02497)			
E	λ=3.35233	-	-	0.12678	0.6739
	(0.61204)				
WE	α=2.00554	β=0.92817	λ=1.17268	0.11254	0.8016
	(3.51420)	(0.25872)	(1.55639)		
EW	α=0.53703	β=1.65814	λ=3.49727	0.11201	0.8061
	(0.48677)	(1.04945)	(1.01122)		
AGPTE	α=11.8543	γ=0.95316	-	0.10887	0.8317
	(0.57215)	(0.13662)			

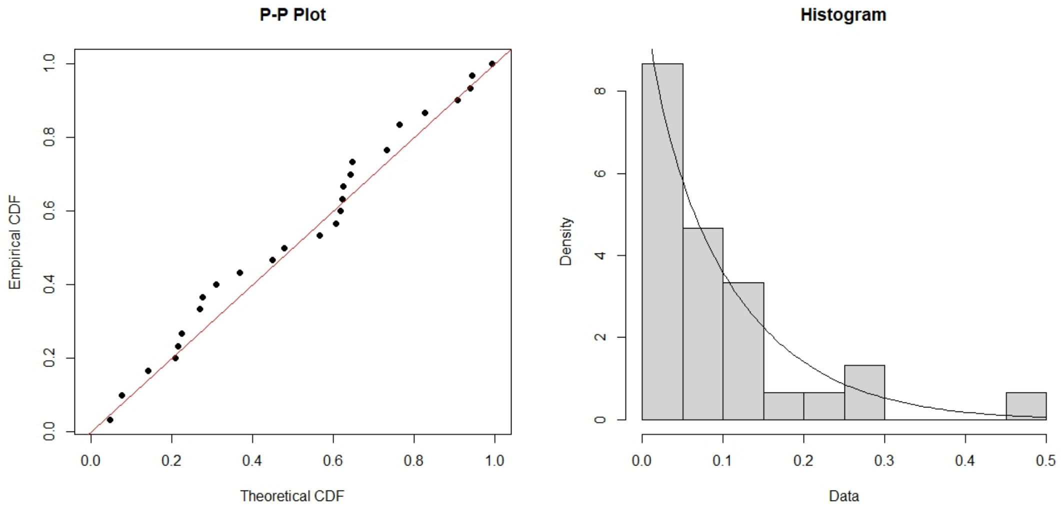

Figure 7.3: P-P plot and histogram for dataset (X)

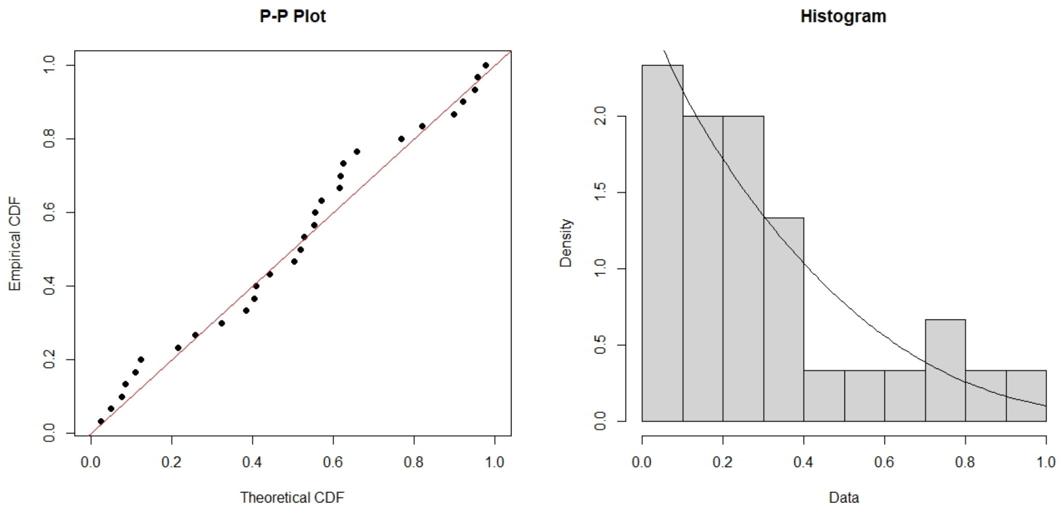

Figure 7.4: P-P plot and histogram for dataset (Y)

The corresponding K-S statistic and P-values are presented in Table 7.7 and Table 7.8. The AGPTE distribution exhibits the lowest K-S statistic and the highest P-value among all considered competing models. The relative histogram and P-P plot for the fitted AGPTE distribution are presented in Figure 7.3 and Figure 7.4. These visualizations further confirm that the AGPTE distribution provides a good fit to the dataset.

We now examine the comparability between the stress and strength parameters, γ_1 and γ_2, using hypothesis testing. We consider the following hypothesis: $H_0 : \gamma_1 = \gamma_2$ Vs $H_1 : \gamma_1 \neq \gamma_2$. Suppose $X \sim$ AGPTE(α_1, γ_1) and $Y \sim$ AGPTE(α_2, γ_2). In this scenario, we obtain the ML estimates of the parameters along with their corresponding log-likelihood values as: $\hat{\alpha}_1 = 1962.45$, $\hat{\alpha}_2 = 11.8459$, $\hat{\gamma}_1 = 0.908191$, $\hat{\gamma}_2 = 0.9500524$, and $l_1 = 46.06371$. Also, for the case $X \sim$ AGPTE(α_1, γ) and $Y \sim$ AGPTE(α_2, γ); the ML estimates for the unknown parameters are determined to be $\hat{\alpha}_1 = 3552.600$, $\hat{\alpha}_2 = 11.66333$, $\hat{\gamma}_1 = 0.940255$, and $l_0 = 46.07341$. The test statistic for evaluating the hypothesis is calculated as $\chi^2 = -2(l_0 - l_1)$. The resultant values of the test statistic and P-values are $\chi^2 = 0.0194$ and P-value= 0.8892, respectively. Thus the P-value indicates that, at a 5% significance level, there is insufficient evidence to reject the null hypothesis. Therefore, we support the assumption that $\gamma_1 = \gamma_2$.

Table 7.9: Estimates and CI of R for the real dataset

ML estimates	$\hat{R}_{MLE}$	$\hat{R}_{MCMC}$	ACI	HPD	BCI
$\hat{\alpha}_1$=3550.60 $\hat{\alpha}_2$=11.6633 $\hat{\gamma}$=0.940255	0.231057	0.261234	(0.172944, 0.289153)	(0.218376, 0.302031)	(0.219024, 0.303985)

We compute the point estimates using MLE and Bayesian estimation via the MCMC method, along with interval estimates, including ACI, HPD, and BCI, for R based on the real dataset. The results are summarized in Table 7.9, indicating that these estimates are relatively close to each other. Furthermore, the HPD intervals are notably shorter than the other two, which aligns well with the findings from our simulation study.

7.9 Summary of the chapter

The estimation of stress-strength reliability for a single-component system is performed by assuming that both the stress and strength components follow a distribution from the AGPT family, sharing a common parameter γ. The estimation is performed using both the MLE and Bayesian approaches for cases where γ is known and unknown. In the case where γ is unknown, obtaining a closed-form expression for the exact Bayesian estimate is challenging. Therefore, the Markov chain Monte-Carlo (MCMC) technique is employed to derive the Bayesian estimate. Further, interval estimation is conducted using ACI, BCI, and HPD credible intervals. To analyze the efficiency of the estimates, a comprehensive simulation study is carried out. The results indicate that all considered estimation techniques perform well, with Bayesian estimates outperforming ML estimates. Furthermore, when γ is known, the MCMC based Bayesian approach provides more precise results than the exact Bayesian estimates. Additionally, for both known and unknown cases of γ, the AIL of the HPD and BCI intervals is smaller compared to that of the ACI. Among these, the HPD interval has the smallest AIL, indicating higher efficiency. For illustration purposes, two real datasets were analyzed, and we observed that the results closely aligned with the findings from the simulation study.

Chapter 8

Stress-strength reliability of s-out-of-k system based on NFE distribution

8.1 Introduction

In the previous chapter, we examined the inference procedure for stress-strength reliability in a single-component system. In practice, we frequently encounter multi-component systems, which offer a more robust and realistic representation of engineering and technological applications. Examples of such systems include power supply systems that consist of multiple generators or power sources to maintain uninterrupted operation and rotor control systems in aerospace, which rely on multiple redundant components to ensure control and stability.

A particular case of multi-component systems is the s-out-of-k system, where the system functions if at least s out of k components operate properly. The reliability analysis of such systems is especially important in engineering, communication networks, and defense applications, where systems are designed to tolerate component failures while maintaining overall functionality. In these settings, each component is subjected to external stress and possesses a certain strength threshold. The system continues to operate as long as the strength of at least s out of k components exceeds the applied stress. Thus, estimating stress-strength reliability in an s-out-of-k system provides a more comprehensive and practical analysis of complex systems across various fields.

Furthermore, we focus on censored samples rather than complete samples, as in many life-testing experiments, some units may be lost or removed before failure, either accidentally or as part of pre-planned strategies to save time and cost. Therefore, studying stress-strength reliability under censored sampling schemes is essential. This chapter examines the estimation of stress-strength reliability for an s-out-of-k system under progressive type-II censoring. We assume that the stress and strength variables follow a special case of the Weibull-G family of distributions, known as the new flexible exponential (NFE) distribution, proposed by Ijaz et al. (2020).

The chapter is organized as follows: Section 8.2 provides an essential background on censoring, with a particular focus on progressive type II censoring. Section 8.3 presents a brief overview of the s-out-of-k system. A comprehensive literature review on the estimation of stress-strength reliability in multi-component systems is given in Section 8.4. Section 8.5 introduces the NFE distribution and discusses some of its key properties. Section 8.6 derives the system reliability function $R_{s,k}$ assuming the stress and strength variables follow independent NFE distributions with a shared parameter b, under progressive type II censoring. Section 8.7 addresses the estimation of $R_{s,k}$ for the case when b is unknown, including classical MLE and Bayesian approaches using Lindley's approximation and MCMC methods. This section also presents interval estimation through ACI, BCI, and HPD intervals. Section 8.8 extends the analysis to the case where b is known, incorporating the same estimation techniques along with the UMVUE. Section 8.9 offers an extensive simulation study to evaluate and compare the performance of the proposed estimation methods under different censoring schemes. In Section 8.10, real-life datasets are analyzed to demonstrate the practical utility of the proposed approach. Finally, Section 8.11

provides a summary and concluding remarks.

8.2 Censoring schemes

In many life testing experiments, censoring is a common phenomenon that arises when the exact time of an event of interest, such as system failure, death, or equipment breakdown, etc., is not completely observed for all experimental units. This may result from various practical constraints such as limited time and cost, insufficient resources, loss of follow-up, or as a part of planned strategies to optimize testing efficiency. Censoring has a wide range of utility in many fields, like medical and clinical trials, engineering and reliability testing, actuarial science, etc.

There are several types of censoring encountered in statistical analyses. Based on the direction of incompleteness, censored data can be classified into three: right censoring, left censoring, and interval censoring. Right censoring occurs when the event of interest has not occurred by the end of the testing period. For example, in a clinical trial, a patient is still alive at the end of the study, so their exact survival time is unknown. Left censoring occurs when the event has already happened before the observation begins, and the exact time is unknown. For example, equipment is found to be in a failed stage at the beginning of the inspection time, and the actual failure time is unknown. Interval censoring occurs when it is known that an event has occurred within a specific time interval, but the exact time of the event is unknown. For example, in an industrial inspection, if a unit is examined every 10 days and is found to have failed during an inspection, we only know that the failure occurred sometime within the interval between two inspections.

Based on the design of the experiment, censoring can be classified into two types: type I censoring, or time censoring, and type II censoring, or failure censoring. Type I censoring occurs when the experiment is terminated at a predetermined time T, regardless of how many failures have occurred. In this case, the failure times of units that failed before time T are observed completely, and the units that survived beyond time T are right censored. Type II censoring occurs when an experiment continues until a pre-specified number of failures, n, have been observed. In this case, the exact failure times of the first n units are known, while the remaining units are considered right-censored. For more details, one may refer to Lawless (1982) and Lee and Wang (2003).

8.2.1 Progressive type II censoring

In certain life testing experiments, it may be necessary to withdraw some of the units that are still functioning during the experiment. For example, when conducting a reliability test on an electronic device, the manufacturer may remove and reassign some active units to meet urgent production demands. As we have seen, type I and type II censoring schemes do not permit the removal of active units during the experiment. To address this limitation, progressive censoring was introduced, which allowed for the withdrawal of active units during the experiment. To benefit from both type II censoring and progressive censoring, the concept of progressive type II censoring was introduced and is defined as follows: Suppose we placed N identical units in a life testing experiment, and the survival life of n units is completely observed. This process is carried out as follows: at the time of the first failure, R_1 units are removed from the remaining $(N-1)$ units. Similarly, at the time of the second failure, R_2 units are removed from the remaining $(N-R_1-2)$ units, and this process continues until the n^{th} failure occurs. At that point all the remaining $R_n = (n - R_1 - R_2 - \cdot - R_n)$ units are removed and the experiment stops. Further, we can observe that for $(R_1 = ... = R_{n-1} = 0)$ and $(N = n,\ R_1 = ... = R_n = 0)$, this scheme reduced to conventional type II right censoring and complete sampling scheme, respectively. For more details on censoring and its applications, one may refer to Balakrishnan and Aggarwala (2000) and Balakrishnan and Cramer (2014).

8.3 s-out-of-k multi-component system

A special case of a multi-component system is the s-out-of-k system, which plays an important role in reliability analysis and various engineering applications. An s-out-of-k system is a multi-component system consisting of k components, where the system is considered operational if and only if at least s components out of the total k components are functioning properly. For example, an automobile generally contains more than one cylinder (k) and assumes that for driving at least 's' cylinders are needed. So, the automobile can be driven if s-out-of-k cylinders fire. Bhattacharyya and Johnson (1974) initially formulated the stress-strength reliability of the s-out-of-k system, which is defined as follows: Let $X_1, X_2, \ldots, X_k$ be the strength variable of k components with CDF $F_X(\cdot)$ and Y be the common stress applied on the system with CDF $F_Y(\cdot)$. Then the stress-strength reliability of a s-out-of-k system is defined as

$$\begin{aligned} R_{s,k} &= P\{\text{at least } s \text{ of } (X_1, X_2, ..., X_k) \text{ exceeds } Y\} \\ &= \sum_{i=s}^{k} \binom{k}{i} \int_{-\infty}^{\infty} (1 - F_X(y))^i ((F_X(y))^{k-i} dF_Y(y). \end{aligned} \tag{8.1}$$

8.4 Review of literature

The study of stress-strength reliability in multi-component systems was initiated by Bhattacharyya and Johnson (1974). Since then, many researchers have contributed to this area, exploring various system configurations, distributional assumptions, and estimation techniques. Norman R and Irwin (1978) investigated the Bayesian estimation of stress-strength reliability, assuming both stress and component strength are independent and identically distributed exponential random variables.

Chandra and Owen (1975) considered the reliability estimation of systems under two practical scenarios: one where each component is subjected to multiple stresses and another where a component consists of several sub-parts, each with its own strength, all being exposed to a single stress. Later, Ebrahimi (1982) explored another complex real-life condition, where a series system composed of p components is subjected to q distinct, independent stresses.

Pandey et al. (1992) proposed an extension to the traditional setup by considering a k component system in which k_1 component strengths follow a common distribution G_1, while the remaining $(k - k_1)$ components follow a different distribution G_2, with all k components facing a common stress. This heterogeneity in strength distribution reflects a more realistic system design. Paul and Uddin (1997) examined the reliability of an s-out-of-k system with non-identical component strengths following an exponential distribution, offering insight into systems with redundancy. Hanagal (2003) studied the reliability of a series system consisting of k components subjected to a common stress. They further considered three distributional assumptions: gamma, Weibull, and Pareto distributions for the stress and strength variables.

Another widely studied multi-component configuration is the consecutive k-out-of-n:G system, which functions if at least k consecutive components operate successfully. Eryilmaz (2008) provided reliability estimation methods for such systems. To reflect the nested system structure investigated the stress-strength reliability of the system, which has n independent components (or subsystems), each consisting of m dependent elements. Similarly, Turkkan and Pham-Gia (2007) addressed the reliability evaluation of a system comprising two subsystems, S_1 and S_2, connected in series, where each subsystem's reliability was modeled using a general stress-strength framework.

Assuming different lifetime models for the stress and strength variables, several studies have been conducted. For instance, Rao and Kantam (2010), Rao (2012a), Rao (2012b), Rao (2012c), Rao et al. (2013), Rao et al. (2015), Kizilaslan and Nadar (2015), Rao et al. (2017), and Dey et al. (2017) considered stress and strength variables following log-logistic, generalized exponential, generalized inverse exponential, Rayleigh, inverse Rayleigh, Burr XII, Weibull, two-parameter exponentiated Weibull, and Kumaraswamy distribution, respectively. Later, Kızılaslan (2017) studied multi-component reliability by assuming that the stress and strength variables belong to the proportional reversed hazard rate model. Similarly, Kızılaslan (2018) considered the case when the stress and strength variables belong to the family of inverse exponentiated distributions. Furthermore, Kizilaslan and Nadar (2018) investigated a system with k statistically independent and identically distributed strength components, where each component is constructed from a pair of statistically dependent elements following a bivariate Kumaraswamy distribution. More recently, Garg et al. (2024) examined the reliability estimation of a multi-component system with non-identical strength components following an inverse Pareto distribution.

The above-mentioned studies primarily focus on the estimation of stress-strength reliability in multi-component systems based on complete samples. However, in many life testing experiments, units may get lost or withdraw from the experiment to reduce time and cost. Thus, estimation procedures based on censored samples have gained importance in recent years. For instance, Kohansal (2019) investigated the estimation of multi-component system reliability using progressively censored data from the Kumaraswamy distribution. Similarly, Ahmadi and Ghafouri (2019), Jha et al. (2020), Maurya and Tripathi (2020), Mahto and Tripathi (2020), and Sauer et al. (2020) considered progressive type II censoring schemes for the generalized half-normal, unit Gompertz, Burr XII, inverted exponentiated Rayleigh, and generalized Pareto distributions, respectively. Later, Saini et al. (2022) and Saini et al. (2023) explored both Bayesian and non-Bayesian approaches for estimating stress-strength reliability using the Burr XII and Topp–Leone distributions under progressive first-failure censoring. Further, Saini and Garg (2022) extended this to multi-component stress-strength models within the Kumaraswamy-G family under progressively first-failure censored schemes. Recently, Hakamipour (2024) addressed an s-out-of-k system where each component comprises two statistically dependent elements subjected to the same random stress, with estimation carried out under progressive censoring.

Chacko and Elizabeth Koshy (2024) examined the inference of multi-component system reliability for the exponentiated Gumbel distribution using ranked set sampling.

These studies show the growing interest in developing robust estimation techniques under various censoring schemes and lifetime distributions for complex systems. Motivated by these studies, the present chapter focuses on the estimation of stress-strength reliability for an s-out-of-k system under progressive type II censoring, assuming that the stress and strength variables are independent and follow the NFE distribution.

8.5 New flexible exponential distribution

Ijaz et al. (2020) proposed a novel family of distributions known as the exponential-H (Exp-H) family, which is similar to the Weibull-G family discussed in Bourguignon et al. (2014). The CDF and PDF of the Exp-H family are defined as

$$\begin{aligned} F(x, a, \Theta) &= 1 - \exp(-aG(x, \Theta)), \quad x, a > 0, \\ f(x, a, \Theta) &= a \exp(-aG(x, \Theta)) g(x, \Theta), \quad x, a > 0, \end{aligned}$$

where $G(x, \Theta) = H(x, \Theta) \exp(x)$, and $H(x, \Theta)$ is a non-decreasing HR depending on the parameter vector Θ and $g(x, \Theta) = \frac{d}{dx}(G(x, \Theta))$. Also, Ijaz et al. (2020) introduced a two-parameter model called the new flexible exponential (NFE) distribution by assuming the HR of the Weibull distribution for $H(x, \Theta)$, *i.e.*, $H(x, \Theta) = ax^{b-1}$. Then, the resulting CDF and PDF are obtained as

$$F(x) = 1 - \exp(-a^2 bx^{(b-1)} \exp(x)), \quad x, a > 0, \ b > 1, \tag{8.2}$$

$$f(x) = a^2 bx^{(b-2)}(x + b - 1) \exp(x - a^2 bx^{(b-1)} \exp(x)), \quad x, \ a > 0, \ b > 1. \tag{8.3}$$

The NFE distribution with parameters a and b is denoted as NFE(a, b). The plot of the density function for various parameter combinations is given in Figure 8.1. Moments, entropies, and inference of NFE are discussed in detail by Ijaz et al. (2020).

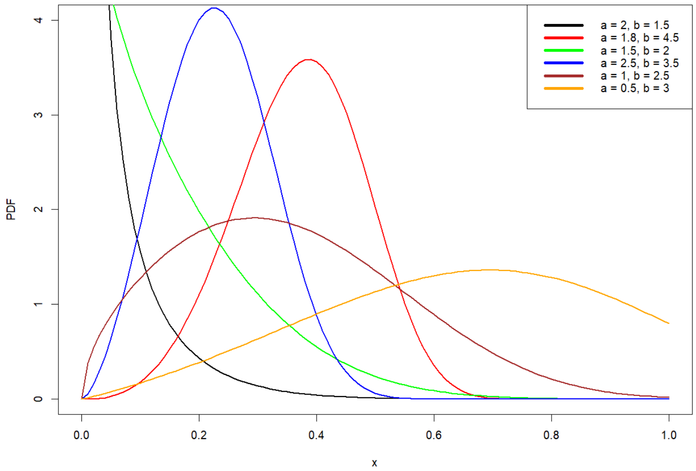

Figure 8.1: The density plot of NFE(a, b) distribution for different values of parameter a and b.

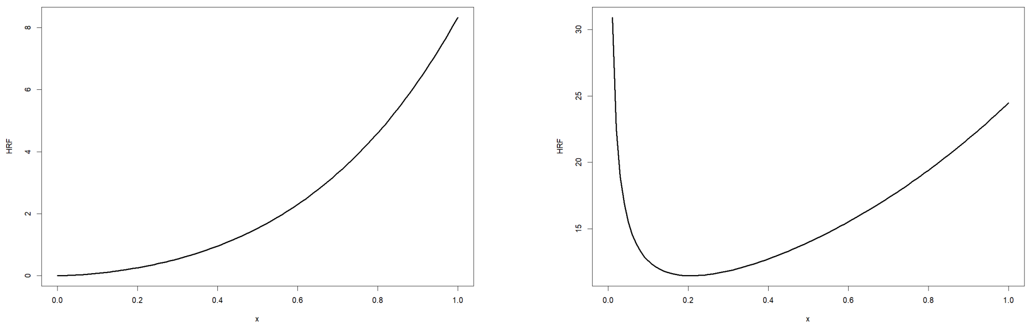

(a) a=0.5, b=3.5 **(b)** a=2, b=1.5

Figure 8.2: The hazard rate plot of NFE(a, b) distribution (a).IHR (b). BT

The HR of NFE(a, b) is given as

$$h(x) = a^2 b x^{(b-2)}(x + b - 1)\exp(x). \tag{8.4}$$

The plot of HR is given in Figure 8.2. It is observed that the shape of the HR varies with respect to b, *i.e.*,

(i) For $1 < b < 2$, it exhibits a bathtub shape, with a change point at $x_0 = \sqrt{(b-1)} - (b-1)$.

(ii) For $b \geq 2$, it shows an IHR behavior.

Notes 6. *The NFE distribution can also be generated using the proposed QT-transformation for suitable choices of $T(\cdot)$, $Q(\cdot)$, and $F(\cdot)$. i.e.,*

$$\begin{aligned} T(x) &= 1 - e^{-ax}, \quad a, x > 0, \\ Q(u) &= \left(\frac{u}{1-u}\right)^{1/\beta}, \quad \beta > 0, \\ F(x) &= \frac{1}{1 + x^{-b}e^{-x}}, \quad x, b > 0, \end{aligned}$$

where $Q(u)$ is the quantile function of the log-logistic distribution, and the baseline $F(x)$ is the modified log-logistic distribution proposed by Kayid (2022).

Notes 7. *The hazard rate exhibits both monotonic and non-monotonic behavior for different parameter values, making the NFE distribution more flexible for modeling lifetime data.*

Notes 8. *Although the parameters are not explicitly designated as location, scale, and shape parameters, perturbation of parameter values of the NFE distribution is observed to have an impact on the location, scale, and shape of the distribution. These intriguing properties motivated us to delve deeply into the stress-strength model based on the NFE distribution.*

To generate a random sample from NFE(a, b), one may use the inverse transformation method. The quantile function of NFE is given by

$$q(u) = (b-1)W\left(\frac{\left(\frac{-\log(1-u)}{a^2 b}\right)^{\frac{1}{b-1}}}{b-1}\right),$$

where, $W(z)$ is the Lambert W function defined as the inverse of $z\exp(z)$, when

$z \geq -1$. The functional form of Lambert W function is

$$W(z) = \sum_{i=1}^{n} \frac{(-1)^n n^{n-2}}{(n-1)!} z^n, \quad z \geq -1.$$

8.6 The system reliability, $R_{s,k}$

Suppose a system consists of k independent components subjected to a common stress Y. Let $X_i,\ i = 1, 2, ..., k$ denote the random strength of each component. Assume that $X_i \sim \text{NFE}(a_1, b)$, for $i = 1, 2, ..., k$ and $Y \sim \text{NFE}(a_2, b)$. Then the stress-strength reliability, $R_{s,k}$, using (8.1), (8.2), and (8.3), can be derived as follows:

$$R_{s,k} = \sum_{i=s}^{k} \binom{k}{i} \int_0^\infty \Big[\big(\exp(-a_1^2 b y^{(b-1)} \exp(y)) \big)^i \big(1 - \exp(-a_1^2 b y^{(b-1)} \exp(y)) \big)^{(k-i)} \\ a_2^2 b y^{(b-2)} (y + b - 1) \exp(y - a_2^2 b y^{(b-1)} \exp(y) \Big] \, dy.$$

Let $t = \exp(-a_1^2 b y^{(b-1)} \exp(y)))$. Upon simplification, we get

$$\begin{aligned} R_{s,k} &= \sum_{i=s}^{k} \binom{k}{i} \left(\frac{a_2}{a_1} \right)^2 \int_0^1 t^{\left(\left(\frac{a_2}{a_1} \right)^2 + i - 1 \right)} (1-t)^{(k-i)} \, dt \\ &= \sum_{i=s}^{k} \sum_{j=0}^{k-i} \binom{k}{i} \binom{k-i}{j} \left(\frac{a_2}{a_1} \right)^2 (-1)^j \int_0^1 t^{\left(i + \left(\frac{a_2}{a_1} \right)^2 + j - 1 \right)} \, dt \\ &= \sum_{i=s}^{k} \sum_{j=0}^{k-i} \binom{k}{i} \binom{k-i}{j} \frac{(-1)^j a_2^2}{a_1^2 (i+j) + a_2^2}. \end{aligned} \tag{8.5}$$

In the upcoming sections, we discuss the classical and Bayesian estimation of $R_{s,k}$, given in (8.5).

8.7 Inference of $R_{s,k}$, when b is unknown

In this section, we address both point estimation and interval estimation of $R_{s,k}$ when b is unknown. Point estimation is performed using MLE and Bayesian estimation. In this case, the exact Bayesian estimates are difficult to obtain in explicit form, leading to the derivation of Bayesian estimates using Lindley's approximation and MCMC techniques. Furthermore, 95% confidence intervals are constructed using the ACI, the HPD, and the BCI.

8.7.1 Maximum Likelihood Estimation

To find the ML estimate of $R_{s,k}$, we first compute the ML estimates of the parameters a_1, a_2, and b under progressive type-II censoring. Suppose N systems are placed in a life-testing experiment, each having K components. Then we observe n systems, each with k components. This sample can be represented as

$$\begin{bmatrix} X_{11} & X_{12} & \dots & X_{1k} \\ \vdots & \vdots & \ddots & \vdots \\ X_{n1} & X_{n2} & \dots & X_{nk} \end{bmatrix} \qquad \text{and} \qquad \begin{bmatrix} Y_1 \\ \vdots \\ Y_n \end{bmatrix}$$

Observed Strength Variables Observed Stress Variables.

Now, assume that $\{X_{i1}, \dots, X_{ik}\},\ i = 1, 2, \dots, n$ is a progressive type II censored sample from NFE(a_1, b) based on the censoring scheme $\{K, k, R_1, R_2, \dots, R_k\}$. Similarly, assume $\{Y_1, Y_2, \dots, Y_n\}$ is a progressive type II censored sample from NFE(a_2, b) with respect to the censoring scheme $\{N, n, S_1, S_2, \dots, S_n\}$. Then the likelihood function of a_1, a_2, and b is given by

$$L(a_1, a_2, b) = C_1 \prod_{i=1}^{n} \left(C_2 \prod_{j=1}^{k} f(x_{ij})[1 - F(x_{ij})]^{R_j} \right) f(y_i)[1 - F(y_i)]^{S_i},$$

where

$$\begin{aligned} C_1 &= N(N-S_1-1)\dots(N-S_1-\dots-S_{n-1}-n+1),\\ C_2 &= K(K-R_1-1)\dots(K-R_1-\dots-R_{k-1}-k+1). \end{aligned}$$

The likelihood function of the observed data is

$$\begin{aligned} L(data|a_1,a_2,b) &= C_1\prod_{i=1}^{n} C_2 \prod_{j=1}^{k} a_1^2 b x_{ij}^{(b-2)}(x_{ij}+b-1)\exp(x_{ij}-a_1^2 b x_{ij}^{(b-1)}e^{(x_{ij})})\\ &\big(\exp(-a_1^2 b x_{ij}^{(b-1)}e^{x_{ij}})\big)^{R_j} a_2^2 b y_i^{(b-2)}(y_i+b-1)\exp(y_i-a_2^2 b y_i^{(b-1)}e^{y_i})\\ &\big(\exp(-a_2^2 b y_i^{(b-1)}e^{y_i})\big)^{S_i}\\ &= C_1 C_2^n (a_1)^{2nk}(a_2)^{2n}(b)^{n(k+1)}\Bigg(\prod_{i=1}^{n}\prod_{j=1}^{k} x_{ij}^{(b-2)}\Bigg)\Bigg(\prod_{i=1}^{n} y_i^{(b-2)}\Bigg)\\ &\Bigg(\prod_{i=1}^{n}\prod_{j=1}^{k} x_{ij}+b-1\Bigg)\Bigg(\prod_{i=1}^{n} y_i+b-1\Bigg)\exp\Bigg(\sum_{i=1}^{n}\sum_{j=1}^{k} x_{ij}+\sum_{i=1}^{n} y_i-\\ &\sum_{i=1}^{n}\sum_{j=1}^{k} a_1^2 b x_{ij}^{(b-1)}e^{x_{ij}}(1+R_j)-\sum_{i=1}^{n} a_2^2 b y_i^{(b-1)}e^{y_i}(1+S_i)\Bigg). \end{aligned}$$

Then the corresponding log-likelihood function is

$$\begin{aligned} l(data|a_1,a_2,b) &\propto 2nk\log(a_1)+2n\log(a_2)+n(k+1)\log(b)+\\ &(b-2)\Bigg(\sum_{i=1}^{n}\sum_{j=1}^{k}\log(x_{ij})+\sum_{i=1}^{n}\log(y_i)\Bigg)+\sum_{i=1}^{n}\sum_{j=1}^{k}\log(x_{ij}+b-1)\\ &+\sum_{i=1}^{n}\log(y_i+b-1)+\sum_{i=1}^{n}\sum_{j=1}^{k} x_{ij}+\sum_{i=1}^{n} y_i\\ &-a_1^2 b\sum_{i=1}^{n}\sum_{j=1}^{k} x_{ij}^{(b-1)}e^{x_{ij}}(1+R_j)-a_2^2 b\sum_{i=1}^{n} y_i^{(b-1)}e^{y_i}(1+S_i). \end{aligned}$$

From the likelihood equations of a_1, a_2, and b, we obtain the ML estimates, say $\hat{a}_1, \hat{a}_2$, and $\hat{b}$ as follows:

$$\frac{\partial l}{\partial a_1} = \frac{2nk}{a_1} - 2a_1 b\sum_{i=1}^{n}\sum_{j=1}^{k} x_{ij}^{(b-1)}\exp(x_{ij})(1+R_j) = 0, \tag{8.6}$$

$$\frac{\partial l}{\partial a_2} = \frac{2n}{a_2} - 2a_2 b\sum_{i=1}^{n} y_i^{(b-1)}\exp(y_i)(1+S_i) = 0, \tag{8.7}$$

$$\frac{\partial l}{\partial b} = \frac{n(k+1)}{b} + \sum_{i=1}^{n}\sum_{j=1}^{k}\log(x_{ij}) + \sum_{i=1}^{n}\log(y_i) + \sum_{i=1}^{n}\sum_{j=1}^{k}\frac{1}{(x_{ij}+b-1)}$$
$$+ \sum_{i=1}^{n}\frac{1}{(y_i+b-1)} - a_1^2\sum_{i=1}^{n}\sum_{j=1}^{k}e^{x_{ij}}(1+R_j)x_{ij}^{(b-1)}[1+b\log(x_{ij})]$$
$$- a_2^2\sum_{i=1}^{n}e^{y_i}(1+S_i)y_i^{(b-1)}[1+b\log(y_i)]. \tag{8.8}$$

From (8.6) and (8.7), we get

$$\hat{a}_1 = \sqrt{\frac{nk}{b\sum_{i=1}^{n}\sum_{j=1}^{k}x_{ij}^{(b-1)}e^{x_{ij}}(1+R_j)}} \quad \text{and} \quad \hat{a}_2 = \sqrt{\frac{n}{b\sum_{i=1}^{n}y_i^{(b-1)}e^{y_i}(1+S_i)}}.$$

It is obvious that from (8.8), b cannot be solved explicitly. Hence, we employ a numerical iterative method to find $\hat{b}$. Rewriting equation (8.8) as $b = f(b)$, we obtain

$$f(b) = n(k+1)\Bigg[a_1^2\sum_{i=1}^{n}\sum_{j=1}^{k}e^{x_{ij}}(1+R_j)x_{ij}^{(b-1)}[1+b\log(x_{ij})]$$
$$+ a_2^2\sum_{i=1}^{n}e^{y_i}(1+S_i)y_i^{(b-1)}[1+b\log(y_i)] - \sum_{i=1}^{n}\sum_{j=1}^{k}\log(x_{ij}) - \sum_{i=1}^{n}\log(y_i)$$
$$- \sum_{i=1}^{n}\sum_{j=1}^{k}\frac{1}{(x_{ij}+b-1)} - \sum_{i=1}^{n}\frac{1}{(y_i+b-1)}\Bigg]^{-1}.$$

From the above equation , we can solve for b using the Newton-Raphson method. Once we compute $\hat{b}$, the estimates $\hat{a}_1$ and $\hat{a}_2$ can be obtained. By using the invariance property of ML estimators, we can derive the ML estimate of $R_{s,k}$, denoted as $\hat{R}_{s,k}$, which is given by

$$\hat{R}_{s,k} = \sum_{i=s}^{k}\sum_{j=0}^{k-i}\binom{k}{i}\binom{k-i}{j}\frac{(-1)^j\hat{a}_2^2}{\hat{a}_1^2(i+j)+\hat{a}_2^2}.$$

8.7.2 Asymptotic confidence interval

To construct the ACI of $R_{s,k}$, we utilize the asymptotic distribution of the ML estimate, $\hat{R}_{s,k}$ of $R_{s,k}$. For this, we consider the following matrix:

$$I(\Theta) = [I_{ij}] = \left[-\frac{\partial^2 l}{\partial\theta_i \partial\theta_j}\right], \quad i, j = 1, 2, 3, 4,$$

where $\Theta = (a_1, a_2, b)$, and the entries I_{ij} are given by

$$\begin{aligned}
I_{11} &= \frac{2nk}{a_1^2} + 2b\sum_{i=1}^{n}\sum_{j=1}^{k} x_{ij}^{(b-1)} \exp(x_{ij})(1 + R_j), \\
I_{12} &= I_{21} = 0, \\
I_{22} &= \frac{2n}{a_2^2} + 2b\sum_{i=1}^{n} y_i^{(b-1)} \exp(y_i)(1 + S_i), \\
I_{13} &= I_{31} = 2a_1\sum_{i=1}^{n}\sum_{j=1}^{k} e^{x_{ij}} x_{ij}^{(b-1)}(1 + b\log x_{ij})(1 + R_j), \\
I_{23} &= I_{32} = 2a_2\sum_{i=1}^{n} e^{y_i} y_i^{(b-1)}(1 + b\log y_i)(1 + S_i), \\
I_{33} &= \frac{n(k+1)}{b^2} + \sum_{i=1}^{n}\sum_{j=1}^{k}\frac{1}{(x_{ij} + b - 1)^2} + \sum_{i=1}^{n}\frac{1}{(y_i + b - 1)^2} + \\
&\quad a_1^2\sum_{i=1}^{n}\sum_{j=1}^{k} e^{x_{ij}}(1 + R_j) x_{ij}^{(b-1)} \log x_{ij}[2 + b\log(x_{ij})] + \\
&\quad a_2^2\sum_{i=1}^{n} e^{y_i}(1 + S_i) y_i^{(b-1)} \log y_i[2 + b\log(y_i)].
\end{aligned}$$

Then, let expectation of $I(\theta)$, $E(I(\theta))$ denote the Fisher information matrix. Since the evaluation of the expectation is quite difficult, we can use the observed information matrix introduced by Cox and Hinkley (1974) as a consistent estimator of the Fisher information matrix. Thus the asymptotic variance-covariance matrix of Θ is $I^{-1}(\Theta)$. Suppose $R^T = \left(\frac{\partial R_{s,k}}{\partial a}, \frac{\partial R_{s,k}}{\partial b}\right)$, where

$$\frac{\partial R_{s,k}}{\partial a_1} = \sum_{i=s}^{k}\sum_{j=0}^{k-i}\binom{k}{i}\binom{k-i}{j}\frac{2a_1a_2^2(-1)^{j+1}(i+j)}{(a_1^2(i+j)+a_2^2)^2},$$
$$\frac{\partial R_{s,k}}{\partial a_2} = \sum_{i=s}^{k}\sum_{j=0}^{k-i}\binom{k}{i}\binom{k-i}{j}\frac{2a_1^2a_2(-1)^{j}(i+j)}{(a_1^2(i+j)+a_2^2)^2}.$$

As $R_{s,k}$ does not depend on b, $\frac{\partial R_{s,k}}{\partial b} = 0$. From Cox and Hinkley (1974), we have $\hat{R}_{s,k}$ is asymptotically normal with mean $R_{s,k}$ and the corresponding asymptotic variance, $V(R_{s,k}) = R^T I^{-1} R$. Thus, a $100(1-\alpha)\%$ confidence interval of $R_{s,k}$ is given as

$$(\hat{R}_{s,k} \pm z_{\alpha/2}\hat{V}(\hat{R}_{s,k})),$$

where $z_{\alpha/2}$ is the upper $(\alpha/2)$ percentile of the standard normal distribution and $\hat{V}(\hat{R}_{s,k})$ is the estimate of $V(\hat{R}_{s,k})$, which can be evaluated by replacing θ with the corresponding ML estimate $\hat{\theta} = (\hat{a}_1, \hat{a}_2, \hat{b})$.

8.7.3 Bayesian estimation

The Bayes estimate of $R_{s,k}$ under the squared error loss function is derived by assuming the parameters a_1, a_2 and b as random variables. In Bayesian inference, the choice of prior distribution plays an essential role. Over the years, various authors have suggested different prior distributions for unknown parameters of interest. However, Arnold et al. (1983) pointed out that there is no clear procedure to check whether a particular prior is better than the other. Here we assume that a_1, a_2 and b follow independent Rayleigh (σ_1), Rayleigh (σ_2), and Rayleigh (σ_3) distributions, respectively.

$$\pi(a_1) = \frac{a_1}{(\sigma_1)^2}e^{-\frac{a_1^2}{2\sigma_1^2}}, \quad \sigma_1 > 0,$$
$$\pi(a_2) = \frac{a_2}{(\sigma_2)^2}e^{-\frac{a_2^2}{2\sigma_2^2}}, \quad \sigma_2 > 0,$$

$$\pi(b) = \frac{b}{(\sigma_3)^2} e^{-\frac{b^2}{2\sigma_3^2}}, \quad \sigma_3 > 0.$$

Based on observed data, the joint posterior density function of a_1, a_2 and b is given by

$$\pi(a_1, a_2, b|data) = \frac{L(data|a_1, a_2, b)\pi(a_1)\pi(a_2)\pi(b)}{\int_0^\infty \int_0^\infty \int_0^\infty L(data|a_1, a_2, b)\pi(a_1)\pi(a_2)\pi(b) \; da_1 \; da_2 \; db}. \tag{8.9}$$

It is observed that the posterior distribution of a_1 and a_2 follows the Nakagami distribution and that of b is not in a known form. The PDF of the Nakagami distribution (also known as Nakagami-m distribution) is defined as

$$f(x; m, \Omega) \quad = \quad \frac{2m^m}{\gamma(m)\Omega^m} x^{2m-1} \exp\left(- \frac{m}{\Omega} x^2 \right), \quad \forall x \geq 0, \quad m \geq 1/2, \quad \Omega > 0.$$

The Nakagami distribution with parameter m and Ω is denoted as $Nakagami\{m, \Omega\}$. A detailed discussion on the Nakagami distribution can be found in Nakagami (1960). Under the squared error loss function, the Bayes estimate of $R_{s,k}$ is the posterior mean. It can be seen that this estimate is in the form of a ratio of two integrals, which cannot be solved analytically. Therefore, we use alternative methods to obtain the Bayes estimate. The two effective procedures used here are:

- Lindley's Approximation.
- MCMC Method.

8.7.3.1 Lindley's approximation

As discussed in the preliminary section of Chapter 2, we employ the Lindley's approximation techniques to evaluate the posterior mean of $R_{s,k}$. For this we consider $(\theta_1, \theta_2, \theta_3) \equiv (a_1, a_2, b)$, $\phi \equiv \phi(a_1, a_2, b) \equiv R_{s,k}$ as in (8.5) and $\rho =$

$C + \log(a_1) + \log(a_2) + \log(b) - \frac{a_1^2}{2\sigma_1^2} - \frac{a_2^2}{2\sigma_2^2} - \frac{b^2}{2\sigma_3^2}$. Then we have

$$\rho_1 = \frac{\partial \rho}{\partial a_1} = \frac{\sigma_1^2 - a_1^2}{a_1\sigma_1^2} \qquad \rho_2 = \frac{\partial \rho}{\partial a_2} = \frac{\sigma_2^2 - a_2^2}{a_2\sigma_2^2} \qquad \rho_3 = \frac{\partial \rho}{\partial b} = \frac{\sigma_3^2 - b^2}{b\sigma_3^2},$$

$$l_{11} = \frac{-2nk}{a_1^2} - 2b\sum_{i=1}^{n}\sum_{j=1}^{k} x_{ij}^{(b-1)} e^{x_{ij}}(1+R_j), \quad l_{22} = \frac{-2n}{a_2^2} - 2b\sum_{i=1}^{n} y_i^{(b-1)} e^{y_i}(1+S_i,$$

$$\begin{aligned}
l_{21} &= l_{12} = 0, \\
l_{13} &= l_{31} = -2a_1\sum_{i=1}^{n}\sum_{j=1}^{k} x_{ij}^{(b-1)}\exp(x_{ij})[1+b\log(x_{ij})](1+R_j), \\
l_{23} &= l_{32} = -2a_2\sum_{i=1}^{n} y_i^{(b-1)}\exp(y_i)[1+b\log(y_i)](1+S_i), \\
l_{33} &= -\frac{n(k+1)}{b^2} - \sum_{i=1}^{n}\sum_{j=1}^{k}\frac{1}{(x_{ij}+b-1)^2} - \sum_{i=1}^{n}\frac{1}{(y_i+b-1)^2}, \\
&\quad -a_1^2\sum_{i=1}^{n}\sum_{j=1}^{k} x_{ij}^{(b-1)}\exp(x_{ij})\log(x_{ij})[2+b\log(x_{ij})](1+R_j) \\
&\quad -a_2^2\sum_{i=1}^{n} y_i^{(b-1)}\exp(y_i)\log(y_i)[2+b\log(y_i)](1+S_i),
\end{aligned}$$

$$\begin{aligned}
l_{111} &= \frac{4nk}{a_1^3}, \qquad l_{222} = \frac{4n}{a_2^3}, \\
l_{113} &= l_{131} = l_{311} = -2\sum_{i=1}^{n}\sum_{j=1}^{k} x_{ij}^{(b-1)}\exp(x_{ij})[1+b\log(x_{ij})](1+R_j), \\
l_{133} &= l_{331} = l_{313} = -2a_1\sum_{i=1}^{n}\sum_{j=1}^{k} x_{ij}^{(b-1)}\exp(x_{ij})\log(x_{ij})[2+b\log(x_{ij})](1+R_j), \\
l_{233} &= l_{323} = l_{332} = -2a_2\sum_{i=1}^{n} y_i^{(b-1)}\exp(y_i)\log(y_i)[2+b\log(y_i)](1+S_i), \\
l_{223} &= l_{322} = l_{232} = -2\sum_{i=1}^{n} y_i^{(b-1)}\exp(y_i)[1+b\log(y_i)](1+S_i), \\
l_{333} &= \frac{2n(k+1)}{b^3} + \sum_{i=1}^{n}\sum_{j=1}^{k}\frac{2}{(x_{ij}+b-1)^3} + \sum_{i=1}^{n}\frac{2}{(y_i+b-1)^3}
\end{aligned}$$

$$-a_1^2 \sum_{i=1}^{n} \sum_{j=1}^{k} x_{ij}^{(b-1)} \exp(x_{ij})(\log(x_{ij})^2[3 + b\log(x_{ij})](1 + R_j)$$
$$-a_2^2 \sum_{i=1}^{n} y_i^{(b-1)} \exp(y_i)(\log(y_i))^2[3 + b\log(y_i)](1 + S_i),$$

and all other $l_{ijk} = 0$, $i, j, k = 1, 2, 3$. Also we have

$$\phi_1 = \sum_{i=s}^{k} \sum_{j=0}^{k-i} \binom{k}{i} \binom{k-i}{j} \frac{2a_1 a_2^2 (-1)^{j+1}(i+j)}{(a_1^2(i+j) + a_2^2)^2},$$
$$\phi_2 = \sum_{i=s}^{k} \sum_{j=0}^{k-i} \binom{k}{i} \binom{k-i}{j} \frac{2a_1^2 a_2 (-1)^{j}(i+j)}{(a_1^2(i+j) + a_2^2)^2},$$

$$\phi_3 = 0, \qquad \text{therefore} \quad \phi_{i3} = 0, \qquad \text{for } i = 1, 2, 3.$$

$$\phi_{11} = \sum_{i=s}^{k} \sum_{j=0}^{k-i} \binom{k}{i} \binom{k-i}{j} \frac{2a_2^2 (-1)^{j+1}(i+j)[a_2^2 - 3a_1^2(i+j)]}{(a_1^2(i+j) + a_2^2)^3},$$
$$\phi_{22} = \sum_{i=s}^{k} \sum_{j=0}^{k-i} \binom{k}{i} \binom{k-i}{j} \frac{2a_1^2 (-1)^{j}(i+j)[a_1^2(i+j) - 3a_2^2]}{(a_1^2(i+j) + a_2^2)^3},$$
$$\phi_{12} = \phi_{21} = \sum_{i=s}^{k} \sum_{j=0}^{k-i} \binom{k}{i} \binom{k-i}{j} \frac{4a_1 a_2 (i+j)(-1)^{j+1}[a_1^2(i+j) - a_2^2]}{(a_1^2(i+j) + a_2^2)^3},$$

$\sigma_{ij},\ i,\ j = 1, 2, 3$ can be obtained by using $l_{ij},\ i\ j = 1, 2, 3$. Hence

$$d_4 = \phi_{12}\sigma_{12}, \qquad d_5 = \frac{1}{2}(\phi_{11}\sigma_{11} + \phi_{22}\sigma_{22}),$$
$$A = l_{111}\sigma_{11} + 2l_{131}\sigma_{13} + l_{333}\sigma_{33}, \qquad B = 2l_{232}\sigma_{23} + l_{222}\sigma_{22} + l_{332}\sigma_{33},$$
$$C = l_{113}\sigma_{11} + 2l_{133}\sigma_{13} + 2l_{233}\sigma_{23} + l_{223}\sigma_{22} + l_{333}\sigma_{33}.$$

Then the Bayes estimator of $R_{s,k}$ using Lindley's approximation is given by

$$\hat{R}_{s,k}^{Li} = R_{s,k} + [\phi_1 d_1 + \phi_2 d_2 + d_4 + d_5] + \frac{1}{2}[A(\phi_1\sigma_{11} + \phi_2\sigma_{12}) + B(\phi_1\sigma_{21} + \phi_2\sigma_{22}) + C(\phi_1\sigma_{31} + \phi_2\sigma_{32})].$$

Here $\hat{R}_{s,k}^{Li}$ is evaluated at $(\hat{a}_1, \hat{a}_2, \hat{b})$. Using this method, we cannot construct the credible intervals for $R_{s.k}$. Hence the following MCMC method is used.

8.7.3.2 Markov Chain Monte-Carlo method

As we mentioned earlier, the posterior PDFs of a_1 and a_2 follow the Nakagami distribution and are given below.

$$a_1|b \sim Nakagami\left\{nk+1, \frac{nk+1}{\sum_{i=1}^{n}\sum_{j=1}^{k} bx_{ij}^{(b-1)}e^{x_{ij}}(1+R_j)+\frac{1}{2\sigma_1^2}}\right\},$$
$$a_2|b \sim Nakagami\left\{n+1, \frac{n+1}{\sum_{i=1}^{n}\sum_{j=1}^{k} by_{i}^{(b-1)}e^{y_{i}}(1+S_i)+\frac{1}{2\sigma_2^2}}\right\},$$

and

$$\pi(b|a_1,a_2,data) \propto b^{n(k+1)+1}e^{-\frac{b^2}{2\sigma_3^2}}\left(\prod_{i=1}^{n}\prod_{j=1}^{k}(x_{ij}+b-1)x_{ij}^{(b-1)}\exp\{-a_1^2 bx_{ij}^{(b-1)}e^{x_{ij}}(1+R_j)\}\right)$$
$$\times\left(\prod_{i=1}^{n}(y_i+b-1)y_i^{(b-1)}\exp\{-a_2^2 by_i^{(b-1)}e^{y_i}(1+S_i)\}\right). \tag{8.10}$$

Thus, the samples for a_1 and a_2 can be generated from their respective marginal posterior distributions. From (8.10), it is clear that the posterior distribution of b is not in a known form, and direct methods cannot be used to generate samples from it. Therefore, we use the Metropolis-Hastings (MH) algorithm with a normal proposal distribution to simulate samples from the posterior distribution of b. For this purpose, we implement the following steps:

1. Choose the initial guess $(a_1^{(0)}, a_2^{(0)}, b^{(0)})$.

2. Initialize $t = 1$.

3. Generate $a_1^{(t)}$ from $Nakagami\left\{nk+1, \frac{nk+1}{\sum_{i=1}^{n}\sum_{j=1}^{k} bx_{ij}^{(b-1)}\exp(x_{ij})(1+R_j)+\frac{1}{2\sigma_1^2}}\right\}$.

4. Generate $a_2^{(t)}$ from $Nakagami\left\{n+1, \frac{n+1}{\sum_{i=1}^{n} by_{i}^{(b-1)}\exp(y_{i})(1+S_i)+\frac{1}{2\sigma_2^2}}\right\}$.

5. Using the following MH algorithm generate $b^{(t)}$ from $\pi(b|a_1^{(t-1)}, a_2^{(t-1)}, data)$ with $N(b^{(t-1)}, V(b))$ as the proposal distribution, where $V(b)$ is obtained from observed fisher information matrix.

- Generate a proposal b^* from $N(b^{(t-1)}, V(b))$.
- Evaluate the acceptance probability

$$\eta_b = \min\left\{1, \frac{\pi(b^*|a_1^{(t-1)}, a_2^{(t-1)}, data)}{\pi(b|a_1^{(t-1)}, a_2^{(t-1)}, data)}\right\}.$$

- Generate U from Uniform$(0,1)$.
- If $U < \eta_b$, accept the proposal and set $b^{(t)} = b^*$, else set $b^{(t)} = b^{(t-1)}$.

6. Compute $R_{s,k}^{(t)} = \sum_{i=s}^{k}\sum_{j=0}^{k-i}\binom{k}{i}\binom{k-i}{j}\frac{(-1)^j(a_2^{(t)})^2}{(a_1^{(t)})^2(i+j)+(a_2^{(t)})^2}$.
7. Set $t = t+1$.
8. Repeat step $3-7$, T times.

The Bayes estimate of $R_{s,k}$ using MCMC method is given by

$$\hat{R}_{s,k}^{MC} = \frac{1}{T}\sum_{t=1}^{T} R_{s,k}^{(t)}.$$

8.7.4 Bayesian credible interval and highest posterior density credible interval

The BCI and HPD of $R_{s,k}$ are constructed using the method suggested by Chen and Shao (1999). Once we compute $R_{s,k}^{(t)}$, $t = 1, 2, \ldots, T$, we obtain the ordered values as $R_{(1)s,k} \le R_{(2)s,k} \le \cdots \le R_{(T)s,k}$. Then the $100(1-\alpha)\%$ BCI for $R_{s,k}$ is given by

$$(R_{([\alpha/2]T)s,k}, R_{([1-\alpha/2]T)s,k}).$$

Also, a $100(1-\alpha)\%$ HPD credible interval of $R_{s,k}$ is constructed by considering the smallest confidence length among all possible $100(1-\alpha)\%$ credible intervals. *i.e.*, $100(1-\alpha)\%$ HPD credible interval for $R_{s,k}$ is obtained as

$$(R_{(j)s,k}, R_{(j+[(1-\alpha)T])s,k}),$$

where j is chosen such that, $R_{(j+[(1-\alpha)T])s,k} - R_{(j)s,k} = \min_{1\leq j\leq T}(R_{(j+[(1-\alpha)T])s,k} - R_{(j)s,k})$, $j = 1, 2, \ldots, T$ and $[\cdot]$ is the greatest integer value function.

8.8 Inference of $R_{s,k}$, when b is known

In this section, we examine both point estimation and interval estimation of $R_{s,k}$ under the assumption that b is known. Point estimates are derived using MLE, Bayesian methods, and uniformly minimum variance unbiased estimation (UMVUE). Although explicit forms of the Bayes estimates are available, we also evaluate the Bayes estimates using Lindley's approximation and the MCMC method for comparative purposes. Furthermore, 95% confidence intervals are constructed using the ACI, the HPD, and the BCI.

8.8.1 Maximum likelihood estimation

Following similar steps, as discussed in Section 8.7.1, the ML estimate of $R_{s,k}$ when b is known can be obtained as

$$\hat{R}_{s,k} = \sum_{i=s}^{k}\sum_{j=0}^{k-i}\binom{k}{i}\binom{k-i}{j}(-1)^j\left[1+\frac{\sum_{i=1}^{n}\sum_{j=1}^{k}x_{ij}^{(b-1)}\exp(x_{ij})(1+R_j)}{k(i+j)\sum_{i=1}^{n}y_i^{(b-1)}\exp(y_i)(1+S_i)}\right].$$

Using the similar procedure as in Section 8.7.1, the ACI of $R_{s,k}$ can be constructed.

8.8.2 UMVUE of $R_{s,k}$

To derive the uniformly minimum variance unbiased (UMVU) estimate of $R_{s,k}$ under progressive type II censoring, it is enough to find the UMVU estimate of $\psi(a_1, a_2)$, where

$$\psi(a_1, a_2) = \frac{a_2^2}{a_1^2(i+j)+a_2^2}.$$

Suppose $\{X_{i1}, \ldots, X_{ik}\}$, $i = 1, 2, \ldots, n$ be a progressively censored sample from NFE(a_1, b) using the censoring scheme $\{K, k, R_1, R_2, \ldots, R_k\}$. Also, let $\{Y_1, Y_2, \ldots, Y_n\}$ be a progressively censored sample from NFE(a_2, b) using the censoring scheme $\{N, n, S_1, S_2, \ldots, S_n\}$. The corresponding likelihood function, when b is known, is given by

$$L(data, b|a_1, a_2) = C_1 C_2^n (a_1)^{2nk} (a_2)^{2n} b^{n(k+1)} \left(\prod_{i=1}^{n} \prod_{j=1}^{k} (x_{ij} + b - 1) x_{ij}^{(b-2)} e^{x_{ij}} \right)$$
$$\left(\prod_{i=1}^{n} (y_i + b - 1) y_i^{(b-2)} e^{y_i} \right) e^{a_1^2 V} e^{a_2^2 U},$$

where

$$U = -\sum_{i=1}^{n} b y_i^{(b-1)} e^{y_i} (1 + S_i) \text{ and } V = -\sum_{i=1}^{n} \sum_{j=1}^{k} b x_{ij}^{(b-1)} e^{x_{ij}} (1 + R_j), \tag{8.11}$$

are complete sufficient statistics for a_2 and a_1, respectively. It is observed that $Y_i^* = Y_i^{(b-1)} e^{Y_i}$, $i = 1, 2, \ldots, n$ is a progressively censored sample from exponential distribution with mean $(a_2^2\, b)^{-1}$. Consider the following transformations

$$\begin{aligned}
Z_1 &= N Y_1^*, \\
Z_2 &= (N - S_1 - 1)(Y_2^* - Y_1^*), \\
&\vdots \\
Z_n &= (N - S_1 - \ldots - S_{n-1} - n + 1)(Y_n^* - Y_{n-1}^*).
\end{aligned}$$

Following Cao and ANg (1986), it is observed that $Z_1, Z_2, \ldots, Z_n$ are independent and identically distributed exponential random variables with mean $(a_2^2\, b)^{-1}$. Further, $U = \sum_{i=1}^{n} Z_i = \sum_{i=1}^{n} (S_i + 1) Y_i^*$ has a gamma distribution with shape parameter n and scale parameter $(a_2^2 b)^{-1}$, *i.e.*,

$$f_U(u) = \frac{(a_2^2 b)^n}{\Gamma n} u^{n-1} e^{-(a_2^2 b) u}, \quad u > 0.$$

Now, we have the following lemma.

Lemma 8.8.1. *Let* $X_{ij}^* = X_{ij}^{b-1}e^{X_{ij}}, i = 1, 2, \ldots, n, \quad j = 1, 2, \ldots, k$ *and* $V = -\sum_{i=1}^n \sum_{j=1}^k (1 + R_j)X_{ij}^*$. *Then the conditional PDF of* Y_i^* *given* $U = u$ *is*

$$f_{Y_i^*|U=u}(y) = \frac{N(n-1)(u-Ny)^{(n-2)}}{u^{n-1}}, \quad 0 < y < \frac{u}{N},$$

and the conditional PDF of X_{11}^* *given* $V = v$ *is*

$$f_{X_{11}^*|V=v}(x) = \frac{K(nk-1)(v-Kx)^{nk-2}}{v^{nk-1}}, \quad 0 < x < \frac{v}{K}.$$

Proof. The conditional PDF of Y_1^* given U is

$$f_{Y_1^*|U=u}(y) = \frac{f_{Y_1^*,U}(y,u)}{f_U(u)},$$

where $f_{Y_i^*,U}(y,u)$ and $f_U(u)$ are the joint PDF of (Y_1^*, U) and PDF of U, respectively. Let $W = \sum_{i=2}^n Z_i$. We can see that W and Z_1 are independent. Then the joint PDF of (Y_1^*, U) can be easily obtained from the joint PDF of (W, Z_1) using the transformation $Z_1 = NY_1^*$ and $U = W + Z_1$. Then,

$$\begin{aligned}
P(Y_1^*, U = u) &= P(Y_1^* = \frac{Z_1}{N}, \sum_{i=1}^n Z_i = u) \\
&= P(Z_1 = NY_1^*, u = Z_1 + \sum_{i=2}^n Z_i) \\
&= P(Z_1 = z_1, W = u - z_1),
\end{aligned}$$

$$\begin{aligned}
f_{Y_1^*|U=u}(y) &= \frac{f_{Y_1^*,U}(y,u)}{f_U(u)} \\
&= \frac{\left((a_2^2b)e^{-(a_2^2b)z_1}\right)\left(\frac{(a_2^2b)^{n-1}}{\Gamma(n-1)}e^{-a_2^2b(u-z_1)}(u-z_1)^{(n-2)}\right)}{\left(\frac{(a_2^2b)^n}{\Gamma n}u^{n-1}e^{-(a_2^2b)u}\right)} \\
&= \frac{(n-1)(u-z_1)^{n-2}}{u^{n-1}} \\
&= \frac{N(n-1)(u-Ny)^{n-2}}{u^{n-1}}, \quad 0 < y < \frac{u}{N}.
\end{aligned}$$

Similarly, we can derive the conditional PDF of X_{11}^* given $V = v$. □

The following theorem provides the UMVU estimate of $\psi(a_1, a_2)$ say, $\hat{\psi}_U(a_1, a_2)$.

Theorem 8.8.1. *Consider the complete sufficient statistics U and V of a_2 and a_1, respectively, given in (8.11). Then the UMVU estimate of $\psi(a_1, a_2) = \frac{a_2^2}{a_1^2(i+j)+a_2^2}$, say $\hat{\psi}_U(a_1, a_2)$ is given by*

$$\hat{\psi}_U(a_1, a_2) = \begin{cases} 1 - \sum\limits_{p=0}^{n-1} (-1)^p \left(\frac{v}{u(i+j)}\right)^p \frac{\binom{n-1}{p}}{\binom{nk+p-1}{p}}, & \text{if} \quad v < u(i+j) \\ \sum\limits_{p=0}^{nk-1} (-1)^p \left(\frac{u(i+j)}{v}\right)^p \frac{\binom{nk-1}{p}}{\binom{n+p-1}{p}}, & \text{if} \quad v > u(i+j). \end{cases}$$

Proof. We know that Y_1^* and X_{11}^* follow an exponential distribution with mean $(Na_2^2 b)^{-1}$ and $(Ka_1^2 b)^{-1}$, respectively. Then

$$\phi(X_{11}^*, Y_1^*) = \begin{cases} 1, & \text{if } KX_{11}^* > (i+j)NY_1^* \\ 0, & \text{if } KX_{11}^* < (i+j)NY_1^*, \end{cases}$$

is an unbiased estimator of $\psi(a_1, a_2)$. Therefore

$$\hat{\psi}_U(a_1, a_2) = E(\phi(X_{11}^*, Y_1^*)|U = u, V = v) = \int\int_A f_{X_{11}^*|V=v}(x) f_{Y_1^*|U=u}(y)\, dx\, dy,$$

where $A = \{(x, y) : 0 < x < v/K,\ 0 < y < u/N\ , Ny(i+j) < Kx\}$. By previous lemma, when $v < u(i+j)$, we have

$$\begin{aligned} \hat{\psi}_U(a_1, a_2) &= \frac{N(n-1)}{u^{n-1}} \frac{K(nk-1)}{v^{nk-1}} \int\limits_0^{\frac{v}{K}} \int\limits_0^{\frac{Kx}{(N(p+q))}} (u - Ny)^{n-2} (v - Kx)^{nk-2}\, dy\, dx \\ &= \frac{NK(n-1)(nk-1)}{u^{n-1} v^{nk-1}} \int\limits_0^{\frac{v}{K}} (v - Kx)^{nk-2} \left[\frac{(u - Ny)^{n-1}}{-N(n-1)} \right]_0^{Kx/N(i+j)} dx \\ &= 1 - \frac{K(nk-1)}{u^{n-1} v^{nk-1}} \int\limits_0^{\frac{v}{K}} (v - Kx)^{nk-2} \left[u - \frac{Kx}{(i+j)} \right]^{n-1} dx \\ & \left[\text{put } t = \frac{Kx}{v},\ dt = \frac{K}{v} dx, \text{ and } v - Kx = v - vt = v(1-t) \right] \end{aligned}$$

$$
\begin{aligned}
&= 1 - (nk-1)\int_0^1 (1-t)^{nk-2}\left(1 - \frac{vt}{u(i+j)}\right)^{n-1} dt \\
&= 1 - (nk-1)\int_0^1 (1-t)^{nk-2}\sum_{p=0}^{n-1}(-1)^p\binom{n-1}{p}\left(\frac{vt}{u(i+j)}\right)^p dt \\
&= 1 - \sum_{p=0}^{n-1}(-1)^p\left(\frac{v}{u(i+j)}\right)^p \frac{\binom{n-1}{p}}{\binom{nk+p-1}{p}}.
\end{aligned}
$$

Proceeding similarly for $v > u(i+j)$, we get

$$
\hat{\psi}_U(a_1, a_2) = \sum_{p=0}^{nk-1}(-1)^p\left(\frac{u(i+j)}{v}\right)^p \frac{\binom{nk-1}{p}}{\binom{n+p-1}{p}}.
$$

□

Now, the UMVU estimate of $R_{s,k}$, say $R_{s,k}^{\hat{U}}$ is

$$
\hat{R}_{s,k}^{U} = \sum_{i=s}^{k}\sum_{j=0}^{k-i}\binom{k}{i}\binom{k-i}{j}(-1)^j\hat{\psi}_U(a_1, a_2). \tag{8.12}
$$

8.8.3 Bayesian estimation

The Bayes estimate of $R_{s,k}$ was derived based on the squared error loss function, assuming that a_1 and a_2 are random variables. Additionally, a_1 and a_2 are assumed to follow independent Rayleigh(σ_1) and Rayleigh(σ_2) distributions, respectively. Then the joint posterior density function of a_1 and a_2 based on the observed sample is

$$
\begin{aligned}
\pi(a_1, a_2|b, data) = &\frac{4a_1^{2nk+1}a_2^{2n+1}}{\Gamma(nk+1)\Gamma(n+1)}\left(\frac{1}{2\sigma_1^2} - V\right)^{nk+1}\left(\frac{1}{2\sigma_2^2} - U\right)^{n+1} \\
&\times \exp\left\{a_1^2\left(V - \frac{1}{2\sigma_1^2}\right) + a_2^2\left(U - \frac{1}{2\sigma_2^2}\right)\right\},
\end{aligned}
$$

where U and V are given in (8.11). The Bayes estimate of $R_{s,k}$, say $\hat{R}_{s,k}^{B}$ under squared error loss function, is given by

$$\hat{R}^B_{s,k} = \int_0^\infty \int_0^\infty R_{s,k}\ \pi(a_1, a_2|b, data)\ da_1\ da_2$$
$$= \sum_{i=s}^{k}\sum_{j=0}^{k-i}\binom{k}{i}\binom{k-i}{j}(-1)^j \int_0^\infty \int_0^\infty \frac{a_2^2}{a_1^2(i+j)+a_2^2}\pi(a_1, a_2|b, data)\ da_1\ da_2. \tag{8.13}$$

Now, by using the idea mentioned in Kizilaslan and Nadar (2018), the Bayes estimate of $R_{s,k}$ can be obtained as follows:

Consider a one-to-one transformation $u_1 = \frac{a_2^2}{a_1^2(i+j)+a_2^2}$, $u_2 = a_1^2(i+j)+a_2^2$. This implies $0 < u_1 < 1$, $0 < u_2 < \infty$, $a_1^2 = \frac{u_2(1-u_1)}{i+j}$, $a_2^2 = u_1u_2$ and the Jacobian of (u_1, u_2) is $J(u_1, u_2) = \frac{1}{4\sqrt{(i+j)u_1(1-u_1)}}$. Then the double integral in (8.13) becomes

$$\frac{\left(\frac{1}{2\sigma_1^2-V}\right)^{nk+1}\left(\frac{1}{2\sigma_2^2-U}\right)^{n+1}}{\Gamma(nk+1)\Gamma(n+1)(i+j)^{nk+1}}\int_0^1\int_0^\infty u_1^{n+1}u_2^{n(k+1)+1}(1-u_1)^{nk}$$
$$\times \exp\left\{-\frac{(u_1-1)}{(i+j)}\left(V-\frac{1}{2\sigma_1^2}\right)-u_1\left(U-\frac{1}{2\sigma_2^2}\right)\right\} du_1du_2$$
$$=\frac{(n+1)(1-z)^{n+1}}{p\beta(n+2, nk+1)}\int_0^1 u_1^{n+1}(1-u_1z)^{nk}(1-u_1z)^{-p}du_1,$$

where $z = 1 - \frac{\left(\frac{1}{2\sigma_2^2}-U\right)(i+j)}{\left(\frac{1}{2\sigma_1^2}-V\right)}$ and $p = n(k+1)+2$. Using the integral form of hyper-geometric series given in Gradshteyn and Ryzhik (1994), we have

$${}_2F_1(\alpha, \beta, \gamma, z) = \frac{1}{B(\beta, \gamma-\beta)}\int_0^1 t^{\beta-1}(1-t)^{\gamma-\beta-1}(1-tz)^{-\alpha}\ dt,\ Re(\gamma) > 0,\ Re(\beta) > 0, |z| < 1.$$

Then,

$$\hat{R}^B_{s,k} = \begin{cases} \displaystyle\sum_{i=s}^{k}\sum_{j=0}^{k-i}\binom{k}{i}\binom{k-i}{j}(-1)^j \frac{(1-z)^{n+1}(n+1)}{p} {}_2F_1(p, n+2, p+1, z), & \text{if } |z| < 1 \\ \displaystyle\sum_{i=s}^{k}\sum_{j=0}^{k-i}\binom{k}{i}\binom{k-i}{j}(-1)^j \frac{n+1}{p(1-z)^{nk+1}} {}_2F_1(p, nk+1, p+1, \tfrac{z}{1-z}), & \text{if } z < -1. \end{cases}$$

Thus, we obtain a closed form for the Bayes estimate of $R_{s,k}$. We also evaluate the Bayes estimates using Lindley's approximation and the MCMC method for the purpose of comparison.

8.8.3.1 Lindley's approximation

In Section (8.7.3), we employed the three-parameter case of Lindley's approximation to determine the Bayes estimates, as all three parameters, a_1, a_2, and b, were assumed to be random variables. However, in this scenario, a_1 and a_2 are treated as random variables, while b is considered known. Hence, the two-parameter case of Lindley's approximation is utilized to compute the Bayes estimates of $R_{s,k}$. *i.e.*, consider $(\theta_1, \theta_2) \equiv (a_1, a_2)$, $\phi \equiv \phi(a_1, a_2) \equiv R_{s,k}$ as in (8.5) and $\rho = C + \log(a_1) + \log(a_2) - \frac{a_1^2}{2\sigma_1^2} - \frac{a_2^2}{2\sigma_2^2}$. Then we the Bayes estimate of $R_{s,k}$ as

$$\hat{R}^{Lin}_{s,k} = R_{s,k} + [\phi_1 d_1 + \phi_2 d_2 + d_3] + \frac{1}{2}[A(\phi_1\sigma_{11} + \phi_2\sigma_{12}) + B(\phi_1\sigma_{21} + \phi_2\sigma_{22})],$$

where

$$\begin{aligned} d_i &= \rho_1\sigma_{i1} + \rho_2\sigma_{i2}, \quad i = 1, 2, \\ d_3 &= \frac{1}{2}[\phi_{11}\sigma_{11} + \phi_{12}\sigma_{12} + \phi_{21}\sigma_{21} + \phi_{22}\sigma_{22}], \\ A &= l_{111}\sigma_{11} + l_{121}\sigma_{12} + l_{211}\sigma_{21} + l_{221}\sigma_{22}, \\ B &= l_{112}\sigma_{11} + l_{122}\sigma_{12} + l_{212}\sigma_{21} + l_{222}\sigma_{22}. \end{aligned}$$

The terms involved in the above expression are the same as those mentioned in Section 8.7.3. Also, note that $\hat{R}^{Lin}_{s,k}$ is evaluated at $(\hat{a}_1, \hat{a}_2)$.

8.8.4 MCMC

It is observed that the marginal posterior densities of a_1 and a_2 follow the Nakagami distribution, with the parameters defined as follows:

$$\begin{aligned}
a_1|data \sim & Nagakami\left\{nk+1, \frac{2(nk+1)\sigma_1^2}{1-2V\sigma_1^2}\right\}, \\
a_2|data \sim & Nakagami\left\{n+1, \frac{2(n+1)\sigma_2^2}{1-2U\sigma_2^2}\right\}.
\end{aligned}$$

Now, we implement the following steps for estimating $R_{s,k}$:

1. Set $t = 1$.
2. Generate $a_1^{(t)}$ from $Nagakami\left\{nk+1, \frac{2(nk+1)\sigma_1^2}{1-2V\sigma_1^2}\right\}$.
3. Generate $a_2^{(t)}$ from $Nakagami\left\{n+1, \frac{2(n+1)\sigma_2^2}{1-2U\sigma_2^2}\right\}$.
4. Compute $R_{s,k}^{(t)} = \sum_{i=s}^{k}\sum_{j=0}^{k-i}\binom{k}{i}\binom{k-i}{j}\dfrac{(-1)^j\left(a_2^{(t)}\right)^2}{\left(a_1^{(t)}\right)^2(i+j)+\left(a_2^{(t)}\right)^2}$.
5. Set $t = t + 1$.
6. Repeat step $2-5$, T times.

Now, the Bayes estimate of $R_{s,k}$ is given by

$$\hat{R}_{s,k}^{MC} = \frac{1}{T}\sum_{t=1}^{T} R_{s,k}^{(t)}.$$

Also, the HPD and BCI of $R_{s,k}$ can be obtained by the method suggested by Chen and Shao (1999). The steps are similar to those given in Section 8.7.4, so we omit them.

8.9 Simulation study

In this section, we conduct an extensive Monte Carlo simulation study to compare the performance of various estimation methods under different censoring schemes (CS). For this purpose, we calculate the AB and MSE of the estimates. Additionally, we examine the efficiency of confidence intervals in terms of AIL and associated CP. These evaluations are carried out for different parameter combinations, hyperparameters, and CS. For computational purposes, we utilize the R statistical software, and the results are based on 1000 replications.

Table 8.1: Censoring Schemes (CS)

(K,k)		CS	(N,n)		CS
(25,15)	R_1	$(0^{*14}, 10)$	(40,20)	S_1	$(0^{*19}, 20)$
	R_2	$(0^{*5}, 1^{*10})$		S_2	(1^{*20})
	R_3	$(0^{*8}, 1^{*4}, 2^{*3})$		S_3	$(0^{*5}, 1^{*10}, 2^{*5})$
(20,12)	R_4	$(0^{*11}, 8)$	(30,18)	S_4	$(0^{*17}, 12)$
	R_5	$(0^{*4}, 1^{*8})$		S_5	$(0^{*6}1^{*12})$
	R_6	$(0^{*4}, 1^{*5}, 2^{*3})$		S_6	$(0^{*7}, 1^{*6}, 2^{*3})$
(15,8)	R_7	$(0^{*7}, 7)$	(22,15)	S_7	$(0^{*14}, 7)$
	R_8	$(0, 1^{*7})$		S_8	$(0^{10}, 1^{*5})$
	R_9	$(0^{*3}, 1^{*3}, 2^{*2})$		S_9	$(0^{*10}, 1^{*3}, 2^{*2})$

We consider three different CS corresponding to each value of (N, n) and (K, k), as reported in Table 8.1. Here N denotes the total number of multi-component systems placed in a life testing experiment, with the failure of n systems observed, and the remaining $(N - n)$ systems assumed to be censored. Similarly, K represents the total number of components in the system, with the failure of k components observed and the rest assumed to be censored. All the results are obtained for $s = 4$ and $s = 6$. To generate random samples from NFE(a_1, b) and NFE(a_2, b) under progressive censoring, we employ the inverse transformation method.

In the case when b is unknown, simulations are performed for two arbitrary sets of parameters: $\Theta_1 = (a_1, a_2, b) = (1.75, 2.5, 3)$ and $\Theta_2 = (a_1, a_2, b) = (2.5, 3.5, 4)$. For computing Bayes estimates, we use two different informative priors: Prior 1: $(\sigma_1, \sigma_2, \sigma_3) = (1.5, 2.5, 3)$ and Prior 2: $(\sigma_1, \sigma_2, \sigma_3) = (1.75, 2, 2.5)$. The AB and MSE of the estimates of $R_{s,k}$ calculated using MLE, Lindley's approximation, and the MCMC method are shown in Table 8.2. To visually analyze the efficiency of various estimation techniques, comparison plots of AB for the unknown case are shown in Figure 8.7. Additionally, we plot the MSE results for a fixed value of (N, n) across varying values of k in Figure 8.5. Moreover, 95% HPD, BCI, and ACI are constructed, and their corresponding AIL along with CP is tabulated in Table 8.4. For the MH algorithm, a proposal distribution similar to $\pi(b|a_1, a_2, b)$ is required. The plots of $\pi(b|a_1, a_2, b)$ for the two sets of parameter combinations for both prior 1 and prior 2 are given in Figure 8.3 and Figure 8.4, respectively. To avoid redundancy, the plots for two specific censoring schemes, (R_1, S_1) and (R_2, S_2), are depicted. By visual inspection, it is observed that the posterior distribution of b is similar to the normal distribution. Hence, a normal proposal distribution is found to be a reasonably good choice. Figures 8.9 to 8.10 present two diagnostic measures, namely the trace plot and ergodic mean plot, to demonstrate the convergence of MCMC for arbitrarily selected censoring schemes (R_3, S_3), (R_5, S_5), and (R_7, S_7).

In the case when b is known ($b = 3.5$), we consider two arbitrary sets of parameters: $\Theta_3 = (a_1, a_2) = (1.5, 2)$ and $\Theta_4 = (a_1, a_2) = (2, 2.5)$. Additionally, for computing Bayes estimates, we use two different informative priors: Prior 3: $(\sigma_1, \sigma_2) = (1, 2)$ and Prior 4: $(\sigma_1, \sigma_2) = (0.75, 1.5)$. Table 8.3 records the AB and MSE of ML estimates, UMVU estimates, exact Bayes estimates, and Bayes estimates using Lindley's approximation and the MCMC method. To visually analyze the efficiency of the different estimation methods, a comparison plot of AB is given in 8.8. Furthermore, we display the MSE outcomes for a fixed (N, n) and varying k in Figure 8.6. Additionally, the AIL and their corresponding CP of

95% HPD, BCI, and ACI are represented in Table 8.5. The following inferences are made from the simulation study:

- From the simulation study, it is inferred that all the considered estimation techniques perform reasonably well, as indicated by the small AB and MSE values, and these values decrease as the sample size increases.
- For all the estimation techniques, the AB and MSE are smaller when $s = 4$ compared to the case when $s = 6$.
- Table 8.2, Figure 8.7, and Figure 8.5 reveal that the AB and MSE of Bayes estimates are smaller than those of ML estimates. Among Bayes estimates, Lindley's estimates are slightly better than MCMC estimates. It is also noted that prior 2 provides better estimates than prior 1.
- The AB and MSE are smaller under Θ_1 compared to Θ_2.
- Table 8.3, Figure 8.8, and Figure 8.6 indicate that Bayes estimates perform better than ML and UMVU estimates. Among Bayes estimates, the exact technique gives better results than the other two. Also, Lindley's estimates are slightly better than MCMC estimates.
- When comparing Bayes estimates between prior 3 and prior 4, it is observed that prior 4 provides better estimates.
- The AB and MSE are smaller under Θ_4 compared to Θ_3.
- From Table 8.4 and Table 8.5, it is observed that all the CP of HPD interval, BCI, and ACI are satisfactory and lie close to the nominal level, and the AIL decreases as the sample size increases.
- The AIL of HPD interval and BCI are smaller when compared to those of ACI. Among HPD interval and BCI, the AIL of HPD interval is the smallest.

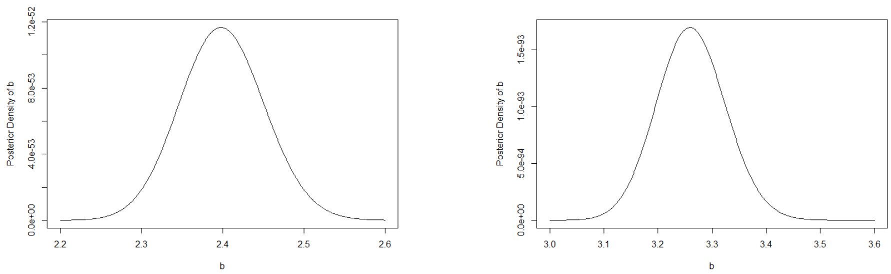

Figure 8.3: The posterior density plot of b corresponding to prior 1 for Θ_1 (*left*) corresponding to (R_1, S_1) and for Θ_2 (*right*) corresponding to (R_2, S_2).

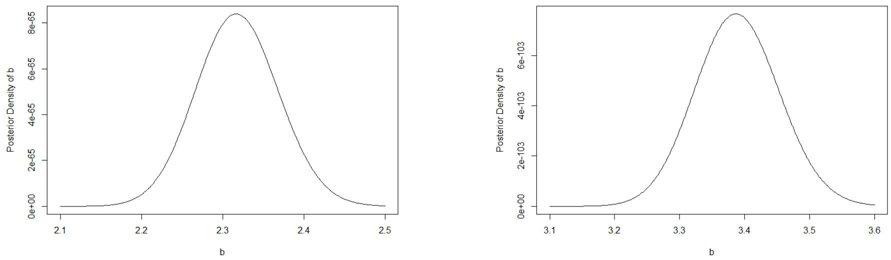

Figure 8.4: The posterior density plot of b corresponding to prior 2 for Θ_1 (*left*) corresponding to (R_1, S_1) and for Θ_2 (*right*) corresponding to (R_2, S_2).

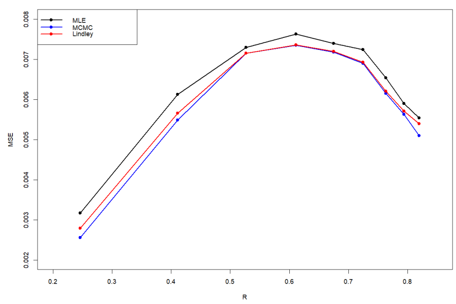

Figure 8.5: MSE plot for Θ_2 (unknown) and $(N, n) = (22, 15)$ and $k = 6, \ldots, 14$

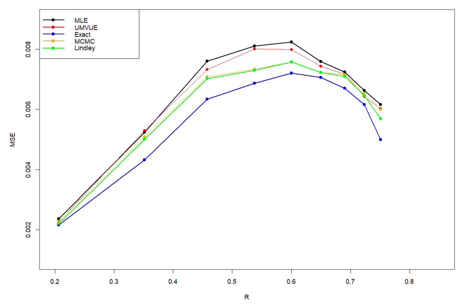

Figure 8.6: MSE plot for Θ_4 (known) and $(N, n) = (22, 15)$ and $k = 6, \ldots, 14$

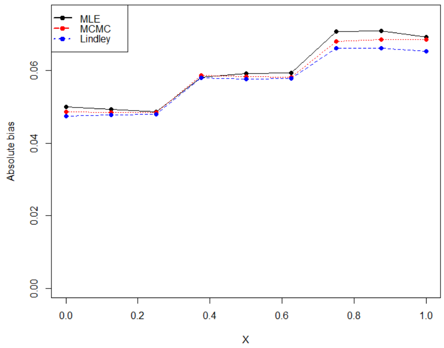

Figure 8.7: AB for Θ_2 (unknown)

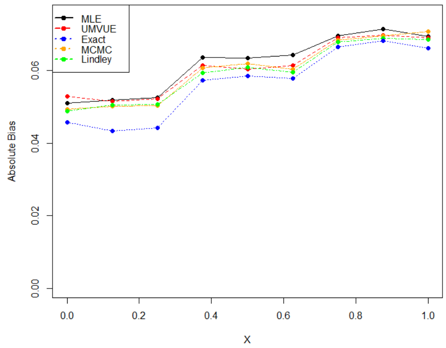

Figure 8.8: AB for Θ_4 (unknown)

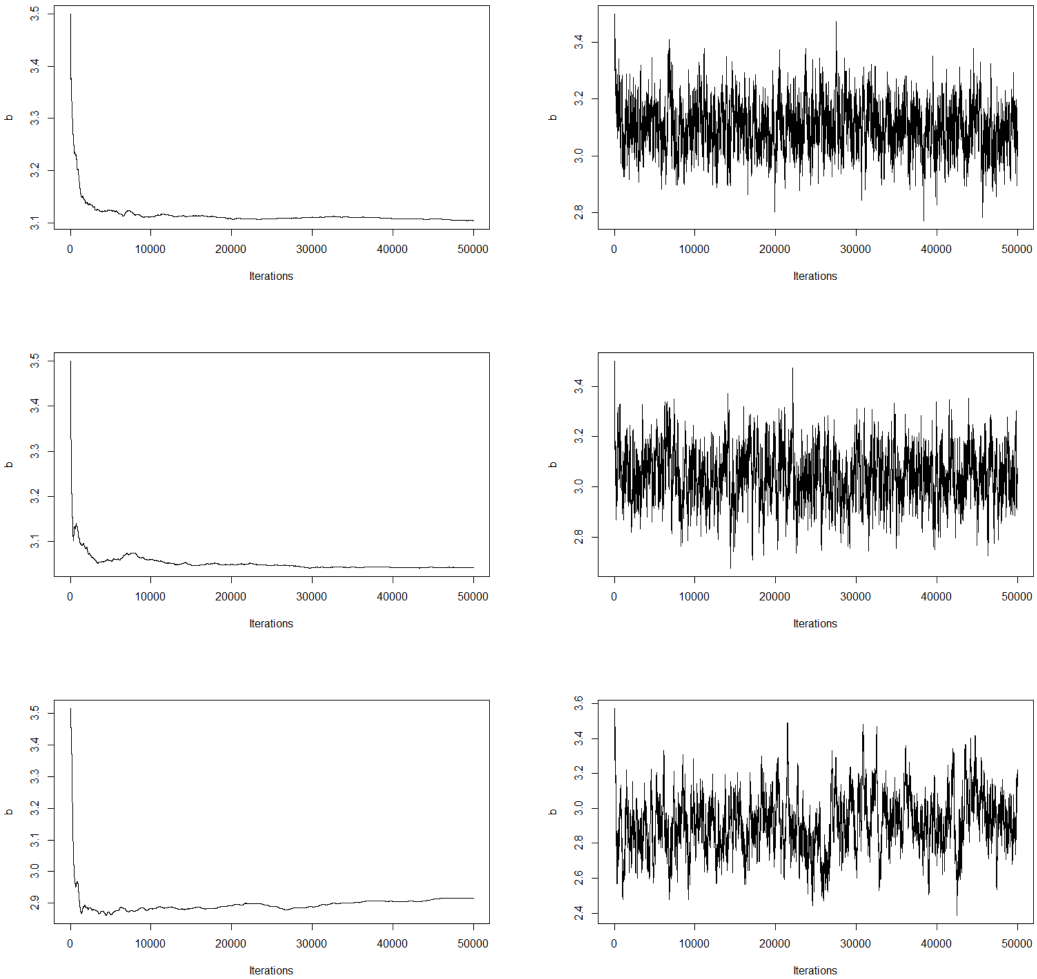

Figure 8.9: Ergodic mean plot and trace plot of Θ_1 for (R_3, S_3), (R_5, S_5) and (R_7, S_7)

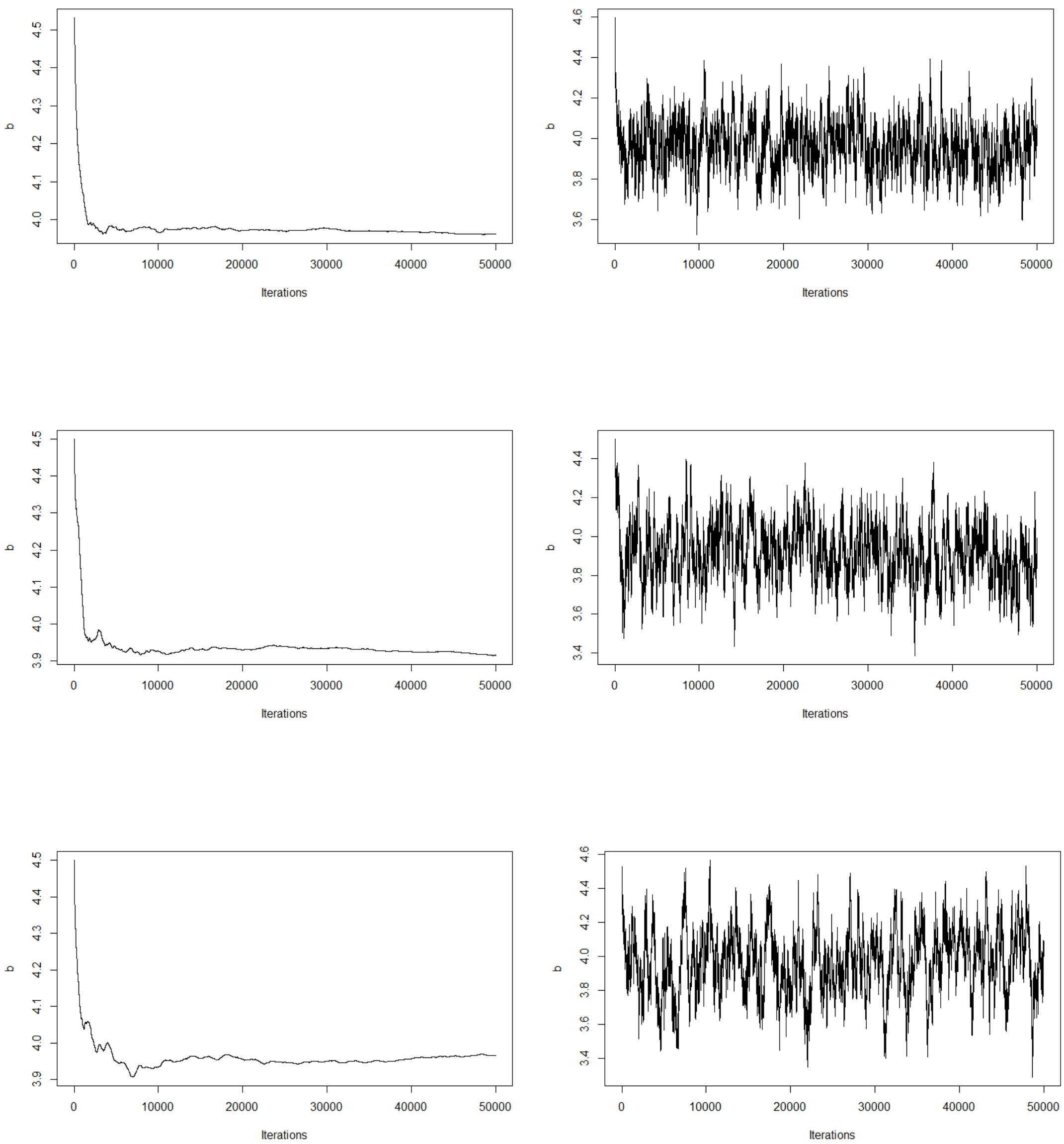

Figure 8.10: Ergodic mean plot and trace plot of Θ_2 for (R_2, S_2), (R_6, S_6) and (R_8, S_8)

Table 8.2: AB and MSE for MLE and Bayes estimates of $R_{s,k}$ (b is unknown)

s	Θ_i	$R_{s,k}$	CS	MLE		Prior 1				Prior 2			
						Lindley		MCMC		Lindley		MCMC	
				Bias	MSE	Bias	MLE	Bias	MSE	Bias	MSE	Bias	MLE
4	Θ_1	0.9298528	(R_1, S_1)	0.031396	0.001549	0.029643	0.001301	0.030119	0.001454	0.029677	0.001315	0.030011	0.001460
			(R_2, S_2)	0.030236	0.001455	0.028477	0.001309	0.029463	0.001370	0.028488	0.001373	0.029232	0.001324
			(R_3, S_3)	0.029865	0.001410	0.029364	0.001419	0.029128	0.001440	0.029370	0.001422	0.029838	0.001298
		0.8943581	(R_4, S_4)	0.040378	0.002538	0.037855	0.002274	0.038948	0.002458	0.037846	0.002275	0.039213	0.002531
			(R_5, S_5)	0.041102	0.002658	0.038085	0.002313	0.039673	0.002402	0.038090	0.002316	0.039575	0.002404
			(R_6, S_6)	0.040241	0.002591	0.037977	0.002173	0.038796	0.002274	0.037998	0.002175	0.039577	0.002344
		0.7835419	(R_7, S_7)	0.063124	0.006075	0.060066	0.005507	0.061045	0.005829	0.059996	0.005499	0.060021	0.005792
			(R_8, S_8)	0.062943	0.005854	0.060700	0.005859	0.060451	0.005890	0.060570	0.005846	0.061771	0.006162
			(R_9, S_9)	0.061767	0.005917	0.059505	0.005301	0.060087	0.005754	0.059445	0.005288	0.061958	0.006065
6	Θ_1	0.850824	(R_1, S_1)	0.047832	0.003393	0.045909	0.003246	0.046294	0.003305	0.045887	0.003246	0.046316	0.003350
			(R_2, S_2)	0.047256	0.003405	0.045094	0.003181	0.045542	0.003162	0.045066	0.003180	0.045397	0.003229
			(R_3, S_3)	0.047964	0.003552	0.045728	0.003343	0.046860	0.003332	0.045718	0.003342	0.046471	0.003355
		0.7753406	(R_4, S_4)	0.060937	0.005504	0.058513	0.005141	0.058863	0.005665	0.058449	0.005132	0.059673	0.005876
			(R_5, S_5)	0.059368	0.005236	0.059276	0.005477	0.058272	0.004978	0.059208	0.005469	0.059102	0.005245
			(R_6, S_6)	0.060265	0.005412	0.059497	0.005620	0.057054	0.005119	0.059391	0.005606	0.059532	0.005652
		0.5396772	(R_7, S_7)	0.069290	0.007565	0.067631	0.007109	0.067996	0.007146	0.067441	0.007055	0.067757	0.007063
			(R_8, S_8)	0.069630	0.007831	0.066465	0.007063	0.068820	0.007352	0.066247	0.007014	0.069049	0.007268
			(R_9, S_9)	0.069242	0.007731	0.067847	0.007589	0.068729	0.007207	0.067642	0.007535	0.069194	0.007424
4	Θ_2	0.9229824	(R_1, S_1)	0.032331	0.001689	0.030878	0.001478	0.030679	0.001464	0.030890	0.001484	0.031722	0.001710
			(R_2, S_2)	0.032276	0.001667	0.030603	0.001506	0.031089	0.001483	0.030646	0.001514	0.031018	0.001586
			(R_3, S_3)	0.032496	0.001716	0.030643	0.001527	0.031588	0.001686	0.030700	0.001535	0.031520	0.001703
		0.8857601	(R_4, S_4)	0.042373	0.002709	0.041764	0.002573	0.041105	0.002589	0.041750	0.002577	0.041375	0.002748
			(R_5, S_5)	0.042628	0.002825	0.041004	0.002762	0.042316	0.002641	0.040997	0.002768	0.041961	0.002726
			(R_6, S_6)	0.043927	0.002991	0.040575	0.002623	0.040406	0.002621	0.040537	0.002629	0.042332	0.003107
		0.7719483	(R_7, S_7)	0.064645	0.006064	0.060611	0.005549	0.061545	0.005700	0.060507	0.005528	0.060634	0.005621
			(R_8, S_8)	0.062998	0.006043	0.060788	0.005693	0.061889	0.006238	0.060605	0.005666	0.060453	0.005693
			(R_9, S_9)	0.064109	0.006236	0.061117	0.005716	0.060947	0.005612	0.061006	0.005707	0.061510	0.005826
6	Θ_2	0.8402593	(R_1, S_1)	0.049933	0.003758	0.047505	0.003543	0.048604	0.003610	0.047441	0.003540	0.048100	0.003740
			(R_2, S_2)	0.049321	0.004082	0.047698	0.003564	0.048423	0.003650	0.047683	0.003643	0.048460	0.003930
			(R_3, S_3)	0.048535	0.003728	0.047900	0.003493	0.048411	0.003592	0.047877	0.003494	0.049115	0.003557
		0.7630574	(R_4, S_4)	0.058133	0.005230	0.057910	0.005049	0.058706	0.005303	0.057840	0.005042	0.058967	0.005551
			(R_5, S_5)	0.059127	0.005497	0.057684	0.004941	0.058380	0.005246	0.057598	0.004922	0.057668	0.005253
			(R_6, S_6)	0.059259	0.005456	0.057815	0.005065	0.058155	0.005141	0.057736	0.005057	0.058904	0.005243
		0.5270025	(R_7, S_7)	0.070679	0.008050	0.066100	0.006852	0.067927	0.007076	0.065604	0.006741	0.068421	0.007428
			(R_8, S_8)	0.070838	0.008118	0.066130	0.006930	0.068530	0.007445	0.065601	0.006802	0.067977	0.007094
			(R_9, S_9)	0.069113	0.008143	0.065222	0.006794	0.068498	0.007351	0.064822	0.006696	0.067196	0.007041

Table 8.3: AB and MSE for ML estimates, UMVU estimates and Bayes estimates of $R_{s,k}$ (b is known)

s	Θ_i	$R_{s,k}$	CS	MLE		UMVUE		Prior 1						Prior 2					
								Exact		Lindley		MCMC		Exact		Lindley		MCMC	
				Bias	MSE	Bias	MSE	Bias	MSE	Bias	MSE	Bias	MSE	Bias	MSE	Bias	MSE		
4	Θ_3	0.8765486	(R_1, S_1)	0.041658	0.002734	0.041618	0.002544	0.036981	0.002028	0.038585	0.002214	0.039710	0.002397	0.036725	0.002022	0.038537	0.002216	0.039321	0.002408
			(R_2, S_2)	0.042719	0.002975	0.041185	0.002545	0.037418	0.002220	0.036843	0.002147	0.038886	0.002359	0.037621	0.002279	0.036801	0.002148	0.039213	0.002384
			(R_3, S_3)	0.041501	0.002610	0.041903	0.002607	0.037013	0.002035	0.039852	0.002412	0.040480	0.002562	0.036495	0.002048	0.039814	0.002412	0.040107	0.002558
		0.8302637	(R_4, S_4)	0.050443	0.003933	0.050649	0.003742	0.048314	0.003681	0.049439	0.003895	0.050085	0.003962	0.047914	0.003758	0.049486	0.003903	0.051020	0.004189
			(R_5, S_5)	0.050884	0.004115	0.049966	0.003740	0.047964	0.003378	0.049306	0.003720	0.050952	0.004043	0.047711	0.003444	0.049249	0.003721	0.049365	0.003770
			(R_6, S_6)	0.052150	0.003986	0.049878	0.003670	0.048918	0.004055	0.049681	0.003850	0.050942	0.003920	0.049549	0.004173	0.049612	0.003848	0.050567	0.003866
		0.7027016	(R_7, S_7)	0.068165	0.006963	0.067583	0.006858	0.064787	0.006437	0.064734	0.006518	0.066768	0.006836	0.064447	0.006088	0.064458	0.006482	0.064602	0.006163
			(R_8, S_8)	0.067090	0.006795	0.066013	0.006723	0.064206	0.006223	0.064679	0.006441	0.065077	0.006391	0.064363	0.006276	0.064409	0.006391	0.065485	0.006782
			(R_9, S_9)	0.067480	0.006974	0.066071	0.006585	0.064763	0.006541	0.065812	0.006598	0.066157	0.006497	0.064073	0.006752	0.065600	0.006542	0.066310	0.007208
6	Θ_3	0.774677	(R_1, S_1)	0.056049	0.004909	0.054836	0.004512	0.051396	0.004254	0.051618	0.004242	0.054774	0.004365	0.050341	0.004194	0.051488	0.004231	0.054862	0.004481
			(R_2, S_2)	0.056516	0.004746	0.055861	0.004620	0.051363	0.004056	0.051723	0.004371	0.055753	0.005106	0.051499	0.004072	0.051654	0.004363	0.056303	0.005017
			(R_3, S_3)	0.055537	0.004743	0.055532	0.004787	0.050746	0.004020	0.053905	0.004482	0.056712	0.005163	0.050409	0.004010	0.053871	0.004476	0.056786	0.005885
		0.6901982	(R_4, S_4)	0.065694	0.006573	0.063827	0.006220	0.058686	0.005253	0.060466	0.005788	0.061434	0.005501	0.060150	0.005533	0.060191	0.005749	0.060166	0.005253
			(R_5, S_5)	0.064551	0.006332	0.064810	0.006435	0.057583	0.005043	0.059637	0.005242	0.063027	0.006159	0.058499	0.005259	0.059447	0.005212	0.061373	0.005820
			(R_6, S_6)	0.063385	0.006181	0.063284	0.005919	0.059170	0.005330	0.060645	0.005671	0.063157	0.006334	0.058003	0.005384	0.060439	0.005626	0.060182	0.005664
		0.4573724	(R_7, S_7)	0.068287	0.007607	0.067934	0.007328	0.066713	0.006317	0.066061	0.007022	0.068487	0.007081	0.064513	0.005796	0.065659	0.006901	0.068857	0.007278
			(R_8, S_8)	0.070091	0.007677	0.066101	0.006786	0.064764	0.006885	0.065055	0.006978	0.069126	0.007135	0.062313	0.006149	0.064646	0.006875	0.068968	0.007371
			(R_9, S_9)	0.070757	0.008138	0.066851	0.006974	0.063245	0.006797	0.064490	0.006656	0.069152	0.007087	0.060355	0.006153	0.063977	0.006548	0.067198	0.006635
4	Θ_4	0.9046318	(R_1, S_1)	0.036938	0.002193	0.036120	0.002094	0.034388	0.001984	0.035602	0.001912	0.035221	0.002317	0.034598	0.002039	0.035597	0.001914	0.034253	0.001601
			(R_2, S_2)	0.035682	0.002166	0.034882	0.001999	0.034947	0.001969	0.035406	0.001911	0.035390	0.001983	0.035358	0.002046	0.035401	0.001914	0.034323	0.001683
			(R_3, S_3)	0.036070	0.002221	0.034746	0.001820	0.034161	0.001922	0.036642	0.002205	0.036537	0.001950	0.034464	0.001996	0.036636	0.002209	0.035678	0.002022
		0.8633435	(R_4, S_4)	0.046345	0.003472	0.045249	0.003133	0.044140	0.003185	0.045150	0.003177	0.046690	0.003427	0.044060	0.003223	0.045144	0.003184	0.045487	0.003237
			(R_5, S_5)	0.045195	0.003192	0.046700	0.003306	0.044306	0.003168	0.045904	0.003364	0.046076	0.003101	0.044656	0.003256	0.045866	0.003365	0.045821	0.003726
			(R_6, S_6)	0.047170	0.003374	0.045847	0.003165	0.045732	0.003238	0.044832	0.003266	0.045420	0.003131	0.046040	0.003300	0.044803	0.003267	0.045414	0.003177
		0.7429363	(R_7, S_7)	0.066979	0.006814	0.063821	0.006086	0.057115	0.004960	0.061318	0.005646	0.063020	0.005953	0.057014	0.004970	0.061123	0.005618	0.061255	0.005680
			(R_8, S_8)	0.066676	0.006727	0.064737	0.006431	0.058573	0.005192	0.063288	0.006164	0.064331	0.006325	0.058000	0.005085	0.063255	0.006158	0.063239	0.006134
			(R_9, S_9)	0.067045	0.006618	0.065964	0.006656	0.059492	0.005421	0.063281	0.006213	0.063955	0.006118	0.058685	0.005281	0.063086	0.006191	0.062586	0.005918
6	Θ_4	0.8132668	(R_1, S_1)	0.051014	0.004040	0.052908	0.004277	0.045781	0.003124	0.048828	0.003584	0.049268	0.003593	0.045177	0.003091	0.048817	0.003587	0.050663	0.003965
			(R_2, S_2)	0.051833	0.004109	0.051441	0.004047	0.043317	0.002804	0.050402	0.004052	0.050098	0.003911	0.043037	0.002760	0.050320	0.004048	0.052235	0.004182
			(R_3, S_3)	0.052582	0.004253	0.052097	0.004185	0.044141	0.002895	0.050652	0.003979	0.050243	0.003930	0.044100	0.002911	0.050646	0.003979	0.049274	0.004061
		0.7324233	(R_4, S_4)	0.063568	0.006134	0.061278	0.005634	0.057320	0.005109	0.059307	0.005141	0.060621	0.005589	0.056481	0.005004	0.059220	0.005128	0.060048	0.005767
			(R_5, S_5)	0.063363	0.006340	0.060291	0.005742	0.058490	0.005207	0.060901	0.005809	0.061922	0.006456	0.057999	0.005097	0.060874	0.005798	0.061403	0.006060
			(R_6, S_6)	0.064269	0.006344	0.061297	0.005738	0.057710	0.005093	0.059445	0.005526	0.060352	0.005612	0.057342	0.005029	0.059414	0.005520	0.060959	0.005903
		0.4966628	(R_7, S_7)	0.069528	0.007836	0.067356	0.007017	0.066479	0.006731	0.067864	0.007083	0.068287	0.007239	0.064545	0.006280	0.067899	0.007151	0.069124	0.007252
			(R_8, S_8)	0.071339	0.007684	0.067291	0.006963	0.068177	0.008268	0.068849	0.007498	0.069498	0.007508	0.065850	0.007600	0.068874	0.007585	0.069675	0.007788
			(R_9, S_9)	0.069305	0.007045	0.066562	0.006898	0.066136	0.006614	0.068535	0.007126	0.070707	0.007647	0.068455	0.007496	0.068197	0.007062	0.068101	0.007215

Table 8.4: Average interval length and coverage probabilities for $R_{s,k}$ ($\alpha = 0.05$) (b is unknown)

s	Θ_i	CS	MLE		Prior 1				Prior 2			
					HPD		BCI		HPD		BCI	
			AIL	CP	AIL	CP	AIL	CP	AIL	CP	AIL	CP
4	Θ_1	(R_1,S_1)	0.306410	0.991	0.125885	0.940	0.245056	0.965	0.135033	0.940	0.24302	0.967
		(R_2,S_2)	0.305136	0.989	0.157413	0.952	0.224693	0.977	0.165106	0.972	0.226632	0.979
		(R_3,S_3)	0.307925	0.989	0.155709	0.956	0.226323	0.973	0.162997	0.960	0.240278	0.985
		(R_4,S_4)	0.372392	0.974	0.259542	0.968	0.290164	0.979	0.265215	0.940	0.29380	0.985
		(R_5,S_5)	0.368672	0.979	0.223239	0.944	0.289899	0.981	0.230927	0.964	0.288719	0.993
		(R_6,S_6)	0.370538	0.989	0.282436	0.944	0.247740	0.989	0.282935	0.976	0.253785	0.977
		(R_7,S_7)	0.519797	0.980	0.310405	0.956	0.235746	0.978	0.315893	0.976	0.246574	0.987
		(R_8,S_8)	0.519845	0.990	0.326576	0.960	0.325039	0.969	0.327885	0.952	0.321228	0.979
		(R_9,S_9)	0.514086	0.977	0.296594	0.964	0.315409	0.973	0.301715	0.940	0.31096	0.979
6	Θ_1	(R_1,S_1)	0.359819	0.974	0.262578	0.968	0.271526	0.985	0.265262	0.956	0.275607	0.977
		(R_2,S_2)	0.354487	0.949	0.250617	0.956	0.271760	0.973	0.254499	0.952	0.282128	0.969
		(R_3,S_3)	0.356613	0.966	0.248442	0.940	0.292891	0.977	0.253515	0.944	0.296808	0.987
		(R_4,S_4)	0.425139	0.985	0.303488	0.964	0.318862	0.985	0.302404	0.956	0.315862	0.973
		(R_5,S_5)	0.425837	0.988	0.298522	0.988	0.316955	0.973	0.299772	0.968	0.311595	0.974
		(R_6,S_6)	0.422835	0.987	0.280728	0.956	0.287654	0.979	0.283843	0.984	0.284320	0.981
		(R_7,S_7)	0.505743	0.988	0.302675	0.956	0.312549	0.979	0.302120	0.968	0.318366	0.973
		(R_8,S_8)	0.499539	0.987	0.310587	0.972	0.280140	0.959	0.310773	0.968	0.275870	0.971
		(R_9,S_9)	0.513683	0.990	0.306757	0.972	0.299923	0.967	0.306290	0.964	0.295866	0.981
4	Θ_2	(R_1,S_1)	0.223586	0.957	0.204750	0.966	0.259031	0.971	0.211311	0.958	0.262831	0.973
		(R_2,S_2)	0.224208	0.966	0.209436	0.955	0.198231	0.989	0.211138	0.949	0.204777	0.985
		(R_3,S_3)	0.221491	0.974	0.185978	0.963	0.201916	0.981	0.192749	0.951	0.208573	0.977
		(R_4,S_4)	0.293484	0.962	0.228548	0.947	0.274995	0.971	0.229538	0.953	0.274500	0.967
		(R_5,S_5)	0.306462	0.987	0.201478	0.955	0.313326	0.981	0.200922	0.959	0.312660	0.979
		(R_6,S_6)	0.291163	0.959	0.215651	0.947	0.240203	0.969	0.215810	0.931	0.236026	0.975
		(R_7,S_7)	0.452381	0.978	0.249143	0.953	0.283519	0.967	0.254885	0.953	0.284954	0.985
		(R_8,S_8)	0.447842	0.988	0.315813	0.971	0.336254	0.971	0.308741	0.963	0.340346	0.987
		(R_9,S_9)	0.446282	0.968	0.304011	0.971	0.277858	0.981	0.305316	0.967	0.277012	0.981
6	Θ_2	(R_1,S_1)	0.300294	0.971	0.236979	0.947	0.262203	0.975	0.235268	0.965	0.264138	0.969
		(R_2,S_2)	0.330593	0.951	0.214037	0.961	0.236327	0.971	0.218637	0.959	0.244958	0.975
		(R_3,S_3)	0.328149	0.950	0.229150	0.967	0.250263	0.975	0.231838	0.951	0.258564	0.969
		(R_4,S_4)	0.371843	0.948	0.300805	0.967	0.281079	0.983	0.307616	0.957	0.282131	0.969
		(R_5,S_5)	0.355595	0.961	0.248653	0.963	0.306871	0.981	0.251008	0.965	0.299836	0.975
		(R_6,S_6)	0.366553	0.972	0.286579	0.977	0.296205	0.975	0.295319	0.965	0.305476	0.969
		(R_7,S_7)	0.468560	0.972	0.312963	0.973	0.312100	0.975	0.305864	0.959	0.311295	0.977
		(R_8,S_8)	0.451303	0.968	0.308540	0.953	0.294627	0.969	0.307289	0.955	0.297632	0.963
		(R_9,S_9)	0.462272	0.992	0.317931	0.949	0.323645	0.981	0.317584	0.959	0.330929	0.973

Table 8.5: Average interval length and coverage probabilities for $R_{s,k}$ ($\alpha = 0.05$) (b is known)

s	Θ_i	CS	MLE		Prior 1				Prior 2			
					HPD		BCI		HPD		BCI	
			AIL	CP	AIL	CP	AIL	CP	AIL	CP	AIL	CP
4	Θ_3	(R_1, S_1)	0.301141	0.992	0.137867	0.948	0.216527	0.972	0.145097	0.940	0.220595	0.968
		(R_2, S_2)	0.294525	0.989	0.142479	0.948	0.220459	0.960	0.149766	0.940	0.224640	0.984
		(R_3, S_3)	0.294378	0.988	0.153041	0.948	0.253253	0.976	0.157998	0.948	0.222619	0.972
		(R_4, S_4)	0.367098	0.982	0.272844	0.972	0.262655	0.976	0.278527	0.956	0.266291	0.968
		(R_5, S_5)	0.367401	0.993	0.200007	0.952	0.247829	0.976	0.204828	0.968	0.252697	0.952
		(R_6, S_6)	0.370190	0.986	0.294179	0.964	0.263029	0.976	0.294548	0.976	0.265535	0.984
		(R_7, S_7)	0.508331	0.982	0.326807	0.98	0.288404	0.960	0.326723	0.956	0.294742	0.988
		(R_8, S_8)	0.511346	0.990	0.309978	0.964	0.318686	0.968	0.312413	0.948	0.322605	0.968
		(R_9, S_9)	0.506694	0.981	0.292275	0.96	0.315604	0.968	0.294204	0.956	0.317073	0.980
6	Θ_3	(R_1, S_1)	0.357302	0.979	0.179328	0.936	0.251945	0.984	0.186532	0.932	0.254948	0.972
		(R_2, S_2)	0.356759	0.995	0.228538	0.976	0.217313	0.984	0.235232	0.956	0.222443	0.984
		(R_3, S_3)	0.355047	0.993	0.263412	0.972	0.269038	0.980	0.268567	0.964	0.273170	0.980
		(R_4, S_4)	0.423249	0.989	0.292323	0.976	0.294931	0.980	0.292316	0.956	0.300174	0.976
		(R_5, S_5)	0.420701	0.982	0.294185	0.972	0.298219	0.984	0.297055	0.948	0.300890	0.980
		(R_6, S_6)	0.422862	0.993	0.297572	0.964	0.303693	0.960	0.297216	0.988	0.307377	0.972
		(R_7, S_7)	0.505598	0.982	0.308255	0.976	0.300167	0.980	0.304085	0.956	0.300200	0.984
		(R_8, S_8)	0.502691	0.991	0.308262	0.960	0.305690	0.976	0.305936	0.976	0.303074	0.968
		(R_9, S_9)	0.497595	0.990	0.311131	0.960	0.323323	0.972	0.310041	0.964	0.319759	0.968
4	Θ_4	(R_1, S_1)	0.230093	0.981	0.132322	0.96	0.165168	0.940	0.136373	0.964	0.169281	0.956
		(R_2, S_2)	0.232625	0.962	0.244285	0.952	0.147492	0.988	0.246742	0.940	0.149868	0.984
		(R_3, S_3)	0.214983	0.971	0.125457	0.936	0.114248	0.976	0.129212	0.948	0.118945	0.984
		(R_4, S_4)	0.306808	0.992	0.166280	0.940	0.149959	0.976	0.172149	0.944	0.157296	0.980
		(R_5, S_5)	0.291753	0.960	0.207753	0.956	0.218347	0.988	0.211333	0.952	0.223060	0.980
		(R_6, S_6)	0.296166	0.968	0.264727	0.944	0.197463	0.968	0.265625	0.960	0.201548	0.972
		(R_7, S_7)	0.446672	0.992	0.286505	0.944	0.321477	0.984	0.290552	0.952	0.326187	0.964
		(R_8, S_8)	0.441952	0.977	0.289095	0.956	0.337957	0.984	0.291770	0.968	0.337471	0.984
		(R_9, S_9)	0.462869	0.992	0.326521	0.948	0.319546	0.984	0.325943	0.964	0.320017	0.984
6	Θ_4	(R_1, S_1)	0.298520	0.964	0.186353	0.952	0.268223	0.968	0.190508	0.944	0.272054	0.956
		(R_2, S_2)	0.292871	0.971	0.211622	0.920	0.263089	0.980	0.217454	0.932	0.264097	0.980
		(R_3, S_3)	0.280039	0.963	0.254795	0.948	0.250377	0.976	0.257685	0.960	0.252884	0.956
		(R_4, S_4)	0.370979	0.985	0.225124	0.960	0.312249	0.988	0.231650	0.976	0.311213	0.968
		(R_5, S_5)	0.354925	0.955	0.268231	0.964	0.314150	0.976	0.271928	0.960	0.315699	0.996
		(R_6, S_6)	0.378124	0.952	0.227604	0.952	0.312049	0.988	0.231763	0.948	0.312798	0.980
		(R_7, S_7)	0.456344	0.991	0.305420	0.98	0.318671	0.96	0.303313	0.968	0.318084	0.980
		(R_8, S_8)	0.460459	0.982	0.306089	0.968	0.313901	0.984	0.307095	0.976	0.312840	0.976
		(R_9, S_9)	0.454589	0.977	0.296999	0.968	0.311727	0.976	0.297496	0.976	0.312636	0.964

8.10 Real Data Analysis

In this section, two real-world datasets are analyzed to demonstrate the computational procedures discussed in this chapter. The fitting performance of the proposed NFE distribution is first assessed using the Kolmogorov–Smirnov (K-S) goodness-of-fit test. The results are then compared with several competing models, including the alpha power exponential (APE) distribution Mahdavi and Kundu (2017b), the exponentiated Weibull (EW) distribution Mudholkar and Srivastava (1993), the sine-exponential (SinE) distribution Isa et al. (2022), the exponentiated generalized inverted exponential (EGIE) distribution Oguntunde et al. (2014), and the classical exponential distribution. The CDF of the competing distributions are given as follows:

- The CDF of exponential distribution (E) is

$$F(x;\lambda) = 1 - \exp\left\{-\lambda x\right\}, \quad x > 0,\ \lambda > 0.$$

- The CDF of exponentiated generalized inverted exponential (EGIE) is

$$F(x;\alpha,\beta,\lambda) = \left(1 - \left(1 - e^{-\frac{\lambda}{x}}\right)^{\alpha}\right)^{\beta}, \quad x > 0,\ \alpha\ \beta > 0\ \lambda > 0.$$

- The CDF of exponentiated Weibul (EW) is

$$F(x;\alpha,\beta,\lambda) = \left(1 - e^{-\lambda x^{\beta}}\right)^{\alpha}, \quad x > 0,\ \alpha\ \beta > 0\ \lambda > 0.$$

- The CDF of sine-exponential (SinE) is

$$F(x;\lambda) = \sin\left(\frac{\pi(1 - e^{-\lambda x})}{2}\right), \quad x > 0,\ \lambda > 0.$$

- The CDF of alpha power exponential (APE) is

$$F(x;\alpha,\beta) = \frac{\alpha^{1-e^{-\beta x}} - 1}{a - 1}, \quad x > 0,\ \alpha > 1,\ \beta > 0.$$

8.10.1 Dataset 1

This dataset consists of 100 observations on the breaking stress of carbon fibers (in GPa), as provided by Nichols and Padgett (2006). We construct an s-out-of-k system using this dataset by assigning the stress variable Y_1 as the first observation in the dataset and the strength variables $X_{1k}, k = 1, \ldots, 10$ as $2nd$ to $11th$ observations. Similarly, Y_2 is assigned as the $12th$ observation, and $X_{2k}, k = 1, \ldots, 10$ as the $13th$ to $22nd$ observations, and this process continues up to the $100th$ observation. Consequently, we obtain data for an s-out-of-k system with $n = 9$. For computational ease and comparison with other models, we normalize each observation by dividing it by $(16 + mean(data))$ as suggested in Jha et al. (2022). The transformed data are as follows:

$$X = \begin{bmatrix} 0.147202 & 0.146665 & 0.134309 & 0.193405 & 0.167080 & 0.175676 & 0.154186 & 0.078973 & 0.167080 & 0.237458 \\ 0.171378 & 0.172990 & 0.090792 & 0.176213 & 0.166006 & 0.100463 & 0.169229 & 0.263245 & 0.201463 & 0.130548 \\ 0.159559 & 0.182123 & 0.159021 & 0.135920 & 0.143442 & 0.157410 & 0.172990 & 0.182123 & 0.150963 & 0.225639 \\ 0.136995 & 0.177825 & 0.177825 & 0.153112 & 0.137532 & 0.191256 & 0.169229 & 0.126250 & 0.136995 & 0.139144 \\ 0.150963 & 0.148814 & 0.116580 & 0.152037 & 0.103149 & 0.075750 & 0.197703 & 0.159559 & 0.073064 & 0.052649 \\ 0.263783 & 0.197703 & 0.098851 & 0.085420 & 0.171378 & 0.084346 & 0.043516 & 0.298703 & 0.092941 & 0.085420 \\ 0.065542 & 0.060170 & 0.091867 & 0.116580 & 0.062856 & 0.272916 & 0.133234 & 0.063393 & 0.188570 & 0.116580 \\ 0.067154 & 0.235309 & 0.098851 & 0.020952 & 0.197703 & 0.133234 & 0.045665 & 0.086495 & 0.149888 & 0.252501 \\ 0.096702 & 0.084346 & 0.058021 & 0.109059 & 0.086495 & 0.113894 & 0.101537 & 0.154724 & 0.151500 & 0.110133 \end{bmatrix}$$

$$Y = \begin{bmatrix} 0.199103 \\ 0.129686 \\ 0.158744 \\ 0.179192 \\ 0.128071 \\ 0.148520 \\ 0.107623 \\ 0.090941 \\ 0.109237 \end{bmatrix}.$$

The corresponding K-S statistics and P-values are tabulated in Table 8.6 and Table 8.7. The NFE distribution exhibits the lowest K-S statistics and highest P-values among all other models, indicating that it provides a satisfactory fit to the considered dataset. Furthermore, the empirical and theoretical CDF plots and probability-probability (P-P) plots for X and Y in Figure 8.11 and Figure 8.12, respectively, support our claim that NFE distribution is a better fit for the data than the competing alternatives.

Table 8.6: The ML estimates (with standard errors in brackets), KS statistics, and P-values for dataset 1 (X)

Model	Parameter estimates			KS Statistic	P-value
APE	α=2.45941 (0.10944)	β=8.71266 (0.70278)	-	0.35899	1.685×10^{-10}
E	λ=5.61641 (0.75066)	-	-	0.23366	0.00010
SinE	λ=3.26284 (0.39712)	-	-	0.22454	0.00022
EGIE	α=34.50021 (0.01432)	β=0.29841 (0.03160)	λ=0.76122 (0.00290)	0.11446	0.1891
EW	α=1.27568 (0.61826)	β=2.36754 (0.64184)	λ=96.51218 (80.62881)	0.07523	0.6883
NFE	α=5.95624 (0.82593)	β=3.73596 (0.21771)	-	0.05649	0.9358

Table 8.7: The ML estimates (with standard errors in brackets), KS statistics, and P-values for dataset 1 (Y)

Model	Parameter estimates			KS Statistic	P-value
APE	α=2.50173 (0.34702)	β=8.54075 (2.22565)	-	0.43677	0.0444
E	λ=8.24667 (2.39776)	-	-	0.36721	0.1354
SinE	λ=8.73688 (1.27078)	-	-	0.35964	0.1509
EGIE	α=32.27370 (12.51432)	β=1.83867 (0.64567)	λ=0.45224 (0.87686)	0.14415	0.9785
EW	α=21.81298 (13.33280)	β=1.36065 (2.30115)	λ=53.25067 (15.2997)	0.14188	0.9815
NFE	α=0.21070 (0.02280)	β=5.12042 (0.10547)	-	0.11988	0.9972

Next, we investigate the equivalence between the stress and strength parameters, b_1 and b_2, through hypothesis testing. The hypotheses under consideration are $H_o : b_1 = b_2$ versus $H_1 : b_1 \neq b_2$. Let $X \sim \text{NFE}(a_1, b_1)$ and $Y \sim \text{NFE}(a_2, b_2)$. In this context, the ML estimates of the parameters, along with their corresponding log-likelihood values, are $\hat{a}_1 = 5.117234$, $\hat{a}_2 = 24.347447$, $\hat{b}_1 = 3.546706$, $\hat{b}_2 = 5.369558$, and $l_1 = 150.9524$. Additionally, let $X \sim \text{NFE}(a_1, b)$ and $Y \sim \text{NFE}(a_2, b)$. Here, the ML estimates of the unknown parameters are obtained as $\hat{a}_1 = 5.455843$, $\hat{a}_2 = 6.153592$, $\hat{b} = 3.638177$, and their respective log-likelihood function is denoted as $l_o = 149.4399$. The test statistic for evaluating the hypothesis is calculated as $\chi^2 = -2(l_o - l_1)$. The resulting values of the test statistic and P-values are $\chi^2 = 3.025$, and P-value $= 0.08199$, respectively. The obtained P-value indicates that, at a 5% level of significance, we cannot reject the null hypothesis. Thus, we justify the assumption that $b_1 = b_2$.

Now, we consider two different censoring schemes for further analysis:

- CS 1: $R = (1, 1, 1, 0, 0, 0, 0)$, $S = (1, 1, 1, 0, 0, 0)$ $(k = 7, s = 4)$.
- CS 2: $R = (2, 1, 1, 0, 0, 0)$, $S = (2, 1, 1, 0, 0)$ $(k = 6, s = 3)$.

The corresponding progressively censored data under these two censoring schemes are

$$X_1 = \begin{bmatrix} 0.147202 & 0.134309 & 0.167080 & 0.154186 & 0.078973 & 0.167080 & 0.237458 \\ 0.159559 & 0.159021 & 0.143442 & 0.172990 & 0.182123 & 0.150963 & 0.225639 \\ 0.150963 & 0.116580 & 0.103149 & 0.197703 & 0.159559 & 0.073064 & 0.052649 \\ 0.065542 & 0.091867 & 0.062856 & 0.133234 & 0.063393 & 0.188570 & 0.116580 \\ 0.067154 & 0.098851 & 0.197703 & 0.045665 & 0.086495 & 0.149888 & 0.252501 \\ 0.096702 & 0.058021 & 0.086495 & 0.101537 & 0.154724 & 0.151500 & 0.110133 \end{bmatrix} Y_1 = \begin{bmatrix} 0.199103 \\ 0.158744 \\ 0.128071 \\ 0.107623 \\ 0.090941 \\ 0.109237 \end{bmatrix},$$

and

$$X_2 = \begin{bmatrix} 0.147202 & 0.193405 & 0.175676 & 0.078973 & 0.167080 & 0.237458 \\ 0.136995 & 0.153112 & 0.191256 & 0.126250 & 0.136995 & 0.139144 \\ 0.263783 & 0.085420 & 0.043516 & 0.298703 & 0.092941 & 0.085420 \\ 0.067154 & 0.020952 & 0.133234 & 0.086495 & 0.149888 & 0.252501 \\ 0.096702 & 0.109059 & 0.113894 & 0.154724 & 0.151500 & 0.110133 \end{bmatrix} Y_2 = \begin{bmatrix} 0.199103 \\ 0.179192 \\ 0.148520 \\ 0.090941 \\ 0.109237 \end{bmatrix}.$$

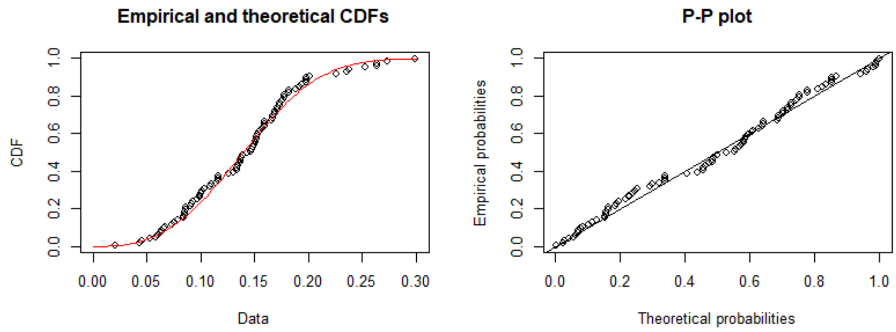

Figure 8.11: Empirical CDF plot and P-P plot for dataset 1 (X)

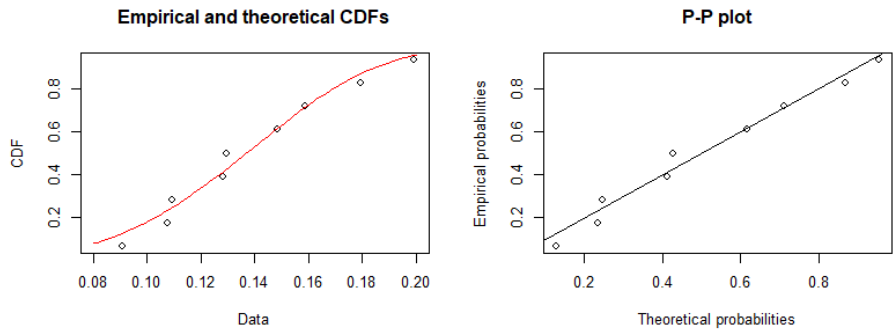

Figure 8.12: Empirical CDF plot and P-P plot for dataset 1 (Y)

We compute the ML estimates of (a_1, a_2, b) and $R_{s,k}$ based on CS 1 and CS 2. Also, the Bayes estimates using Lindley's approximation and MCMC techniques have been computed by arbitrarily choosing the hyper-parameters $\sigma_1 = 1$, $\sigma_2 = 2$, and $\sigma_3 = 2.5$. The results are recorded in Table 8.8. From this table, it is observed that these estimates are relatively close to each other. The 95% ACI and credible intervals of $R_{s,k}$ are calculated for the considered CS and are noted in Table 8.9. We infer that the length of HPD intervals is shorter than the other two, and thus these results satisfactorily coincide with the simulation study.

Table 8.8: Estimates of $R_{s,k}$ under the considered censoring schemes for real datasets.

Data	CS	ML Estimates	$\hat{R}_{s,k}^{MLE}$	$\hat{R}_{s,k}^{Lind}$	$\hat{R}_{s,k}^{MCMC}$
dataset 1	CS 1	$\hat{a}_1 = 4.852867$ $\hat{a}_2 = 4.887101$ $\hat{b} = 3.657667$	0.504466	0.468303	0.495559
dataset 1	CS 2	$\hat{a}_1 = 3.315296$ $\hat{a}_2 = 3.062496$ $\hat{b} = 3.357611$	0.520122	0.506302	0.537114
dataset 2	CS 1	$\hat{a}_1 = 0.330725$ $\hat{a}_2 = 0.503861$ $\hat{b} = 5.260297$	0.643226	0.645401	0.648820
dataset 2	CS 2	$\hat{a}_1 = 0.240729$ $\hat{a}_2 = 0.506653$ $\hat{b} = 10.75583$	0.874396	0.868149	0.863389

Table 8.9: ACI ,BCI and HPD intervals of $R_{s,k}$ under the considered censoring schemes for real datasets.

Data	CS	ACI	BCI	HPD
dataset 1	CS 1	(0.2443469, 0.7645864)	(0.2568185, 0.7345171)	(0.2607467, 0.7249613)
dataset 1	CS 2	(0.2276842, 0.8125616)	(0.2589857, 0.7902811)	(0.2732228, 0.8032365)
dataset 2	CS 1	(0.3995118, 0.8869413)	(0.3960188, 0.8558818)	(0.4106793, 0.8598368)
dataset 2	CS 2	(0.7491164, 0.9996756)	(0.6642133, 0.9316638)	(0.6736229, 0.9277599)

8.10.2 Dataset 2

We examine the monthly water capacity of Trinity Reservoir in California, USA, specifically for June, along with the average annual water capacity of the reservoir from 1980 to 2021. The dataset is accessible at http://cdec.water.ca.gov. Similar datasets have been utilized by various researchers as seen in Kizilaslan and Nadar (2018), Nadar et al. (2013), Kohansal (2019), and Ahmadi and Ghafouri (2019). The maximum and minimum water levels of Trinity Reservoir are mostly observed in June and November, respectively. In this context, we create a scenario related to excessive drought. The claim is that there will be no excessive drought if, for every June over a five-year span, the water capacity of the reservoir exceeds the average annual capacity of the previous year at least two times. Here we set $k = 5$ and $s = 2$. The complete dataset includes Y_1, representing the average annual capacity in the year 1980 and $X_{1j}, j = 1, 2, .., 5$, representing the water capacity in June from 1981 to 1985. Similarly, Y_2 denotes the average annual water capacity in the year 1986, and $X_{2j}, j = 1, 2, ..., 5$, represents the water capacity in June from 1987 to 1991. Continuing this up to 2021, we obtain $n = 7$. For computational ease, data are divided by the total capacity of Trinity reservoir, 2448000 acre-foot. Then the transformed data are as follows:

$$X = \begin{bmatrix} 0.895343 & 0.992402 & 0.994690 & 0.992034 & 0.868913 \\ 0.941996 & 0.847783 & 0.779885 & 0.664966 & 0.473355 \\ 0.844218 & 0.688553 & 0.975538 & 0.948558 & 0.767386 \\ 0.968813 & 0.950884 & 0.782410 & 0.779254 & 0.966773 \\ 0.878157 & 0.930193 & 0.756379 & 0.635813 & 0.516260 \\ 0.988303 & 0.902450 & 0.740257 & 0.434087 & 0.379987 \\ 0.885269 & 0.721991 & 0.945337 & 0.716095 & 0.474733 \end{bmatrix}, \; Y = \begin{bmatrix} 0.845711 \\ 0.829792 \\ 0.343489 \\ 0.865310 \\ 0.754051 \\ 0.605497 \\ 0.461555 \end{bmatrix}$$

First, we assess whether the NFE distribution fits the considered dataset 2. The goodness of fit is checked using the K-S test. Similar to dataset 1, we compare the NFE distribution with several competing alternatives, and the results are presented in Table 8.10 and Table 8.11. The NFE distribution exhibits the lowest K-S statistics and highest P-values among all other models, indicating that it provides a satisfactory fit to the considered dataset. Empirical and theoretical CDFs and P-P plots for X and Y are given in Figure 8.13 and Figure 8.14, respectively, which shows that the NFE distribution is a good fit to the considered dataset.

Table 8.10: The ML estimates (with standard errors in brackets), KS statistics, and P-values for dataset 2 (X)

Model	Parameter estimates			KS Statistic	P-value
APE	α=2.49817 (0.13565)	β=1.84128 (0.00150)	-	0.42356	3.273×10^{-6}
E	λ=1.06145 (0.21106)	-	-	0.34793	0.0002
SinE	λ=0.61311 (0.11177)	-	-	0.34278	0.0003
EGIE	α=112.12249 (7.75899)	β=0.88402 (0.33137)	λ=4.13370 (0.81764)	0.15197	0.3575
EW	α=0.10715 (0.01812)	β=37.83348 (0.11930)	λ=1.31753 (0.11930)	0.11683	0.6826
NFE	α=0.36063 (0.03399)	β=6.54492 (0.87565)	-	0.10703	0.7783

Table 8.11: The ML estimates (with standard errors in brackets), KS statistics, and P-values for dataset 2 (Y)

Model	Parameter estimates			KS Statistic	P-value
E	λ=1.23084 (0.56225)	-	-	0.34478	0.3024
SinE	λ=0.71690 (0.29761)	-	-	0.33618	0.3308
EGIE	α=56.30176 (9.20828)	β=0.59257 (0.49429)	λ=3.27247 (1.73871)	0.25393	0.6702
APE	α=1.00010 (0.39335)	β=1.48770 (0.52349)	-	0.23056	0.7769
EW	α=0.08541 (0.03228)	β=36.60994 (0.00489)	λ=59.69783 (0.00489)	0.21764	0.8309
NFE	α=0.50934 (0.10373)	β=4.73259 (0.14346)	-	0.18271	0.9417

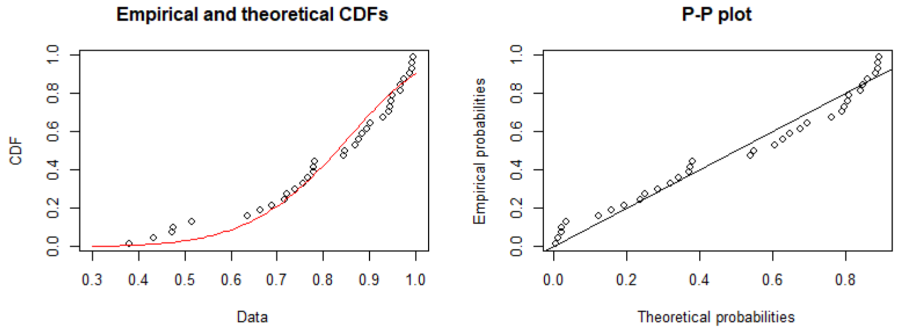

Figure 8.13: Empirical CDF plot and P-P plot for dataset 2 (X)

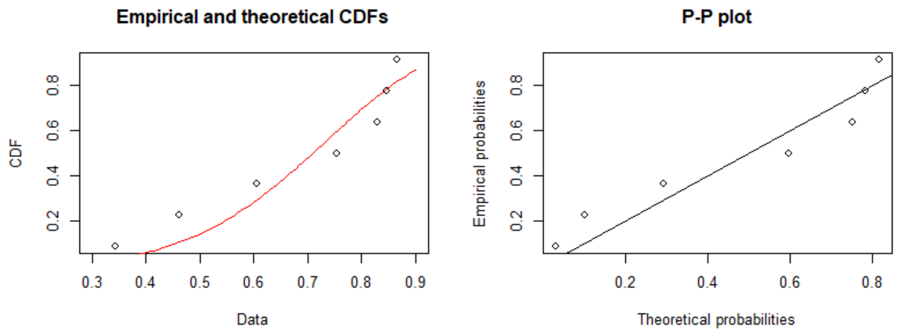

Figure 8.14: Empirical CDF plot and P-P plot for dataset 2 (Y)

We now investigate the comparability between the stress and strength parameters, b_1 and b_2, through hypothesis testing. The hypotheses in focus are $H_o : b_1 = b_2$ Vs $H_1 : b_1 \neq b_2$. Let $X \sim \text{NFE}(a_1, b_1)$ and $Y \sim \text{NFE}(a_2, b_2)$. In this scenario, we derive the ML estimates of the parameters, accompanied by their respective log-likelihood values: $\hat{a}_1 = 0.3752720$, $\hat{a}_2 = 0.5491581$, $\hat{b}_1 = 0.2476823$, $\hat{b}_2 = 4.7159116$, and $l_1 = 16.22642$. Furthermore, consider the cases where $X \sim \text{NFE}(a_1, b)$ and $Y \sim \text{NFE}(a_2, b)$; the ML estimates for the unknown parameters are determined to be $\hat{a}_1 = 0.3802394, \hat{a}_2 = 0.555526, \hat{b} = 5.915725$, with the associated log-likelihood value $l_0 = 15.85517$. The test statistic for evaluating the hypothesis is calculated as $\chi^2 = -2(l_o - l_1)$. The resultant values of the test statistic and P-values are $\chi^2 = 0.7425$, and P-value $= 0.3889$, respectively. The P-value implies that, at a significance level of 5%, there is insufficient evidence to reject the null hypothesis. Thus, we substantiate the assumption that $b_1 = b_2$. For further analysis, we consider two different censoring schemes as given below:

- CS 1 : $R = (1, 0, 0, 0),\ S = (1, 0, 0, 0, 0, 0)\ (k = 4, s = 2)$.
- CS 2 : $R = (0, 0, 2),\ S = (0, 0, 0, 0, 2)\ (k = 3, s = 1)$.

The corresponding progressively censored data under these two censoring schemes are

$$X_1 = \begin{bmatrix} 0.895343 & 0.994690 & 0.992034 & 0.868913 \\ 0.844218 & 0.975538 & 0.948558 & 0.767386 \\ 0.968813 & 0.782410 & 0.779254 & 0.966773 \\ 0.878157 & 0.756379 & 0.635813 & 0.516260 \\ 0.988303 & 0.740257 & 0.434087 & 0.379987 \\ 0.885269 & 0.945337 & 0.716095 & 0.474733 \end{bmatrix},\ Y_1 = \begin{bmatrix} 0.845711 \\ 0.343489 \\ 0.865310 \\ 0.754051 \\ 0.605497 \\ 0.461555 \end{bmatrix}$$

and

$$X_2 = \begin{bmatrix} 0.895343 & 0.992402 & 0.994690 \\ 0.941996 & 0.847783 & 0.779885 \\ 0.844218 & 0.688553 & 0.975538 \\ 0.968813 & 0.950884 & 0.782410 \\ 0.878157 & 0.930193 & 0.756379 \end{bmatrix},\ Y_2 = \begin{bmatrix} 0.845711 \\ 0.829792 \\ 0.343489 \\ 0.865310 \\ 0.754051 \end{bmatrix}$$

Here also, we compute the MLE and Bayes estimates of $R_{s,k}$ based on CS 1 and CS 2, where the Bayes estimates are evaluated using Lindley's approximation and the MCMC technique. The results are recorded in Table 8.8. Also, the 95% ACI and credible intervals are evaluated and are given in Table 8.9. From this table, we can conclude that estimates of $R_{s,k}$ are relatively close to each other, and the HPD interval has the shortest AIL compared to the other two. Thus, we can say that the results obtained under real data analysis satisfactorily coincide with those observed in the simulation study.

8.11 Summary of the chapter

This chapter focused on the estimation of stress-strength reliability in an s-out-of-k system under progressive Type II censoring. The analysis was carried out under the assumption that the stress and strength variables are independent and follow the NFE distribution, sharing a common parameter. The MLE and Bayesian estimation are carried out for both known and unknown cases of the common parameter. For Bayesian estimation, Lindley's approximation and the MCMC method are employed. Additionally, for the case of a known common parameter, the UMVUE is also derived. Interval estimation is performed using ACI, BCI, and HPD credible intervals. A detailed simulation study was conducted to compare the performance of these estimation methods and censoring schemes in terms of AB and MSE. The results revealed that Bayesian methods outperformed classical methods in all cases. In the case of unknown parameter, among the Bayesian techniques, Lindley's approximation is marginally better than the MCMC method. However, no significant difference was observed between them in terms of AB and MSE. In the case of known parameter, UMVUE was found to be marginally better than MLE, and among the Bayesian estimations, the exact Bayesian method yielded the smallest AB and MSE. The AIL of the HPD interval is smaller than those of BCI and ACI for all the cases. It was observed that the coverage probability of the intervals is satisfactory and lies close to the nominal level. For illustration purposes, two real datasets were analyzed; it was observed that the results obtained under real data analysis satisfactorily coincide with those observed in the simulation study.

Chapter 9

Conclusion and recommendations for future research

9.1 Introduction

This chapter summarizes the key findings of the study, highlighting the significance of the proposed method in statistical modeling and reliability analysis. Through this study, we have introduced a novel method for constructing families of distributions, namely QT-transformation and QT_d-transformation, based on the quantile function $Q(\cdot)$ and a continuous function $T(\cdot)$. By selecting well-known mathematical functions, standard transformations, and arbitrarily chosen forms for the function $T(\cdot)$, we developed several new families of distributions. Their statistical properties were thoroughly investigated and demonstrated their applicability through real-world data analysis and stress-strength reliability estimation. Finally, this chapter discusses the limitations of the study and proposes future research directions aimed at enhancing the flexibility, applicability, and efficiency of the proposed methodology in diverse real-world scenarios.

9.2 Summary of the thesis

The study introduced a method for constructing families of distributions that facilitated the development of models with desirable properties derived from commonly used mathematical functions. The proposed method was built using the Q-transformation rule, combined with fundamental properties of the quantile function. Since the method involves a combination of the quantile function $Q(\cdot)$ and a continuous function $T(\cdot)$ that satisfies certain properties, we referred to it as the QT-transformation. Additionally, we proposed an alternative concept called the QT_d-transformation. By selecting well-known functions, widely used transformations, or even arbitrarily chosen functions for $T(\cdot)$, the proposed method generates flexible and robust families of distributions. The statistical properties and parameter estimation of the resulting distributions were examined and validated through extensive real-world data analysis. The usefulness of the models was further demonstrated through their applications in stress-strength reliability estimation. The thesis is structured into nine chapters, each addressing a different aspect of the study.

Chapter 1 provided a brief introduction to lifetime distributions and their significance in various fields. It also included the background, motivation, and objectives of the study. Additionally, a comprehensive review of statistical distributions was conducted.

Chapter 2 provided the essential theoretical background on probability distributions and statistical modeling, covering key properties such as quantiles, moments, reliability measures, order statistics, entropies, stochastic ordering, and tail behavior. It also introduced important distributional classes, estimation techniques, and model selection criteria, forming the basis for the methodological developments in subsequent chapters.

In Chapter 3, we discussed the construction and theoretical foundation of the QT-transformation and its dual concept, the QT_d-transformation. A framework of these approaches is developed by defining their mathematical structure and the necessary conditions for their implementation. Further, we provided the fundamental rules of the quantile function, which were essential for developing the proposed methodology.

As discussed earlier, we considered the widely recognized sigmoid function as the choice for $T(\cdot)$, and the resulting models and their properties were presented in Chapter 4. Among the various types of sigmoid functions, we focused on the logistic sigmoid function, the arctangent sigmoid function, and the error sigmoid function. For the quantile function, we chose the Gumbel distribution. Based on these choices, we proposed the logistic sigmoid Gumbel family, the arctangent sigmoid Gumbel family, and the error sigmoid Gumbel family. Within this framework, we introduced modified exponential distributions, namely LSGE, ASGE, and ESGE, and examined their reliability properties and tail behavior. It was also observed that the proposed models belong to certain significant classes of distributions. For illustration purposes, an extensive simulation study was conducted, followed by a real data analysis to check the practical applicability.

Chapter 5 introduced two families of distributions using the QT-transformation. Specifically, we considered the function $T(\cdot)$ as two well-known transformations: the Yun transformation and the sigmoidal transformation. Since both these transformations have a range between 0 and 1, we select the quantile function $Q(\cdot)$ as the quantile function of the unit Gumbel distribution and the unit exponential distribution. Based on these choices, we introduced two new families of distributions, namely the Yun {unit Gumbel} (YUG) family and the sigmoidal type-I {unit exponential} (SUE) family. Since the study primarily focuses on the generalization of the exponential distribution, we constructed submodels by considering the exponential distribution as the baseline, resulting in the YUGE and SUEE distributions. Also, we examined their structural properties, reliability characteristics, and tail behavior. It is noted that the proposed models belong to some significant classes of distributions. Parameter estimation was performed using the maximum likelihood method, and the performance of the estimators was assessed through an extensive Monte Carlo simulation. Finally, the practical utility of these models was demonstrated through applications to two real-world datasets.

Besides well-known functions, we selected an arbitrary function for $T(\cdot)$ that met all necessary conditions. The resulting model was called the alpha gamma power transformation (AGPT), as it involved the parameters α and γ. Their properties and some results based on a general baseline distribution are discussed. Further, we express the CDF and PDF of AGPT using the series representations and derived key statistical properties, including ordinary moments, incomplete moments, moment generating function, mean residual life, mean waiting time, Rényi entropy, q-entropy, and order statistics. We also explored characterization results based on truncated moments and HR. Using this framework, we introduced a three-parameter generalization of the exponential distribution, called the alpha gamma power transformed exponential (AGPTE) distribution, and studied their parameter estimation using MLE, and their ACI was also constructed. The model performance was evaluated through an extensive simulation study and real-data analysis. These concepts and results were discussed in detail in Chapter 6.

Stress-strength reliability is one of the key metrics in reliability analysis used to measure a system's ability to withstand applied stress. In Chapter 7, we discussed the stress-strength reliability of a system, assuming that the stress and strength variables followed a distribution from the AGPT family sharing a common parameter γ. The estimation procedure was carried out using MLE and Bayesian techniques for cases where γ was known and unknown. In situations where γ is unknown, obtaining the exact form of the Bayesian estimates was challenging, so we employed the MCMC method. Interval estimation for the reliability parameter R was constructed using the ACI, HPD, and BCI. To assess the performance of the estimation methods, an extensive simulation study was conducted. Finally, a real-data analysis was performed to illustrate the practical applicability of the proposed approach.

Chapter 8 focused on the estimation of stress-strength reliability in the s-out-of-k system under progressive type-II censoring. We assumed that the system consists of components facing the common stress where the stress and strength variable follows the NFE distribution, a special submodel of the proposed framework, sharing a common parameter. The estimation procedures used in this chapter are MLE, UMVUE, and Bayesian estimation. MLE was derived for both known and unknown common parameters. We used Lindley's approximation and MCMC to get estimates for the Bayesian approach because it was hard to get exact Bayesian estimates when the common parameter is unknown. We also derive UMVUE when the common parameter is known. The 95% ACI, HPD, and BCI were obtained. A comprehensive simulation study was performed to evaluate the performance of different censoring schemes and estimation methods. Finally, two real datasets with progressive censoring were analyzed for illustration.

Finally, the current chapter concludes the findings and summarizes the study, highlighting its limitations and providing recommendations for future research.

9.3 Limitations of the study

Despite the significant findings and contributions of this study, the limitations also need to be acknowledged. The proposed methods QT-transformation and QT_d-transformation involve a composition of three functions based on specific criteria. The complexity of the resulting model depends on the choice of these three functions, especially the function $T(\cdot)$ and $T_d(\cdot)$, which serves as the outermost function. Thus the behavior of $T(\cdot)$ and T_d plays a crucial role in shaping the distribution. Selecting a highly complex function may increase model flexibility but can also introduce challenges in parameter estimation, computational efficiency, and model interpretability. Additionally, in stress-strength reliability analysis, estimation under the Bayesian framework requires computationally intensive methods such as MCMC and Lindley's approximation, which can be time-consuming and sensitive to prior specifications. Furthermore, the availability of stress-strength data, especially for s-out-of-k systems under censoring, is often limited. Thus, based on the available dataset, the study constructed the required system conditions.

9.4 Recommendations for Future Research

- In this study, we introduced the dual concept of the QT-transformation, termed as the QT_d-transformation. However, its potential applications and practical implications were not explored. Future research may focus on developing its applicability to statistical modeling, reliability analysis, and real data applications.
- In Chapter 4, we considered only three types of sigmoid functions as the choice for $T(\cdot)$. Besides these, there are other sigmoid functions such as the hyperbolic tangent, Gompertz, Gudermannian, and generalized logistic functions could be explored to develop new families of distributions and investigate their statistical properties.
- In Chapter 5, we considered the sigmoidal transformation by choosing the real-valued function $f(x) = x^{\beta}$, as defined in **Theorem 5.3.1**. For the convenience of the study, we named the resulting transformation the sigmoidal type-I transformation. Exploring different functional forms for $f(x)$ could lead to the generation of various sigmoidal transformations, contributing to the development of new flexible classes of distributions.
- Since the study focuses on the exponential distribution, it was used as the baseline model throughout. Additionally, the quantile function $Q(\cdot)$ in the QT-transformation was chosen from the Gumbel, unit Gumbel, and unit exponential distributions. By choosing different combinations of $Q(\cdot)$ and baseline distributions, a broader class of flexible distributions can be constructed.
- The analysis of stress-strength reliability in this study can be extended in various directions, such as exploring other censoring techniques (e.g., hybrid or adaptive censoring), modeling systems under varying stress levels,

and investigating scenarios where stress and strength variables are dependent.

- Specifically, we applied the proposed models in stress-strength reliability. It can also be utilized in other reliability contexts, such as accelerated life testing and degradation modeling, to further expand their applicability.
- The QT-transformation can be extended to a multivariate setup to construct multivariate statistical models, which can be effectively applied to various real-life scenarios.

List of Publications

1. Greeshma Chandran & M. Manoharan (2024) Estimation of stress-strength reliability in s-out-of-k system for new flexible exponential distribution under progressive type-II censoring, *Journal of Statistical Computation and Simulation*, 94(10), 2143-2188, DOI: 10.1080/00949655.2024.2323940

2. Greeshma Chandran & M. Manoharan (2024) A Method for Generating Family of Distributions Using Sigmoid Functions and Its Applications. (Communicated).

3. Greeshma Chandran & M. Manoharan (2025) Generating families of distributions using Yun and sigmoidal transformations with an application to exponential distribution. (under revision in Journal of Applied Statistics).

4. Greeshma Chandran & M. Manoharan (2025) On Alpha Gamma Power Transformation for Life Distributions with Applications to Real-Life Data (Communicated).

5. Greeshma Chandran & M. Manoharan (2025) Estimation of Stress-Strength Reliability for the AGPT-Family of Distributions (Communicated).

Presentations in Seminars/Conferences

1. "Reliability Estimation of Multi-component stress-strength model for New Flexible Exponential distribution under progressive type II Censored Samples" in the International Virtual Conference on Statistics and Data Science: Theory and Practice for Progress and Prosperity, held during 11th – 13th March 2022, organized jointly by the Department of Statistics, University College of Science, Osmania University, Hyderabad and ISPS.

2. "Estimation of stress-strength reliability in s-out-of-k system for New Flexible Exponential distribution under progressive type II censoring" in the Eighth International Conference on Statistics for Twenty-first Century-2022 (ICSTC - 2022) organized by the International Statistics Fraternity(ISF), School of Physical and Mathematical Sciences and Department of Statistics, University of Kerala, Trivandrum during 16 - 19 December, 2022.

3. "On Alpha Gamma Power Transformation for Life Distributions with Applications to Real Life Data" in the International Conference on Statistics, Probability, Data Science and Related Areas, held during 04th - 06th January 2023, organized jointly by the Department of Statistics, Cochin University of Science and Technology & ISPS.

4. “Generating families of distributions using sigmoidal and yun transformations with an application to exponential distribution” in the International Conference on Innovative Trends in Statistics, Optimization, and Data Science (IC-ITSODS-2024), to be held during December 21-23, 2024 at Department of Statistics and Operational Research, Kurukshetra University, Kurukshetra.

5. “A method for generating family of distributions using sigmoid functions and its applications” in the Annual Conference of International Indian Statistical Association 2024, held at Cochin University of Science and Technology, jointly organized by Department of Statistics, Cochin University of Science and Technology and IISA.

Bibliography

[1] Abd El-Monsef, M. M. E., Marei, G. A., and Kilany, N. M. (2022). Poisson modified Weibull distribution with inferences on stress-strength reliability model. *Quality and Reliability Engineering International*, 38(5):2649–2669.

[2] Ahmad, Z., Ilyas, M., and Hamedani, G. G. (2019). The extended alpha power transformed family of distributions: properties and applications. *Journal of Data Science*, 1(1):13–27.

[3] Ahmadi, K. and Ghafouri, S. (2019). Reliability estimation in a multicomponent stress-strength model under generalized half-normal distribution based on progressive type-II censoring. *Journal of Statistical Computation and Simulation*, 89(13):2505–2548.

[4] Ahmed, M. A. (2020). On the alpha power Kumaraswamy distribution: Properties, simulation and application. *Revista Colombiana de Estadística*, 43(2):285–313.

[5] Akhila, P., Girish Babu, M., and Bakouch, H. (2023). A versatile probabilistic model based on Yun-G family of distributions and its applications in engineering sector. *J. Kerala Stat. Assoc*, 34(1):52–83.

[6] Akinsete, A., Famoye, F., and Lee, C. (2008). The beta-Pareto distribution. *Statistics*, 42(6):547–563.

[7] Al-Mutairi, D. K., Ghitany, M. E., and and, D. K. (2013). Inferences on stress-strength reliability from Lindley distributions. *Communications in Statistics - Theory and Methods*, 42(8):1443–1463.

[8] Aljarrah, M. A., Lee, C., and Famoye, F. (2014). On generating T-X family of distributions using quantile functions. *Journal of Statistical Distributions and Applications*, 1(1):1–17.

[9] Aljohani, H. M., Almetwally, E. M., Alghamdi, A. S., and Hafez, E. (2021). Ranked set sampling with application of modified Kies exponential distribution. *Alexandria Engineering Journal*, 60(4):4041–4046.

[10] Alshawarbeh, E., Lee, C., and Famoye, F. (2012). The beta-Cauchy distribution. *Journal of Probability and Statistical Science*, 10(1):41–57.

[11] Alzaatreh, A., Lee, C., and Famoye, F. (2012). On the discrete analogues of continuous distributions. *Statistical Methodology*, 9(6):589–603.

[12] Alzaatreh, A., Lee, C., and Famoye, F. (2013). A new method for generating families of continuous distributions. *Metron*, 71(1):63–79.

[13] Anastassiou, G. A. (2022). Multivariate fuzzy-random and stochastic arctangent, algebraic, gudermannian and generalized symmetric activation functions induced neural network approximations. In *International Workshop of Mathematical Modelling, Applied Analysis and Computation*, pages 1–32. Springer.

[14] Anastassiou, G. A. (2025). Parametrized arctangent sigmoid function based Banach space valued neural network approximation. *Neural, Parallel, and Scientific Computations*, 33(1):25–38.

[15] Andrews, L. C. (1998). *Special Functions of Mathematics for Engineers*. SPIE Press, Washington, USA.

[16] Arellano-Valle, R. B., Gómez, H. W., and Quintana, F. A. (2004). A new class of skew-normal distributions. *Communications in Statistics-Theory and Methods*, 33(7):1465–1480.

[17] Arnold, B. C., Press, S. J., et al. (1983). Bayesian inference for Pareto populations. *Journal of Econometrics*, 21(3):287–306.

[18] Arslan, T. (2023). A new family of unit-distributions: Definition, properties and applications. *TWMS Journal of Applied and Engineering Mathematics*, 13(2):782–791.

[19] Azzalini, A. (1985). A class of distributions which includes the normal ones. *Scandinavian Journal of Statistics*, 12(2):171–178.

[20] Azzalini, A. and Valle, A. D. (1996). The multivariate skew-normal distribution. *Biometrika*, 83(4):715–726.

[21] Bader, M. and Priest, A. (1982). Statistical aspects of fibre and bundle strength in hybrid composites. In *Progress in Science and Engineering of Composites*, pages 1129–1136. Tokyo: ICCM-IV.

[22] Baklizi, A. (2014). Bayesian inference for Pr $(Y < X)$ in the exponential distribution based on records. *Applied Mathematical Modelling*, 38(5):1698–1709.

[23] Bakouch, H. S., Hussain, T., Tošić, M., Stojanović, V. S., and Qarmalah, N. (2023). Unit exponential probability distribution: Characterization and applications in environmental and engineering data modeling. *Mathematics*, 11(19):4207.

[24] Balakrishnan, N. and Aggarwala, R. (2000). *Progressive Censoring: Theory, Methods, and Applications.* Birkhäuser, Boston.

[25] Balakrishnan, N. and Cramer, E. (2014). *The Art of Progressive Censoring: Applications to Reliability and Quality Statistics for Industry and Technology.* Springer, New York.

[26] Barlow, R. and Campo, R. (2024). *Total Time on Test Processes and Applications to Failure Data Analysis.* Society for Industrial and Applied Mathematics, Berkeley, California, USA.

[27] Basu, A. P. and Ebrahimi, N. (1983). On the reliability of stochastic systems. *Statistics & Probability Letters*, 1(5):265–267.

[28] Basu, S. and Lingham, R. T. (2003). Bayesian estimation of system reliability in Brownian stress-strength models. *Annals of the Institute of Statistical Mathematics*, 55(1):7–19.

[29] Bhattacharyya, G. and Johnson, R. A. (1974). Estimation of reliability in a multicomponent stress-strength model. *Journal of the American Statistical Association*, 69(348):966–970.

[30] Bhuyan, P. and Dewanji, A. (2014). *Dynamic Stress-Strength Modeling with Cumulative Stress and Strength Degradation*. Technical Report No. ASU/2014/7, Applied Statistics Unit, Indian Statistical Institute, Kolkata.

[31] Bhuyan, P. and Dewanji, A. (2017a). Estimation of reliability with cumulative stress and strength degradation. *Statistics*, 51(4):766–781.

[32] Bhuyan, P. and Dewanji, A. (2017b). Reliability computation under dynamic stress–strength modeling with cumulative stress and strength degradation. *Communications in Statistics-Simulation and Computation*, 46(4):2701–2713.

[33] Birnbaum, Z. et al. (1956). On a use of the Mann-Whitney statistic. In *Proceedings of the third Berkeley symposium on mathematical statistics and probability*, volume 1, pages 13–17. University of California Press Berkeley, CA, USA.

[34] Birnbaum, Z. and McCarty, R. (1958). A distribution-free upper confidence bound for $\Pr\{Y < X\}$, based on independent samples of X and w. *The Annals of Mathematical Statistics*, 29(2):558–562.

[35] Bourguignon, M., Silva, R. B., and Cordeiro, G. M. (2014). The Weibull-G family of probability distributions. *Journal of Data Science*, 12(1):53–68.

[36] Bryson, M. C. and Siddiqui, M. (1969). Some criteria for aging. *Journal of the American Statistical Association*, 64(328):1472–1483.

[37] Burr, I. W. (1942). Cumulative frequency functions. *The Annals of mathematical statistics*, 13(2):215–232.

[38] Cao, J, H. and ANg, K. (1986). *An introduction to Reliability Mathematics.* Science Press, Beijing.

[39] Chacko, M. and Elizabeth Koshy, A. (2024). Estimation of multicomponent stress–strength reliability for exponentiated Gumbel distribution. *Journal of Statistical Computation and Simulation*, 94(7):1595–1630.

[40] Chandra, N. K. and Roy, D. (2001). Some results on reversed hazard rate. *Probability in the Engineering and Informational Sciences*, 15(1):95–102.

[41] Chandra, S. and Owen, D. B. (1975). On estimating the reliability of a component subject to several different stresses (strengths). *Naval Research Logistics Quarterly*, 22(1):31–39.

[42] Chang, S.-M. and Genton, M. G. (2007). Extreme value distributions for the skew-symmetric family of distributions. *Communications in Statistics—Theory and Methods*, 36(9):1705–1717.

[43] Chen, M.-H. and Shao, Q.-M. (1999). Monte carlo estimation of Bayesian Credible and HPD intervals. *Journal of Computational and Graphical Statistics*, 8(1):69–92.

[44] Cheng, K. F. and Chao, A. (1984). Confidence intervals for reliability from stress-strength relationships. *IEEE Transactions on Reliability*, 33(3):246–249.

[45] Chesneau, C., Babu, M. G., and Bakouch, H. S. (2021). The Yun transform in probabilistic and statistical contexts: Weibull baseline case and its applications in reliability theory. *Journal of Computational Mathematics and Data Science*, 1:100002.

[46] Church, J. D. and Harris, B. (1970). The estimation of reliability from stress-strength relationships. *Technometrics*, 12(1):49–54.

[47] Cordeiro, G. M. and De Castro, M. (2011). A new family of generalized distributions. *Journal of Statistical Computation and Simulation*, 81(7):883–898.

[48] Cordeiro, G. M., Ortega, E. M., and da Cunha, D. C. (2013). The exponentiated generalized class of distributions. *Journal of Data Science*, 11(1):1–27.

[49] Cox, D. R. and Hinkley, D. V. (1974). *Theoretical Statistics*. Chapman and Hall, London.

[50] Dey, S., Ghosh, I., and Kumar, D. (2019). Alpha-power transformed Lindley distribution: properties and associated inference with application to earthquake data. *Annals of Data Science*, 6(4):623–650.

[51] Dey, S., Mazucheli, J., and Anis, M. (2017). Estimation of reliability of multicomponent stress-strength for a Kumaraswamy distribution. *Communications in Statistics-Theory and Methods*, 46(4):1560–1572.

[52] Dunning, K. A. and Hanson, J. N. (1977). Generalized Pearson distributions and nonlinear programing. *Journal of Statistical Computation and Simulation*, 6(2):115–128.

[53] Eberly, L. E. and Casella, G. (2003). Estimating Bayesian credible intervals. *Journal of Statistical Planning and Inference*, 112(1-2):115–132.

[54] Ebrahimi, N. (1982). Estimation of reliability for a series stress-strength system. *IEEE Transactions on Reliability*, 31(2):202–205.

[55] Ebrahimi, N. and Ramallingam, T. (1993). Estimation of system reliability in brownian stress-strength models based on sample paths. *Annals of the Institute of Statistical Mathematics*, 45(1):9–19.

[56] Eghwerido, J. T., Nzei, L. C., and Agu, F. I. (2021). The alpha power Gompertz distribution: characterization, properties, and applications. *Sankhya A*, 83(1):449–475.

[57] Elbatal, I., Ahmad, Z., Elgarhy, M., and Almarashi, A. M. (2018). A new alpha power transformed family of distributions: properties and applications to the Weibull model. *Journal of Nonlinear Science and Applications*, 12(1):1–20.

[58] Elliot, D. and Prössdorf, S. (1995). An algorithm for the approximate solution of integral equations of Mellin type. *Numerische Mathematik*, 70(4):427–452.

[59] Elliott, D. (1998). Sigmoidal transformations and the trapezoidal rule. *Anziam Journal*, 40(E):E77–E137.

[60] Epstein, B. and Sobel, M. (1953). Life testing. *Journal of the American Statistical Association*, 48(263):486–502.

[61] Eryilmaz, S. (2008). Consecutive k-out-of-n: G system in stress-strength setup. *Communications in Statistics—Simulation and Computation®*, 37(3):579–589.

[62] Eugene, N., Lee, C., and Famoye, F. (2002). Beta-normal distribution and its applications. *Communications in Statistics-Theory and methods*, 31(4):497–512.

[63] Fisher, R. A. (1912). On an absolute criterion for fitting frequency curves. *Messenger of mathematics*, 41(1):155–156.

[64] Foss, S., Korshunov, D., Zachary, S., et al. (2011). *An Introduction to Heavy-Tailed and Subexponential Distributions*, volume 6. Springer New York, NY.

[65] Galton, F. (1883). *Inquires into Human Faculty and its Development.* Macmillan, London.

[66] Garg, R., Kumari, M., Sahoo, R. K., and Kumari, A. (2024). Stress-strength reliability estimation of multicomponent system with non-identical strength components from inverse pareto distribution. *Life Cycle Reliability and Safety Engineering*, 13(3):351–363.

[67] Gera, A. (1997). The modified exponentiated-Weibull distribution for life-time modeling. In *Annual Reliability and Maintainability Symposium*, volume 1, pages 149–152.

[68] Gilchrist, W. (2000). *Statistical Modelling with Quantile Functions.* Chapman and Hall/CRC,New York.

[69] Glänzel, W. (1987). A characterization theorem based on truncated moments and its application to some distribution families. In *Mathematical Statistics and Probability Theory: Volume B Statistical Inference and Methods Proceedings of the 6th Pannonian Symposium on Mathematical Statistics, Bad Tatzmannsdorf, Austria, September 14–20, 1986*, pages 75–84. Springer.

[70] Govindarajulu, Z. (1968). Distribution-free confidence bounds for P $(X < Y)$. *Annals of the Institute of Statistical Mathematics*, 20(1):229–238.

[71] Gradshteyn, I. and Ryzhik, I. (1994). *Table of Integrals, Series, and Products.* 6th edn New York: Academic Press.

[72] Gupta, R. C., Gupta, P. L., and Gupta, R. D. (1998). Modeling failure time data by Lehman alternatives. *Communications in Statistics-Theory and Methods*, 27(4):887–904.

[73] Gupta, R. D. and Kundu, D. (1999). Theory & methods: Generalized exponential distributions. *Australian & New Zealand Journal of Statistics*, 41(2):173–188.

[74] Gupta, R. D. and Kundu, D. (2001). Exponentiated exponential family: an alternative to gamma and Weibull distributions. *Biometrical Journal: Journal of Mathematical Methods in Biosciences*, 43(1):117–130.

[75] Gupta, R. D. and Kundu, D. (2007). Generalized exponential distribution: Existing results and some recent developments. *Journal of Statistical Planning and Inference*, 137(11):3537–3547.

[76] Hakamipour, N. (2024). Stress–strength reliability estimation of s-out-of-k multicomponent systems based on copula function for dependent strength elements under progressively censored sample. *International Journal of General Systems*, 54(4):440–462.

[77] Hanagal, D. D. (2003). Estimation of system reliability in multicomponent series stress-strength models. *Journal of the Indian Statistical Association*, 41(1):1–7.

[78] Hashempour, M. and Alizadeh, M. (2023). A new weighted half-logistic distribution: Properties, applications and different method of estimations. *Statistics, Optimization & Information Computing*, 11(3):554–569.

[79] Hashempour, M. and Alizadeh, M. (2024). A new two-parameter extension of half-logistic distribution: Properties, applications and different method of estimations. *Thailand Statistician*, 22(3):720–735.

[80] Hastings, W. K. (1970). Monte Carlo sampling methods using Markov chains and their applications. *Biometrika*, 57(1):97–109.

[81] Hastings Jr, C., Mosteller, F., Tukey, J. W., and Winsor, C. P. (1947). Low moments for small samples: a comparative study of order statistics. *The Annals of Mathematical Statistics*, 18(3):413–426.

[82] Hollander, M. and Proschan, F. (1975). Tests for the mean residual life. *Biometrika*, 62(3):585–593.

[83] Hussein, M., Elsayed, H., and Cordeiro, G. M. (2022). A new family of continuous distributions: properties and estimation. *Symmetry*, 14(2):276.

[84] Ijaz, M., Mashwani, W. K., and Belhaouari, S. B. (2020). A novel family of lifetime distribution with applications to real and simulated data. *PLOS ONE*, 15(10):1–15.

[85] Isa, A. M., Bashiru, S. O., Ali, B. A., Adepoju, A. A., and Itopa, I. I. (2022). Sine-exponential distribution: Its mathematical properties and application to real dataset. *UMYU Scientifica*, 1(1):127–131.

[86] Ismail, R., Jeyaratnam, S., and and, S. P. (1986). Estimation of pr[X >Y] for gamma distributions. *Journal of Statistical Computation and Simulation*, 26(3-4):253–267.

[87] Ivshin, V. (1996). Unbiased estimators of P$(X < Y)$ and their variances in the case of uniform and two-parameter exponential distributions. *Journal of Mathematical Sciences*, 81(4):2790 – 2793.

[88] Jha, M. K., Dey, S., Alotaibi, R., Alomani, G., and Tripathi, Y. M. (2022). Multicomponent stress-strength reliability estimation based on unit generalized exponential distribution. *Ain Shams Engineering Journal*, 13(5):101627.

[89] Jha, M. K., Dey, S., Alotaibi, R. M., and Tripathi, Y. M. (2020). Reliability estimation of a multicomponent stress-strength model for unit Gompertz distribution under progressive Type II censoring. *Quality and Reliability Engineering International*, 36(3):965–987.

[90] Jiang, R., Ji, P., and Xiao, X. (2003). Aging property of unimodal failure rate models. *Reliability Engineering & System Safety*, 79(1):113–116.

[91] Jiménez, J., Arunachalam, V., and Serna, G. (2015). A generalization of Tukey'sg—h family of distributions. *Journal of Statistical Theory and Applications*, 14(1):28–44.

[92] Johnson, N. L. (1949). Systems of frequency curves generated by methods of translation. *Biometrika*, 36(1/2):149–176.

[93] Jónás, T. (2007). Sigmoid functions in reliability based management. *Periodica Polytechnica Social and Management Sciences*, 15(2):67–72.

[94] Kamruzzaman, J. (2002). Arctangent activation function to accelerate backpropagation learning. *IEICE Transactions on Fundamentals of Electronics, Communications and Computer Sciences*, 85(10):2373–2376.

[95] Karakaya, K., Kınacı, İ., Kuş, C., and Akdoğan, Y. (2021). On the DUS-Kumaraswamy distribution. *Istatistik Journal of The Turkish Statistical Association*, 13(1):29–38.

[96] Karian, Z. A., Dudewicz, E. J., and Mcdonald, P. (1996). The extended generalized lambda distribution system for fitting distributions to data: history, completion of theory, tables, applications, the "final word" on moment fits. *Communications in Statistics-Simulation and Computation*, 25(3):611–642.

[97] Kavya, P. and Manoharan, M. (2021). Some parsimonious models for lifetimes and applications. *Journal of Statistical Computation and Simulation*, 91(18):3693–3708.

[98] Kayid, M. (2022). Applications of bladder cancer data using a modified log-logistic model. *Applied Bionics and Biomechanics*, 2022:6600278.

[99] Khan, A. H. and Jan, T. (2015). Estimation of stress-strength reliability model using finite mixture of two parameter Lindley distributions. *Journal of Statistics Applications and Probability*, 4(1):147–159.

[100] Kızılaslan, F. (2017). Classical and Bayesian estimation of reliability in a multicomponent stress–strength model based on the proportional reversed hazard rate mode. *Mathematics and Computers in Simulation*, 136(June):36–62.

[101] Kızılaslan, F. (2018). Classical and bayesian estimation of reliability in a multicomponent stress–strength model based on a general class of inverse exponentiated distributions. *Statistical Papers*, 59(3):1161–1192.

[102] Kizilaslan, F. and Nadar, M. (2015). Classical and Bayesian estimation of reliability in multicomponent stress-strength model based on Weibull distribution. *Revista Colombiana de estadistica*, 38(2):467–484.

[103] Kizilaslan, F. and Nadar, M. (2018). Estimation of reliability in a multicomponent stress-strength model based on a bivariate Kumaraswamy distribution. *Statistical Papers*, 59(1):307–340.

[104] Klüppelberg, C. (1988). Subexponential distributions and integrated tails. *Journal of Applied Probability*, 25(1):132–141.

[105] Kohansal, A. (2019). On estimation of reliability in a multicomponent stress-strength model for a Kumaraswamy distribution based on progressively censored sample. *Statistical Papers*, 60(6):2185–2224.

[106] Kotz, S., Lumelskii, Y., and Pensky, M. (2003). *The Stress-Strength Model and its Generalizations: Theory and Applications*. World Scientific Press, Singapore.

[107] Kumar, D., Singh, U., and Singh, S. K. (2015a). A method of proposing new distribution and its application to bladder cancer patients data. *J. Stat. Appl. Pro. Lett*, 2(3):235–245.

[108] Kumar, D., Singh, U., and Singh, S. K. (2015b). A new distribution using sine function-its application to bladder cancer patients data. *Journal of Statistics Applications & Probability*, 4(3):417.

[109] Kundu, D. and Gupta, R. D. (2005). Estimation of $\mathbf{P}(\mathbf{Y}<\mathbf{X})$ for generalized exponential distribution. *Metrika*, 61(3):291–308.

[110] Kundu, D. and Gupta, R. D. (2006). Estimation of P $[Y < X]$ for Weibull distributions. *IEEE Trans. Reliab.*, 55(2):270–280.

[111] Kundu, D. and Raqab, M. Z. (2009). Estimation of $\mathbf{R} = \mathbf{P}(\mathbf{Y}<\mathbf{X})$ for three-parameter Weibull distribution. *Statistics & Probability Letters*, 79(17):1839–1846.

[112] Kundu, D. and Raqab, M. Z. (2015). Estimation of $\mathbf{R} = \mathbf{P}(\mathbf{Y}<\mathbf{X})$ for three-parameter generalized Rayleigh distribution. *Journal of Statistical Computation and Simulation*, 85(4):725–739.

[113] Lawless, J. F. (1982). *Statistical Models and Methods for Lifetime Data.* John Wiley & Sons, New York.

[114] Lee, C., Famoye, F., and Alzaatreh, A. Y. (2013). Methods for generating families of univariate continuous distributions in the recent decades. *Wiley Interdisciplinary Reviews: Computational Statistics*, 5(3):219–238.

[115] Lee, E. T. and Wang, J. (2003). *Statistical Methods for Survival Data Analysis*, volume 476. John Wiley & Sons, Belmont, CA.

[116] Leipus, R., Siaulys, J., and Konstantinides, D. (2023). *Closure Properties for Heavy-Tailed and Related Distributions.* Springer Nature, Cham.

[117] Lindley, D. V. (1980). Approximate Bayesian methods. *Trabajos de Estadística y de Investigación Operativa*, 31(1):223–245.

[118] Lio, Y. L. and and, T.-R. T. (2012). Estimation of $\delta = P(X < Y)$ for Burr XII distribution based on the progressively first failure-censored samples. *Journal of Applied Statistics*, 39(2):309–322.

[119] Liu, H., Xu, M., Gu, H., Gupta, A., Lafferty, J., and Wasserman, L. (2011). Forest density estimation. *The Journal of Machine Learning Research*, 12(3):907–951.

[120] Mahdavi, A. and Kundu, D. (2017a). A new method for generating distributions with an application to exponential distribution. *Communications in Statistics-Theory and Methods*, 46(13):6543–6557.

[121] Mahdavi, A. and Kundu, D. (2017b). A new method for generating distributions with an application to exponential distribution. *Communications in Statistics - Theory and Methods*, 46(13):6543–6557.

[122] Mahto, A. K. and Tripathi, Y. M. (2020). Estimation of reliability in a multicomponent stress-strength model for inverted exponentiated Rayleigh distribution under progressive censoring. *OPSEARCH*, 57(4):1043–1069.

[123] Malik, A. and Ahmad, S. (2019). Transmuted alpha power inverse Rayleigh distribution: properties and application. *Journal of Scientific Research*, 11(2):185–194.

[124] Marshall, A. W. and Olkin, I. (1997). A new method for adding a parameter to a family of distributions with application to the exponential and Weibull families. *Biometrika*, 84(3):641–652.

[125] Matis, J. and Al-Muhammed, M. (2010). Theory and application of the logistic probability density function as a population growth model. *Damascus University Journal for Basics Science*, 26(1):9–19.

[126] Maurya, R. K. and Tripathi, Y. M. (2020). Reliability estimation in a multicomponent stress-strength model for Burr-XII distribution under progressive censoring. *Brazilian Journal of Probability and Statistics*, 34(2):345–369.

[127] Maurya, S., Kaushik, A., Singh, S., and Singh, U. (2017a). A new class of distribution having decreasing, increasing, and bathtub-shaped failure rate. *Communications in Statistics-Theory and Methods*, 46(20):10359–10372.

[128] Maurya, S. K., Kaushik, A., Singh, S. K., and Singh, U. (2017b). A new class of exponential transformed Lindley distribution and its application to yarn data. *International Journal of Statistics and Economics*, 18(2):135–151.

[129] Menon, A., Mehrotra, K., Mohan, C. K., and Ranka, S. (1996). Characterization of a class of sigmoid functions with applications to neural networks. *Neural Networks*, 9(5):819–835.

[130] Metropolis, N., Rosenbluth, A. W., Rosenbluth, M. N., Teller, A. H., and Teller, E. (1953). Equation of state calculations by fast computing machines. *The Journal of Chemical Physics*, 21(6):1087–1092.

[131] Mokhlis, N. A., Ibrahim, E. J., and and, D. M. G. (2017). Stress-strength reliability with general form distributions. *Communications in Statistics - Theory and Methods*, 46(3):1230–1246.

[132] Moors, J. (1988). A quantile alternative for kurtosis. *Journal of the Royal Statistical Society: Series D (The Statistician)*, 37(1):25–32.

[133] Mudholkar, G. and Srivastava, D. (1993). Exponentiated Weibull family for analyzing bathtub failure-rate data. *IEEE Transactions on Reliability*, 42(2):299–302.

[134] Mudholkar, G. S., Srivastava, D. K., and Freimer, M. (1995). The exponentiated Weibull family: A reanalysis of the bus-motor-failure data. *Technometrics*, 37(4):436–445.

[135] Murthy, D. P., Xie, M., and Jiang, R. (2004). *Weibull Models*. John Wiley, New York.

[136] Muth, E. J. (1977). Reliability models with positive memory derived from the mean residual life function. In *The Theory and Applications of Reliability*, volume 2, pages 401–435. Academic Press New York, NY, USA.

[137] Nadar, M., Kızılaslan, F., and and, A. P. (2014). Classical and Bayesian estimation of P($Y < X$) for Kumaraswamy's distribution. *Journal of Statistical Computation and Simulation*, 84(7):1505–1529.

[138] Nadar, M., Papadopoulos, A., and Kizilaslan, F. (2013). Statistical analysis for Kumaraswamy's distribution based on record data. *Statistical Papers*, 54(2):355–369.

[139] Nadarajah, S. (2002). Reliability for beta models. *Serdica Mathematical Journal*, 28(3):267p–282p.

[140] Nadarajah, S. (2004). Reliability for Laplace distributions. *Mathematical Problems in Engineering*, 2004(2):169–183.

[141] Nadarajah, S., Cordeiro, G. M., and Ortega, E. M. (2013). The exponentiated Weibull distribution: a survey. *Statistical Papers*, 54(3):839–877.

[142] Nadarajah, S. and Gupta, A. (2004). The beta Fréchet distribution. *Far East Journal of Theoretical Statistics*, 14(1):15–24.

[143] Nadarajah, S. and Kotz, S. (2004). The beta Gumbel distribution. *Mathematical Problems in Engineering*, 2004(4):323–332.

[144] Nadarajah, S. and Kotz, S. (2006a). The beta exponential distribution. *Reliability Engineering & System Safety*, 91(6):689–697.

[145] Nadarajah, S. and Kotz, S. (2006b). The exponentiated type distributions. *Acta Applicandae Mathematica*, 92(2):97–111.

[146] Nadarajah, S. and Kotz, S. (2006c). Skew distributions generated from different families. *Acta Applicandae Mathematica*, 91(1):1–37.

[147] Nakagami, M. (1960). The m-distribution: A general formula of intensity distribution of rapid fading. In *Statistical Methods in Radio Wave Propagation*, pages 3–36. Pergamon Press.

[148] Nassar, M., Alzaatreh, A., Abo-Kasem, O., Mead, M., and Mansoor, M. (2018). A new family of generalized distributions based on alpha power transformation with application to cancer data. *Annals of Data Science*, 5(3):421–436.

[149] Nassar, M., Alzaatreh, A., Mead, M., and Abo-Kasem, O. (2017). Alpha power weibull distribution: Properties and applications. *Communications in Statistics-Theory and Methods*, 46(20):10236–10252.

[150] Nichols, M. D. and Padgett, W. (2006). A Bootstrap control chart for Weibull percentiles. *Quality and Reliability Engineering International*, 22(2):141–151.

[151] Norman R, D. and Irwin, G. (1978). Bayesian analysis of reliability in multi-component stress-strength models. *Communications in Statistics - Theory and Methods*, 7(5):441–451.

[152] Oguntunde, P., Adejumo, A., and Balogun, O. (2014). Statistical properties of the exponentiated generalized inverted exponential distribution. *Applied Mathematics*, 4(2):47–55.

[153] Oguntunde, P., Balogun, O., Okagbue, H., and Bishop, S. (2015). The Weibull-exponential distribution: Its properties and applications. *Journal of Applied Sciences*, 15(11):1305–1311.

[154] Ord, J. K. (1967). On a system of discreate distributions. *Biometrika*, 54(3-4):649–656.

[155] Pandey, M., Uddin, M. B., and Ferdous, J. (1992). Reliability estimation of an s-out-of-k system with non-identical component strengths: the Weibull case. *Reliability Engineering & System Safety*, 36(2):109–116.

[156] Paul, R. K. and Uddin, M. B. (1997). Estimation of reliability of stress-strength model with non-identical component strengths. *Microelectronics Reliability*, 37(6):923–927.

[157] Pearson, K. (1895). X. contributions to the mathematical theory of evolution.—ii. skew variation in homogeneous material. *Philosophical Transactions of the Royal Society of London.(A.)*, 186:343–414.

[158] Pewsey, A. (2000). The wrapped skew-normal distribution on the circle. *Communications in Statistics-Theory and Methods*, 29(11):2459–2472.

[159] Prössdorf, S. and Rathsfeld, A. (1991). On an integral equation of the first kind arising from a cruciform crack problem. *Integral Equations and Inverse Problems, Petkov V, Lazarov R (eds). Longman: Coventry*, pages 210–219.

[160] Punathumparambath, B. (2011). Estimation of P $(X > Y)$ for the double Lomax distribution. In *Probstat Forum*, volume 4, pages 1–11.

[161] Raeside, R. (1988). The use of sigmoids in modelling and forecasting human populations. *Journal of the Royal Statistical Society Series A: Statistics in Society*, 151(3):499–513.

[162] Ramadan, D. A. and Magdy, W. (2018). On the alpha-power inverse Weibull distribution. *International Journal of Computer Applications*, 181(11):6–12.

[163] Ramberg, J. S., Dudewicz, E. J., Tadikamalla, P. R., and Mykytka, E. F. (1979). A probability distribution and its uses in fitting data. *Technometrics*, 21(2):201–214.

[164] Ramberg, J. S. and Schmeiser, B. W. (1972). An approximate method for generating symmetric random variables. *Communications of the ACM*, 15(11):987–990.

[165] Ramberg, J. S. and Schmeiser, B. W. (1974). An approximate method for generating asymmetric random variables. *Communications of the ACM*, 17(2):78–82.

[166] Rao and Kantam (2010). Estimation of reliability in multicomponent stress-strength model: Log-Logistic distribution. *Electronic Journal of Applied Statistical Analysis*, 3(2):75–84.

[167] Rao, G. S. (2012a). Estimation of reliability in multicomponent stress-strength based on generalized exponential distribution. *Revista Colombiana de Estadística*, 35(1):67–76.

[168] Rao, G. S. (2012b). Estimation of reliability in multicomponent stress-strength based on generalized inverted exponential distribution. *International Journal of Current Research & Review*, 4(21):48–56.

[169] Rao, G. S. (2012c). Estimation of reliability in multicomponent stress-strength model based on Rayleigh distribution. *ProbStat Forum*, 5(1):150–161.

[170] Rao, G. S., Aslam, M., and Arif, O. H. (2017). Estimation of reliability in multicomponent stress–strength based on two parameter exponentiated Weibull distribution. *Communications in Statistics - Theory and Methods*, 46(15):7495–7502.

[171] Rao, G. S., Aslam, M., and Kundu, D. (2015). Burr-XII distribution parametric estimation and estimation of reliability of multicomponent stress-strength. *Communications in Statistics-Theory and Methods*, 44(23):4953–4961.

[172] Rao, G. S., Kantam, R., Rosaiah, K., and Reddy, J. P. (2013). Estimation of reliability in multicomponent stress-strength based on inverse Rayleigh distribution. *Journal of Statistics Applications & Probability*, 2(3):261–7.

[173] Rezaeian Zadeh, M., Amin, S., Khalili, D., and Singh, V. P. (2010). Daily outflow prediction by multi layer perceptron with logistic sigmoid and tangent sigmoid activation functions. *Water Resources Management*, 24(11):2673–2688.

[174] Ruiz, J. and Navarro, J. (1996). Characterizations based on conditional expectations of the doubled truncated distribution. *Annals of the Institute of Statistical Mathematics*, 48(3):563–572.

[175] Saini, S. and Garg, R. (2022). Reliability inference for multicomponent stress–strength model from kumaraswamy-g family of distributions based on progressively first failure censored samples. *Computational Statistics*, 37(4):1795–1837.

[176] Saini, S., Tomer, S., and Garg, R. (2022). On the reliability estimation of multicomponent stress–strength model for Burr-XII distribution using progressively first-failure censored samples. *Journal of Statistical Computation and Simulation*, 92(4):667–704.

[177] Saini, S., Tomer, S., and Garg, R. (2023). Inference of multicomponent stress-strength reliability following Topp-Leone distribution using progressively censored data. *Journal of Applied Statistics*, 50(7):1538–1567.

[178] Sauer, L., Lio, Y., and Tsai, T.-R. (2020). Reliability inference for the multicomponent system based on progressively type II censored samples from generalized Pareto distributions. *Mathematics*, 8(7):1176.

[179] Shaked, M. and Shanthikumar, J. G. (2007). *Stochastic Orders*. Springer, New York, NY.

[180] Shannon, C. E. (1948). A mathematical theory of communication. *The Bell System Technical Journal*, 27(3):379–423.

[181] Silva, G. O., Ortega, E. M., and Cordeiro, G. M. (2010). The beta modified Weibull distribution. *Lifetime Data Analysis*, 16(3):409–430.

[182] Sivri, T. T., Akman, N. P., and Berkol, A. (2022). Multiclass classification using arctangent activation function and its variations. In *2022 14th International Conference on Electronics, Computers and Artificial Intelligence (ECAI)*, pages 1–6. IEEE.

[183] Su, C., Chen, J., and Hu, Z. (2004). Some discussions on the class L (γ). *Journal of Mathematical Sciences*, 122(4):3416–3425.

[184] Tukey, J. W. (1960). *The Practical Relationship Between the Common Transformations of Percentages of Counts and of Amounts*. Technical Report 36. Statistical Techniques Research Group, Princeton University, Princeton, NJ.

[185] Tukey, J. W. (1977). Modern techniques in data analysis. In *Proceedings of the NSF-Sponsored Regional Research Conference*, volume 7. Southern Massachusetts University, North Dartmouth, MA, USA.

[186] Turkkan, N. and Pham-Gia, T. (2007). System stress-strength reliability: The multivariate case. *IEEE Transactions on Reliability*, 56(1):115–124.

[187] ul Haq, M. A. and Elgarhy, M. (2018). The odd Fréchet-G family of probability distributions. *Journal of Statistics Applications & Probability*, 7(1):189–203.

[188] Verhulst, P.-F. (1838). Notice sur la loi que la population suit dans son accroissement. *Correspondence Mathematique et Physique*, 10(1838):113–129.

[189] Vicari, D. and Kotz, S. (2005). Survey of developments in the theory of continuous skewed distributions. *Metron*, 63(2):225–261.

[190] Weerahandi, S. and Johnson, R. A. (1992). Testing reliability in a stress-strength model when X and Y are normally distributed. *Technometrics*, 34(1):83–91.

[191] Weibull, W. (1951). A statistical distribution function of wide applicability. *Journal of Applied Mechanics*, 18(3):293–297.

[192] Xu, H., Yu, P. L., and Alvo, M. (2019). Detecting change points in the stress-strength reliability P $(X < Y)$. *Applied Stochastic Models in Business and Industry*, 35(3):837–857.

[193] Yang, S., Li, N., and Zhang, X. (2021). Improved variable step size LMS algorithm based on arctangent function. In *2021 China Automation Congress (CAC)*, pages 4666–4669. IEEE.

[194] Yun, B. I. (2014). An ad hoc approximation to the gauss error function and a correction method. *Applied Mathematical Sciences*, 8(86):4261–4273.

[195] ZAIDI, A. (2022). Mathematical justification on the origin of the sigmoid in logistic regression. *Central European Management Journal*, 30(4):1327–1337.